CHAPTER 1

INTRODUCTION

Parkinson's disease (PD) is a progressive neurodegenerative disorder of the brain characterized by a deficiency of dopamine (DA) in nigrostriatal nerve terminals. Monoamine oxidase B (MAO-B) and the neuronal form of nitric oxide synthase (nNOS), two enzymes present in the brain, have been suggested to be involved in the neurodegenerative events leading to PD. The inhibition of these enzyme systems has been proposed to have a protective effect against the degeneration of dopaminergic neurons. An inhibitor of both enzyme systems, 7-nitroindazole (7-NI), has been shown to be neuroprotective in the MPTP mouse model of neurodegeneration. During our previous studies,[1] we have synthesized and evaluated the potential of tetrahydropyridinyl bearing water soluble "prodrugs" of 7-NI and related indazoles. As part of our synthetic efforts, we investigated systematically the nucleophilic aromatic substitution reaction between indazole and 4-chloro-1-methylpyridium iodide. These studies led to the successful regiospecific syntheses of the 1*H*- and the 2*H*- isomeric indazolylpyridinium idodides. During the course of these studies we encountered an unusual rearrangement reaction resulting in the isomerization of 4-(2*H*-indazolyl)-1-methylpyridinium iodide to the corresponding 1*H*- isomer. The mechanism of this unexpected rearrangement remained unclear.

This dissertation describes our studies on the mechanism of the rearrangement reaction and its exploitation leading to the synthesis of various indazolylpyridinium derivatives. The tetrahydropyridinyl analogues derived from these newly available indazolylpyridinium species were designed to have MAO substrate properties and to provide information concerning the active sites of MAO-A and MAO-B. Also, the potential "prodrug" properties of substituted tetrahydropyridinylindazoles may lead to *in vivo* neuroprotection studies.

---

[1] The results of our previous studies have been described in detail in: Isin, E.M. (2000) Potential prodrugs of the neuronal nitric oxide synthase and monoamine oxidase inhibitor 7-nitroindazole and structurally related compounds. M.S. thesis, VPI&SU, Blacksburg, VA, 2000. Some of these results will be summarized in the introduction part of this dissertation with reference to the above work.

The results on the MAO-A substrate properties of the previously synthesized nitroindazolyl "prodrugs" and identification of metabolites will be also presented. The dockings studies carried out on these compounds utilizing the x-ray crystal structure of MAO-B will be described in an attempt to explain the MAO-B substrate and inhibitor properties of synthetically accessible nitroindazolyl "prodrugs".

Before summarizing our previous results on the synthesis and evaluation of the "prodrugs" of indazole derivatives, a brief introduction to PD and the discovery, function and structure of MAO and NOS will be presented in relation to their significance to neurodegenerative pathways leading to PD.

1.1. Parkinson's Disease (PD)

PD is defined as a progressive neurodegenerative disorder of the basal ganglia. It is characterized by the degeneration of or injury to nigrostriatal dopaminergic neurons leading to a DA deficiency state.[2] Loss of 50% of these neurons is observed even in the patients with mild symptoms.[3] The DA loss in the striatum of these patients is as high as 70-80%.[4] Resting tremor, muscular rigidity, difficulty in initiating motor activity, and loss of postural reflexes are the main symptoms of the disease.[5] The high incidence (1%) among the population over 55 years of age emphasizes the importance of PD research.

The etiology of and the treatment strategies for PD were discussed previously in detail.[6] Therefore, only the relationship between PD and the two enzyme systems, MAO and nNOS, will be summarized here.

In 1983, 1-methyl-4-phenyl-1,2,3,6-tetrahydropyridine [MPTP (**1**)] was recognized as a human neurotoxin that causes motor deficits similar to those observed in patients with PD.[7,8] The neurotoxic properties of MPTP are dependent on its conversion

---

[2] Marsden, C.D. (1990) Parkinson's disease. *The Lancet.* **335**, 948-952.
[3] Fearnley, J.M., Lees, A.J. (1991) Ageing and Parkinson's disease: substantia nigra regional selectivity. *Brain* **114**, 2283-2301.
[4] Rieder, P., Wuketich, S. (1976) Time course of nigra-striatal degeneration in Parkinson's disease. *J. Neurol. Transm*. **38**, 377-382.
[5] Bernheimer, H., Birkmayer, W., Harnykiewicz, O., Jellinger, K., Seitelberger, F. (1973) Brain dopamine and syndromes of Parkinson and Huntington. *J. Nuerol. Sci.* **20**, 415-455.
[6] Reference 1, pages 1-3 and 26-28.
[7] Langston, J.W., Ballard, P., Tetrud, J.W., Irwin, I. (1983) Chronic parkinsonism in humans due to a product of meperidine-analog synthesis. *Science* **219**, 979-980.
[8] For a detailed account of the discovery of MPTP see Reference 1, pages 8-11.

to the pyridinium species MPP^+ (**3**).[9] As shown in Scheme 1, MPTP undergoes a two electron ring α-carbon oxidation in the brain, a reaction catalyzed by MAO-B, to form the corresponding dihydropyridinium species $MPDP^+$ (**2**) which is oxidized further by a poorly defined pathway to MPP^+.[10,11]

Scheme 1. MAO-B catalyzed oxidation of MPTP (1).

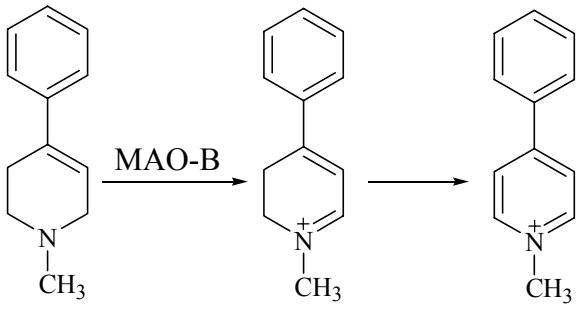

1 **2** **3**

Interestingly, MPP^+ is a substrate for the DA transporter and is actively transported into the nigrostriatal nerve terminals.[12,13] This behavior may explain the selective damage to dopaminergic neurons. Following the transport, MPP^+ localizes within inner mitochondrial membranes and inhibits complex I of the mitochondrial respiratory chain resulting in cell death and DA deficieny.[14,15,16] Although the role of

---

[9] Chiba, K., Trevor, A., Castagnoli, N., Jr. (1984) Metabolism of the neurotoxic tertiary amine, MPTP, by brain monoamine oxidase. *Biochem. Biophys. Res. Commun.* **120**, 574-578.

[10] Chiba, K., Peterson, L.A., Castagnoli, K.P., Trevor, A.J., Castagnoli, N., Jr. (1985) Studies on the molecular mechanism of bioactivation of the selective nigrostriatal toxin 1-methyl-4-phenyl-12,3,6-tetrahydropyridine. *Drug Metabolism and Disposition* **13**, 342-347.

[11] Peterson, L.A., Caldera, P.S., Trevor, A., Chiba, K., Castagnoli, N., Jr. (1985) Studies on the 1-methyl-4-phenyl-2,3-dihydropyridinium species 2,3-$MPDP^+$, the monoamine oxidase catalayzed oxidation product of the nigrostriatal toxin 1-methyl-4-phenyl-1,2,3,6-tetrahydropyridine (MPTP). *J. Med. Chem.* **28**, 1432-1436.

[12] Javith, J.A., Snyder, S.H. (1984) Uptake of $MPP^{(+)}$ by dopamine neurons explains selecetivity of parkinsoniism-inducing neurotoxin, MPTP. Eu*r. J. Pharmacol.* **106**, 455-456.

[13] Chiba, K., Trevor, A.J., Castagnoli, N., Jr. (1985) Active uptake of MPP^+, a metabolite of MPTP, by brain synaptosomes. (1985) *Biochem. Biophys. Res. Commun*. **128**, 1228-1232.

[14] Nicklas, W.J., Youngster, S.K., Kindt, M.V., Heikkila, R.E. (1987) MPTP, MPP^+ and mitochondrial funstion. *Life Sci.* **40**, 721-729.

[15] Schapira, A.H.V., Cooper, J.M., Dexter, D., Clark, J.B., Jenner, P., Marsden,C.D. (1990) Mitochondrial complex I deficieny in Parkinson's disease. *J. Neurochem.* **54**, 823-827.

[16] Singer, T.P., Castagnoli, N., Jr., Ramsay, R.R., Trevor, A.J. (1987) Biochemical events in the development of parkinsonism induced by 1-methyl-4-phenyl-1,2,3,6-tetradhyropyridine. *J. Neurochem.* **49**, 1-8.

MAO in MPTP toxicity is already well-documented, a recent study using MAO-B deficient knock-out mice provides further evidence.[17] In this strain of mice, MPTP does not cause damage to the dopaminergic neurons in the substantia nigra.

The neurotoxicity of MPTP led to the development of the MPTP mouse model of PD.[18] In this model MPTP administration leads to a decrease in striatal DA levels. Several MAO-B inhibitors have been tested in this mouse model.[19,20] The results demonstrate that MAO-B inhibition protects against MPTP induced neurotoxicity in the brain.

In the recent years, a lower incidence of PD in smokers compared to non-smokers has been documented.[21,22] Furthermore, brain imaging using positron emission tomography (PET) demonstrated decreased MAO-B activities in the brains of smokers compared to non-smokers.[23] This rather surprising finding lends further relevance to the importance of MAO-B and MAO-B inhibition studies related to the incidence of PD.[24]

Another enzyme system that is thought to be involved in neurodegenerative pathways leading to PD is nNOS. NOS (EC 1.14.13.39) catalyzes the conversion of *L*-arginine (**4**) to *L*-citrulline (**6**) via the intermediate *L*-N-hydroxyarginine (**5**), a process

---

[17] Grimsby, J., Toth, M., Chen, K., Kumazawa, T., Klaidman, L. Adams, J.D., Karoum, F., Gal, J., Shih, J.C. (1997) Increased stress response and B-phenylethylamine in MAO-B deficient mice. *Nature Genet.* **17**, 1-5.

[18] For a review: Schmidt, N., Ferger, B. (2001) Neurochemical findings in the MPTP model of Parkinson's diseae. *J. Neural Trans*. **108**, 1263-1282. Lau, Y.-S., Meredith, G.E. (2003) From drugs of abuse to Parkinsonism: The MPTP mouse model of Parkinson's disease. *Methods in Molecular Medicine* **79**, 103-116.

[19] Castagnoli, N.; Petzer, J.P.; Steyn, S.; Castagnoli, K.; Chen, J.-F.; Schwarzschild, M.A.; Van der Schyf, C.J. (2003) Monoamine oxidase B inhibition and neuroprotection**:** Studies on selective adenosine A_{2A} receptor antagonists. *Neurology* **61**, S62-S68.

[20] Castagnoli, K.; Petzer, J.B.; Steyn, S.J.; Van Der Schyf, C.J.; Castagnoli, N., Jr. (2003) Inhibition of human MAO-A and MAO-B by a compound isolated from flue-cured tobacco leaves and its neuroprotective properties in the MPTP mouse model of neurodegeneration. *Inflammopharmacology* **11**, 183-188.

[21] Honig, L.S. (1999) Smoking and Parkinson's disease. *Neurology* **53**, 1158.

[22] Checkoway, H., Nelson, L.M. (1999) Epidemiologic approaches to the study of Parkinson's disease etiology. *Epidemiology* **10**, 327-336.

[23] Fowler, J.S., Volkow, N.D., Wang, G.J., Pappas, N., Logan, J., MacGregor, R.R, Alexoff, D., Shea, C., Schleyer, D.J., Wolf, A.P., Warner, D., Zezulokova, I., Cilento, R. (1996) Inhibition of monoamine oxidase B in the brains of smokers. *Nature* **379**, 733-736.

[24] Castagnoli, K., Murugesan, T. (2004) Tobacco leaf, smoke and smoking, MAO inhibitors, Parkinson's disease and neuroprotection; Are there links? *Neurotoxicology* **11**, 183-188.

that leads to the formation of the free radical nitric oxide [NO (**7**)], as shown in Scheme 2.[25]

Scheme 2. NOS catalyzed conversion of *L*-arginine (4) to *L*-citrulline (6) and NO (7).

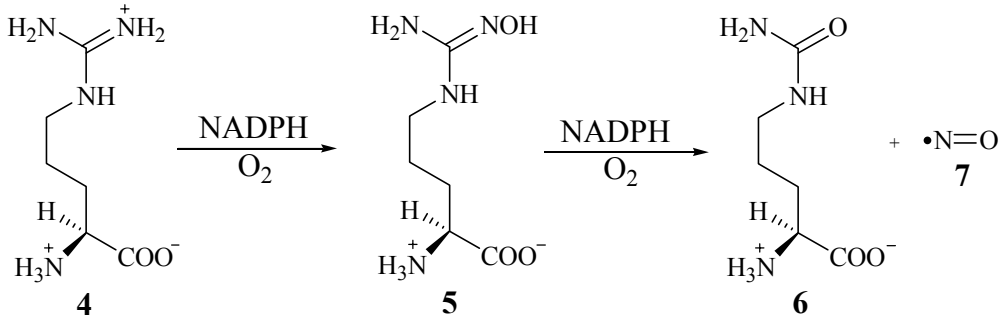

In addition to its diverse functions throughout the human body, NO, a freely diffusible gas, is suspected to lead to neurotoxicity[26,27] possibly through its reactions with oxygen radicals present *in vivo*.[28,29,30] For example, it was suggested that NO could react with superoxide radical anion (**8**) in cells to form peroxynitrite (**9**) as shown in Scheme 3. Peroxynitrite formation can lead eventually to lipid peroxidation, DNA alkylation and tyrosine nitration, possibly through the more reactive protonated form peroxynitrous acid (**10**).

Scheme 3. Reaction of NO (7) with superoxide radical anion (8) forming peroxynitrite (9) which is in equilibrium with peroxynitrous acid (10).

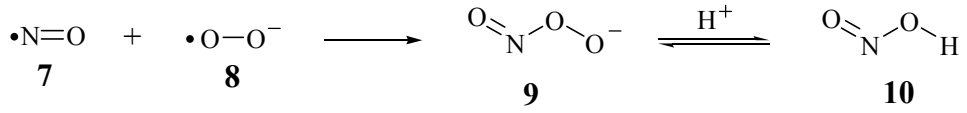

[25] For a detailed mechanism of this conversion see Reference 1, pages 15-16.
[26] Gerlach, M., Blum-Degen, D., Lan, J., Riederer, P. (1999) Nitric oxide in the pathogenesis of Parkinson's disease. *Adv. Neurol.* **80**, 239-245.
[27] Olanow, C.W. (1993) A radical hypothesis for neurodegeneration. *Trends. Nuerosci.* **16**, 439-444.
[28] Beckman, J.S., Crow, J.P., (1993) Pathological implications of nitric oxide, superoxide and peroxynitrite formation. *Biochem. Soc. Trans.* **21**, 330-334.
[29] Squadrito, G.L., Pryor, W.A.(1998) Oxidative chemistry of nitric oxide: the roles of superoxide, peroxynitrite and carbon dioxide. *Free Radical Biol. Med.* **25**, 392-403
[30] For a detailed review of the reactions of NO with reactive oxygen species see Reference 1, pp. 17-25.

An alternative toxication pathway involves the formation of nitrosoperoxycarbonate (**12**) via the reaction of **9** with carbon dioxide (**11**) as shown in Scheme 4. Decomposition of **12** releases two reactive species, nitrogen dioxide (**13**) and carbonate (**14**) radicals. These free radicals may cause the oxidation and nitration of biological target molecules.

Scheme 4. Formation of nitrosoperoxycarbonate (12) from peroxynitrite and carbon dioxide followed by fragmentation to yield nitrogen dioxide (1) and carbonate radicals (14).

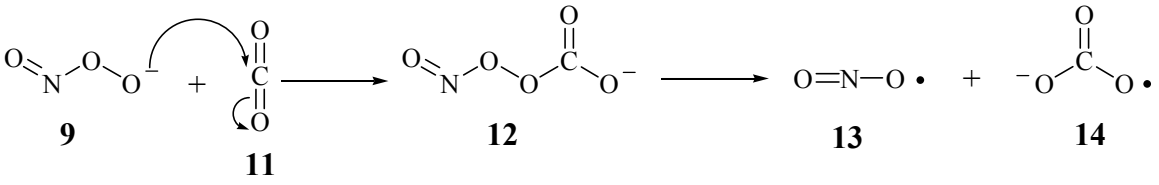

Due to the possible involvement of MAO and nNOS in neurodegeneration, the inhibition of these two enzyme systems has been of interest to us as a possible approach to neuroprotection. An exhaustive review of these enzyme systems is beyond the scope of this dissertation. However, a brief discussion of the discovery, the structure, function and biological significance of MAO and NOS will be presented in the following section.

1.2. Monoamine Oxidase (MAO)

In 1928, Mary L. C. Hare (Mary Bernheim), a graduate student at Duke University, reported her discovery of tyramine oxidase as a new enzyme system present in the liver.[31] The oxidation differed from known pathways by being cyanide-resistant and iron-insensitive. She proposed the main function of the enzyme system to be the metabolism of exogenous amines with potential toxicity. Later catecholamines were also

[31] Hare, M.L.C. (1928) Tyramine Oxidase. 1. A new enzyme system in liver. *Biochem. J.* **22**, 968-979.

reported to be metabolized by this new enzyme system.[32,33] In 1951 the name of this new enzyme system was changed to monoamine oxidase (MAO).[34]

MAO [monoamine; oxygen oxidoreductase (deaminating) (flavin containing) EC 1.4.3.4] is an outer membrane bound mitochondrial enzyme that catalyzes the oxidative deamination of endogenous amines. In 1968, Johnston discovered the presence of two forms of MAO. One form of the enyme (MAO-A) was inactivated by clorgyline (**15**) but not the other (MAO-B).[35] The presence of two forms of MAO was confirmed after the observation that (*R*)-deprenyl (**16**) inactivated only the B form.[36]

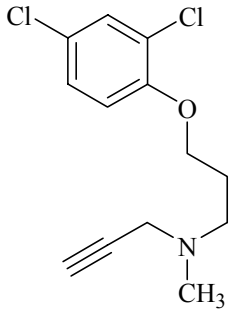

15

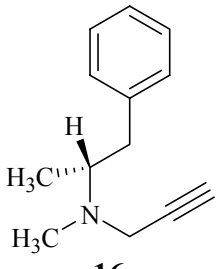

16

Biogenic amine substrates include the neurotransmitters serotonin [5-hydroxytryptamine (5-HT)] (**17**), dopamine (**18**) and norepinephrine (**19**). Serotonin and norepinepherine were shown to be MAO-A selective substrates and dopamine to be a mixed A and B substrate.[37] Benzylamine (**20**) and 2-phenylethylamine (**21**) are MAO-B selective substrates.[38]

---

[32]Blaschko, H., Richter, D., Schlossmann, H. (1937) The inactivation of adrenaline. *J. Physiol.* **90**, 1-19.
[33] Zeller, E.A. (1938) Uber den enzymatischen abbau von histamin und diaminen. *Helv. Chim. Acta* **21**, 881-890.
[34] Zeller, E. A. (1951) Oxidation of amines**.** *Enzymes* **2**, 536-58.
[35] Johnston, J.P. (1968) Some observations upon a new inhibitor of monoamine oxidase in brain tissue. *Biochem Pharmacol.* **17**, 1285-1297.
[36] Knoll, J., Magyar, K. (1972) Some puzzling pharmacological effects of monoamine oxidase inhibitors. *Adv. Biochem. Psychopharmacol.* **5**, 393-408.
[37] Fowler, C.J., Tipton, K.F. (1984) On the substrate specificity of the two forms of monoamine oxidase. *J. Pharm. Pharmacol.* **36**, 111-115.
[38] Neff, N.H., Yang, H.Y.T., Goridis, C. (1974) Degradation of transmitter amines by specific types of monoamine oxidases. *Biochem. Pharmacol.* **Suppl. 1**, 86-90.

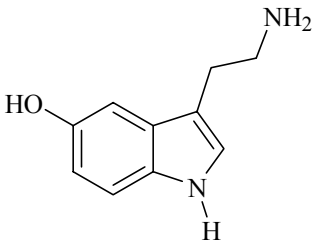

17

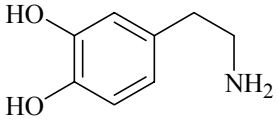

18

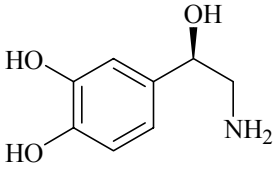

19

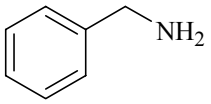

20

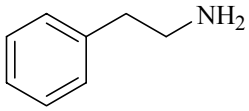

21

In 1988, cDNAs for human liver MAO-A and MAO-B were cloned[39] and in 1989 they were expressed in mammalian cells.[40] Amino acid sequence comparison revealed 70% identity between the two isoforms.[41] Both forms of the enzyme are widely distributed throughout the human body.[42] Both MAO-A and MAO-B are expressed in the human brain, liver[43] and intestine. In the placenta only the A form is present[44] whereas in the blood platelets and lymphocytes only MAO-B is expressed.[45]

Interestingly, MAO-A levels in new-born humans and rodents are almost at adult levels.[46] On the other hand, the postmortem studies of Fowler *et al.* demonstrated that brain MAO-B levels increase with age.[47,48,49]

---

[39] Bach, A.W., Lan, N.C., Johnson, D.L., Abell, C.W., Bembenek, M.E., Kwan, S-W., Seeburg, P.H., Shih, J.C. (1988) cDNA cloning of human liver monoamine oxides A and B: molecular basis of differences in enzymatic properties. *Proc. Natl. Acad. Sci. USA* **85**, 4934-4938.

[40] Lan, N.C., Chen, C.H., Shih, J.C. (1989) Expression of functional human monoamine oxidase A and B cDNAs in mammalian cells. *J. Neurochem*. **52**, 1652-1654.

[41] For a sequence comparison of human MAO-A and MAO-B from different species, see Appendix 1.

[42] O'Carroll, A.M., Anderson, M.C., Tobbia, I., Phillips, J.P., Tipton, K.F. (1989) Determination of the absolute concentrations of monoamine oxidase A and B in human tissues. *Biochem. Pharmacol*. **38**, 901-905.

[43] Denney, R.M., Fritz, R.R., Patel, N.T., Abell, C.W. (1982) Human liver MAO-A and MAO-B separated by imminoaffinity chromatography with MAO-B specific monoclonal antibody. *Science* **215**, 1400-1403.

[44] Weyler, W., Salach, J.I. (1985) Purification and properties of mitochondrial monoamine oxides type A from human placenta. *J. Biol. Chem*. **260**, 13199-13207.

[45] Weyler, W., Hsu, Y.P., Breakefield, X.O. (1990) Biochemistry and genetics of monoamine oxidase. *Pharmacol. Therapeut.* **47**, 391-417.

[46] Mahy, N., Andres, N., Andrade, C., Saura, J. (2000) Age-related changes of MAO-A and -B distribution in human and mouse brain. *Neurobiology* **8**, 47-54.

Investigations of MAO activity in different species have revealed greater similarities between the activity profiles of humans and rodents compared to humans and subhuman primates.[50,51]

1.2.1. Disease States Related to MAO

The relation between MAO and human behavior has been the subject of intense investigation in recent years. However, the first finding related to the link between MAOs and human behavior dates back to the 1950s. One of the side effects of iproniazid (**22**), an anti-tuberculosis drug, was recognized to be mood-elevation. Subsequently it was shown that **22** was an MAO inhibitor.[52] This observation led to the exploration of MAO inhibitors as anti-depressants.

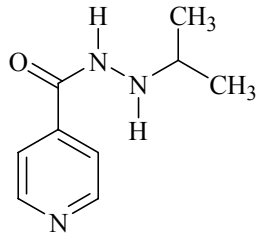

22

The first generation of MAO inhibitors were irreversible and non-selective, properties that caused severe side effects due to the interference with the metabolism of dietary amines[53] and the inhibition of the various subtypes of the cytochrome P450

---

[47] Fowler, C.J., Wiberg, A., Oreland, L., Marcusson, J., Winblad, B. (1980) The effect of age on the activity and molecular properties of human brain monoamine oxidase. *J. Neural Transm.* **49**, 1-20.
[48] Saura, J., Richards, J.G., Mahy, N. (1994) Differential age-related changes of MAO-A and MAO-B in mouse brain and peripheral organs. *Neurobiol. Aging* **15**, 399-408.
[49] Saura, J., Richards, J.G., Mahy, N. (1994) Age-related changes in MAO in Bl/C57 mouse tissues: a quantitative radioautographic study. *J. Neural. Transm.* **41**, 89-94.
[50] Squires, R.F. (1972) Multiple forms of monoamine oxidase in intact mitochondria as characterized by selective inhibitors and thermal stability: A comparison of eight mammalian species. *Adv. Biochem. Pharmacol.* **5**, 355-369.
[51] Inoue, H., Castagnoli, K., Cornelis, V.D.S., Mabic, S., Igarashi, K. Castagnoli, N., Jr. (1999) Species-dependent differences in monoamine oxidase A and B-catalyzed oxidation of various C4 substituted 1-methyl-4-phenyl-1,2,3,6-tetrahydropyridinyl derivatives. *J. Pharmacol. Exp. Ther.* **291**, 856-864.
[52] Pletscher, A. (1991) The discovery of antidepressants: a winding path. *Experientia* **47**, 4-8.
[53] Davies, B., Bannister, R., Sever, P. (1978) Pressor amines and monoamine-oxidsae inhibitors for treatment of postural hypotension in autonomic failure. Limitations and hazards. *Lancet* **1**, 172-175.

(cP450) family of enzymes.[54] Due to the side effects caused by the non-selective MAO inhibitors, efforts concentrated on developing selective and potent MAO-A inhibitors. These efforts led to the discovery of toloxatone [**23**, (K_i = 0.38 μM for MAO-A and 15 μM for MAO-B)][55] the first member in the "second generation" of MAO inhibitors to be used clinically as an antidepressant.[56,57] A more recent example is moclobemide [**24**, (K_i = 10 μM for MAO-A and 1.6 mM for MAO-B)][58] another reversible and selective MAO-A inhibitor with antidepressant properties.

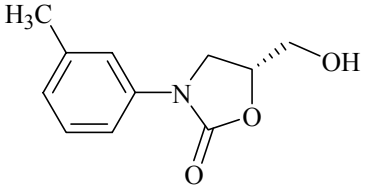

23

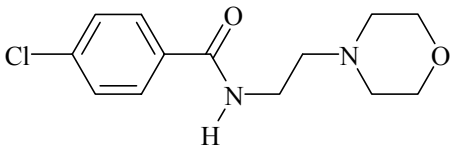

24

The inhibition of MAO-A is targeted for the treatment of depression whereas selective MAO-B inhibitors have been shown to be beneficial in symptomatic treatment of PD. The mechanism based, MAO-B selective inactivator (*R*)-deprenyl (**16**) is used in the treatment of early stage PD.[59] It was studied initially as an antidepressant in Hungary.[60] Despite the initial success of (*R*)-deprenyl, further studies involving large patient groups led to the conclusion that it did not have any long term benefits. Its use has been associated with an increased rate of mortality.[61]

---

[54] De Master, E.G., Summer, H.W., Kaplan, E., Shirota, F.N., Nagasaw, H.T. (1982) Pargyline-induced hepatotoxicity: possible mediation by the reactive metabolite, propiolaldehyde. *Toxicol. Appl. Pharmacol.* **65**, 390-401.

[55] Mai, A., Artico, M., Esposito, M., Ragno, R., Sbardella, G., Massa, S. (2003) Synthesis and biological evaluation of enantiomerically pure pyrrolyl-oxazolidinones as a new class of potent and selective monoamine oxidase type A inhibitors. *Il Farmaco* **58**, 231-241.

[56] Raynaud, G., Gouret, C. (1973) Activity of toloxatone, antidepressants, and various reserpine antagonists in 3 behavioral experiments in mice treated with nialamide. *Chim. Ther.* **3**, 328-330.

[57] Kan, J.P., Malone, A., Strolin-Bendetti, M. (1978) Monoamine oxidsae inhibitory properties of 5-hydroxymethyl-3-m-tolyloxazolidin-2-one (toloxatone). *J. Pharm. Pharmacol.* **30**, 190-192.

[58] Ulus, H.I., Maher, T.J., Wurtman, R.J. (2000) Characterization of phentermine and related compounds as monoamine oxidase (MAO) inhibitors. *Biochem. Pharmacol.* **59**, 1611-1621.

[59] Calne, D.B. (1993) Treatment of Parkinson's disease. *N. Engl. J. Med.* **14**, 1021-1027.

[60] Vargar, E., Tringer, L. (1967) Clinical trial of a new type promptly acting psychoenergic agent (phenyl-isopropyl-methylpropinyl-HCl, E-250) *Acta Med. Acad. Sci. Hung. Tomus* **23**, 289-295.

[61] Calne, D.B. (1995) Selegiline in Parkinson's disease-No neuroprotective effect: Increased mortality. *Br Med. J.* **311**, 1583-1584.

MAO levels are thought to correlate with several other disease states and further studies are being pursued in order to understand these correlations.[62] For example, low MAO-B activity in platelets is correlated with bipolar disorder, suicidal behavior and alcoholism.[63] In schizophrenic patients, blood platelet MAO-B activity was shown to be significantly reduced.[64] A positive correlation is reported between increased salivary MAO-A and B activity and stress.[65] Also, in knock-out mice lacking the MAO-A gene, enhanced aggressive behavior was observed.[66]

1.3. Nitric Oxide Synthase (NOS)

As mentioned above, the neuronal form of NOS is another enzyme that has been linked to PD. NOS catalyzes the conversion of *L*-arginine to *L*-citrulline forming the free radical NO which may cause oxidative damage in the brain.

Endothelial cells long were known to mediate the dilation of blood vessels via the production of some unknown substance which was named the endothelial-derived relaxation factor (EDRF).[67] In 1987, the research groups of Ignarro and Moncada independently identified EDRF as NO.[68,69] NO was named the molecule of the year by Science in 1992 and the Nobel Prize in medicine in 1998 was given to Robert R. Furchgott, Ferid Murad and Louis J. Ignarro for their contributions to nitric oxide research.

---

[62] Shih, J.C., Chen, K., Ridd, M.J. (1999) Monoamine oxidase: from genes to behavior. *Annu. Rev. Neurosci.* **22**, 197-217.
[63] Devor, E.J., Cloninger, C.R., Hoffman, P.L., Tabakoff, B. (1993) Association of monoamine oxidase (MAO) activity with alcoholism and alcoholic subjects. *Am. J. Med. Genet.* **48**, 209-213.
[64] Simpson, G.M., Shih, J.C., Chen, K., Flowers, C., Kumazawa, T., Spring, B. (1999) Schizophrenia, monoamine oxidase activity, and cigarette smoking. *Neuropsychopharmacology* **20**, 392-394.
[65] Doyle, A. ,Hucklebridge, F. Evans, P, Clow, A. (1996) Salivary monoamine oxidase A and B inhibitory activities correlate with stress. *Life. Sci*. **59**, 1357-1362.
[66] Cases, O., Seif, I., Gaspar, P., Chen, K., Pournin, S., Muller, U., Aguet, M., Babinet, C. (1995) Aggressive behavior and altered amounts of brain serotonin and norepinephrine in mice lacking MAO-A. *Science* **268**, 1763-1766.
[67] Furchgott, R.F., Zawadski, J.V. (1980) The obligatory role of the endothelial cells in the relaxation of arterial smooth muscle by acetylcholine. *Nature* **288**, 373-376.
[68] Ignarro, L.J. Byrns, R.E., Buga, G.M., Wooks, K.S. (1987) Endothelium-derived relaxing factor from pulmonary artery and vein possesses pharmacological and chemical properties that are identical to those for nitric oxide radical. *Circ. Res.* **61**, 866-879.
[69] Palmer, R.M., Ferrige, A.G., Moncada, S. (1987) Nitric oxide release accounts for the biological activity of endothelium derived relaxing factor. *Nature* **327**, 524-526.

Despite its possible involvement in neurodegenerative pathways, NO is a biologically important molecule with diverse functions throughout the body. It is a neurotransmitter and regulates blood pressure. In the immune system, NO acts as cytotoxic agent.[70]

Although it was known for 70 years that humans excrete more nitrate than can be accounted for by dietary intake,[71] the pathways leading to nitrate synthesis were not clear. In 1987, Marletta' s research group discovered that the source of nitrite and nitrate in the body was the amino acid *L*-arginine (**4**).[72] The source of the nitrate nitrogen was determined to be the guanidine nitrogen of *L*-arginine (via ^{15}N labeling experiments). [73] It was shown that *L*-arginine is converted to *L*-citrulline (**6**) and NO which is the precursor to nitrite and nitrate.[74] It was suggested that this unusual conversion had to be carried out by a specific monooxygenase-like enzyme.[75] In 1990, Bredt and Snyder achieved the purification of NOS from rat cerebellum.[76] Following the purification, the same research group reported the cloning of the cDNA and expression of NOS.[77]

There are three isoforms of NOS. The neuronal isoform (nNOS), present predominantly in the brain, and the endothelial isoform (eNOS), present in the endothelial cells, are constitutive enzymes that are activated by a calcium-calmodulin dependent pathway. The inducible form (iNOS) is found predominantly in macrophages and smooth muscle cells.[78] eNOS is known to be involved in blood pressure regulation [79] and its inhibition causes vasoconstriction leading to an increase in blood pressure and

---

[70] Kerwin, J.F., Lancaster, J.R., Feldman, P.L. (1995) Nitric oxide: A new paradigm for second messengers. *J. Med. Chem.* **38**, 4342-4362.
[71] Mitchell, H.H., Shonle, H.A., Grindley, H.S. (1916) The origin of the nitrates in the urine. *J. Biol. Chem.* **24**, 461-490.
[72] Iyengar, R., Stuehr, D.J., Marletta, M.A. (1987) Macrophage synthesis of nitrite, nitrate, and N-nitrosamines:precursors and role of the respiratory burst. *Proc. Natl. Acad. Sci. U.S.A.* **84**, 6369-6373.
[73] Reference 139 and Hibbs, J.B., Jr., Taintor, R.R., Vavrin, Z. (1987) Macrophage cytotoxicity: role for L-arginine deiminase and imino nitrogen oxidation to nitrite. *Science*, **235**, 473-476.
[74] Marletta, M.A., Yoon, P.S., Iyengar, R., Leaf, C.D., Wishnok, J.S. (1988) Macrophage oxidation to L-arginine to nitrite and nitrate:nitric oxide is an intermediate. *Biochemistry* **27**, 8706-8711.
[75] Marletta, M.A. (1988) Mammalian synthesis of nitrite, nitrate, nitric oxide and N-nitrosating agents. *Chem. Res. Toxicol.* **1**, 249-257.
[76] Bredt, D.S., Snyder, S.H. (1990) Isolation of nitric oxide synthetase, a calmodulin-requiring enzyme. *Proc. Acad. Natl. Sci. U.S.A*. **87**, 682-685.
[77] Bredt, D.S., Hwang, P.M., Glatt, C.E., Lowenstein, C., Reed, R.R., Snyder, S.H. (1991) Cloned and expressed nitric oxide synthase structurally resembles cythochrome P-450 reductase. *Nature*, **351**, 714-718.
[78] Snyder, S., Bredt, D.S. (1992) Biological roles of nitric oxide. *Sci. Am.* **166**, 28-35.
[79] Vane, J.R. (1994) The Croonian lecture, 1993: The endothelium:Maestro of the blood circulation. *Proc. R. Soc. Lond. B* **345**, 225-246.

decrease in blood flow to organs.[80] nNOS is responsible for the synthesis of NO in the brain where it is thought to act as a secondary messenger to activate neurotransmitters including glutamate, acetylcholine and histamine.[81] Since enhanced production of NO is thought to have a role in central nervous system injury,[82] nNOS inhibition has been investigated as a therapeutic approach to prevent neurodegeneration[83] and nNOS inhibitors have been evaluated as potential neuroprotective agents.[84] One such nNOS inhibitor is 7-nitroindazole (7-NI).[85] After the recognition of 7-NI as a novel, selective nNOS inhibitor *in vivo*, further studies revealed interesting and rather controversial information on its potential role in neuroprotection which eventually led us to undertake the design and synthesis of a "prodrug" of 7-NI. In the following section, the studies on the neuroprotective properties of 7-NI as well as its potential utility as a therapeutic agent in relation to its low aqueous solubility will be described.

1.4. 7-Nitroindazole (7-NI)

Efforts by Moore *et al.* led to the identification of 7-NI (**25**) as an nNOS inhibitor.[86] It was reported to have potent antinociceptive activity in the mouse with no effect on blood pressure. [87] Although *in vitro* IC_{50} values for nNOS and eNOS inhibition by 7-NI are very close (0.71 μM and 0.78 μM respectively), 7-NI was suggested to be an nNOS selective inhibitor *in vivo* due to the absence of cardiovascular effects expected to

---

[80] Southan, G.J., Szabo, C. (1996) Selective pharmacological inhibition of distinct nitric oxide synthase isoforms. *Biochem. Pharmacol.* **51**, 383-394.
[81] Bredt, D.S., Snyder, S.H. (1992) Nitric oxide, a novel neuronal messenger. *Neuron* **8**, 211-216.
[82] Dawson, V.L., Dawson, T.M., London, E.D., Bredt, D.S., Snyder, S.H. (1991) Nitric oxide mediates glutamate neurotoxicity in primary cortical cultures. *Proc. Natl. Acad. Sci. U.S.A.* **88**, 6368-6371.
[83] Beal, M.F. (1997) Therapeutic effects of nitric oxide synthase inhibition in neuronal injury *Neuroprotection in CNS Diseases* 131-145.
[84] Matthews, R.T., Yang, L., Beal, F.M. (1997) S-methylthiocitrulline, a neuronal nitrice oxide synthase inhibitor protects against malonate and MPTP neurotoxicity. *Exp. Neurol.* **143**, 282-286.
[85] Babbedge, R.C., Bland-Ward, P.A., Hart, S.L., Moore, P.K. (1993) Inhibition of rat cerebellar nitric oxide synthase by 7-nitroindazole and related substituted indazoles. *Br. J. Pharmacol.* **110**, 225-228.
[86] Moore, P.K., Bland-Ward, P.A. (1996) 7-nitroindazole: An inhibitor of nitric oxide synthase *Methods. In Enzymology* **268**, 393-399.
[87] Moore, P.K., Wallace, P., Gaffen, Z., Hart, S.L., Babbedge, R.C. (1993) 7-nitro indazole, an inhibitor of nitric oxide synthase, exhibits antinociceptive activity in the mouse without increasing blood pressure. *Br. J. Pharmacol.* **108**, 296-297.

be seen following eNOS inhibition. [88] Subsequently, Beal's research group reported that 7-NI protected against MPTP induced neurotoxicity in mice[89] and in baboons.[90]

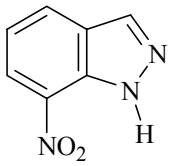

25

The mechanism or mechanisms responsible for the neuroprotective properties of 7-NI have been a controversial area of research. Since 7-NI did not inhibit the MAO-B catalyzed oxidation of benzylamine by mouse brain mitochondrial preparations, the neuroprotective mechanism was reported to be independent of MAO-B inhibition.[91] As part of their studies to characterize the 7-NI mediated protection against the toxicity of MPTP, Przedborski *et al.* compared the striatal levels of MPP^+ in MPTP-treated mice versus 7-NI injected and control mice and reported that the striatal MPP^+ levels were unaffected by neuroprotective doses of 7-NI.[92] This led the authors to conclude that the neuroprotective effect of 7-NI must be due to nNOS inhibition.

Since 7-NI is a planar, heterocylic compound, similar to many known MAO-B inhibitors,[93,94] its potential MAO-B inhibition properties were reinvestigated. Results of

---

[88] Moore, P.K., Wallace, P., Gaffen, Z., Hart, S.L., Babbedge, R.C. (1993) Characterization of the novel nitric oxide synthase inhibitor 7-nitro indazole and related indazoles: antinociceptive and cardiovascular effects. *Br. J. Pharmacol.* **110**, 219-224.

[89] Schulz, J.B., Matthew, R.T., Muqit, M.M., Browne, S.E., Beal, M.F. (1995) Inhibition of neuronal nitric oxide synthase by 7-nitroindazole protects against MPTP-induced neurotoxicity in mice. *J. Neurochem.* **64**, 936-939.

[90] Hantraye, P., Brouillet, E., Ferrante, R., Palfi, S., Dolan, R., Matthew, R.T., Beal, M.F. (1996) Inhibition of neuronal nitric oxide synthase prevents MPTP-induced parkinsonism in baboons. *Nature Med*. **2**, 1017-1021.

[91] Reference 89.

[92] Przedborski, S., Jackson-Lewis, V., Yokoyama, R., Shibata, T., Dawson, V.L., Dawson, T.M. (1996) Role of neuronal nitric oxide in 1-methyl-4-phenyl-1,2,3,6-tetrahydropyridine (MPTP)-induced dopaminergic neurotoxicity. *Proc. Natl. Acad. Sci. USA* **93**, 4565-4571.

[93]Kneubuehler, S., Thull, U., Altomare, C., Carta, V., Gaillard, P., Carrupt, P.A., Carotti, A., Testa, B. (1995) Inhibition of monoamine oxidase-B by 5H-indeno[1,2,-c]pyridazines. Biological activities, quantitative structure-activity relationships (QSARs) and 3D-QSARs. *J. Med. Chem.* **38**, 3974-3883.

[94] Lebreton, L., Curet, O., Gueddari, S., Mazouz, F., Bernard, S., Burstein, C., Milcent, R. (1995) Selective and potent monoamine oxidase type B inhibitors:2-substituted 5-aryltetrazole derivatives. *J. Med. Chem*. **38**, 4876-4792.

these studies demonstrated that 7-NI is indeed a competitive inhibitor of MAO-B (K_i = 4 μM for mouse brain mitochondrial MAO-B).[95] Related studies established that 7-NI protected against MPTP induced depletion of DA. Furthermore, 7-NI treatment led to a significant decrease in the striatal MPP^+ levels.[96] A non-selective NOS inhibitor, N^{γ}-nitro-*L*-arginine (**26**),[97] did not have any effect on MPTP-induced striatal ATP depletion in mice whereas 7-NI prevented the striatal ATP loss in the same animal model providing further evidence for the significance of MAO-B inhibition in neuroprotection by 7-NI.[98] These findings support a role for MAO-B inhibition in mediating the neuroprotective effects of 7-NI.

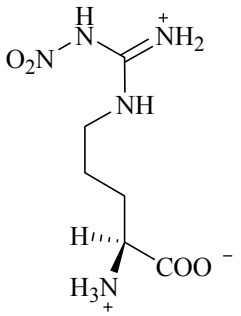

26

In a more recent study,[99] Tipton and O'Byrne have examined the effect of 7-NI on brain slices obtained from female Wistar rats exposed to MPP^+ only, 7-NI + MPP^+ and **26** + MPP^+. Compound **26** only partially prevented the decrease in DA levels at a concentration that was expected to inhibit all three isoforms of NOS. On the other hand

---

[95] Castagnoli, K., Palmer, S., Anderson, A., Bueters, T., Castagnoli, N. Jr. (1998) The neuronal nitric oxide synthase inhibitor 7-nitroindazole also inhibits the monoamine oxides-B-catalyzed oxidation of 1-methyl-4-phenyl-1,2,3,6-tetrahydropyridine. *Chem. Res. Toxicol.* **11**, 716-717.

[96] Di Monte, D.A., Royland, J.E., Anderson, A., Castagnoli, K., Castagnoli N. Jr., Langston, J.W. (1997) Inhibition of monoamine oxidase contributes to the protective effect of 7-nitroindazole against MPTP neurotoxicity. *J. Neurochem.* **69**, 1771-1773.

[97] Reif, D.W., McCreedy, S.A. (1995) N-nitro-L-arginine and N-monomethyl-L-arginine exhibit a different pattern of inactivation toward the three nitric oxide synthases. *Arch. Biochem. Biophys.* **320**, 170-176.

[98] Royland, J.E., Delfani, K., Langston, J.W., Janson, A.M., Di Monte, D.A. (1999) 7-nitroindazole prevents 1-methyl-4-phenyl-1,2,3,6-tetrahydropyridine-induced ATP loss in the mouse striatum. *Brain Res.* **839**, 41-48.

[99] O'Byrne, M.B., Tipton, K.F. (2002) Inhibition of the neuronal isoform of nitric oxide synthase significantly attenuates 1-methyl-4-phenylpyridinium (MPP^+) toxicity in vitro. *J. Neural. Transm*. **109**, 585-596.

treatment with 7-NI led to a significant increase in DA levels. The use of MPP^+ in place of MPTP in this study excludes the involvement of MAO-B in the conversion of MPTP to MPP^+ as a route to neurotoxicity. In other words, even though the neuroprotective effect of 7-NI may be due to MAO-B inhibition, this effect cannot be explained exclusively by the lack of MPP^+ formation. On the other hand a lesser degree of increase in DA levels observed with **26** compared to 7-NI suggests that there may be additional pathways through which these compounds exert their protective effects rather than nNOS inhibition.

According to these results, the neuroprotective effects of 7-NI may be due to MAO-B inhibition, nNOS inhibition, inhibition of both enzymes or still unknown pathways. The low solubility of 7-NI at pH 7.4 in physiological media limits the scope of *in vivo* studies that can be pursued to understand better the role of 7-NI in neuroprotection. Silva *et al.* reports that 7-NI is insoluble above a concentration of 100 μM in physiological media.[100] Therefore, these investigators formulated the monosodium salt of 7-NI to be used in *in vivo* studies. In this preparation, 7-NI, in a 3:1 mixture of methanol:chloroform, is treated with and 1 equivalent of NaOH. After evaporation of the solvents, the salt is reported to be soluble in a pH 7.5 buffer. This is likely to be a semi-stable solution only, since the pK_a of 7-NI is 12.5[101] and at pH 7.5, 7-NI is expected to be present mainly in neutral form in solution.

7-NI usually is administered intraperitoneally (i.p.) as a suspension in peanut oil. This is rather problematic due to the disadvantages associated with the use of a suspension rather than a solution and the large volume of peanut oil that must be used. In an attempt to characterize the pharmacokinetic properties of 7-NI, Bush *et al.* evaluated the use of solubility enhancers to develop an aqueous vehicle that will allow i.v. infusion.[102] They were able to dissolve 20 mg of 7-NI in 6 mL of an aqueous vehicle containing ethanol, polyethyleneglycol (PEG) 400 and Tween 80

---

[100] Silva, M.T., Rose, S., Hindmarsh, J.G., Aislaitner, G., Gorrod, J.W., Moore, P.K., Jenner, P., Marsden, C. (1994) Increased striatal dopamine efflux in vivo following inhibition of cerebral nitric oxide synthase by the novel monosodium salt of 7-nitroindazole. *Br. J. Pharmacol.* **114**, 257-258.

[101] Terrier, F., Millot, F., Schaal, R. (1969) Acidity of various indole derivatives in alkali metal methoxide solutions. *Bull. Soc. Chim. France* **9**, 3002-3007.

[102] Bush, M.A., Pollack, G.M. (2000) Pharmacokinetics and protein binding on the selective neuronal nitric oxide synthase inhibitor 7-nitroindazole. *Biopharmaceutics and Drug Disposition* **21**, 221-228.

(polyoxyethylenesorbitan monooleate). However, the results of the animal experiments showed that the clearance of 7-NI from the systemic circulation was inhibited by the vehicle.

1.5. Design and Synthesis of Potential "Prodrugs" of 7-NI and Structurally Related Indazoles

In an attempt to overcome the problems associated with the low solubility of 7-NI, we elected to pursue a "prodrug" approach utilizing a tetrahydropyridinyl (THP) moiety as the carrier. The THP moiety was to be attached to the N-1 nitrogen of the indazolyl ring of 7-NI to form the potential 1*H*-prodrug **27**. Alternatively the attachment could be via the N-2 nitrogen to form the potential 2*H*-prodrug **28**.

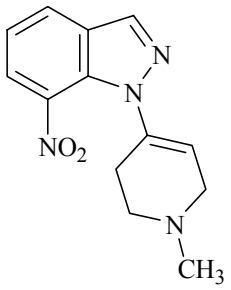

27

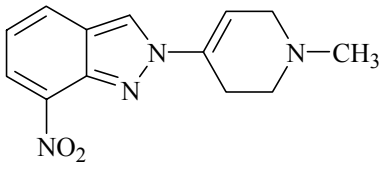

28

According to the proposed bioactivation pathway, compound **27** (or **28**) is expected to undergo a two electron ring α-carbon oxidation catalyzed by MAO or alternatively by cP450 to form the corresponding dihydropyridinium species **29**. Spontaneous hydration of **29** followed by C-N bond cleavage of the resulting intermediate **30** leads to the release of the 2*H*- tautomer of the active drug 7-NI (**31**) and the aminoenone **32**. The resulting 2*H*-isomer will tautomerize to the more stable 1*H*-tautomer **25** (Scheme 5).

Scheme 5. Proposed bioactivation pathway for the potential 7-NI prodrug resulting in the release of active compound 7-NI.

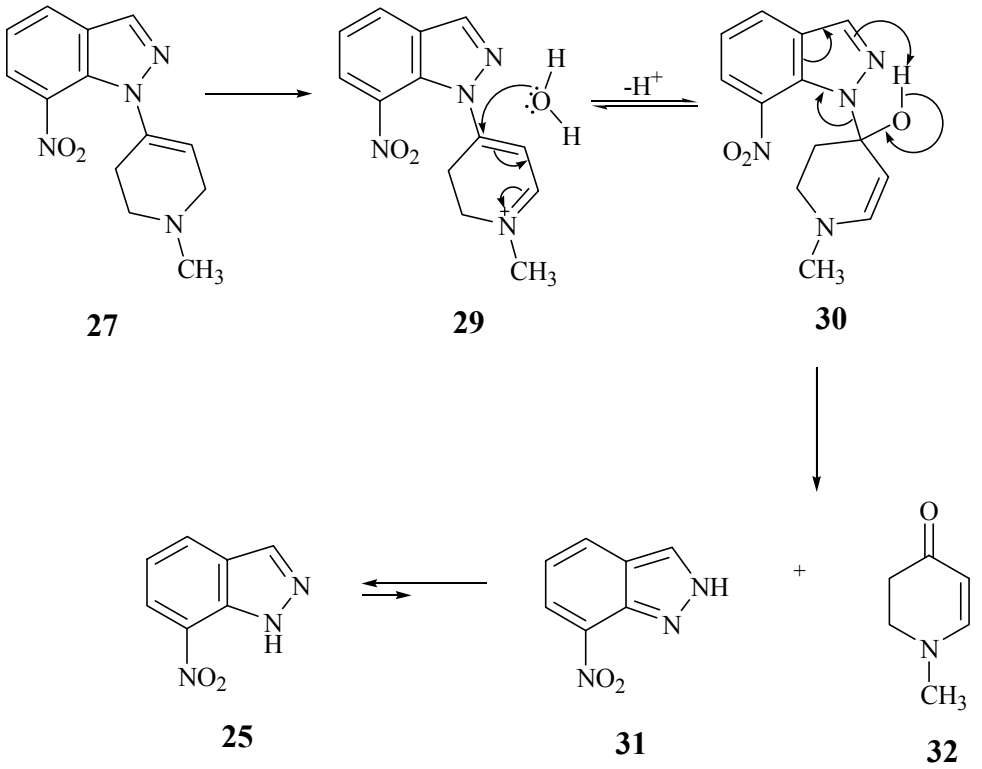

The proposed "prodrug" approach mimics partially the bioactivation pathway by which MPTP is converted in the brain to neurotoxin MPP^+ (Scheme 1). Therefore, in addition to overcoming the solubility problem, it is possible that the approach would target the central nervous system where MAO-B activity is high.

The utility of this approach has been explored earlier with a "prodrug" of (*R*)-nordeprenyl (**33**), an effective and selective inactivator of MAO-B that is equipotent with (*R*)-deprenyl (**16**).[103] In this study, a carbamate linkage was utilized to overcome the hydrolytic instability of the enamine functionality that results from the direct attachment of the THP carrier. The prodrug **34** of (*R*)-nordeprenyl was shown to result in the release of the active compound *in vivo*. The hydration of the dihydropyridinium species **35** is followed by the C-N bond cleavage of the resulting intermediate **36**. In this case, the

[103] Flaherty, P., Castagnoli, K., Wang, Y.W., Castagnoli, N., Jr. (1996) Synthesis and selective monoamine oxidase B inhibiting properties of 1-methyl-1,2,3,6-tetrahydropyrid-4-yl carbamate derivatives: Potential prodrugs of (R)- and (S)-nordeprenyl. *J. Med. Chem.* **39**, 4756-4761.

product of the cleavage, the carbamic acid derivative **37**, undergoes decarboxylation to release (*R*)-nordeprenyl (**33**) as shown in Scheme 6.

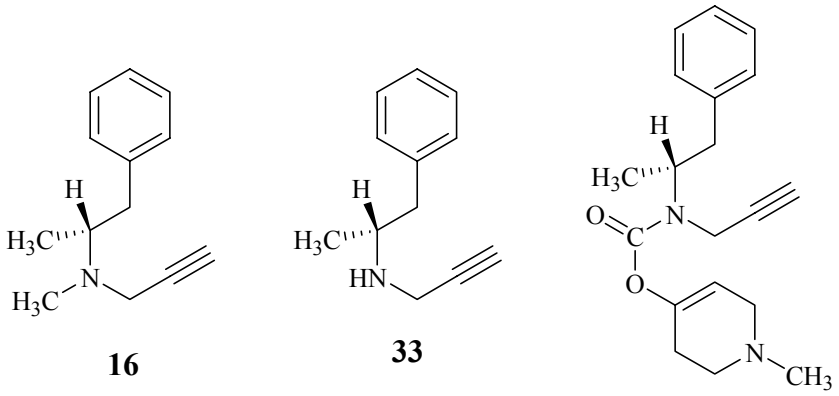

Scheme 6. Bioactivation pathway for the prodrug of (*R*)-nordeprenyl (34) resulting in the release of (*R*)-nordeprenyl (33).

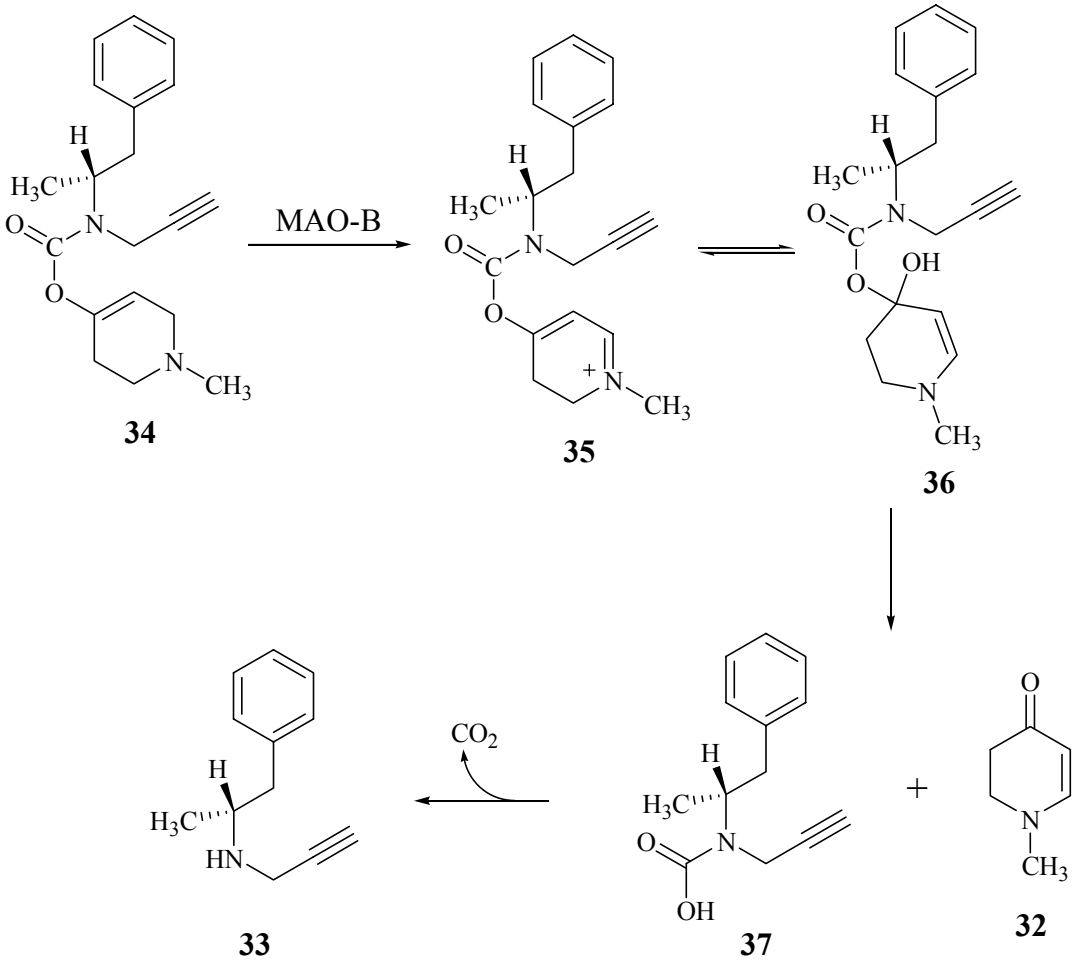

Another interesting observation that supports the feasibility of the "prodrug" approach is related to the benzimidazolyltetrahydropyridinyl species **38**. The MAO-B substrate properties of compound **38** have been evaluated and the metabolites analyzed by HPLC-DA.[104] In addition to the expected pyridinium species **40**, the presence of benzimidazole (**41**) was observed. This observation suggests that the dihydropyridinium species **39**, formed by the two electron oxidation of **38**, undergoes hydration followed by cleavage. Further oxidation of **39** yields the pyridinium species **40** as shown in Scheme 7.

Scheme 7. The formation of pyridinium species 40 and the parent benzimidazole (41) as a result of *in vitro* MAO-B metabolism of prodrug 38.

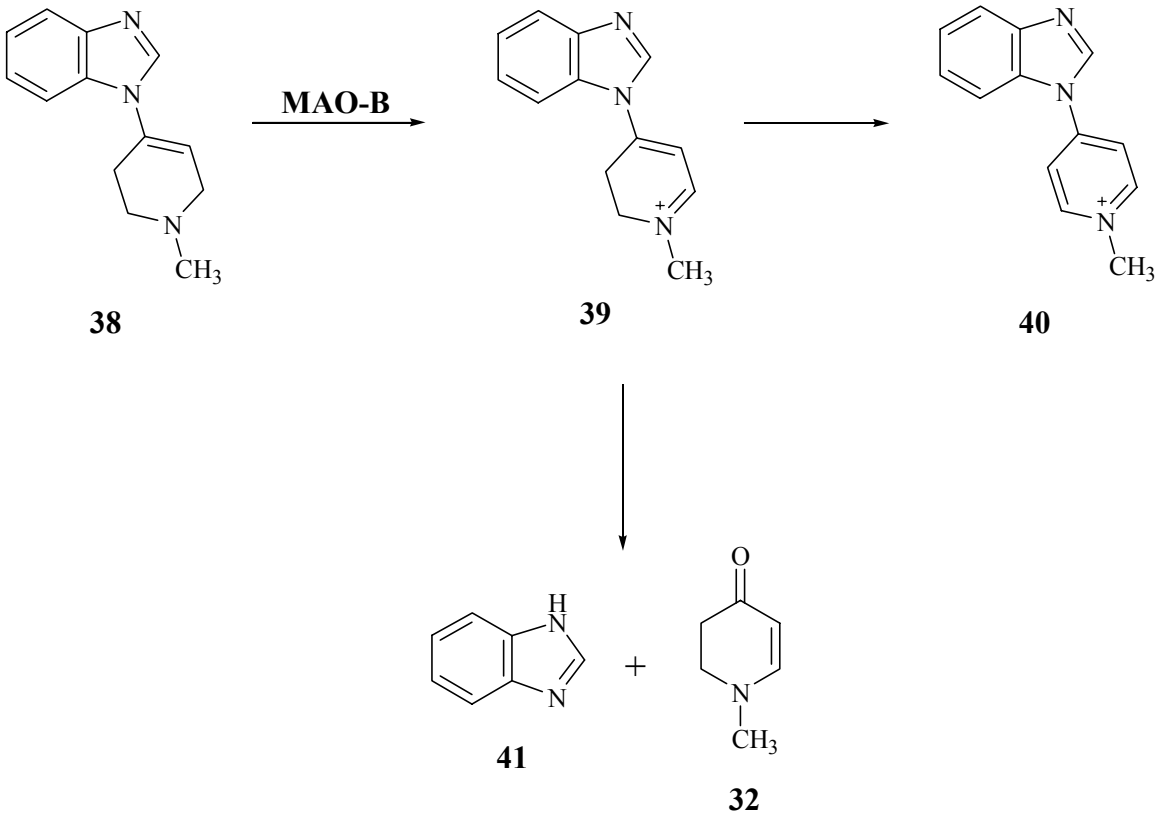

[104] Nimkar, S.K., Mabic, S., Anderson, A.H., Palmer, S.L., Graham, T.H., de Jonge, M., Hazelwood, L., Hislop, S.J., Castagnoli, N., Jr. (1999) Studies on the monoamine oxidase-B-catalyzed biotransformation of 4-azaaryl-1-methyl-1,2,3,6-tetrahydropyridine derivatives. *J. Med. Chem.* **42**, 1828-1835.

Encouraged by these results in support of the feasibility of the "prodrug" approach, we undertook the syntheses of potential prodrugs of 7-NI.[105] In this study we also included the regioisomers 5- and 6-nitroindazoles [5-NI (**42**) and 6-NI (**43**)]. These two molecules have been reported to possess slightly better MAO inhibition properties than 7-NI. Their nNOS inhibitory properties, however, differ significantly from those of 7-NI as shown in Table 1.[98,99] Due to these differences in inhibitory properties, investigation of neuroprotective potential of 5- and 6-NI may reveal important information of the contribution of MAO-B and/or nNOS inhibition in neuroprotection.

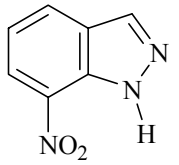

25

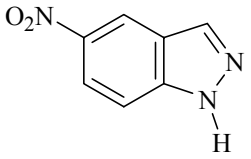

42

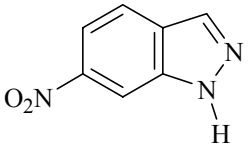

43

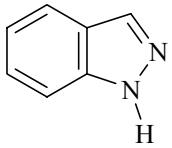

44

Table 1. MAO and nNOS inhibitor properties of indazole derivatives.

	Inhibitory Activity - IC_{50} (μM)		
	nNOS[106]	**MAO-A**[107]	**MAO-B**[103]
Indazole (**44**)	177.0	>100	72
7-NI (**25**)	0.9	70	41
5-NI (**42**)	47.3	44	3.3
6-NI (**43**)	31.6	46	2.8

A brief review of our previously reported[108] synthetic studies on nitroindazoles is included as part of this literature review. Synthetic approaches to these types of prodrugs were attempted via the nucleophilic aromatic substitution reaction of 4-chloro-1-methylpyridinium iodide (**54**) and the nitroindazoles to give the corresponding

[105]The results are reported in Reference 1 in detail. Here, only a summary will be included as an introduction to our studies following the completion of the M.S. degree.
[106] Babbedge, R.C., Bland-Ward, P.A., Hart, S.L., Moore, P.K. (1993) Inhibition of rat cerebellar nitric oxide synthase by 7-nitroindazole and related substituted indazoles. *Br. J. Pharmacol.* **110**, 225-228.
[107] Grandi, T., Sparatore, F., Gnerre, C., Crivori, P., Carrupt, P.-A., Testa, B. (1999) Monoamine oxidase inhibitory properties of some benzazoles: Structure-; Activity relationships. *AAPS Pharmsci.* **1**, 1-4.
[108] Reference 1.

indazolylpyridinium adducts which, in turn, would be reduced to the desired tetrahydropyridinyl prodrugs as shown in Scheme 8.

Scheme 8. Retrosynthetic approach to the prodrugs of nitroindazoles.

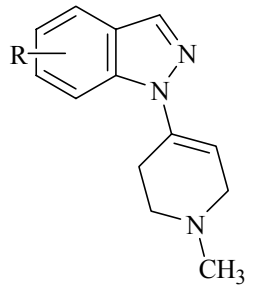

45: R = 5-NO_2
46: R = 6-NO_2
47: R = 7-NO_2

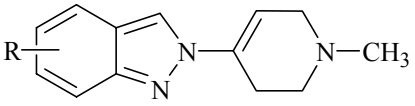

47: R = 5-NO_2
48: R = 6-NO_2
28: R = 7-NO_2

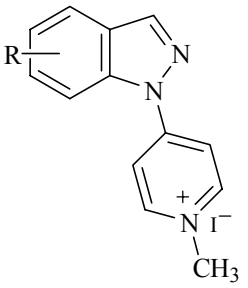

49: R = 5-NO_2
50: R = 6-NO_2
51: R = 7-NO_2

and/or

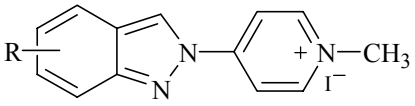

52: R = 5-NO_2
53: R = 6-NO_2
54: R = 7-NO_2

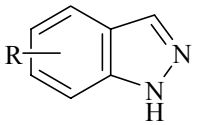

42: R = 5-NO_2
43: R = 6-NO_2
25: R = 7-NO_2

+

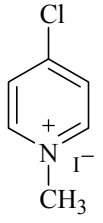

55

According to an earlier report,[109] the nucleophilic aromatic substitution reaction between 7-NI and **55** in the presence of the sterically hindered base 2,2,6,6-tetramethylpiperidine [TMP (**56**)] in refluxing N,N-dimethylformamide (DMF) resulted in the formation of a single product in poor yield as shown in Scheme 9. The structure of this product had been assigned tentatively to 4-(7-nitroindazol-2-yl)pyridine (**57**).

Scheme 9. Reported formation of 4-(7-nitroindazol-2-yl)pyridine (57) via the reaction of 7-NI and with 55 in the presence of base.

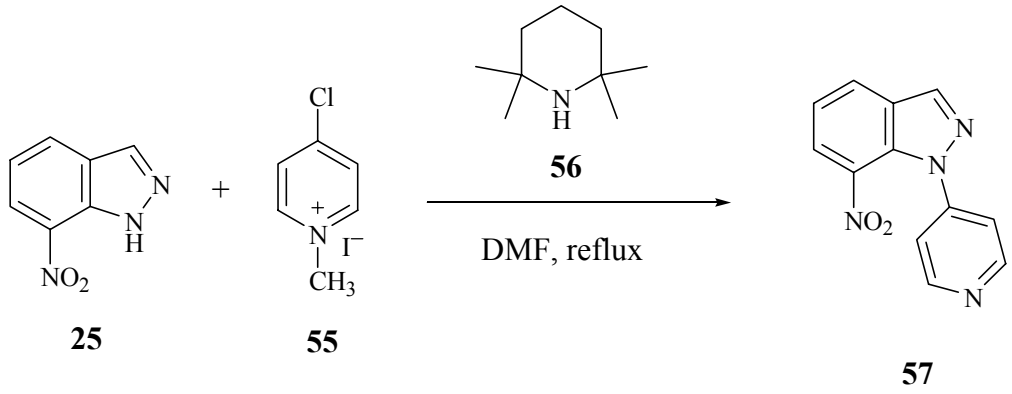

We repeated the reaction shown in Scheme 9 and an ethyl acetate extract of the reaction mixture was analyzed by GC-MS. The total ion current (TIC) tracing was complex and there were two peaks present corresponding to the m/z of the expected 7-nitroindazolylpyridine products in a ratio of approximately 5:1. The yield of the reaction was very low making the pathway shown in Scheme 9 unfeasible for the syntheses of the desired 7-nitroindazolylpyridines. Nevertheless, we were able to isolate enough material for GC-MS and NMR comparisons of the two isomeric products which allowed us to assign unambiguously the structure of the major product as the 2*H*-isomer **58** and the minor product as the 1*H*-isomer **57**.[110] We have concluded that the previous tentative assignment, therefore, was incorrect. The formation of compounds **57** and **58** instead of the expected pyridinium species **51** and **54** was rationalized by an in situ demethylation reaction at high temperatures as shown in Scheme 10.

---

[109] Unpublished results carried out by Millie de Jonge in the research group of Professor Neal Castagnoli, Jr. at Harvey W. Peters Center, Chemistry Department, VPI&SU.
[110] For the details of the assignment procedure see Reference 1, pages 53-69.

Scheme 10. Thermal demethylation of the pyridinium species 51 and 54 in the reaction mixture to form the corresponding pyridinyl species 57 and 58.

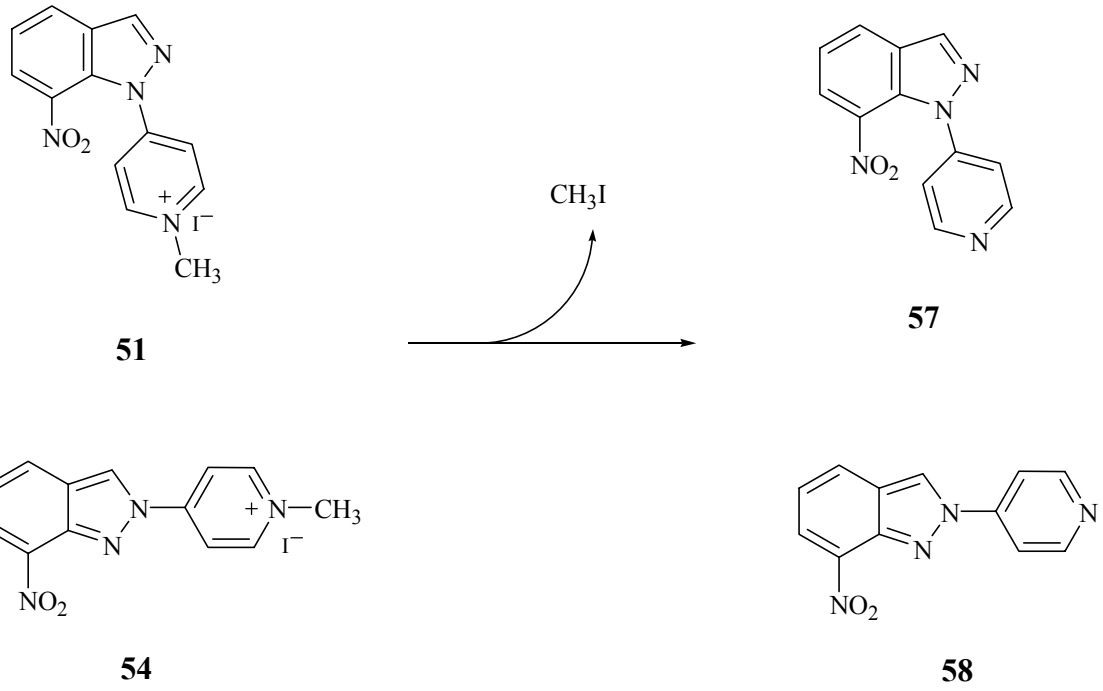

51 **57**

54 **58**

The presumed requirement of TMP in the reaction was based on the anticipated involvement of the 7-nitroindazolyl anion (**59**) in the initial nucleophilic aromatic substitution reaction. In an attempt to confirm the role of TMP as a base, we monitored the UV chromophore of 7-NI in the absence of base and in the presence of excess TMP or excess NaOH. In the presence of NaOH, a shift to higher wavelengths (from λ_{max} = 370 nm to λ_{max} = 460 nm) was observed consistent with the formation of 7-nitroindazolyl anion whereas addition of TMP did not result in any significant shift in the UV spectrum. However, when the reaction shown in Scheme 9 was attempted in the absence of TMP no product formation was observed even at elevated temperatures. This led to the conclusion that only a small amount of the 7-nitroindazolyl anion is required to catalyze the reaction.[111] It is important to note that the delocalized 7-nitroindazolyl anion formed after the deprotonation of 7-NI constitutes an ambident nucleophile as shown in Scheme 11.

[111] Reference 1, pages 70-72.

Scheme 11. Deprotonation of 7-NI leads to the formation of ambident nucleophile 59.

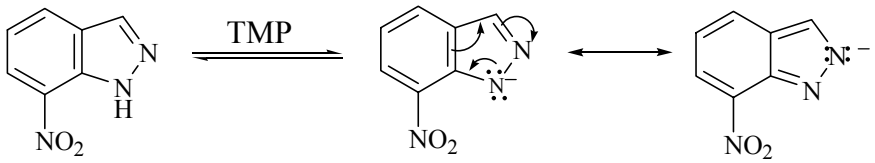

25 **59a** **59b**

Due to the ambident nature of the nitroindazolyl anion, both the N-1 and N-2 nitrogen atoms can react with the electrophilic pyridinium species **55** which, in turn, can lead to the formation of both the 1*H*- and the 2*H*-nitroindazolylpyridinium species **51** and **54** as shown in Scheme 12. However, the formation of the more stable benzenoid 1*H*-isomer **51** is expected to be favored over the less stable 2*H*-isomer with the quinoid structure.[112]

Scheme 12. Reaction of the 7-nitroindazolyl anion with 55 to form two possible isomeric 7-nitroindazolylpyridiniums 51 and 54.

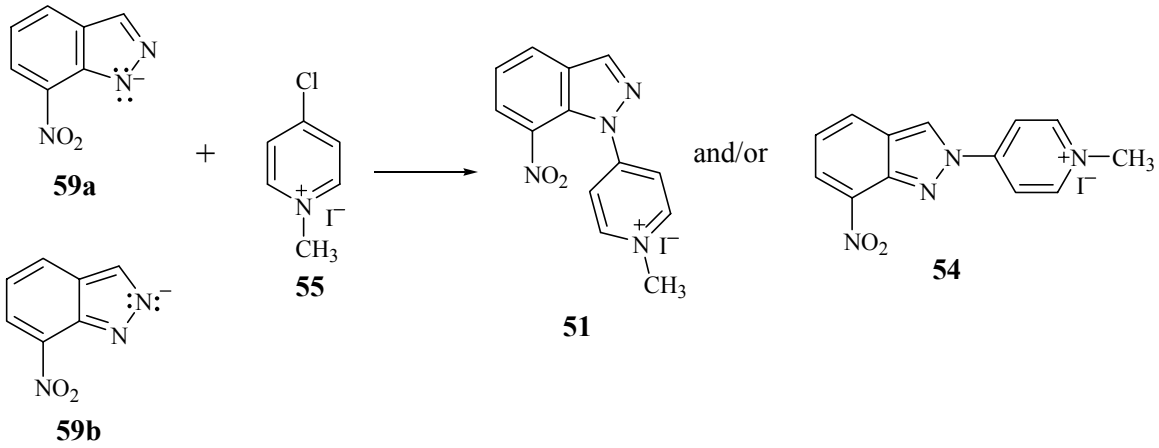

We monitored the progress of the reaction shown in Scheme 9 at various temperatures via GC-MS. However, the GC-MS TIC tracings obtained were complex and

[112] See pages 32-35 below for a detailed discussion of relative stabilities of indazole tautomers.

were not conclusive with respect to the fate of the reaction.[113] Therefore we decided to monitor the reaction progress using HPLC-DA. HPLC-DA would allow us also to distinguish between the pyridinium species **51** and **54** and pyridinyl species **57** and **58**. This was not possible with GC-MS since the thermal demethylation reaction shown in Scheme 10 will take place in the injection port as well.

When the reaction between 7-NI and **55** in the presence of TMP was carried out in DMF at room temperature, HPLC-DA tracings showed the formation of a single product. Subsequently, the product, which crystallized out of the reaction mixture, was isolated in 58 % yield and identified as the 2*H*- isomer **54**.[114] We rationalized the exclusive formation of the 2*H*- isomer by the steric hindrance caused by the nitro group at the C-7 position which causes the attack by N-1 to be unfavorable. The 2*H*-7-nitroindazolylpyridinium species **54** was reduced to the corresponding THP compound **28** in 74 % yield.

Although the formation of **54** in the presence of TMP was shown to take place readily at room temperature, GC-MS monitoring of the reaction had indicated that the product was forming only at elevated temperatures. In an attempt to clarify the controversy, we analyzed the pyridinium product **54** by GC-MS. The TIC spectrum showed that **54** decomposed under GC-MS conditions to yield 7-NI.[115] Due to the decomposition of **54**, GC-MS analysis of the room temperature reaction mixture failed to show product formation. However, as the reaction temperature was increased, the demethylation of the pyridinium product **54** was taking place in the reaction mixture to form **58** which was stable under GC-MS conditions. These results led to the incorrect conclusion that product formation occurred only at high temperatures. The advantage of HPLC-DA monitoring over the GC-MS was made clear by these outcomes.

After obtaining the potential 2*H*- "prodrug" of 7-NI, we applied the same methodology to the syntheses of the potential "prodrugs" of 5- and 6-NI. When 5-NI and 6-NI were treated with **55**, a single isomeric product again was detected by HPLC-DA. This time, however, the products were shown to be the 1*H*-isomers **49** (86% yield) and

---

[113] For the results of GC-MS monitoring of the reaction see Reference 1, pages 72-75.
[114] For the identification method see Reference 1, page 79.
[115] For a detailed account of the studies on the thermal stability of **54**, see Reference 1, pages 80-85.

50 (83% yield). Unlike 7-NI, N-1 attack is not hindered in 5- and 6-NI. Therefore, the reaction proceeds to form exclusively the 1*H*-isomers which are more stable than the corresponding 2*H*-isomers due to the presence of the benzenoid structure. These products were reduced readily with $NaBH_4$ to the corresponding "prodrugs" **93** (92% yield) and **94** (96% yield).

At this point, it was possible to obtain only the 2*H*- "prodrug" of 7-NI and only the 1*H*- "prodrugs" of 5- and 6-NI. This was a potential limitation for anticipated biological studies where the evaluation of MAO-B and MAO-A substrate properties of both isomeric "prodrugs" was desired. Therefore, we decided to undertake a detailed investigation of the nucleophilic aromatic substitution reaction of **55** with indazoles. In this study, we chose the parent indazole as a model compound to understand better the effect of the nitro group on the regiochemistry of the reaction. Before reporting our results on the reaction between indazole and **55**, a brief review on the characteristics of indazoles will be given.

1.6. Indazoles

Indazole, first defined by Emil Fischer as a "pyrazole ring condensed with the benzene ring", has been studied extensively due to its interesting chemical and biological properties. A SciFinder search on indazole results in more than 3000 hits.

1.6.1. History

In 1880 Emil Fischer reported that heating *o*-hydrazinobenzoic acid (**60**) results in the formation of **61** which was later named as indazolone (Scheme 13).[116]

[116] Fischer, E. (1880) *Ber.* **13**, 679.

Scheme 13. First reported synthesis of indazolone (61)

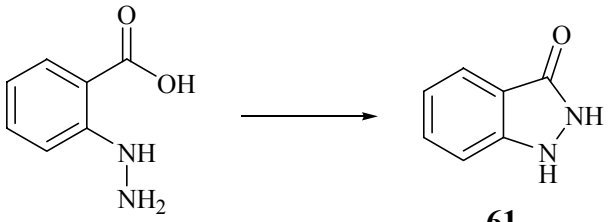

60 **61**

Since indazolone can be regarded as the anhydride of **60**, Emil Fischer and Kuzel attempted to apply the same strategy to obtain the anydride of *o*-hydrazinocinnamic acid (**62**). Among other products, they isolated a molecule that did not contain any oxygen. Upon further analysis the product was assigned the structure **44** (Scheme 14). According to Fischer and Kuzel, this was a transformation which was "remarkable in the highest degree" and they named the molecule indazole, by analogy with the name indole.[117]

Scheme 14. First reported synthesis of indazole (44).

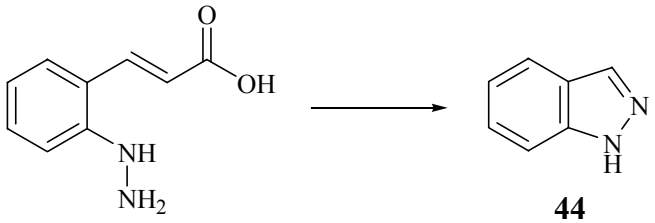

62 **44**

Most of the earlier studies on indazole have been carried out by Karl von Auwers, mainly between 1920 and 1930. Some of his work as well as more recent studies will be reviewed in the following sections.

[117] Fischer, E., Kuzel, H. (1883) *Ann.* **221**, 261.

1.6.2. Tautomerism of Indazole

1.6.2.1. Annular Tautomerism

Tautomerism in heterocyclic systems has been studied in considerable detail. In 2000, Elguero *et al.* published the "Decalogue of tautomerism".[118] The second item of the Decalogue states "Do not ignore a tautomer even if it is a minor one". It also is noted that "tautomerism and aromaticity are intimately linked" and that "an understanding of tautomerism is vital for understanding chemical reactivity". These statements clearly show how critical the issue of tautomerism is. During our studies on indazole derivatives, we repeatedly recognized the importance of this advice.

As Von Auwers first observed, indazole may exist in two forms as shown in Scheme 15.[119] These two forms result from the movement of the labile proton between the two nitrogen atoms, a process decribed as prototropic annular tautomerism.[120] Annular tautomerism has been more difficult to study than other types of prototropic tautomerism due to the fast proton transfer rate between the annular atoms.

Scheme 15. Annular prototropic tautomerism of indazole.

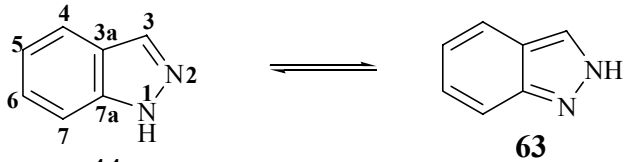

44 **63**

Von Auwers had shown qualitatively that the unsubstituted indazole exists predominantly as the 1*H*-tautomer (**44**) based on results from molecular refractivity studies.[121] This was supported by the finding that the UV and Raman spectra of unsubstituted indazole were similar to the spectra obtained for 1-substituted indazoles but

---

[118] Elguero, J., Katritzky, A.R., Denisko, O.V. (2000) Protropic tautomerism of heterocycles: Heteroaromatic tautomerism-general overview and methodology. *Advances in Heterocyclic Chemistry* **76**, 1-84.
[119] Von Auwers, K., Von Meyenburg, ?. (1891) *Ber.* **24**, 2370-
[120] Elguero, J., Marzin, C., Katritzky, A.R., Linda, P. (1976) Preface *Adv. Heterocycl. Chem.*, Suppl. 1, 2-4.
[121] Von Auwers, K. (1937) Structure of indazoles. *Liebig's Ann. Chem*. **527**, 291-298.

different than the spectra of 2-substituted indazoles.[122,123] Comparison of ^{1}H[124] and ^{14}N[125] NMR spectra of indazole with 1-methyl and 2-methylindazoles as well as more comprehensive ^{13}C and ^{15}N NMR studies reported recently[126,127] provide further evidence for the 1*H*-tautomer. X-ray crystallography studies show that indazole crystallizes as the 1*H*- desmotrope.[128,129]

Basicity measurement is another method that has been used to demonstrate the predominance of the 1*H*-tautomer.[130] In this approach, experimental pK_a values for indazole, 1-methyl and 2-methylindazoles were determined and, with the aid of computational methods, K (defined as [**44**]/[**63**]) for the equilibrium shown in Scheme 15) was estimated to be 51.4. Tautomerism of indazole has been studied also in the gas phase using mass spectrometry,[131] photoelectron,[132] microwave,[133] and IR

---

[122] Fries, K., Fabel, K.., Eckhardt, H. (1942) Bicyclic compounds and their comparison with naphthalene. VI. Indazole series. *Ann.* **550**, 31-49.

[123] Kohlrausch, K.W.F., Seka, R. (1940) Raman effect and constitution problems. XVI. 1- and 2-methylated benzotriazole and indazole. *Ber*. **73B**, 162-166.

[124] Elguero, J., Fruchier, A., Jacquier, R. (1966) The azole series. V. Nuclear magnetic resonance study of indazoles. *Bull. Soc, Chim. Fr.* 2075-2084.

[125] Witanowski, M., Stefaniak, L., Januszewski, H., Grabowski, Z. (1972) Nitrogen-14 nuclear magnetic resonance of azoles and their benzo derivatives. *Tetrahedron* **28**, 637-653.

[126] Elguero, J, Fruchier, A., Tjiou, E.M., Trofimenko, S. (1995) ^{13}C NMR of indazoles. *Chemistry of Heterocyclic Compounds* **31**, 1006-1026.

[127] Claramunt, R.M., Sanz, D., Lopez, C., Jimenz, J.A., Jimeno, M.L., Elguero, J., Fruchier, A. (1997) Substituent effect on the ^{15}N NMR parameters of azoles. *Magn. Reson. Chem.* **35**, 35-75.

[128] Escande, E., Lapasset, R., Faure, R., Vincent, E.-J., Elguero, J. (1974) Molecular structure and fundamental properties of the benzazoles indazole, benzimidazole and benzotriazole. *Tetrahedron* **30**, 2903- 2909.

[129] Desmotropy is defined as "observation of crytallization of a compound in two different tautomers" in Garcia, M.A., Lopez, C., Claramunt, R.M., Kenz, A., Pierrot, M., Elguero, J. (2002) Polymorphism vs. Desmotropy: The cases of 3-phenyl- and 5-phenyl-1*H*-pyrazoles and 3-phenyl-1*H*-indazole Helv. Chim. Acta 85, 2763-2776.

[130] Catalan, J., del Valle, J.C., Claramunt, R.M., Boyer, G., Laynez, J., Gomez, J., Jimenez, P., Tomas, F., Elguero, J. (1994) Acidity and basicity of indazole and its N-methyl derivatives in the ground and in the excited state. *J. Phys. Chem.* **98**, 10606-10612.

[131] Maquestiau, A., Van Heverbeke, Y., Flemming, R., Pardo, M.C.P., Elguero, J. (1975) Fragmentation of azoles under electron impact. *Org. Mass. Spectrom.* **10**, 558-560.

[132] Palmer, M.H., Kennedy, S.M.F. (1978) The electronic structure of aromatic molecules: ab initio molecular orbital studies and photoelectron spectra for the aza-derivatives of indole, benzofuran, benzothiopene. *J. Mol. Struct*. **43**, 33-48 and 203-220.

[133] Velino, B., Cane, E., Trombetti, A., Corbelli, G., Zerbetto, F., Caminati, W. (1992) Microwave spectrum and ab initio calculations of indazole. *J. Mol. Spectrosc*. **155**, 1-10.

spectroscopy.[134] In all cases, the it was concluded that the major tautomer of indazole was the 1*H*- tautomer **44**.

The structure determination of 2-substituted indazoles has been more controversial. Initially the tricyclic structure **64** was suggested due to the evidence for the presence of a benzene ring based on the reactivity of 2-substituted indazoles in electrophilic aromatic substitution reactions and molecular refractivity measurements.[135,136] However, a tricyclic formula creates a stereogenic center at C-3 and efforts to resolve putative indazole-3-carboxylic acid (**65**) were unsuccessful. Eventually, von Auwers proposed the quinoid structure **66**.

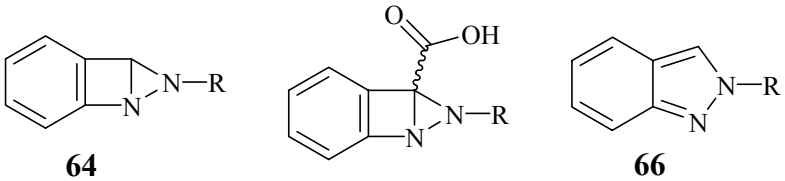

64 **65** **66**

Another important observation reported by von Auwers is related to the structure of 3-phenylindazole. When 3-phenylindazole, which has a melting point of 107-108 ^{o}C, is heated slightly above its melting point and allowed to resolidify, it forms crystals with a melting point of 115-116 ^{o}C.[137] Acetylation of both compounds (low melting and high melting) results in the formation of the same product which is converted to the low melting 3-phenylindazole upon hydrolysis. Von Auwers had interpreted these results as 3-phenylindazole existing in the solid as two forms, **67** and **68**, differing in the location of the imino hydrogen.

---

[134] Cane, E., Palmieri, P., Tarroni, R., Trombetti, A. (1993) Gas-phase infrared spectrum of indazole. Scaled quantum mechanical force field and complete spectrum assignment. *J. Chem. Soc. Faraday Trans.* **89**, 4005-4011.

[135]Von Auwers, K., Duesberg, M. (1920) Structural and spatial isomerism of indazole derivatives and the constitution of indaoles. *Ber.* **53B**, 1179-1210.

[136] Von Auweres, K., Schaich, W. (1921) N-alkyl derivatives and N-carboxylic esters of indazaole. *Ber.* **54B**, 1738-1770.

[137] Von Auwers, K., Huttenes, K. (1922) 3-phenylindazole and 2-hydroxy-3-phenylindazole. *Ber.* **55B**, 1112-1138.

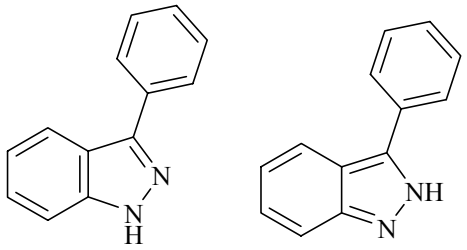

67 **68**

In 1950, Lindwall and Rousseau compared the UV spectra of various 3-substituted indazoles with 1,3- and 2,3-disubstituted indazoles.[138] The UV spectra of 3-substituted indazoles were similar to 1,3-disubstituted indazoles but different from 2,3-disubstituted indazoles. This finding led the authors to conclude that 3-phenylindazole should possess the benzenoid form **67** rather than the quinoid form **68**.

Recently, 80 years after Karl von Auwers' first paper on the subject,[139] Elguero *et al.* concluded that crystallization of 3-phenylindazole in two forms represents polymorphism rather than desmotropy.[140] In other words, both forms have the same structure and connectivity as **67** but form crystals in two different habits (one as long needles the other one as cube shaped crystals) rather than two different tautomers (desmotropy) as von Auwers had previously suggested. The authors attributed this to the rather high energy difference between the two tautomers (tautomer **67** being more stable than tautomer **68** by about 4.4 kcal/mol). The reasons for this difference in stability will be discussed in detail.

1.6.2.2. Relative Stabilities of 1*H*- and 2*H*-Indazoles

The stability of indazole tautomers has been extensively studied using various computational methods. Although the 1*H*- tautomer was shown to be more stable than the 2*H*- tautomer in all of these studies, the energy differences between the two tautomers in the gas phase reported in the literature vary between 12.9 kcal/mol and 8 kcal/mol,

---

[138] Rousseau, V., Lindwall, H.G. (1950) Structure and ultraviolet absroption spectra of indazole, 3-substituted indazole and some of their derivatives. *J. Am. Chem. Soc.* **72**, 3047-3051.

[139] Elguero *et al.* acknowledges Karl von Auwers in their paper "… we feel that present research work is posthumous homage to the memory of the great German chemist, Karl von Auwers, who was the most prominent figure in the pyrazole and indazole chemistry in the last century".

[140] Garcia, M. A., Lopez, C., Claramunt, R. M., Kenz, A., Pierrot, M., Elguero, J. (2002) Polymorphism vs. desmotropy: The cases of 3-phenyl and 5-phenyl 1*H*-pyrazoles and 3-phenyl-1*H*-indazole. *Helvetica Chemica Acta*, **85**, 2763-2776.

depending on the method of calculation. The *ab initio* calculations at MP2/6-31G** level carried out by Catalan *et al*. show that the 1*H*-tautomer is more stable than the 2*H*-tautomer by 4.1 kcal/mol (ΔG^{o}_{298}).[141] At this level of calculation, experimental microwave rotational constants were reproduced accurately which supports the reliability of the estimated energy difference between the two tautomers. An energy difference of 4.1 kcal/mol is comparable with the energy difference in water which was reported to be 2.3 kcal/mol utilizing pK_a measurements.[142]

It is not trivial to explain the difference in stability between the two tautomers in terms of aromaticity since both the benzenoid and the quinoid tautomers can be considered as aromatic. Although aromaticity is a commonly used concept in chemistry, quantification of aromaticity has been a problem. In recent years, the multidimensional characteristics of aromaticity with "magnetic" and "classic" components have been debated frequently.[143]

Bird introduced an index of aromatic character by evaluating the variation of ring bond orders[144] and he later extended his studies to establish a unified aromaticity index which shows good correlation with resonance energies.[145] A unified aromaticity index (I_A) of 144 is assigned to 1*H*-indazole (having more aromatic character than benzene which has an I_A=100). The resonance energies for 1*H*- and 2*H*-indazole are reported to be 75.7 and 73.3 kcal/mol, respectively.[146]

Clar discussed the topic of aromaticity in his book "The Aromatic Sextet" in 1972.[147] One of the key examples described in the book is the comparison of phenanthrene (**69**) with anthracene (**70**). Although both molecules are aromatic, phenanthrene possesses more benzenoid character than anthracene which leads to greater

---

[141] Catalan, J., De Paz, J.L.G., Elguero, J. (1996) Importance of aromaticity on the relative stabilites of indazole annular tautomers: an ab initio study. *J. Chem. Soc. Perkin Trans. 2* 57-60.
[142] Catalan, J., Del Valle, J.C., Claramunt, R.M.., Boyer, G., Laynez, J., Gomez, J., Jimenez, P., Tomas, F., Elguero, J. (1994) Acidity and basicity of of indazole and its N-methyl derivatives in the ground and in the excited state. *J. Phys. Chem.* **98**, 10606-10612.
[143] Katritzky, A.R., Karelson, M., Sild, S., Krygowski, T.M., Jug, K. (1998) Aromaticity as a quantitative concept. 7. Aromaticity reaffirmed as a multidimensional characteristic. *J. Org. Chem.* **63**, 5228-5231.
[144] Bird, C.W. (1985) A new aromaticity index and its application to five-membered ring heterocycles *Tetrahedron* **41**, 1409-1414.
[145] Bird, C.W. (1992) Heteroaromaticity.5.A unified aromaticity index. *Tetrahedron* **48**, 335-340.
[146] Bird, C.W. (1996) The relationship of classical and magnetic criteria of aromaticity. *Tetrahedron* **52**, 9945-9952.
[147] Clar E. "Aromatic Sextet", New York, John Wiley, 1972.

stability by 7-12 kcal/mol.[148,149] Clar explains this difference as being due to the presence of two "inherent sextets" and one "induced sextet" in **69** vs. one "inherent sextet" and two "induced sextets" in **70**. Therefore, the formulation **69b** is chosen over **69c** to represent phenanthrene.

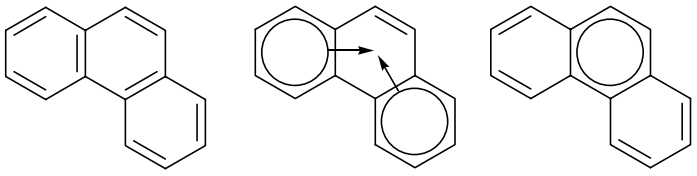

69a **69b** **69c**

70a **70b**

Formulation **69b** creates a fixed double bond in the center ring which was demonstrated experimentally to be the case. Phenanthrene undergoes bromination even in the absence of a catalyst to yield the corresponding dibromide (**71**) as shown in Scheme 16.[150]

Scheme 16. Bromination of the "fixed" double bond of phenanthrene to form the corresponding dibromide 71.

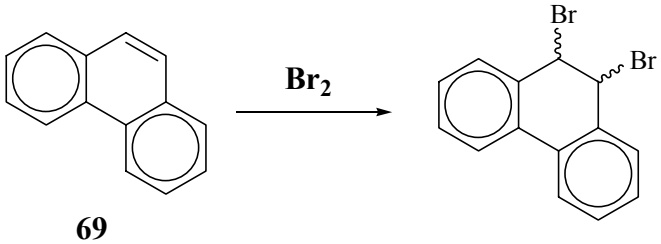

69 **71**

[148] Richardson, J.W., Parks, G.S. (1939) Thermal data on organic compounds. XIX. Modern combustion data for some nonvolatile compounds containing carbon, hydrogen and oxygen. *J. Am. Chem. Soc.* **61**, 3543-3546.
[149] Magnus, A., Becker, F. (1951) Bond ratios in the higher aromatic hydrocarbons on the basis of new precision measurements of their heats of combustion *Erdoel und Kohle* **4**, 115-118.
[150] Altschuler, L., Berliner, E. (1966) Rates of bromination of polynuclear aromatic hydrocarbons. *J. Am. Chem. Soc.* **88**, 5837-5845.

This concept applies to indazole as well. The 1*H*-tautomer, which has one "inherent sextet" and one "induced sextet", is expected to be (and is) more stable than the 2*H*- tautomer with two "intrinsic sextets".

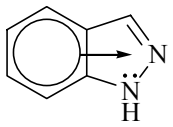

44

1.6.2.3. Non-Prototropic Tautomerism of Indazole

The migration of a substituent from one indazolyl nitrogen to the other has been observed and referred to as non-protropic tautomerism. One of the well-documented examples is the acyl group migration or acylotropy as shown in Scheme 17.

Scheme 17. Isomerization of 2*H*-acetylindazole (72) to 1*H*-acetylindazole (73).

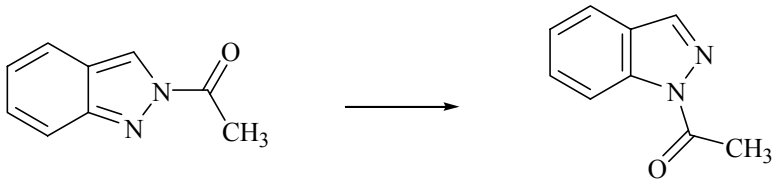

72 **73**

This type of rearrangement reaction was first reported by von Auwers in 1919.[151] In his first paper on the subject, 2-acetylindazole was reported to be converted into 1-acetylindazole upon heating with acetic anyhdride. In a following paper, von Auwers describes two poorly defined stereoisomeric 2-acetylindazoles, one of which is "labile" and the other which is stable.[152] Meisenheimer and Dietrich challenged the possibility of stereoisomerism and suggested that they may be structural isomers (1-acetylindazole or

[151] Von Auwers, K., Marburg, K. (1919) Isomerism phenomena in indazole derivatives. Preliminary communication. *Ber.* **52B**, 1330-1339.
[152] Von Auwers, K., Schwegler, K, Marburg, K. (1920) Stereoisomeric acyl derivatives of substituted indazoles. *Ber.* **53B**, 1211-1232.

3-acetylindazole).[153] In 1925 von Auwers concluded that "…stable and labile "2-acylindazoles" are in reality structural isomers, 1- and 2-acyl derivatives."[154] The mechanism of this thermal rearrangement reaction leading to isomerization was proposed by von Auwers to be intramolecular.[155]

In their study on the rearrangement of acylindazoles, Yamazaki *et al.* concluded that light and oxygen did not have any effect on the reaction. [156] Furthermore, they could not find any evidence for a free radical process. The rearrangement, which was monitored by NMR spectroscopy, was shown to follow first order kinetics. Polar solvents increased the rate of the reaction and carboxylic acids as well as boron trifluoride/ethyl ether were shown to catalyze the conversion. In the light of the above findings the authors suggested that the isomerization of 2*H*-acylindazoles to 1*H*-acylindazoles proceeds through heterolytic cleavage which results in the formation of the indazolyl anion (**74**) and acylium species (**75**). The recombination of **74** and **75** yields the 1*H*-acetylindazole (**73**).

---

[153] Meisenheimer, J., Dietrich, A. (1924) The isomeric acylindazoles of Karl von Auwers. *Ber*. **57B**, 1715-1723.
[154] Von Auwers, K. (1925) Constitution of the stable and labile acylindazoles. *Ber.* **58B**, 2081-2088.
[155] Von Auwers, K., Ernecke, A., Wolter, E. (1930) Influence of substituents on the formation and rearrangement tendency of acylated indazoles. *Ann.* **478**, 154-175.
[156] Yamazaki, T., Baum, G., Shechter, H. (1974) Consecutive [1,5]-sigmatropic and dissociation-recombination processes in rearrangements of 3-substituted 3-acyl-3H-indazoles to 1-acylindazoles *Tett. Lett.* **49-50**, 4421-4424.

Scheme 18. Suggested mechanism for the isomerization of 2*H*-acetylindazole (72) to 1*H*-acetylindazole (73).

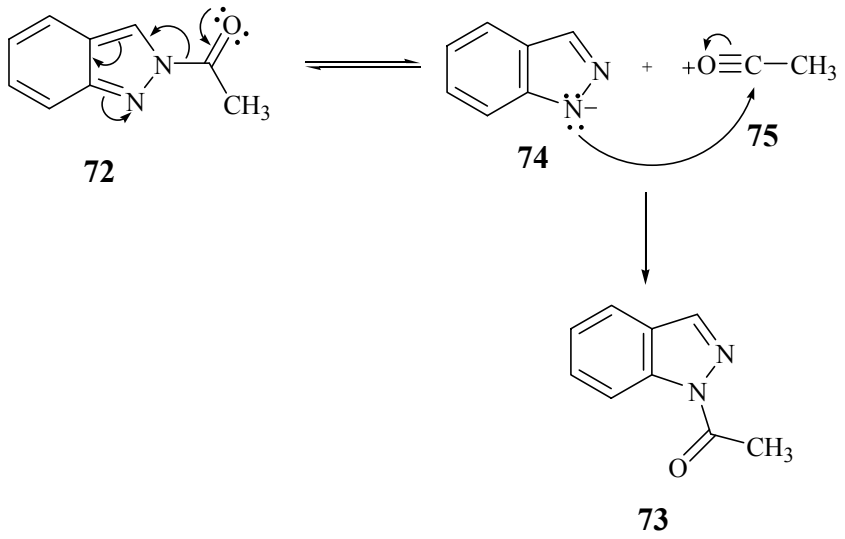

The key evidence to support the above mechanism comes from the product analysis. When a mixture of 2*H*-3-phenylacylindazole (**76**) and 2*H*-6-nitroacylindazole (**77**) is heated in chlorobenzene, cross-over products **78** and **79** are obtained in addition to the expected 1*H*-isomers. Although consistent with the products obtained, the pathway described in Scheme 18 does not provide an explanation for the increased rate of rearrangement in the presence of carboxylic acids.

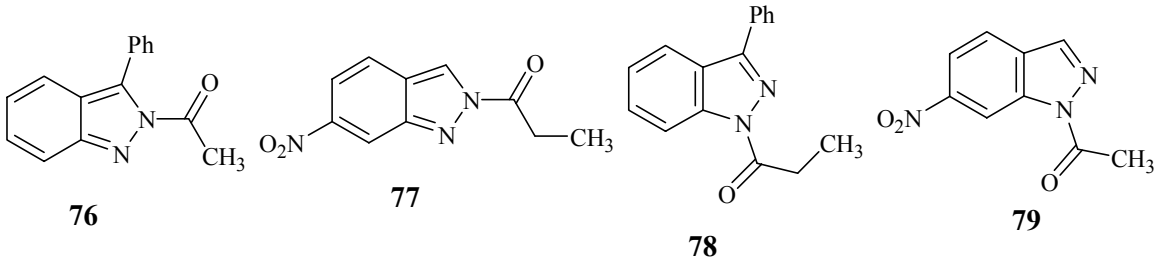

A more recent example of 2*H*- to 1*H*-isomerism of indazoles is reported in the nucleoside literature.[157] As shown in Scheme 19, the 2*H*-deoxynucleoside species **80** rearranges to the corresponding 1*H*-derivative **81** when heated in the presence of acid.

Scheme 19. Isomerization of 2*H*-deoxynucleoside species 80 to the corresponding 1*H*-derivative 81.

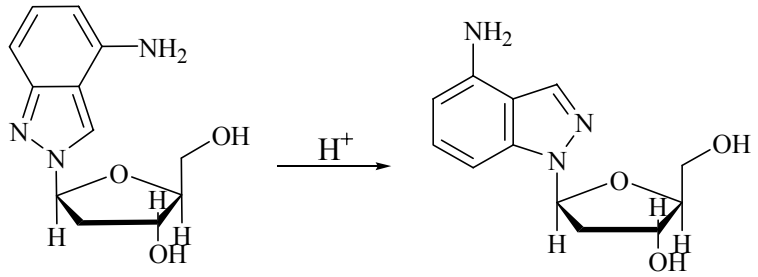

80 **81**

For the above rearrangement of deoxynucleosides the authors propose the mechanism shown in Scheme 20 where, in the presence of acid, compound **80** decomposes to form 1*H*-4-aminoindazole (**82**) and the oxonium species **83**. Reaction of **82** with **83** at elevated temperature forms irreversibly the more stable 1*H*-isomer **81**.

[157] Boryski, J. (1999) Acylnucleosides of indazole and their rearrangements. *Polish Journal of Organic Chemistry* **73**, 1019-1027.

Scheme 20. Proposed mechanism for the rearrangement of 2*H*-deoxynucleoside species 80 to the corresponding 1*H*-derivative 81.

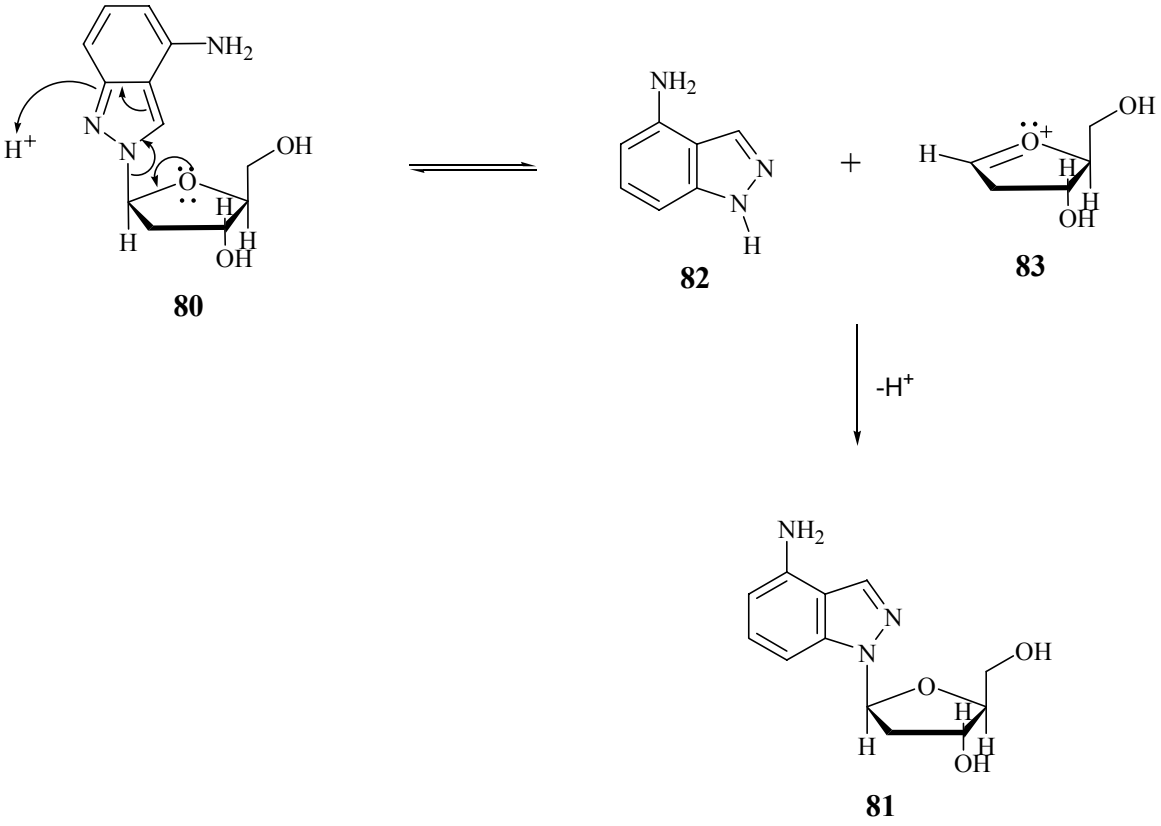

1.6.3. Preparation of N-alkylated and N-arylated Derivatives

As in many other aspects of indazole chemistry, the first results on the alkylation of indazole were reported by Karl von Auwers. In 1924, he reported that "…alkylation of indazole may give 1- or 2-derivatives or mixtures of both, the course of the reaction depending both on the experimental conditions and on the nature of the alkyl halide. Further investigation in various directions has shown that the relationships are very complicated and it is not possible as yet to establish with certainty the ultimate causes of the phenomena involved".[158] Some of his findings are quite valuable and will be described briefly.

---

[158] Von Auwers, K., Allardt, H.-G. (1924) Further investigations on the alkylation of indazole *Ber*. **57B**, 1098-1106.

Scheme 21. Alkylation of indazole to give 1*H*- and/or 2*H*-alkyl indazoles.

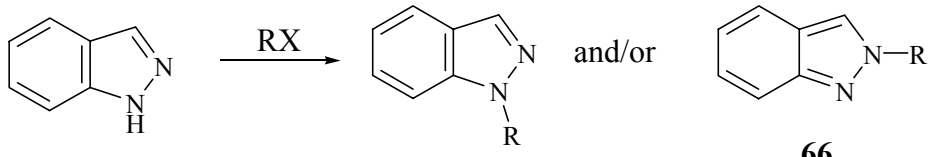

44 **84** **66**

When indazole and an alkyl halide are heated in the absence of base, the product is **66** regardless of the halide. The outcome is variable when the silver salt of indazole is used as the starting material. In this case, the reaction proceeds at room temperature when methyl, allyl and benzyl iodides are used. The use of methyl iodide results in the exclusive formation of the 2*H*-derivative whereas the allyl and benzyl iodides give exclusively the 1*H*-derivatives. The effect of temperature on the ratio of regioisomeric products is not clear. Von Auwers reported that the reaction between the silver salt of indazole and ethyl iodide resulted in a mixture of products and the ratio of 1*H*- to 2*H*- was 94:6 at 37 ^{o}C, 76:24 at 50 ^{o}C and 50:50 at 100 ^{o}C. When the reaction was carried out in the presence of an aqueous base, both regioisomers form in varying ratios depending on the alkyl halide used. There was no mechanistic interpretation offered for these observations.

Jaffari *et al.* reported the methylation of indazole using various alkylating agents. The regioselectivity was dependent on the nature of the alkylating agent.[159] A later report describes the methylation of indazole using dimethyl sulfate in the presence of potassium hydroxide which yields an approximately 1:1 mixture of 1*H*- and 2*H*-isomers.[160,161] An efficient and regioselective synthesis of 2-methyl and 2-ethyl substituted indazoles is described by Stafford *et al.*[162] The use of trimethyloxonium tetrafluoroborate [$(CH3)_3O^+BF_4^-$)] as the alkylating agent results in the exclusive formation of the 2*H*-isomer in 93% yield at room temperature. This approach was shown to be applicable for

---

[159] Jaffari, G.A., Nunn, A.J. (1973) Methylation of indazoles and related reactions. *J. Chem. Soc. Perkin Trans*. 1, 2371-2374.
[160] Morel, S., Boyer, G., Coullet, F., Galy, J.-P. (1996) A synthesis of 9-methoxy-1-methyl-1H,6H-pyrazolo[4,3-c]carbazole. *Synth. Commun.* **26**, 2443-2447.
[161] Boyer, G., Galy, J.-P., Barbe, J. (1995) Synthesis of substituted pyrazolo[3,4-b]- and pyrazolo[4,3-c]phenothiazine derivatives. *Heterocycles* **41**, 487-496.
[162] Cheung, M., Boloor, A., Staffiord, J.A. (2003) Efficient and regioselective synthesis of 2-alkyl-2*H*-indazoles. *J. Org. Chem.* **68**, 4093-4095

indazole derivatives bearing electron withdrawing groups as well as electron donating groups.

Arylation of indazoles is more challenging due to decreased electrophilicity of the aryl group. Regardless of the approach, the problem of regioselectivity applies to the arylation reactions as well. Use of *p*-tolyllead triacetate (**85**) in the presence of copper diacetate results in a 2:1 mixture of 1*H*- and 2*H*-tolylindazoles[163] whereas *p*-tolylboronic acid (**86**) in the presence of copper diacetate and pyridine is reported to give a mixture of isomers with a 1*H*- to 2*H*-ratio of 9:2.[164] Finet *et al.* reports the formation of 1*H*- and 2*H*-phenylindazoles in a 1:1 ratio with triphenylbismuth diacetate in the presence of a catalytic amount of copper diacetate and tetramethylguanidine as the base.[165]

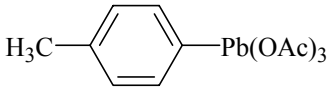

85

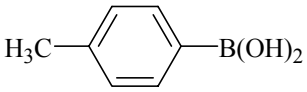

86

Although various methods of alkylation and arylation of indazoles are reported in the literature, it is still a serious challenge to achieve the efficient regioselective synthesis of one isomer over the other. In many instances the applicability is limited to specific alkyl/aryl groups reacting with certain indazole derivatives.

An alternative approach to arylindazoles proceeds through cyclization reactions. One early method involves heating benzeneazo-*o*-benzyl alcohol (**87**) in the presence of sulfuric acid which gives the corresponding 2*H*-arylindazole (**88**) as shown in Scheme 22.[166]

---

[163]Lopez-Alvarado, P., Avendano, C., Menendez, J.C. (1993) New synthetic applications of aryllead triacetates.N-arylation of azoles. *J. Org. Chem.* **60**, 5678-5682.

[164] Lam, P.Y.S., Clark, C.G., Saubern, S., Adams, J., Winters, M.P., Chan, D.M.T., Combs, A. (1998) New aryl/heteroaryl C-N bond cross-coupling reactions via arylboronic acid/cupric acetate arylation. *Tett. Lett.* **39**, 2941-2944

[165] Federov, A.Y., Finet, J.-P. (1999) N-Phenylation of azole derivatives by triphenylbismuth derivatives/cupric acetate *Tett. Lett.* **40**, 2747-2748.

[166] Freundler, P. (1907) Researches on the azo compounds. Transformation of the orthocarboxylic azo compounds into oxyindazoles. *Bull. Soc. Chim.* [4] **1**, 206-216.

Scheme 22. Regioselective synthesis of 2*H*-phenylindazole (88) via the ring closing of benzeneazo-*o*-benzyl alcohol (87).

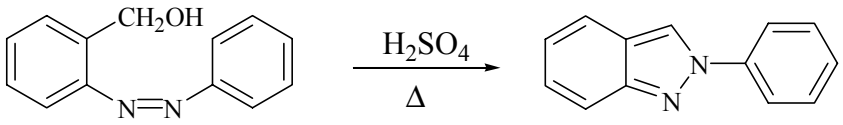

87 **88**

Another approach involves an N-N bond making reaction starting with (*o*-nitrobenzyl)amines (**89**) or (*o*-nitrobenzylidene)amines (**91**). Reductive cyclization of **89** using Sn, (or Zn or Fe) in the presence of hydrochloric acid (or acetic acid) results in the formation of the corresponding 2*H*-indazole derivatives as shown in Scheme 23.

Scheme 23. Synthesis of 2*H*-arylindazoles (90) via the cyclization of (*o*-nitrobenzyl)amines (89).

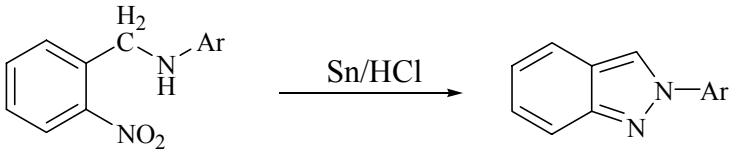

89 **90**

In a similar reaction, **91** can be converted to the corresponding 2*H*-indazole (**90**) upon treatment with $P(OEt)_3$[167] (or $PdCl_2(PPh)_3/SnCl_2/CO(g)$[168]) as shown in Scheme 24.

[167] Armour, M.A., Cadogan, J.I.G., Grace, D.S.B. (1975) Reduction of nitro and nitroso compounds by tervalent phosphorous reagents, XI. Kinetic study of the effects of varying the reagent and the nitro compound in the conversion of o-nitrobenzylidene amines to 2 –substituted indazoles. *J. Chem. Soc. Perkin Trans*. **2**, 1185-1189.

[168] Akazome, M., Kondo, T., Watanabe, Y. (1994) Palladium complex-catalzyed reductive N-heterocyclization of nitroarenes: Novel synthesis of indole and 2H-indazole derivatives. *J. Org. Chem.* **59**, 3375-3380.

Scheme 24. Synthesis of 2*H*-arylindazoles (90) via the cyclization of (*o*-nitrobenzylidene)amines (91).

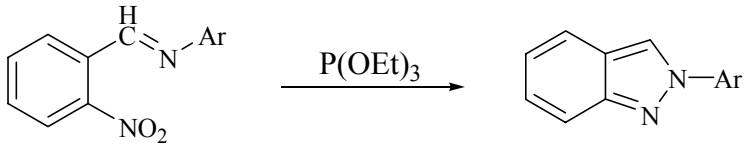

91 **90**

Cyclization of hydrazones (**93**) in the presence of a base at high temperatures results in the formation of the corresponding 1*H*-arylindazoles (**94**). The hydrazones, in turn, can be prepared by the treatment of an *o*-halogenated aldehyde (**92**) with the desired hydrazine hydrate as shown in Scheme 25.

Scheme 25. Synthesis of 1*H*-arylindazoles (94) via the base catalyzed cyclization of hydrazones (X = F or Br).

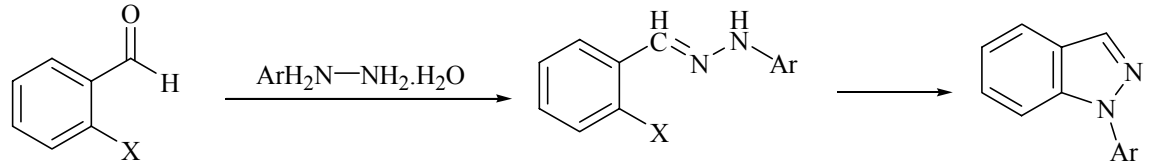

92 **93** **94**

Recently, Song *et al.* published two papers describing an efficient way of obtaining 1*H*- and 2*H*-arylindazoles utilizing a palladium catalyzed cyclization reaction. The first paper reports the synthesis of 2*H*-arylindazoles via the intramolecular amination of N-aryl-N-(*o*-bromobenzyl)hydrazines (**95**)shown in Schemes 26.[169]

[169] Song, J.J., Yee, N.K. (2000) A novel synthesis of 2-aryl-2H-indazoles via a palladium-catalyzed intramolecular amination reaction. *Organic Letters* **2**, 529-521.

Scheme 26. Regioselective synthesis of 2*H*-arylindazoles (96) via palladium catalyzed intramolecular amination reactions.

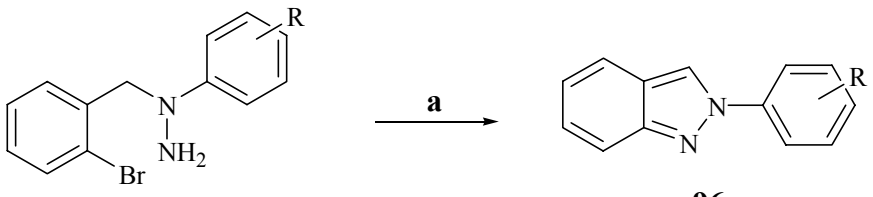

95 **96**

[a]Reagents and conditions: $Pd(OAc)_2$/1,1'-bis(diphenylphosphino)ferrocene (ddpf)/*t*-BuONa/toluene/90°C

In the subsequent paper, the authors describe the application of their methodology to the synthesis 1*H*-arylindazoles.[170] In this reaction, the starting N-1-aryl substituted hydrazines (**98**) are prepared from the N-2-tripenylphosphine protected hydrazine (**97**) as shown in Scheme 27.

Scheme 27. Preparation of [N-aryl-N'-(*o*-bromobenzyl)-hydrazinato-N']triphenylphosphonium bromides (99) as precursors to 1*H*-arylindazole.

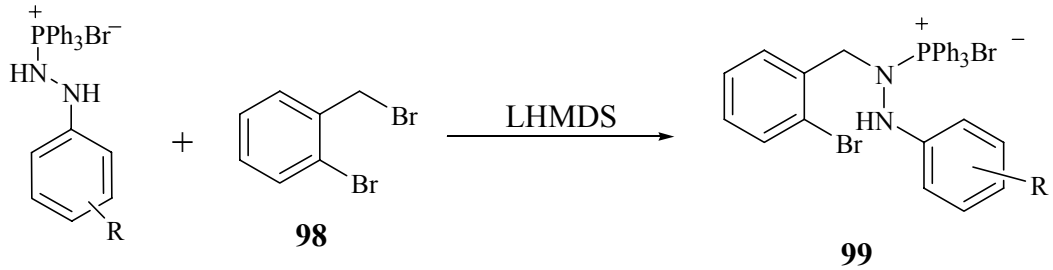

97 **98** **99**

Although the cyclization of **99** results in the formation of the desired 1*H*-arylindazoles (**101**), higher yields were obtained when **99** was deprotected to give hydrazines (**100**) prior to the cyclization reaction as shown in Scheme 28.

[170] Song, J.J, Yee, N.K. (2001) Synthesis of 1-aryl-1H-indazoles via the palladium-catalyzed cyclization of N-aryl-N'-(o-bromobenzyl)hydrazine and [N-aryl-N'-(o-bromobenzyl)-hydrazinato-N']-triphenylphopshoniumbromides *Tett. Lett.* **42**, 2937-2940.

Scheme 28. Regioselective synthesis of 1*H*-arylindazoles (101) via palladium catalyzed ring closing reactions.

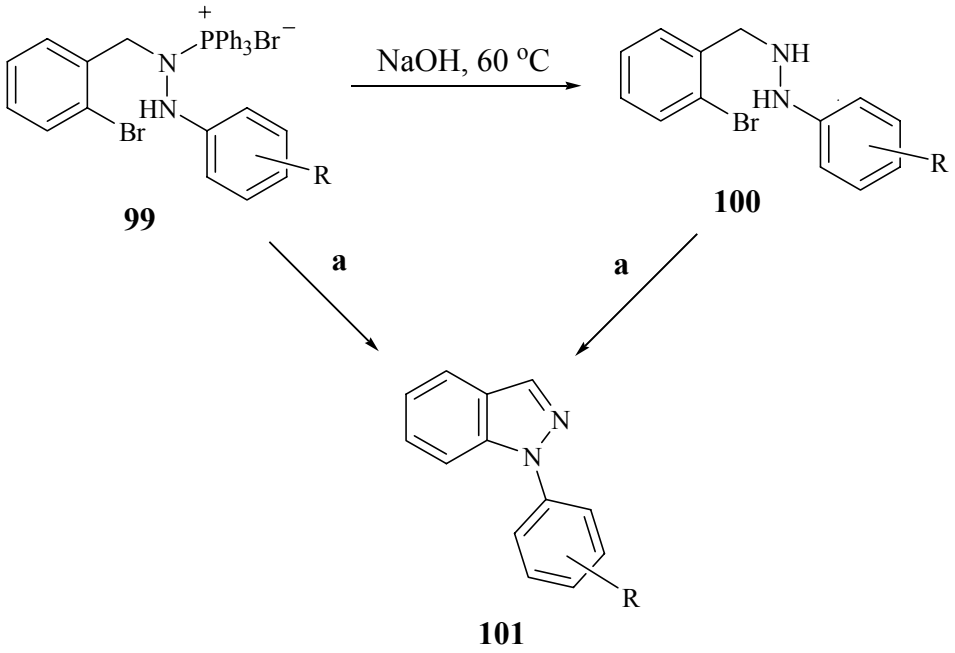

[a]Reagents and conditions: $Pd(OAc)_2$/1,1'-bis(diphenylphosphino)ferrocene (ddpf)/t-BuONa/tolune/90°C

1.6.4. Biologically Important Indazoles

Indazolyl derivatives have been tested in various biological test systems and some of them have been shown to have important pharmacological activities.

Compound **102**, an indazolyl substituted cyclic urea derivative, was reported to be an extremely potent HIV protease inhibitor. Molecular modeling studies underline the biological importance of the hydrogen bond donor properties of indazolyl nitrogen atoms in **102**.[171]

[171] Rodgers, J.D., Johnson, B.L., Wang, H., Greenberg, R.A., Erickson-Viitanen, S., Klabe, R.M., Cordova, B.C., Rayner, M.M., Lam, G.N., Chang, C.-H. (1996) Potent cyclic urea HIV protease inhibitors with benzofused heterecycles as P2/P2' groups *Bioorg. Med. Chem.Lett.* **6**, 2919-2924.

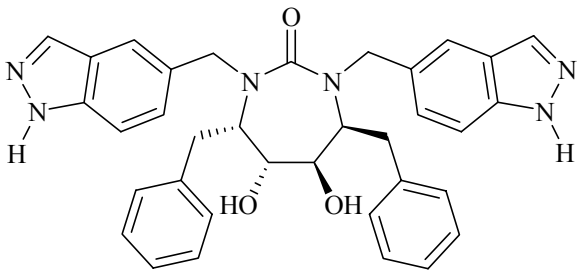

102

Antispermatogenic activity of 1-*p*-chlorobenzyl-1*H*-indazole-3-carboxylic acid (**103**)[172] has led to the synthesis of a large number of 1*H*-indazole-3-carboxylic acid derivatives.[173] One of these compounds, lonidamine (**104**), was shown to have antitumor properties as well.[174,175] The results of phase II and III studies for the treatment of advanced breast, ovarian and lung cancers are encouraging.

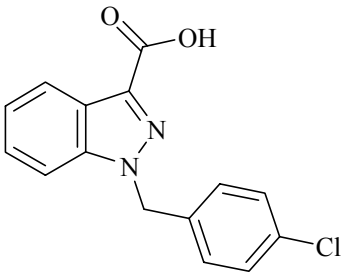

103

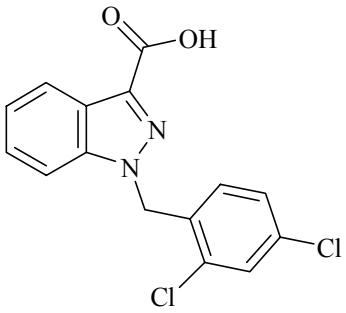

104

[172] Silvestrini, B., Burberi, S., Catanese, B., Cioli, V., Coulston, F., Lisciani, R., Barcellona, P.S (1975) Antispermatogenic activity of 1-p-chlorobenzyl-1H-indazole-3-carboxylic acid (AF 1312/TS) in rats. I. Trials of single and short-term administrations with study of pharmacologic and toxicologic effects. *Exp. Mol. Pathol.* **23**, 288-307.

[173] Corsi, G., Palazzo, G., Germani, C., Barcellona, P.S., Silvestrini, B. (1976) 1-Halobenzyl-1H-indazole-3-carboxylicacids. A new class of antispermatogenic agents. *J. Med. Chem.* **19**, 778-783.

[174] Caputo, A., Silvestrini, B., (1984) Lonidamine, a new approach to cancer therapy. *Oncology* **41 (Suppl. 1)**, 2-6.

[175] Di Cosimo, S., Ferretti, G., Papaldo, P., Carlini, P., Fabi, A., Cognetti, F. (2003) Lonidamine: efficacy and safety in clinical trials for the treatment of solid tumors *Drugs Today* **39**, 157-173.

The piperidine derivative of indazole HP818 (**105**) has been examined[176] and together with its derivatives has been patented[177] as a nonnarcotic analgesic and antipsychotic drug.

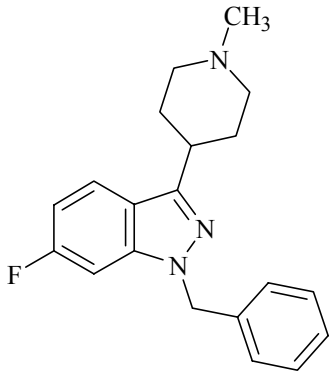

105

The indazole derivatives **106**[178] and **107**[179] were shown to have significant anti-inflammatory properties.

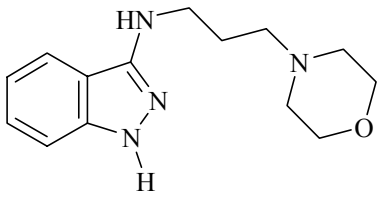

106

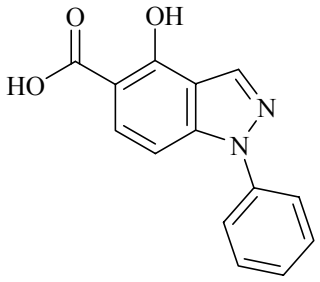

107

The 7-NI derivative **108** was tested for its effects in the treatment of alcohol dependence.[180]

---

[176] Locke, K.W., Dunn, R.W., Hubbard, J.W., Vanselous, C.L., Cornfeldt, M., Stuart, F., Strupczewski, J.T. (1990) HP 818: a centrally acting analgesic with neuroleptic properties *Drug Development Research* **19**, 239-256.

[177] Strupczewski, J.T., Bordeau, K.J. (1990) Preparation of 3-(1-substituted-4-piperazinyl)-1H-indazoles as analgesics and antipsychotics U.S. 89-405161

[178] Kawakubo, H. Sone, T., Wakigawa, K., Narita, T. (1987) Anti-inflammatory, analgesic and antipyretic actions of 3-aminoindazole derivatives. *Yakugaki Zasshi* **107**, 28-36.

[179] Mosti, L., Sansebastiano, L., Fossa, P., Schenone, P., Mattioli, F. (1992) 1-Phenyl-1H-indazole derivatives with analgesic and anti-inflammatory activities *Farmaco*, **47**, 357-365.

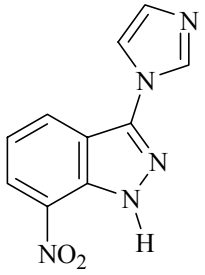

108

Inspired by the above mentioned "multitude of pharmacological activities" and as part of their interest in antimutagenesis and antioxidants, Mitscher's group recently reported their successful attempt to create a library of tri-substituted indazoles.[181] During their in vitro screening efforts they have identified the 1,3,5-trisubstituted derivative **109** as an extremely potent antioxidant.

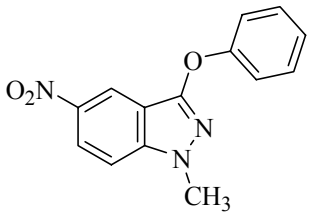

109

[180] Beauge, F., Dingeon, P., Rault, S., Boulouard, M. (2003) Substituted 7-nitroindazoles (7-NI), process for their preparation, and their therapeutic use, particularly for the treatment of alcohol dependence. Fr. Demande.

[181] Menon, S., Vaidya, H., Pillai, S., Vidya, R., Mitscher, L.A. (2003) A parallel synthesis demonstration library of tri-substituted indazoles containing new antimutagenic/antioxidant hits related to benzylamine *Combinatorial chemistry and high throughput screening* **6**, 79-99.

CHAPTER 2
SYSTEMATIC INVESTIGATION OF THE REACTION BETWEEN INDAZOLE (44) AND 4-CHLORO-1-METHYLPYRIDINIUM IODIDE (55)

2.1. Summary of Earlier Results[182]

Our goal of synthesizing both isomeric 1*H*- and 2*H*-indazolylpyridinium species as precursors to the corresponding "prodrugs" prompted the development of regioselective synthetic routes. The cyclization reactions reported in the literature are multi-step processes with limited applicability. Therefore we have decided to investigate systematically the nucleophilic aromatic substitution reaction of indazole derivatives with 4-chloro-1-methylpyridinium iodide. As reported, indazole was chosen as a model compound.[183] As the starting point for our further studies on the chemistry of indazolylpyridiniums, a brief summary of these results will be included here.

The reaction between indazole and **55** in refluxing DMF in the presence of 2 equivalents of TMP gave exclusively the demethylated 1*H*-indazolypyridine species **111**. This outcome can be explained by the demethylation reaction described in Scheme 10 for the corresponding 7-nitroindazolylpyridinium species **51** and **54**.[183] In a similar manner, the initial formation of the indazolylpyridinium species **110** is followed by demethylation at elevated temperatures to form the 4-indazolylpyridine (**111**) and iodomethane as shown in Scheme 29.

[182] These results were reported in Reference 1, pages 98-107.
[183] At the time the reaction was carried out with indazole, the demethylation step has not been fully understood.

Scheme 29. Exclusive formation of 1*H*-4-indazolylpyridine via the reaction between indazole and 55.

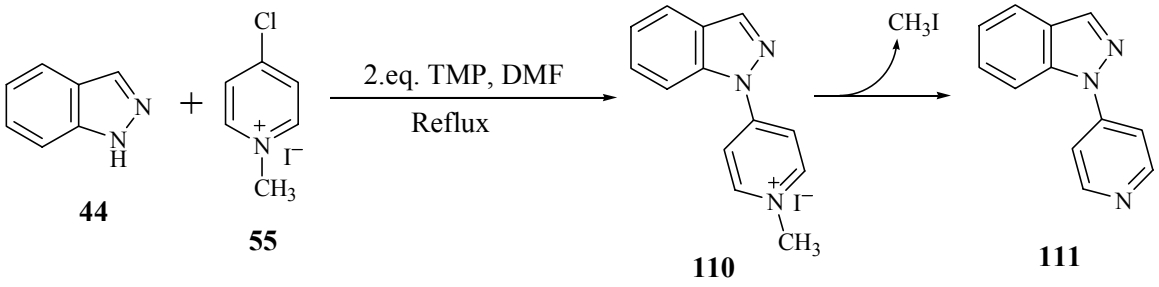

As in the case of 7-NI, the reaction of indazole (**44**) with **55** was carried out in the presence of TMP at 22 ^{o}C to prevent the undesired demethylation of **110**. The progress of the reaction was monitored by HPLC-DA as well as GC-MS. In agreement with results obtained with nitroindazoles,[184] we observed product formation at room temperature. There was no evidence for the demethylation reaction. Much to our surprise, however, instead of the exclusive formation of the 1*H*-indazolypyridinium **110**, the formation of a mixture of two isomeric products with a ratio of 3 parts to 1 part was observed. We identified the major product to be the 1*H*-isomer **110** and the minor product to be the 2*H*-isomer **112** (Scheme 30). After isolation, the resulting indazolylpyridinium derivatives were determined by elemental analysis to be the iodide salts.

Scheme 30. The reaction between indazole and 55 at room temperature resulting in the formation of a mixture of isomeric indazolylpyridiniums 110 and 112.

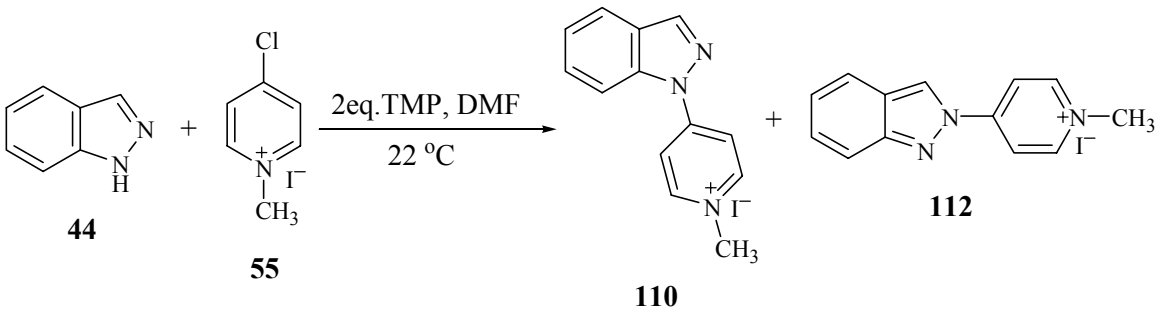

[184] See Section 1.5. Design and Synthesis of Potential "Prodrugs" of 7-NI and Structurally Related Indazoles.

Exclusive formation of 1*H*-indazolylpyridine species **111** at elevated temperatures in contrast to the formation of a mixture of isomeric indazolylpyridiniums at room temperature suggested the possibility of a thermal rearrangement of the 2*H*-isomer **112** to the more stable 1*H*-isomer **110**.

The possible thermal rearrangement of **112** to **110** was examined under various conditions using HPLC-DA. Both the 1*H*- and the 2*H*-isomers were found to be stable at 150^{o} C in DMF in the absence of TMP. The 2*H*-isomer also was stable in the presence of TMP at 22 ^{o}C. At 60 ^{o}C, however, **112** rearranged quantitatively to the 1*H*-isomer in the presence of 1 equivalent of TMP. On the other hand, the 1*H*-isomer was stable under these conditions. These results demonstrated unambiguously the TMP dependent irreversible rearrangement of the 2*H*-indazolylpyridinium **112** to the 1*H*-indazolylpyridinium **110** at 60 ^{o}C. Furthermore, the rearrangement reaction also reached completion at 60 ^{o}C in the presence of 0.1 equivalent of TMP consistent with a catalytic role for TMP. The results are summarized in Table 2.

Table 2. Stability of 110 and 112 under various reaction conditions.

Starting Material	Temperature	TMP	Results
110	150 ^{o}C	0	No reaction
110	150 ^{o}C	1 equivalent	No reaction
112	150 ^{o}C	0	No reaction
112	22 ^{o}C	1 equivalent	No reaction
112	60 ^{o}C	1 equivalent	100 % conversion to **110**
112	60 ^{o}C	0.1 equivalent	100 % conversion to **110**

After establishing the conditions required for the quantitative isomerization of **112** to **110**, we decided to take advantage of the rearrangement reaction to obtain regiospecifically the 1*H*-indazolylpyridinium **110**. We carried out the reaction between indazole and **55** in the presence of 2 equivalents of TMP at 60 ^{o}C to ensure the completion of the rearrangement reaction. As expected we obtained exclusively the 1*H*-isomer in good yield as shown in Scheme 31.

Scheme 31. Regiospecific synthesis of 1*H*-indazolylpyridinium species 110.

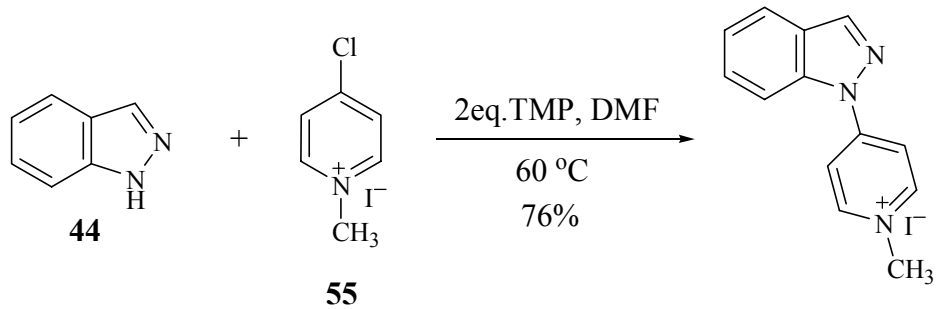

44 **55** **110**

The obligatory role of TMP for the rearrangement reaction led us to investigate the requirement of the base for the reaction between indazole (**44**) and 4-chloro-1-methylpyridinium iodide (**55**). We examined the reaction in the absence of TMP. No product formation was observed at room temperature suggesting the requirement of base for the reaction to proceed. However, as the temperature was increased gradually, HPLC-DA monitoring showed the formation of a single product at 100 °C. We identified this product to be the 2*H*-isomer **112** (Scheme 32).

Scheme 32. Regiospecific synthesis of 2*H*-indazolylpyridinium species 112.

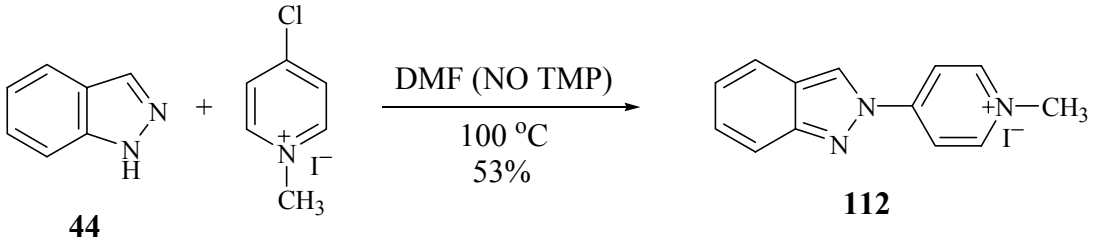

44 **55** **112**

Our systematic investigation of the nucleophilic aromatic substitution reaction between indazole and 4-chloro-1-methylpyridinium iodide provided regiospecific routes to both the 1*H*- and the 2*H*-isomers in good yield. Since the products crystallize out of the reaction mixtures in good yield, the ease of work-up increased further the efficiency

of our synthetic pathway. Also an interesting rearrangement reaction in which the 2*H*-indazolylpyridinium species isomerizes to the 1*H*-indazolylpyridinium **108** was observed. These results are summarized in Scheme 33.[185]

Scheme 33. Summary of the results obtained from the systematic investigation of the reactions between indazole and 55.

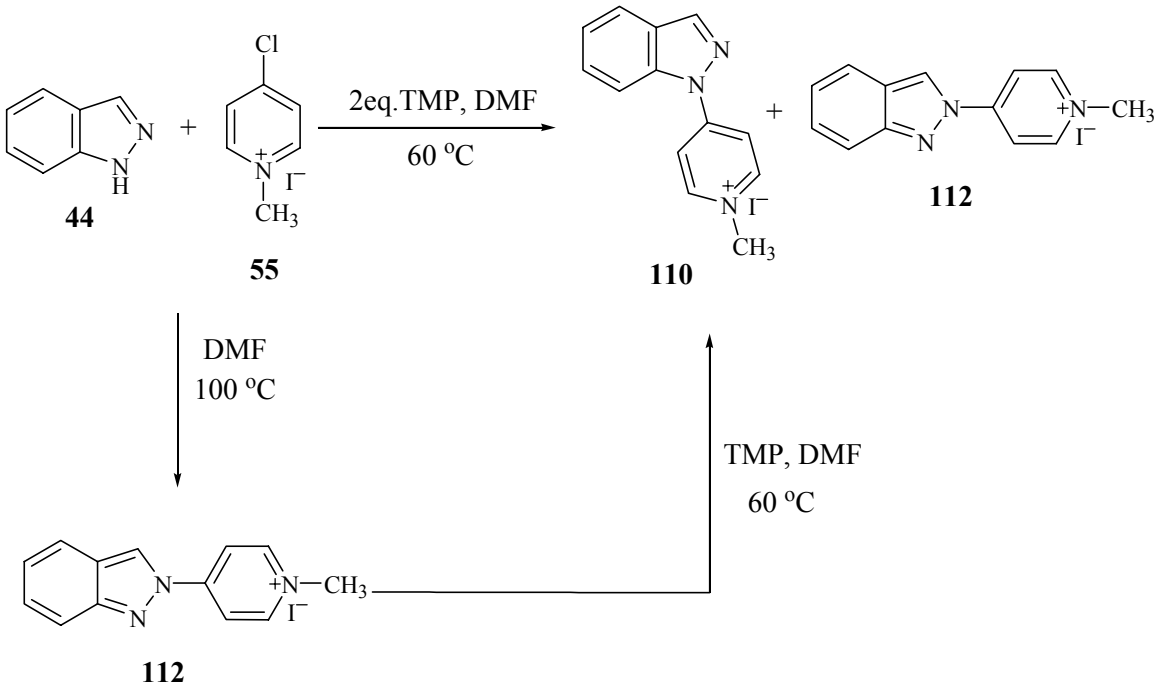

2.2. Evaluation of the Results[186]

2.2.1. Kinetic and Thermodynamic Evaluation of the Reaction Between Indazole and 55

2.2.1.1. TMP Catalyzed Product Formation

Our results demonstrated that the reaction between indazole and **55** leads to product formation both in the presence and absence of base. When the base is included the reaction proceeds readily at room temperature to give a mixture of products. In the

[185] Isin, E.M., de Jonge, M., Castagnoli, N., Jr. (2001) Studies on the synthetic approaches to 1*H*- and 2*H*-indazolyl derivatives. *J. Org. Chem.* **66**, 4220-4226.

[186] Although, a preliminary interpretation of the results was attempted in Reference 1, the complete evaluation will be presented in this dissertation supported by molecular modeling calculations.

presence of TMP, indazole is converted to the indazolyl anion which is expected to be the attacking nucleophile. Since the indazolyl anion is an ambident nucleophile, attack by N-1 and N-2 to give the neutral intermediates **113** and **114**, respectively, is possible.

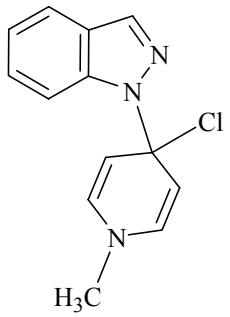

113

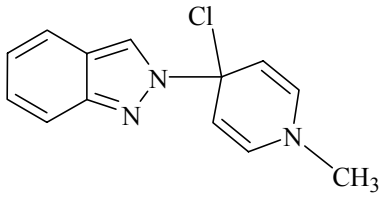

114

The benzenoidal intermediate **113**, leading to the 1*H*-indazolylpyridinium **110**, is expected to be more stable than the quinoidal intermediate **114**, leading to the 2*H*-indazolylpyridinium **112**. Therefore, according to the Hammond Postulate, the pathway leading to the 1*H*-isomer via intermediate **113** should proceed via a lower energy barrier compared to the pathway to **114** which forms the less stable 2*H*-isomer as shown in Fig. 2. The 1*H*- to 2*H*- product ratio is dictated kinetically by the difference in activation energies when a base is included in the reaction mixture. Our molecular modeling calculations at the AM1 level showed that intermediate **113** is more stable than **114** by 5 kcal/mol. This value is consistent with the reported difference of energy between the indazole tautomers.[187]

[187] For a discussion of the stability comparison of indazole tautomers see Section 1.6.2.2. Relative Stabilities of 1*H*- and 2*H*-Indazoles.

Figure 1. Reaction progress vs. energy diagram for the reaction between indazole and 55 in the presence of TMP.

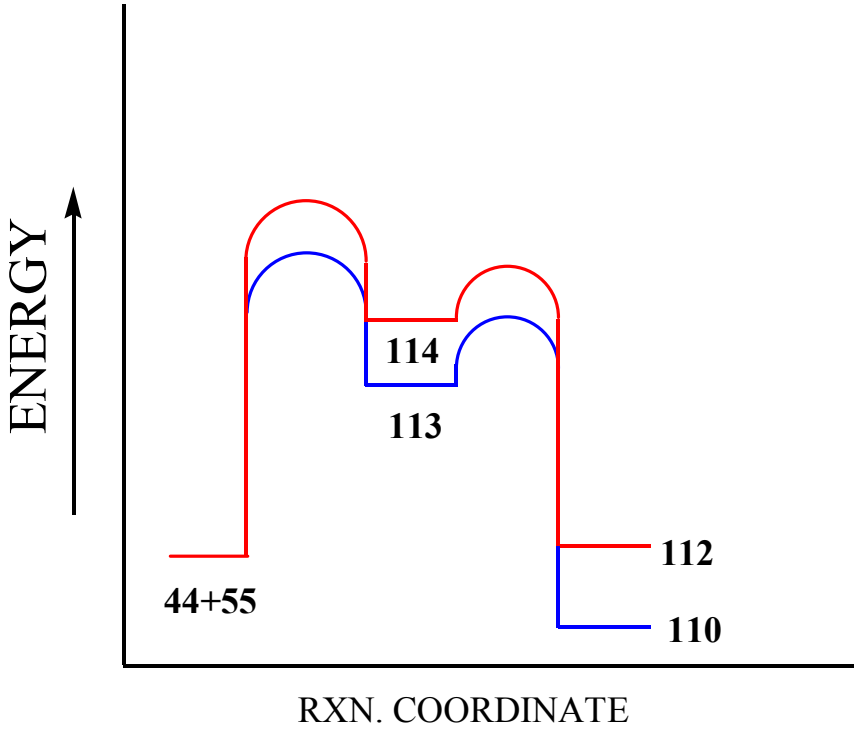

2.2.1.2. Product Formation in the Absence of TMP

In the absence of base, the attacking species is a neutral indazolyl species which is expected to be less reactive than the indazolyl anion. Therefore, the activation energy for product formation must be higher compared to the reaction in the presence of TMP. Due to the increased energy of activation, the reaction between indazole and **55** will proceed only at elevated temperatures (100 ^{o}C).

In contrast to the TMP mediated reaction, the only product obtained in the absence of base is the 2*H*-indazolylpyridinium species **112**. An examination of the intermediates leading to the 1*H*-isomer **110** vs. the 2*H*-isomer **112** justifies the formation of the less stable2*H*-product under these conditions. In the absence of base, N-1 attack of the neutral indazole leads to the charged localized intermediate **115** whereas N-2 attack results in the formation of intermediate **116** which is stabilized via charge delocalization as shown in Scheme 33.

Scheme 34. Comparison of intermediates 115 and 116 leading to the 1*H*- and 2*H*-indazolylpytidiniums, respectively.

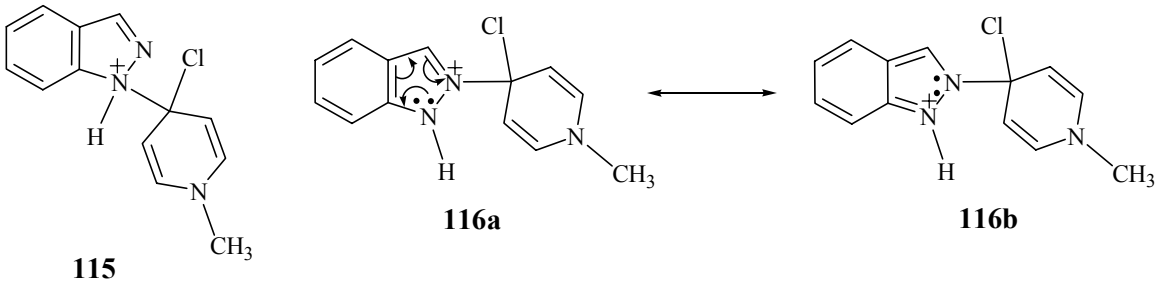

115 **116a** **116b**

In agreement with this analysis, our molecular modeling calculations at the semi empirical AM1 level show that intermediate **116** is more stable than intermediate **115** by 9 kcal/mol. The energy difference between the 1*H*- and the 2*H*-indazolylpyridiniums was calculated to be 11 kcal/mol. In the absence of base, a higher energy barrier must be mounted to obtain the thermodynamically more stable 1*H*-isomer **110** as shown in Fig. 2. In other words, formation of the less stable isomer is rationalized as a kinetically controlled outcome.

Figure 2. Reaction progress vs. energy diagram for the reaction between indazole and 55 in the presence of TMP.

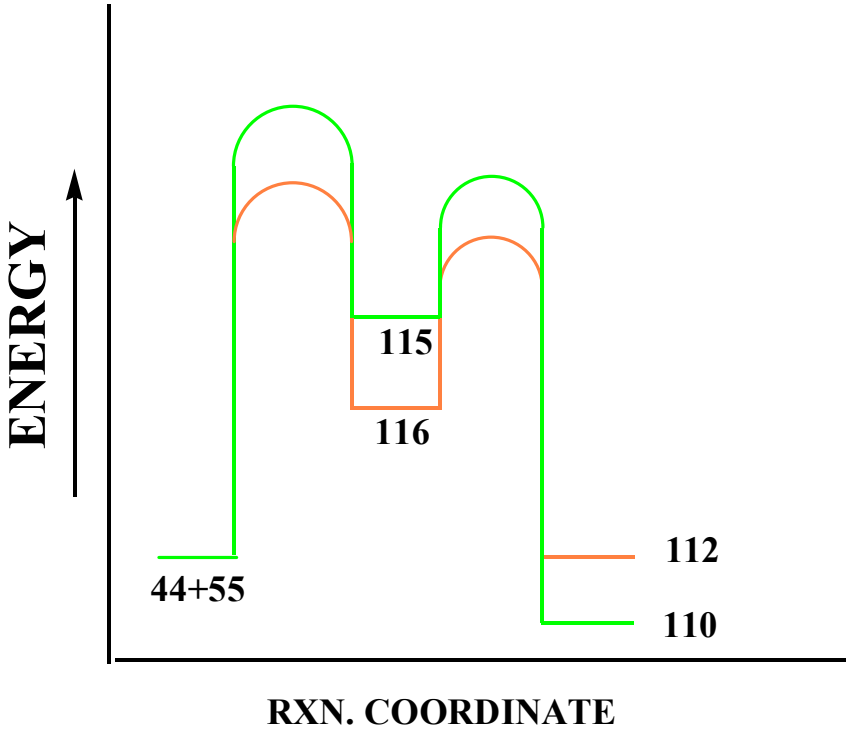

CHAPTER 3

PROPOSED MECHANISMS FOR THE ISOMERIZATION OF THE 2*H*-INDAZOLYLPYRIDINIUM 112 TO THE 1*H*-INDAZOLYLPYRIDINIUM 110

As described in Section 2.1 the less stable 2*H*-indazolylpyridinium species **112** isomerizes to the more stable 1*H*-isomer **110** through a TMP mediated thermal rearrangement reaction which takes place at 60 ^{o}C. It is important to note that TMP is required for the rearrangement reaction to take place. However, only a catalytic amount of TMP is sufficient for the quantitative conversion of **112** to **110**. We have considered two possible mechanisms for this isomerization reaction. These mechanisms will be presented in the following sections.

3.1. Thermal Decomposition of 112 Followed by Recombination

We have considered the mechanism shown in Scheme 34 as a possible pathway for the rearrangement reaction. At elevated temperatures, the attack of iodide at C-4 of the pyridinium ring may form reversibly intermediate **117**. Cleavage of intermediate **117** results in the formation of indazolyl anion (**118**) and 4-iodo-1-methylpyridinium iodide (**119**). The reaction between the indazolyl anion and **119** is expected to form selectively the intermediate **120** which is the precursor species to the more stable 1*H*-indazolypyridinium **110**.

Scheme 35. Proposed mechanism for the isomerization of 112 to 110.

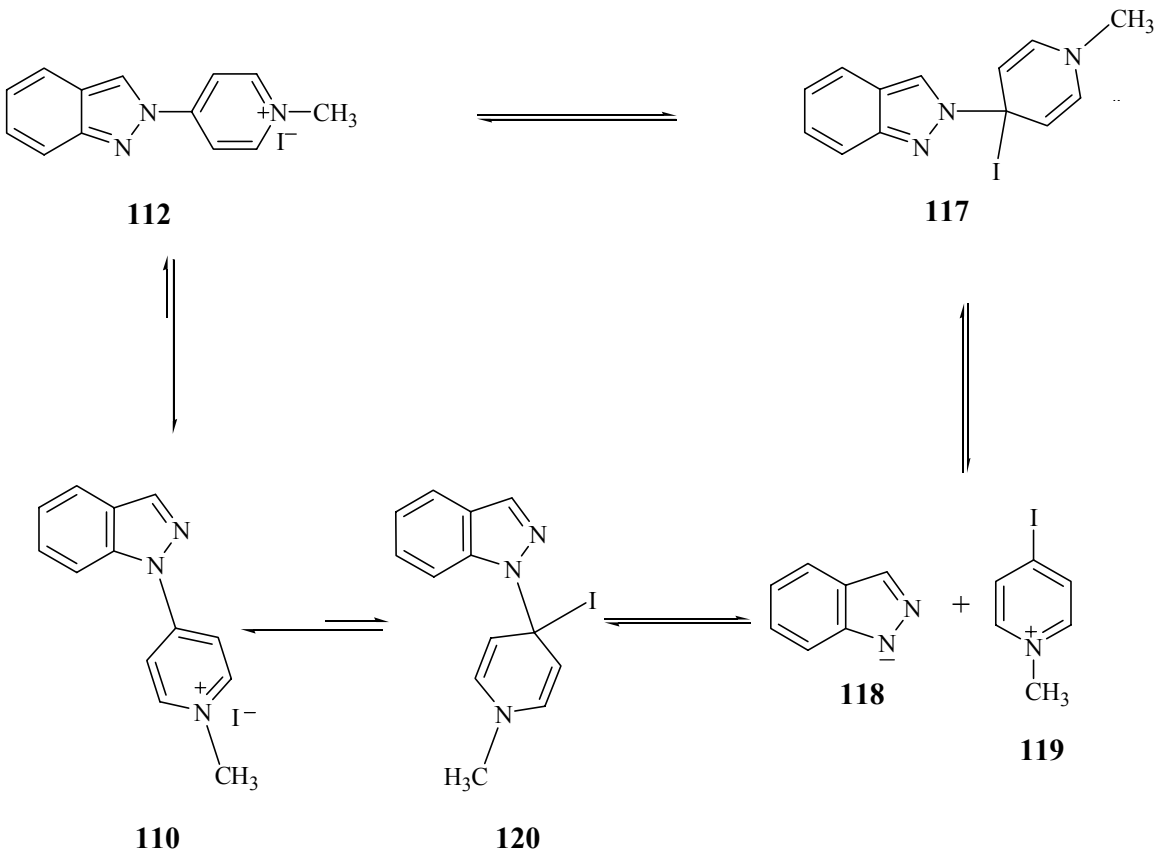

This pathway does not provide an explanation for the obligatory requirement of TMP as a catalyst. It is possible that TMP may act exclusively as a base and maintain indazole in the anionic form. In case the reaction mixture is contaminated with a trace amount of water, the presence of TMP will prevent the protonation of indazolyl anion. However, all of our efforts to exclude water from the reaction mixture failed to overcome the requirement for TMP. Furthermore, in the absence of base at 60 ^{o}C, the collapse of the tetrahedral intermediate **117** should be irreversible due to the anticipated protonation of indazolyl anion as shown in Scheme 36. If this were the case, the 2*H*-isomer **112** would be expected to decompose to indazole and 4-iodo-1-methylpyridinium when heated to 60 ^{o}C in DMF in the absence of TMP (Scheme 36). However, we have demonstrated that the 2*H*-isomer is stable in the absence of TMP even at 150 ^{o}C.

Scheme 36. Irreversible decomposition of 112 to indazole (44) and 119 in the presence of a trace amount of water via the formation of intermediate 117.

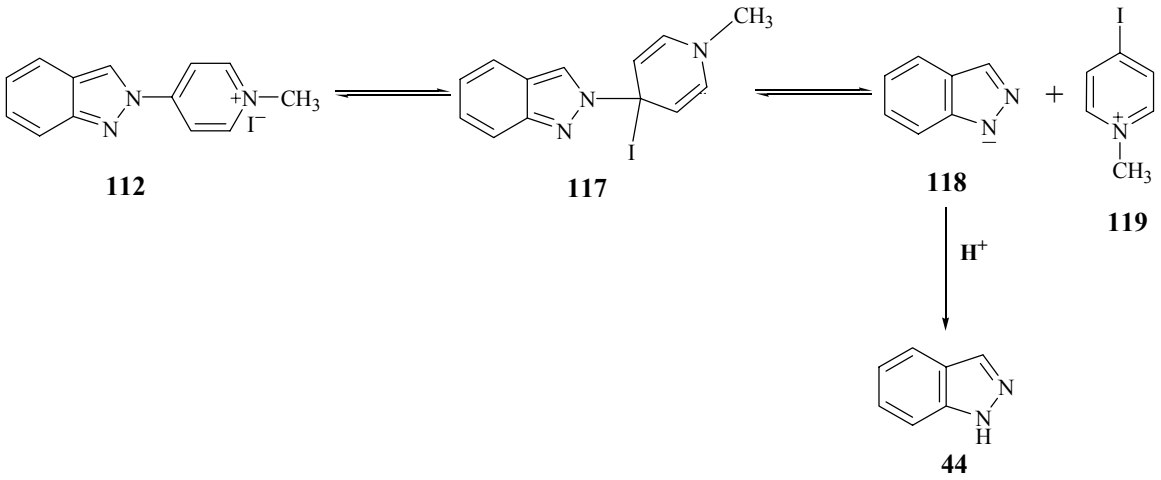

112 **117** **118** **119** **44**

3.2. Addition-Elimination of TMP

Since our results do not support the pathway described in Scheme 35, we considered an alternative mechanism in which TMP acts as a nucleophile instead of a base.[188] The attack of TMP at C-3 (or C-4 or C-6 or C-7a) of the indazolyl ring of the 2*H*-indazolylpyridinium species **112** can lead to the formation of the spirodiaziridinyl intermediate **121** which should collapse preferentially to form the more stable 1*H*-indazolylpyridinium **110**. The catalyst, TMP, is regenerated as shown in Scheme 37. (See Appendix 2 for Favorskii rearrangement which is an example of a rearrangement reaction also involving a three-membered ring as an intermediate).

[188] This alternative mechanism was pointed out initially by a reviewer of the manuscript cited in Reference 185.

Scheme 37. Addition of TMP to 2*H*-indazolylpyridinium 112 followed by elimination to form selectively 1*H*-indazolylpyridinium 110.

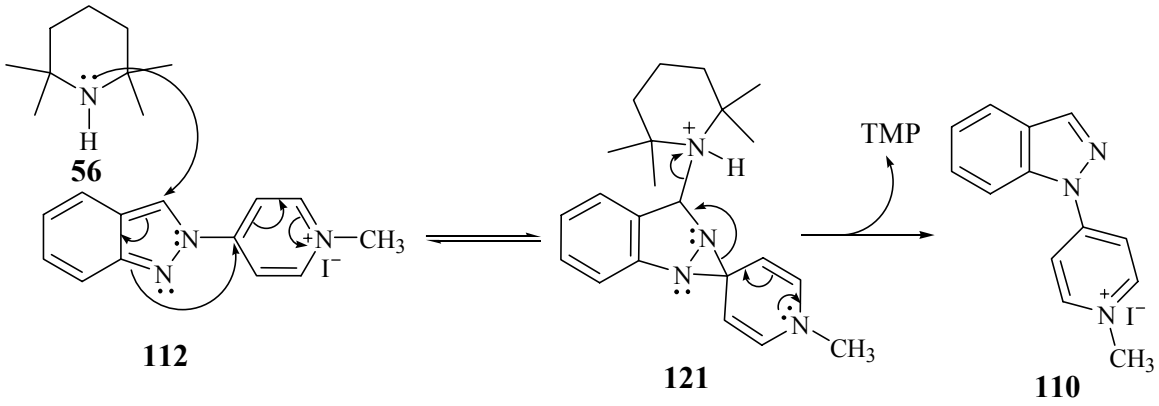

Although TMP is a sterically hindered base with low nucleophilicity, Michael addition reactions of TMP to electron-deficient acetylenes, which can be considered as a distant analogy to the first step of the rearrangement reaction shown in Scheme 37, have been reported previously in the literature.[189] For example, TMP adds to the acetylene **122** to form the corresponding α,β-unsaturated ester **123** (Scheme 38).

Scheme 38. Michael addition of TMP to activated acetylene 120 to form exclusively the *E*-isomer of 123.

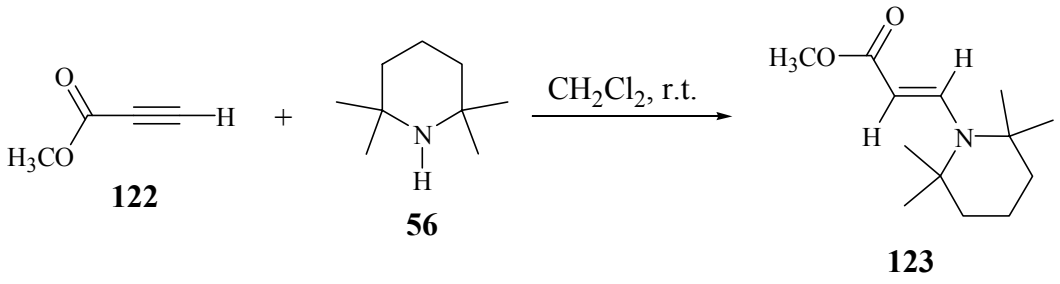

The above addition reaction results in the exclusive formation of the *E* isomer. However, the addition reaction between TMP and the disubstituted acetylene **124** gives

[189] Cossu, S., De Lucchi, O., Durr, R. (1996) Nucleophilic addition of highly hindered amines to electron-deficient acetylenes. *Synth. Commun*. **26**, 4597-4601.

exclusively the *Z* isomer **125** as shown in Scheme 39. This observation is of particular interest to us as will be discussed in detail in Section 4.3.

Scheme 39. Michael addition of TMP to activated acetylene 124 to form exclusively the *Z*-isomer of 125.

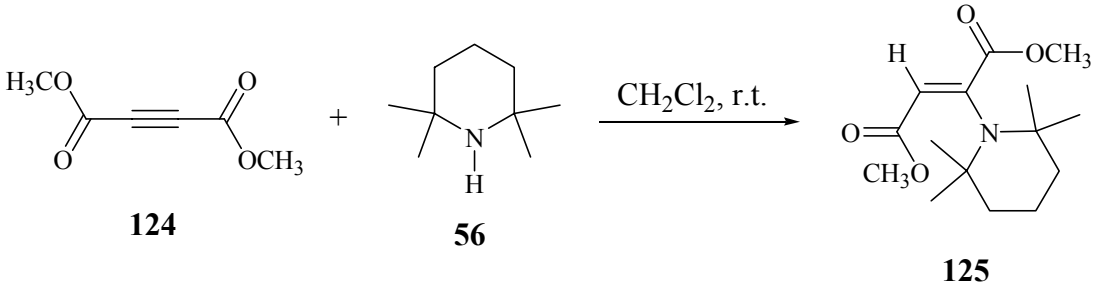

3.2.1. Comparison of the Possible Sites of Attack

The attack of TMP at the four possible sites, C-3, C-4, C-6 and C-7a, results in the formation of the corresponding putative intermediates **121**, **126**, **127** and **128,** all of which can collapse to give the 1*H*-indazolylpyridinium **110**.

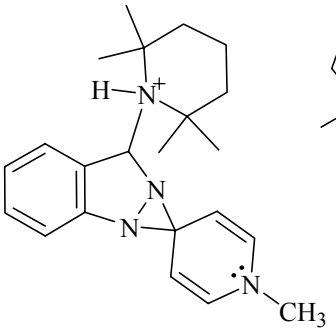

121

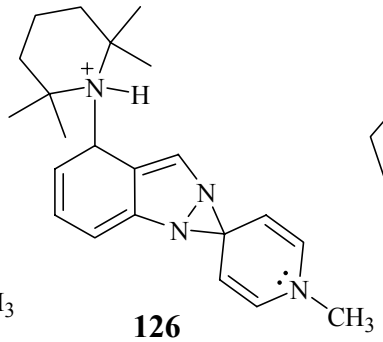

126

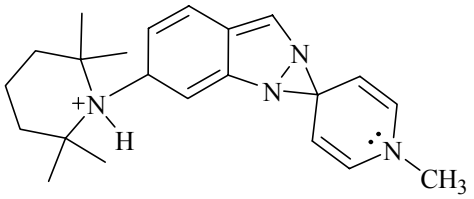

127

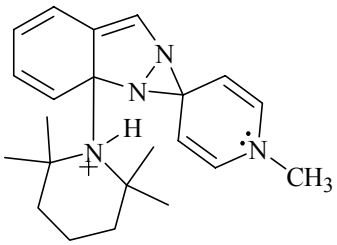

128

An examination of the possible intermediates shows that **121** possesses the benzenoid moiety whereas attack at C-4, C-6 or C-7a disrupts the aromaticity of the indazole system. The calculated enthalpy for the formation of each intermediate from **112** [$\Delta H_{rxn} = \Delta H_{intermediate} - (\Delta H_{\mathbf{112}} + \Delta H_{TMP})$], provide quantitative evidence for the stability of **121** over the other three possible intermediates (Table 3). This energy difference is comparable to the resonance stabilization energy of benzene which underlines the important stabilizing effect of the benzenoid moiety in **121**.

Table 3. The calculated energies of possible spirodiaziridinyl intermediates as precursors to 110.

	Calculated ΔH_{rxn} (kcal/mol) (Semi Empirical AM1)	**Calculated ΔH_{rxn} (kcal/mol) (ab initio 6-31G*)**
121	29	51
126	56	92
127	52	84
128	70	107

3.3. Kinetics of the Rearrangement Reaction

As supported by the molecular modeling calculations described in Section 3.2.1, the first step proposed for the rearrangement reaction involves nucleophilic attack by TMP, most likely at C-3, to form intermediate **121** (Scheme 37). After the formation of this high energy spirodiaziridinyl intermediate, the second step, involving the collapse of **121** to form irreversibly the thermodynamically stable 1*H*-isomer, is expected to be a rapid downhill process as shown in Figure 3. According to this analysis, the rate determining step of the rearrangement reaction is most likely to be the first step leading to intermediate **121**.

Figure 3. Proposed reaction progress vs. energy diagram for the rearrangement of 112 to 110.

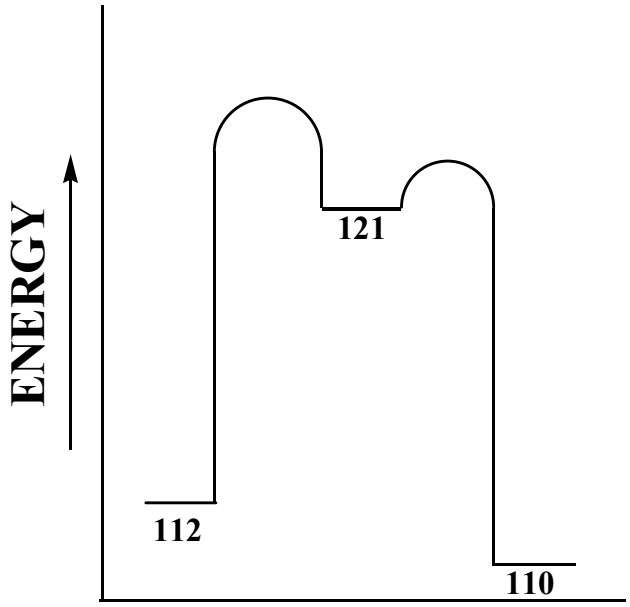

In an attempt to generate experimental support for this proposal, we undertook a kinetic study to determine the rate equation for the rearrangement reaction. The 2*H*-indazolylpyridinium species **112** was found not to be suitable for kinetic studies due to the poor HPLC separation of this compound and the corresponding 1*H*- isomer **110**. Instead, 4-(2*H*-6-bromoindazolyl)-1-methylpyridinium iodide (**174**)[190] was utilized. Compound **174** was baseline separated from the corresponding 1*H*- isomer **176** in the HPLC tracings.

The rate dependence of the rearrangement reaction on TMP concentration was investigated first in DMF at 90° C. The concentration of TMP was varied and the rate of formation of **176** was monitored by HPLC.[191] The rate did not increase linearly with TMP concentration. Furthermore, the rate of rearrangement in the presence of 2 equivalents of TMP was found to be slower than in the presence of 1 equivalent of TMP. These conflicting results led us to evaluate the stability of TMP in DMF at 90° C.

[190] Syntheses of the 1*H* and 2*H*-6-bromoindazolylpyridinium species will be described in detail in Section 3.5.2. Studies on 6-Bromoindazolylpyridinium Derivatives.
[191] In all of the kinetic studies, TMP was distilled prior to use.

Solutions of TMP in DMF were heated for 30 minutes, 1.5 hours and 2.5 hours at 90^{o} C before the addition to a solution of **174** in DMF. The HPLC tracings for the rearrangement reaction in the presence of 2 equivalents of TMP pre-heated for different periods of time are given in Figure. 4.

Figure 4. HPLC-DA tracings obtained for the rearrangement of 174 after 30 minutes at 90 ^{o}C in the presence of 2 equivalents of TMP pre-equilibrated for 30 minutes (a) and 2.5 hours (b).

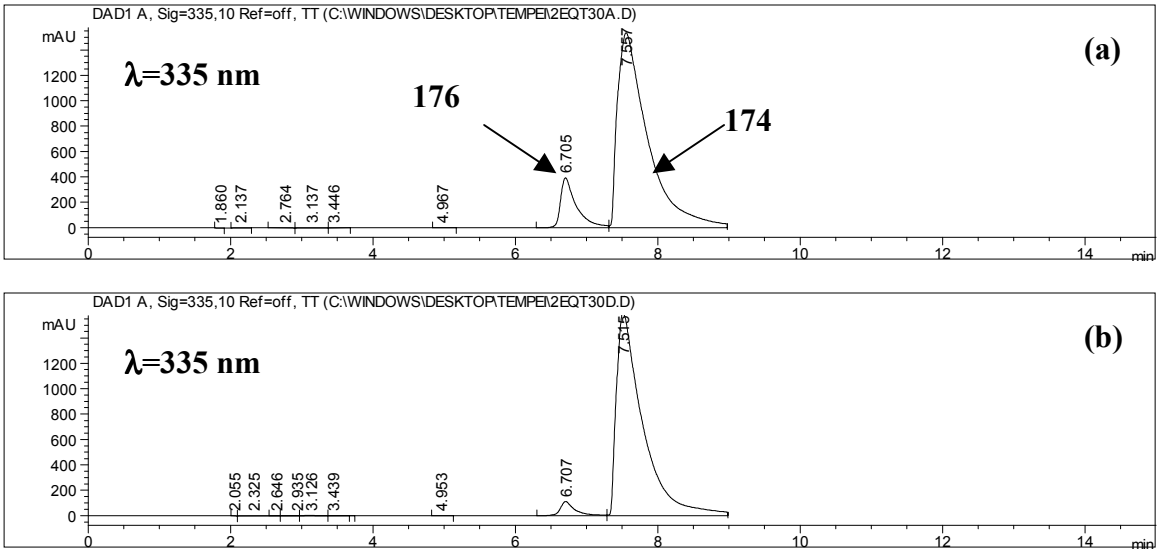

The results of this experiment showed that the amount of rearranged product decreased when TMP had been pre-heated. It appeared therefore, that TMP was not stable in DMF at high temperatures. The loss of TMP in the presence of DMF is likely to be due to the documented formylation reaction of TMP by DMF as shown in Scheme 40.[192]

[192] Takahashi, K., Shibagaki, M., Matsushita, H. (1988) Formylation of amines by dimethylformamide in the presence of hydrous zirconium oxide. *Agricultural and Biological Chemistry* **52**, 853-854.

Scheme 40. Formylation of TMP by DMF.

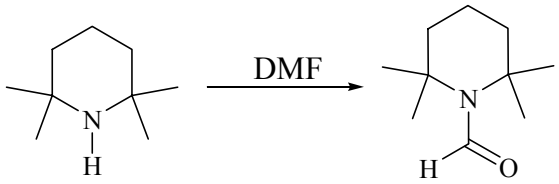

56 **129**

This finding led us to study the kinetics of the rearrangement reaction in DMSO instead of DMF. The rearrangement of **174** ($[\mathbf{174}]_{initial}$ = 0.01 M) was monitored in the presence of 0.001, 0.002, 0.003, 0.005, 0.01 and 0.02 M TMP. The amount of **174** converted to **176** versus time at these concentrations is shown in Figure 5. The initial rates were determined from the linear part of the plots (conversion of **174** to **176** was between 10 to 20 %).

Figure 5. Formation of 1*H*-isomer 176 over time at various TMP concentrations.

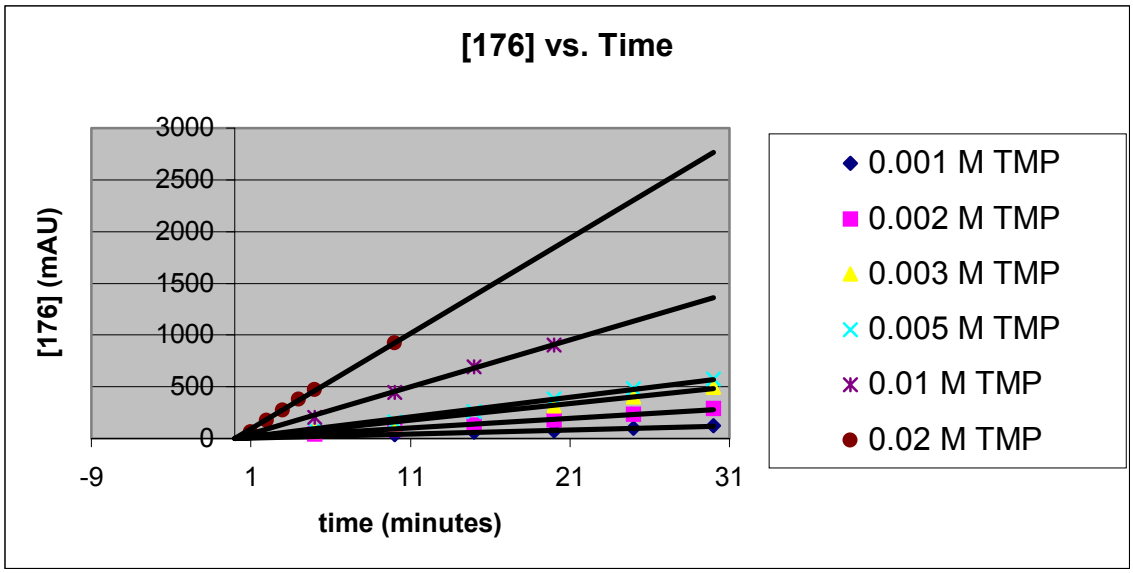

Figure 6. Rate of rearrangement vs. TMP concentration.

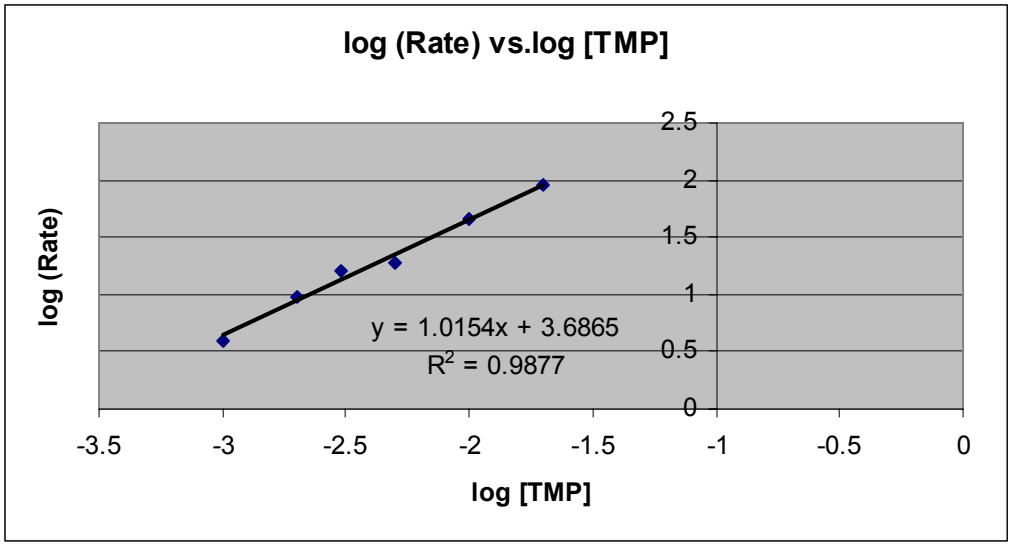

When the logarithm of the rate of the rearrangement was plotted versus the logarithm of TMP concentration, a straight line with a slope of 1 was obtained (Fig. 6). This outcome showed clearly that the rearrangement reaction was first order in TMP (rate = $k[TMP]^n$ and therefore log(rate) = logk + nlog [TMP] where k=rate constant, n=reaction order). In a separate set of experiments, the rate of the rearrangement reaction was measured as the concentration of **174** was varied at constant TMP concentration. The results of these experiments are summarized in Figures 7 and 8.

Figure 7. Formation of 1*H*-isomer 176 over time at various concentrations of 174.

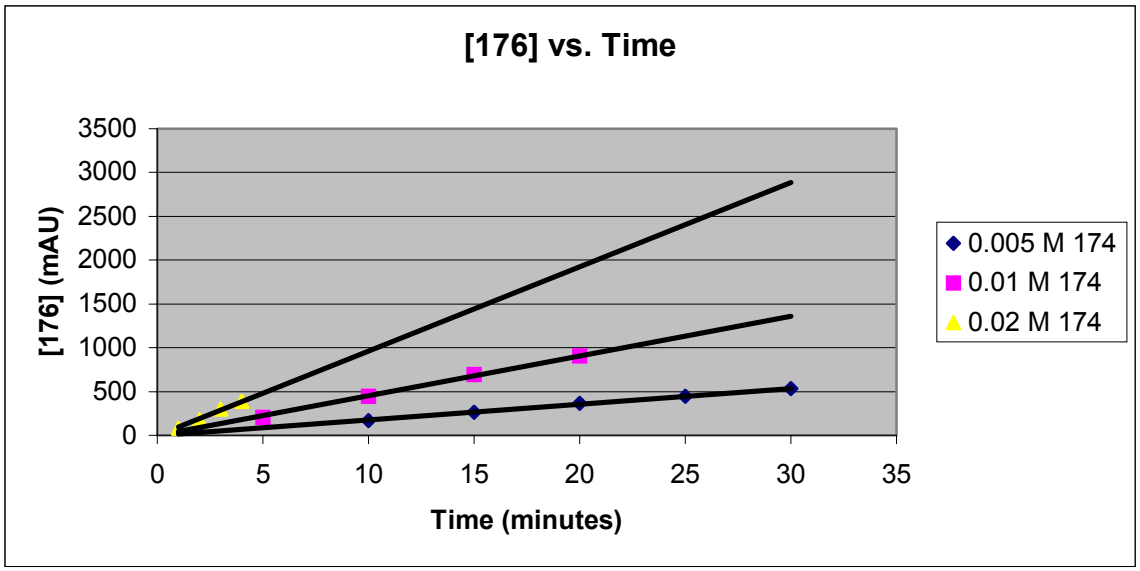

Figure 8. Rate of rearrangement vs. concentration of 174.

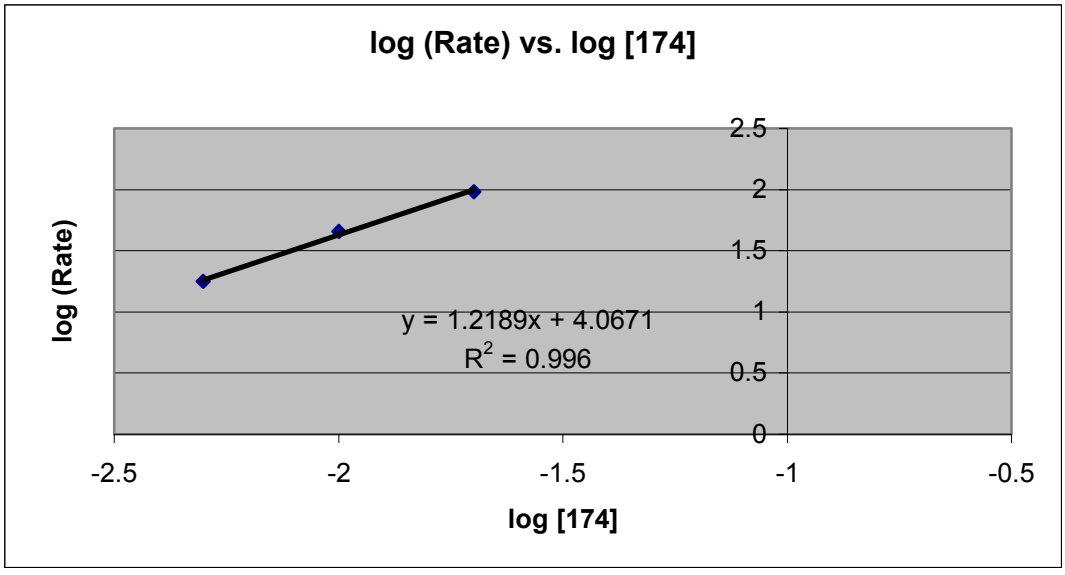

The results establish that the rearrangement reaction was first order also in **174** (Figs. 7 and 8). Consequently, this is a bimolecular reaction which is first order in the 2*H*- isomer and in TMP. This outcome is consistent with the pathway proposed in Scheme 37 involving the nucleophilic attack of TMP in the rate determining step.

3.4. The Effect of Different Bases on the Rearrangement Reaction

According to our proposed nucleophilic pathway, replacement of TMP with a less hindered, more nucleophilic amine with comparable basicity to TMP would be expected to increase the rate of the rearrangement reaction. Therefore, we examined the effect of piperidine (**130**) on the reaction rate. The 2*H*-indazolylpyridinium species **112** was treated with 1 equivalent of piperidine in DMF at room temperature and the reaction was monitored by HPLC-DA. The HPLC-DA tracings showed the rapid disappearance of the peak corresponding to **112**. However, instead of the expected formation of the 1*H*-isomer **110**, two new peaks appeared with retention times 3.58 minutes and 4.44 minutes. After 30 minutes the peak corresponding to **112** had disappeared completely and been replaced with the two new peaks (Fig. 9).

Figure 9. HPLC-DA monitoring of possible piperidine catalyzed rearrangement of 112.

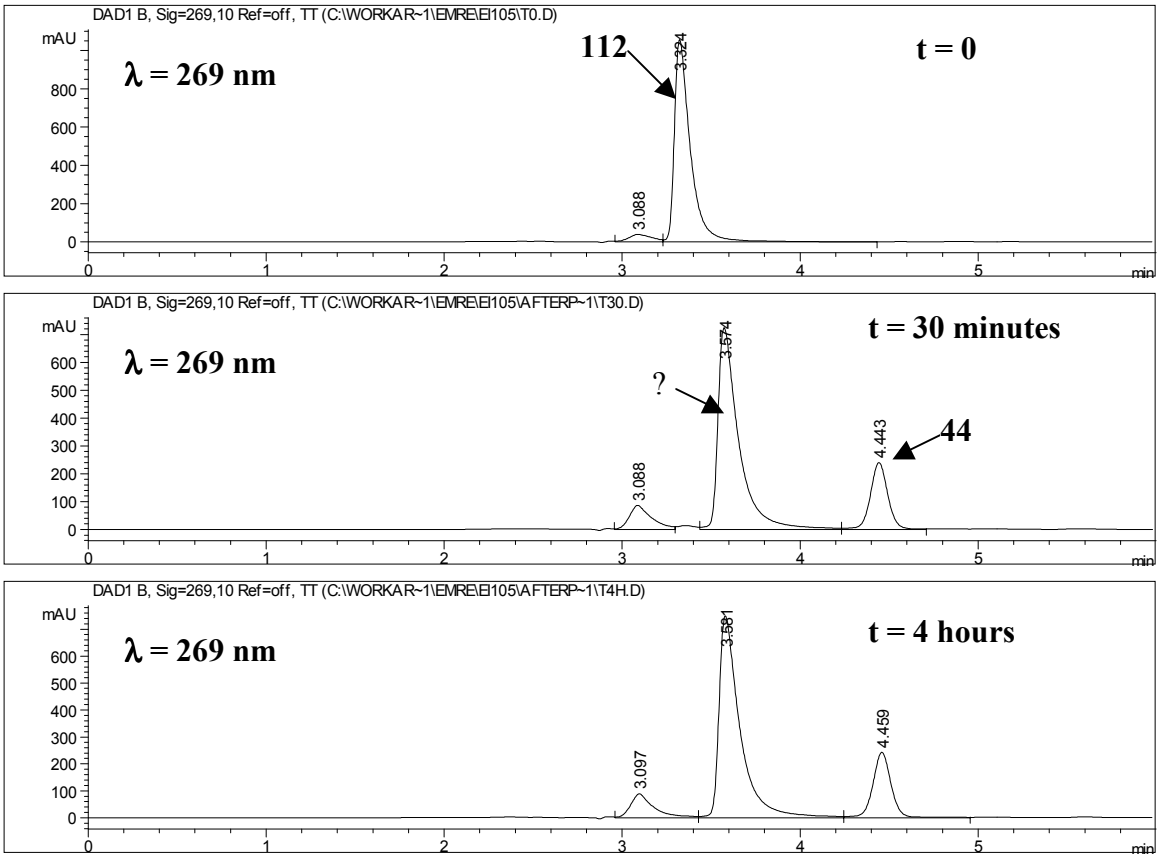

One of the two new peaks (t_R=4.44 min) showed an identical retention time and UV spectrum with that of indazole. This led us to consider the possibility of aminolysis of **112** via the attack of piperidine at C-4 of the pyridinium moiety to form intermediate **131**. The unstable intermediate **131** can collapse to give indazole and the 1-methyl-4-piperidin-1-ylpyridinium species **132** as shown in Scheme 41.

Scheme 41. Aminolysis of 112 in the presence of piperidine to give indazole and 132.

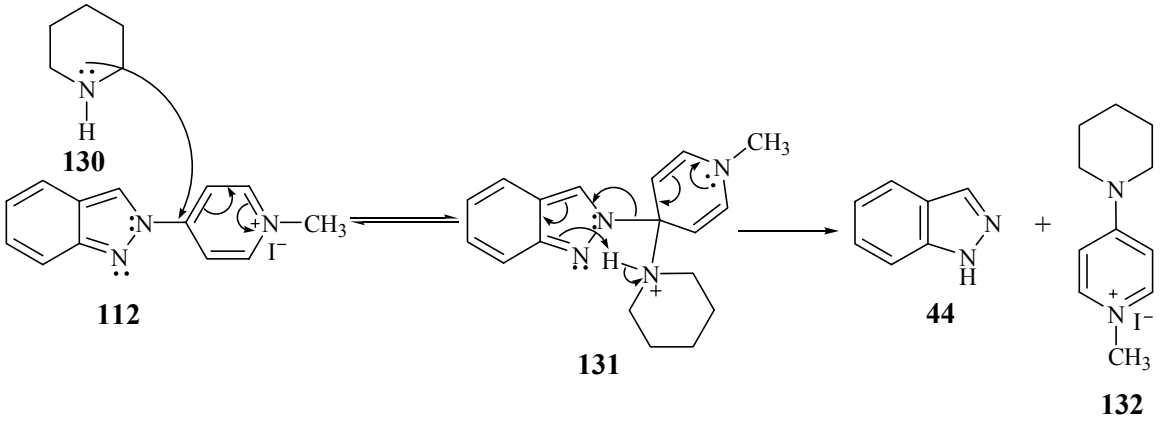

In order to assign unambiguously the structure of the second peak (t_R=3.58 min), compound **132** was prepared via the reaction of 4-chloro-1-methylpyridinium iodide (**55**) with piperidine (**130**) as shown in Scheme 42. HPLC-DA analysis showed that synthetic **132** had an identical retention time and UV spectrum with the peak eluting at 3.58 minutes. A precipitate was obtained from the reaction mixture upon addition of ether. The ^{1}H NMR spectrum of the isolated solid was identical to that of synthetic **132** confirming the formation of the aminolysis product **132**.

Scheme 42. Synthesis of 1-methyl-4-piperidin-1-ylpyridinium iodide (132).

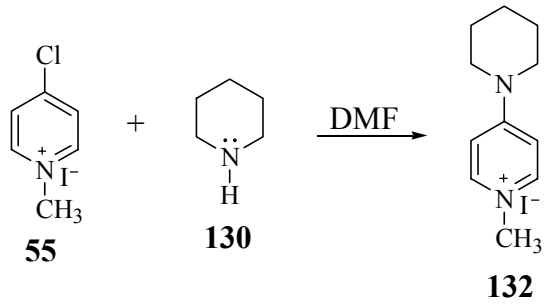

A second approach to this question involved triethylamine (**132**) as the catalyst. In this case, steric hindrance should prevent the attack at C-4 of the pyridinium moiety. Furthermore, triethylamine lacks the amine proton which is required for the irreversible decomposition of **134** via intramolecular proton transfer as shown in Scheme 43.

Scheme 43. Unfavorable decomposition of 112 in the presence of triethylamine.

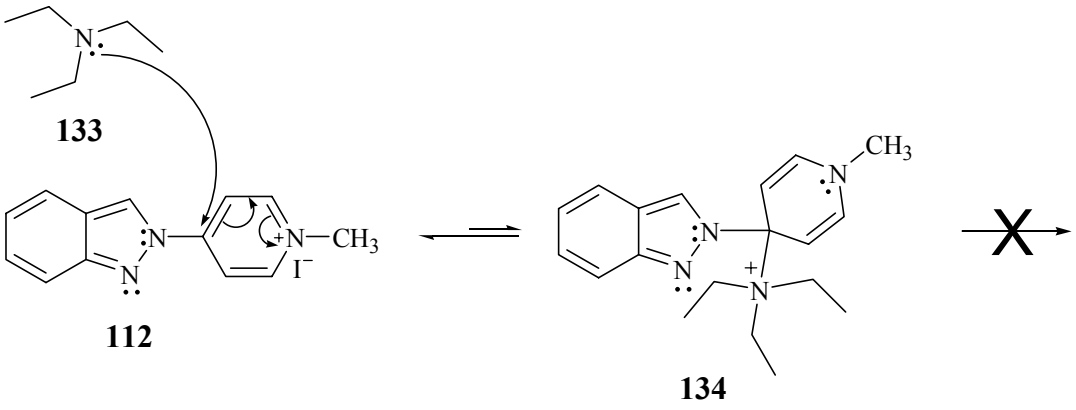

HPLC-DA tracings showed that **112** was stable at room temperature as well as at 60 ^{o}C in the presence of triethylamine (Fig. 10). The rearrangement reaction was found to proceed at a comparable rate with that obtained with TMP at 60^{o} C but only when the temperature was raised to 90 ^{o}C.

Figure 10. HPLC-DA monitoring of triethylamine catalyzed rearrangement of 112.

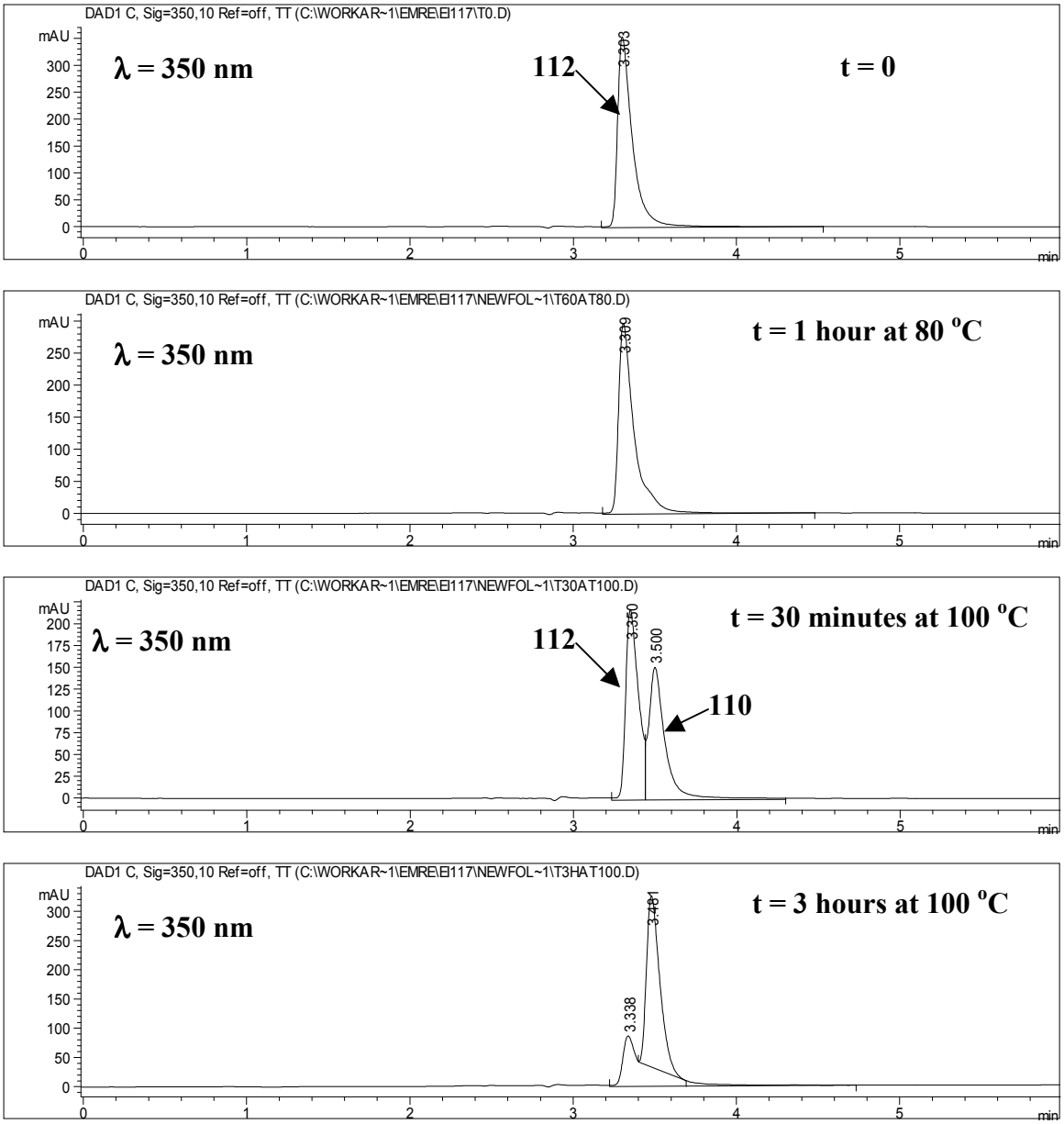

When the rearrangement reaction was attempted in the presence of 1,4-diazabicyclo[2.2.2]octane [DABCO (**135**)], rate of rearrangement comparable to that of triethylamine was obtained at 90 °C. The use of 1,4-dithiane (**136**) did not result in the rearrangement reaction even at 90 °C. An attempt to compare the rate of rearrangement in the presence of triethylamine versus DABCO by ^{1}H NMR showed that the rearrangement was taking place more readily in the presence of DABCO than it was in triethylamine.

135

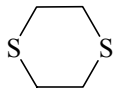

136

The heats of reaction for the formation of the expected intermediates **121**, **137**, **138** and **139** upon attack by TMP, triethylamine, DABCO, or 1,4-dithiane respectively, at C-3 of 2*H*-indazolylpyridinium **112** [$\Delta H_{rxn} = \Delta H_{intermediate} - (\Delta H_{\mathbf{112}} + \Delta H_{attackng\ species})$] were calculated. On the basis of the calculated energies, the rearrangement in the presence of DABCO is expected to take place at a rate at least comparable to that observed with TMP. However, TMP, a secondary amine, is likely to be more nucleophilic than DABCO, a tertiary amine, resulting in a faster rate of rearrangement. When the rates of rearrangement observed in the presence of the two tertiary amines are compared, triethylamine reacts slower than DABCO due to the higher energy requirement for the formation of the sterically more hindered intermediate **137** compared to intermediate **138**. It is likely that the poor nucleophilicity of 1,4-dithiane makes the attack at C-3 unfeasible, preventing the rearrangement reaction to take place.

Table 4. Calculated heats of reaction for the expected formation of intermediates upon attack by various bases.

	Calculated ΔH_{rxn} (kcal/mol) (Semi Empirical AM1)	**Calculated ΔH_{rxn} (kcal/mol) (ab initio 6-31G*)**
121	29	51
137	36.5	40
138	29	35
139	19	Not available

3.5. Investigation of the Site of TMP Attack

The results presented so far are consistent with a nucleophilic pathway for the rearrangement reaction. However, there is not sufficient evidence to identify unambiguously the site of nucleophilic attack. Although the attack of TMP at C-3, C-4, C-6 or C-7a is possible, energy considerations suggest that the most likely site of attack is C-3. Therefore, we decided to examine the effect of substitution at the C-3 position on the rate of the rearrangement reaction. The preparation of the targeted 3-substituted indazolylpyridinium derivatives and their rearrangement reactions are described in the following section.

3.5.1. Studies on the 3-Substituted Indazolylpyridinium Derivatives

If C-3 of the indazolyl ring is the site of attack, increasing the steric hindrance at this position via substitution may prevent or slow down the rearrangement reaction. In order to investigate this possibility, we undertook the syntheses of the 3-methyl and 3-bromo substituted 2*H*-indazolylpyridinium derivatives **140** and **141**, respectively.

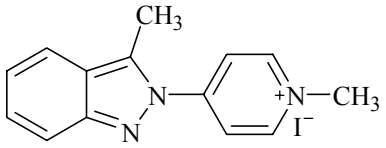

140

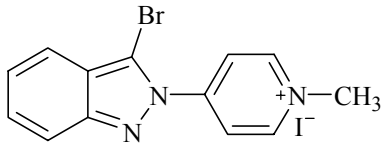

141

For the preparation of **140** and **141** advantage was taken of the regiospecific syntheses developed for 1*H*- and 2*H*-indazolylpyridinium derivatives **110** and **112**. The reaction between 3-substituted indazoles **142** and **143** and 4-chloro-1-methylpyridinium iodide (**55**) in the presence of excess TMP at 60 ^{o}C was expected to give exclusively the 1*H*-indazolylpyridinium products **144** and **145**. On the other hand the 2*H*-indazolylpyridinium analogs **140** and **141** were expected to be the only products when the reactions were carried out in the absence of TMP at 100 ^{o}C (Scheme 44).

Scheme 44. Proposed synthetic route to 1*H*- and 2*H*-3-substituted indazolylpyridiniums.

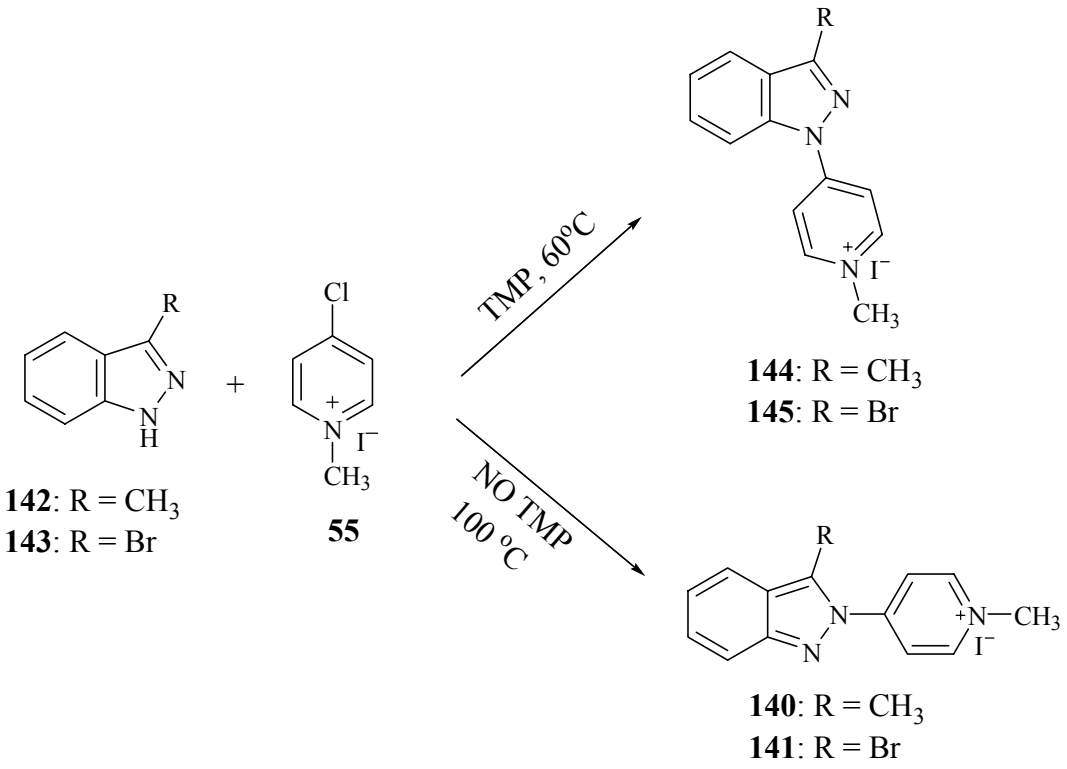

The synthesis of 3-bromoindazole (**143**) was achieved via the reported selective bromination of indazole at C-3 using bromine/dioxane complex as shown in Scheme 45.[193]

Scheme 45. Selective bromination of indazole to yield 3-bromoindazole (143).

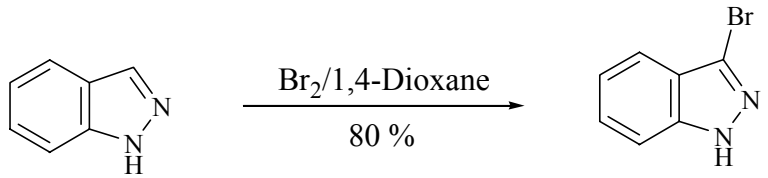

44 **143**

[193] Pozhanskii, F.T., Sayopin, V.G., Martsokha, B.K. (1964) Halogenation of indazole and its derivatives by complex compounds of halogens with dioxane. *Zhurnal Obshchei Khimii* **34**, 2777-2778.

The reaction shown in Scheme 44 is thought to proceed through the bromonium species **145** which is formed by the reaction between 1,4-dioxane (**144**) and bromine as shown in Scheme 46.

Scheme 46. Formation of brominating agent 145.

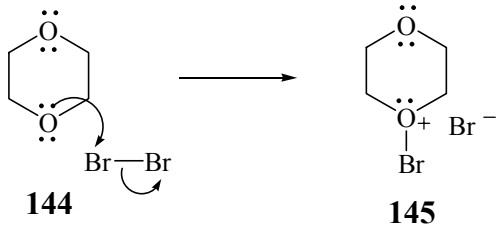

The increased reactivity at the C-3 position of indazole in electrophilic aromatic substitution reactions is expected due to the stability of intermediate **146** in which the 6 π electron system is retained as shown in Scheme 47.

Scheme 47. Regioselective bromination of indazole (44) at C-3.

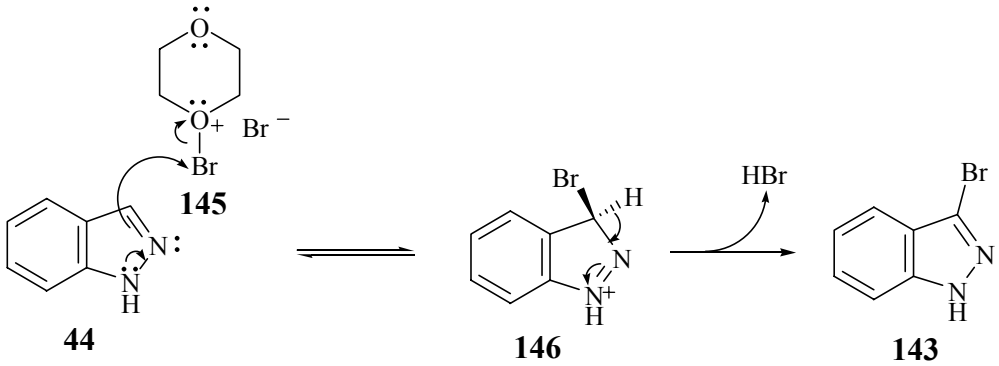

The synthesis of the 3-methyl analog **142** was attempted via a lithium-bromine exchange reaction using *sec*-butyllithium and *t*-butyllithium followed by quenching with iodomethane as described in the literature.[194] The addition of *t*-butyllithium was carried out –78^{o} C and the temperature was kept between –70 ^{o}C to –65 ^{o}C during the iodomethane addition. After working-up the reaction mixture the GC-MS tracing

[194] Welch, W.M., Hanau, C.E., Whalen, W.M. (1992) A novel synthesis of 3-substituted indazole derivatives. *Synthesis* **10**, 937-939.

suggested the presence of the N-methyl (**147**), 1,3-dimethyl (**148**) and indazole (**44**) in addition to the desired 3-methylindazole (**142**) as shown in Scheme 48.

Scheme 48. Methylation of 3-bromoindazole (143) resulting in a mixture of products.

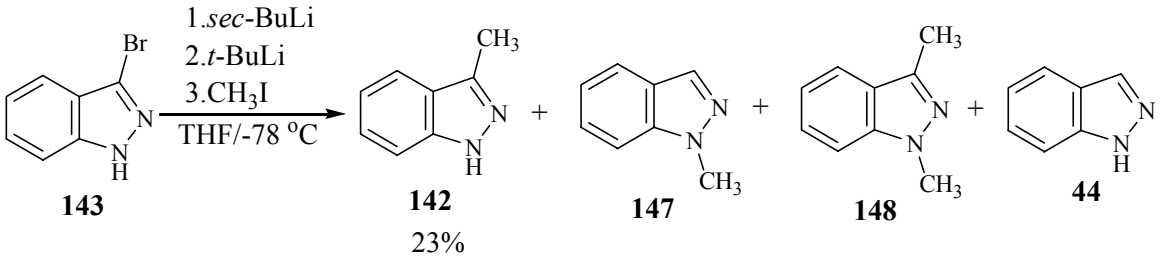

The outcome of the reaction shown in Scheme 48 suggested, that even at temperatures as low as –70° C, methylation takes place at C-3 as well as N-1 to give **142**, **147** and **148**. An alternative and more efficient pathway to 3-methylindazole was examined.[195] Diazotization of 3-ethylaniline (**149**) using sodium nitrite in fluoroboric acid gave the corresponding fluoroborate salt **150** in good yield. Treatment of the fluoroborate salt with potassium acetate in chloroform in the presence of 18-crown-6 resulted in the cyclization of the starting diazonium intermediate to give 3-methylindazole in 72 % yield as shown in Scheme 49.

Scheme 49. Synthesis of 3-methylindazole via the cyclization of the diazonium salt 150.

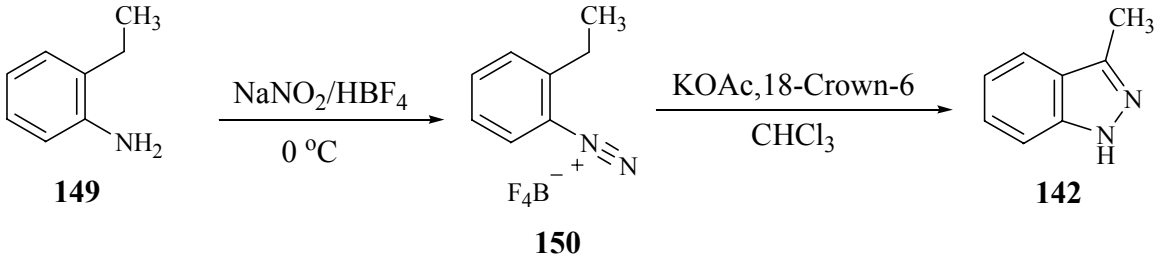

[195]Bartsch, R.A., Yang, I.-W. (1984) Phase transfer catalysis of indazoles from *o*-alkylbenzenediazonium tetrafluoroborates. *J. Heterocyclic Chem.* **21**, 1063-1064.

The reaction of **142** with 4-chloro-1-methylpyridinium iodide (**55**) in the absence of base in DMF was expected to give **140** through the formation of the charge delocalized intermediate **151** as shown in Scheme 50. The presence of the methyl substituent at C-3 was expected to stabilize **151** further, favoring the product formation.

Scheme 50. Formation of the stabilized intermediate 151 leading to the 2*H*-3-methylindazolylpyridinium 140.

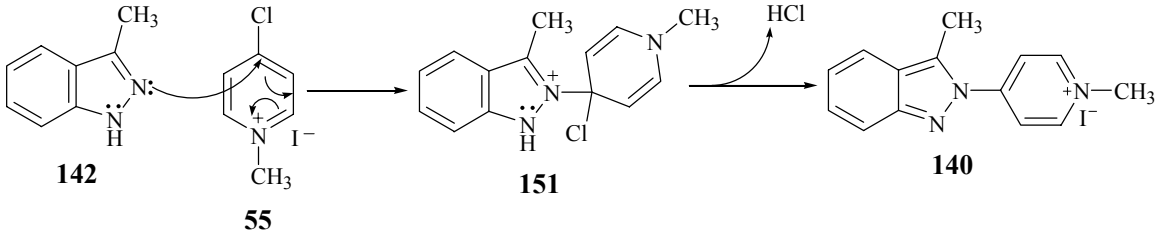

HPLC-DA monitoring of the reaction between 3-methylindazole (**142**) and **55** in the absence of TMP at 100 ^{o}C showed the very slow disappearance of the peak corresponding to 3-methylindazole (t_R= 5.06 min) and the appearance of one major (t_R=3.93 min) and one minor peak (t_R=3.35 min) as shown in Figure 11. Even after 2 days at 100 ^{0}C approximately 75 % of the starting 3-methylindazole remained unreacted.

Figure 11. HPLC-DA monitoring of the reaction between 3-methylindazole and 55 in the absence of TMP at 100 °C at two different wavelengths.

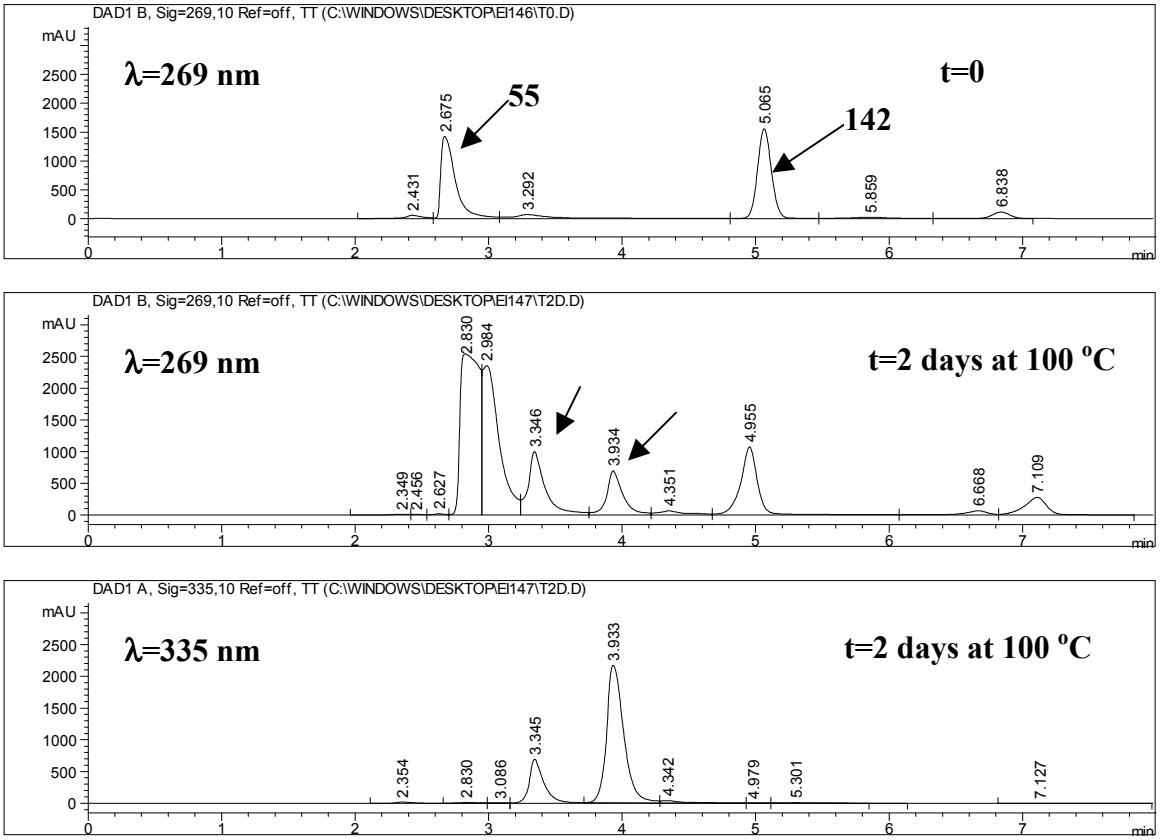

The decrease in the rate of the reaction compared to the parent indazole (**44**) can be attributed to the steric hindrance exerted by the methyl group at C-3 of **142**. Although the methyl group is expected to stabilize the positively charged intermediate **151**, the unfavored steric interactions appear to counter this stabilizing effect.

Based on our previous observations we assumed that the major product peak (t_R=4.17 min) was the 2*H*-isomer **140**. The appearance of a second peak was unexpected. We proposed that the minor peak may be the 1*H*-isomer **144**.

In order to confirm the proposed structure of the minor product we undertook the preparation of the 1*H*-3-methylindazolylpyridinium **144** via the reaction of 3-methylindazole (**142**) with **55** in the presence of TMP at room temperature. The HPLC-DA tracing obtained after 30 minutes at room temperature showed the appearance of a single product with a retention time of 3.92 minutes (Fig. 12). A solid subsequently separated from the reaction mixture.

Figure 12. HPLC-DA monitoring of the reaction between 3-methylindazole and 55 in the presence of TMP at room temperature.

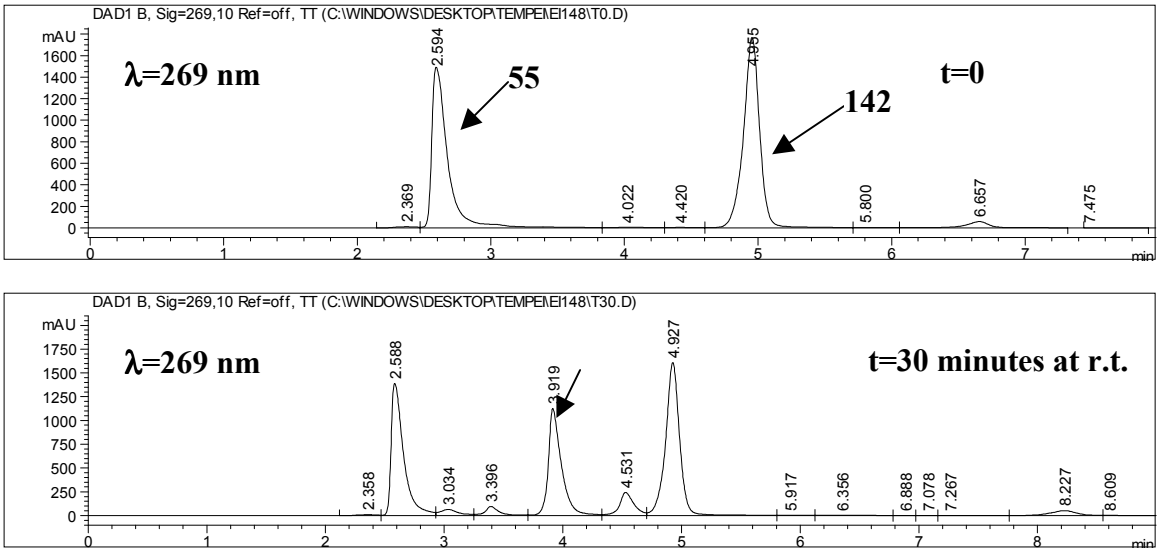

The retention time and UV spectrum of this product corresponded to the major peak rather than the minor peak observed in the HPLC-DA tracings obtained from the reaction in the absence of TMP. The product was isolated and the ^{1}H NMR spectrum obtained (Fig. 13) was consistent with the 1*H*-isomer **144**.

Figure 13. ^{1}H NMR spectrum (500 MHz) of the product obtained from the reaction between 3-methylindazole and 55 in the presence of base with tentative peak assignments.

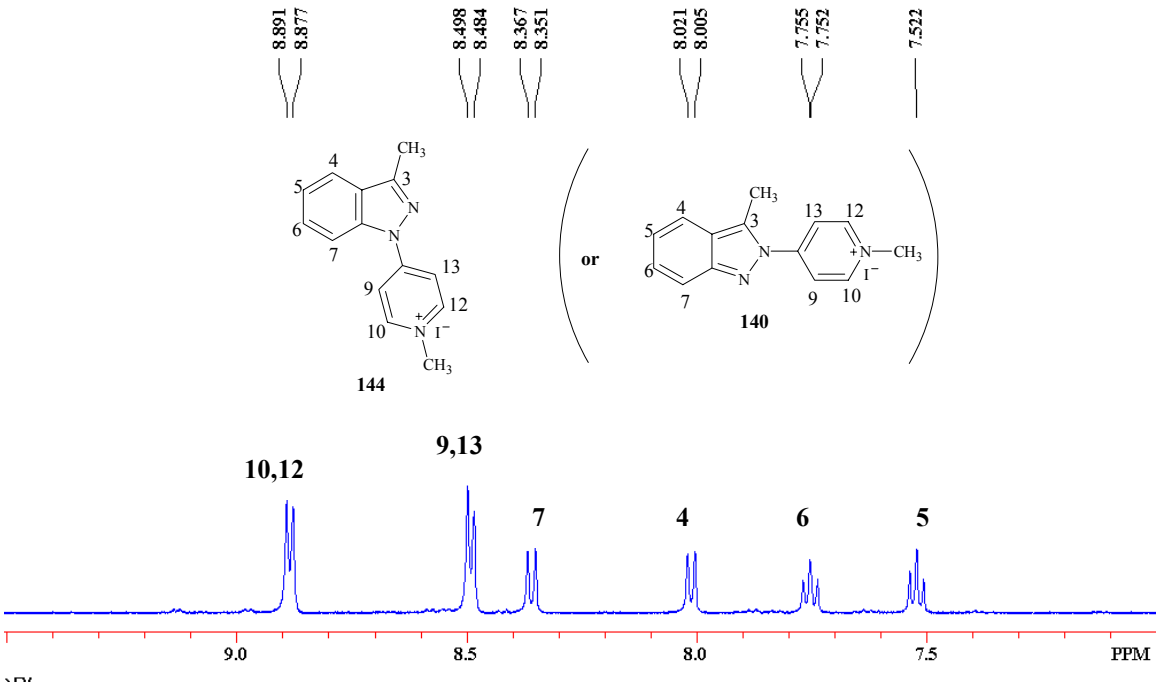

A DPFGSE NOE ^{1}H NMR experiment also was performed to confirm the regiochemistry of the product. The irradiation of the signal corresponding to the protons attached to the C-9 and C-13 of the pyridinium ring resulted in an enhancement for the signal corresponding to the proton attached to the C-7 of the indazolyl ring, consistent with the 1*H*-isomer **144** (Fig. 14).

Figure 14. Irradiation of protons attached to C-9 and C-13 resulting in an enhancement for proton attached to C-7.

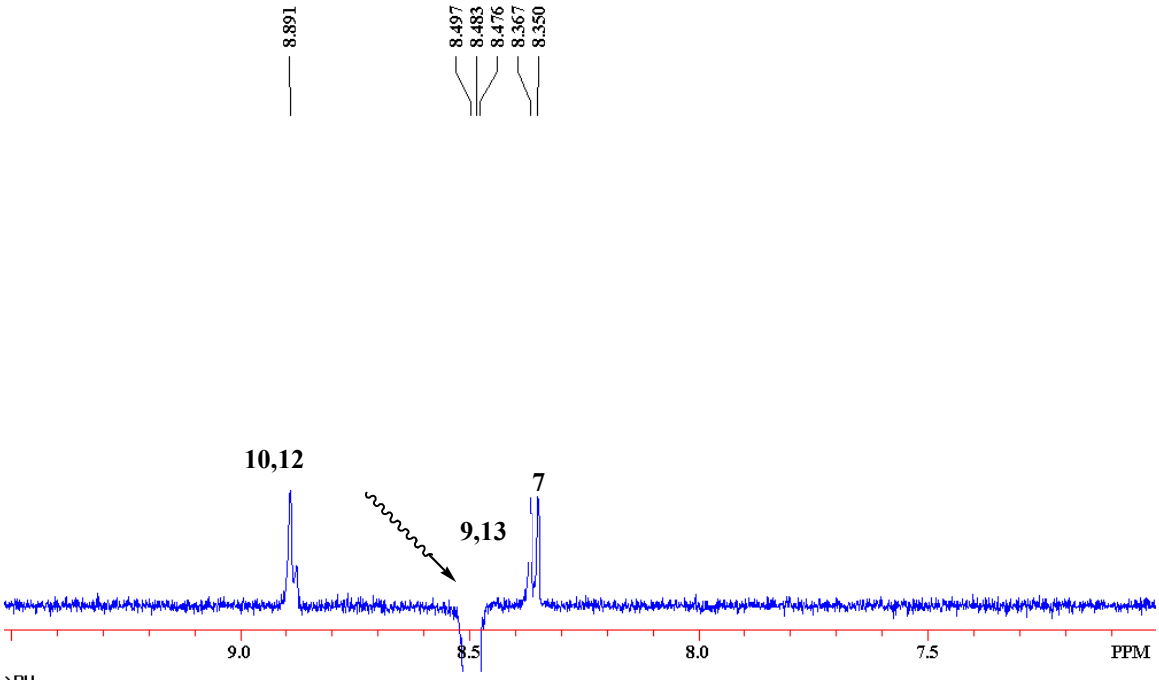

Another irradiation experiment was carried out to provide additional structure evidence. The irradiation of the peak corresponding to the proton attached to C-4 (the doublet which did not show any enhancement in the previous experiment) resulted in an enhancement for the peak at 7.52 ppm (Fig. 15). This allowed us to distinguish between the peaks corresponding to the protons attached to C-5 (7.52 ppm) and C-6 (7.75 ppm), both of which appear as triplets.

Figure 15. Assignment of the peaks to the protons attached to C-5 and C-6 via the irradiation of the peak corresponding to the proton attached to C-4.

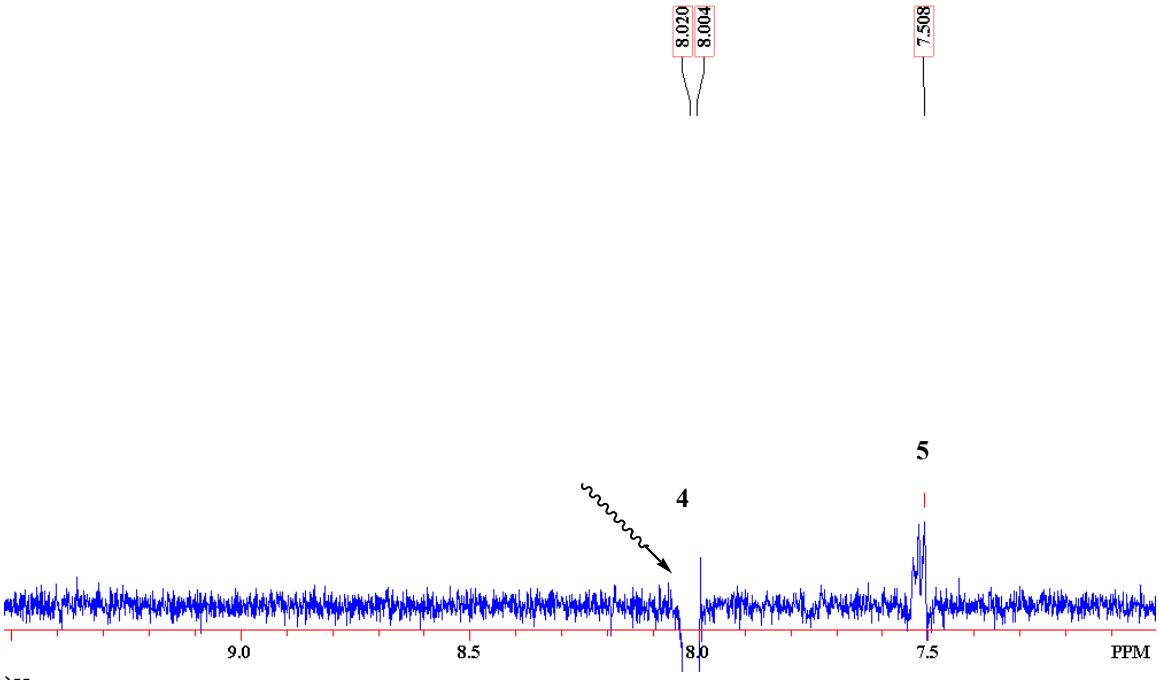

According to these observations, 4-(1*H*-3-methlindazolyl)-1-methylpyridinium iodide (**144**) is the only product obtained from the reaction between 3-methylindazole and **55** in the presence of TMP at room temperature as shown in Scheme 51.

Scheme 51. Formation of the 1*H*-3-methylindazolylpyridinium 144 from the reaction between 3-methylindazole and 55 in the presence of TMP at room temperature.

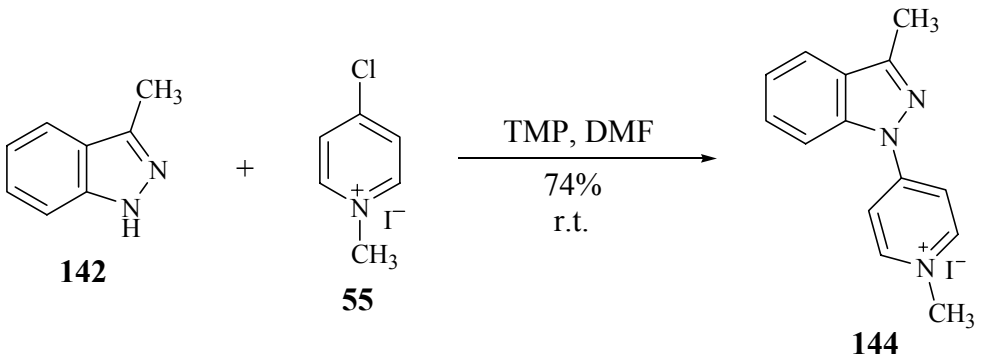

The exclusive formation of the 1*H*-isomer in the presence of TMP at room temperature can be rationalized by the decreased reactivity of the sterically hindered N-2 nitrogen atom. This is consistent with the slow rate of reaction observed when TMP is excluded from the reaction. However, the formation of the 1*H*-isomer as the major product in the absence of base was unexpected based on the previous results obtained for the reaction between indazole (**44**) and **55** in the absence of base. This outcome led us to investigate the kinetics of the coupling reaction in an attempt to confirm that the neutral 3-methylindazole is the species participating in the rate determining step of the nucleophilic aromatic substitution reaction as expected. The reaction between **142** and **55** ($[\mathbf{55}]_{initial}$ = 0.25 M) in the absence of TMP was carried out in the presence of 0.25 and 0.5 M 3-methylindazole. The rate of the reaction was monitored by HPLC-DA. The resulting initial rates (consumption of 3-methylindazole after 2 hours was 12 % and 20 % , respectively, for $[\mathbf{142}]_{initial}$ = 0.25 M and 0.5 M) of the reaction are shown in Fig. 16.

Figure 16. Rate of reaction between 142 and 55 in the presence of 0.25 and 0.5 M 3-methylindazole.

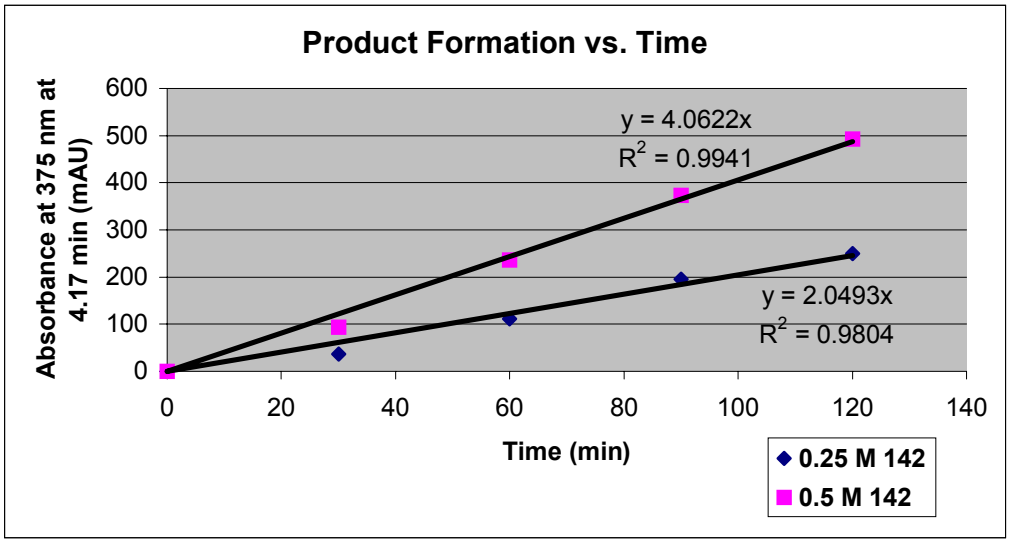

The rate of the reaction doubled when the concentration of **142** was increased from 0.25 M to 0.5 M. The reaction, therefore, is first order in 3-methylindazole. Consistent with this analysis, one rationale for the formation of the 1*H*-isomer **144** as the

major product in the absence of base is the attack of the N-1 nitrogen of 3-methylindazole to form intermediate **152** which will give the 1*H*- isomer **144** (Scheme 52). However, considering the high energy of the charge localized intermediate **152**, this pathway seems unlikely. Furthermore, the analogous reaction between indazole (**44**) and **55** in the absence of TMP at 100 ^{o}C had not proceeded to a detectable level suggesting that the energy requirement for the formation of the charged intermediate involving attack by N-1 of **44** could not be met under reaction conditions similar to those encountered in the corresponding reaction with 3-methylindazole.

Scheme 52. Formation of 144 in the absence of TMP through intermediate 152.

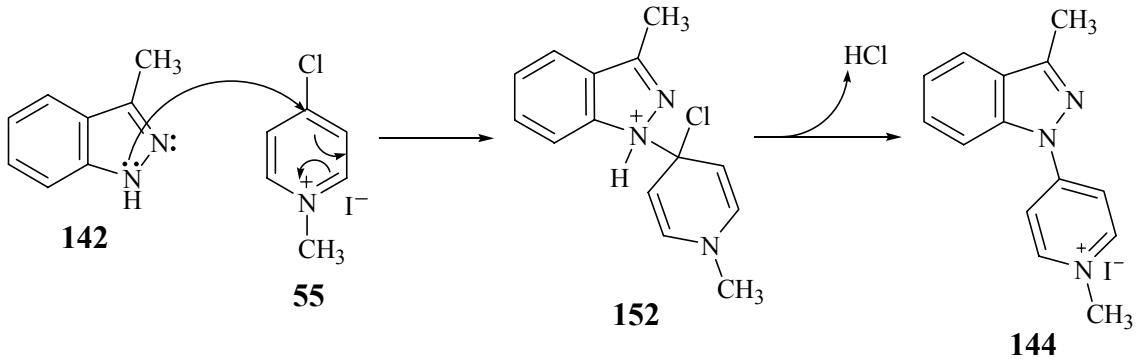

This evaluation led us to consider the formation of the 2*H*-isomer **140** as the initial product of the reaction between **142** and **55** followed by a spontaneous thermal rearrangement to the stable 1*H*-isomer **144**. In the absence of base, the rearrangement reaction should proceed through the benzylic tertiary carbocation intermediate **153** as shown in Scheme 53.

Scheme 53. Proposed formation of the 1*H*-3-methylindazolylpyridinium species 144 via the spontaneous thermal rearrangement of the 2*H*-isomer 140.

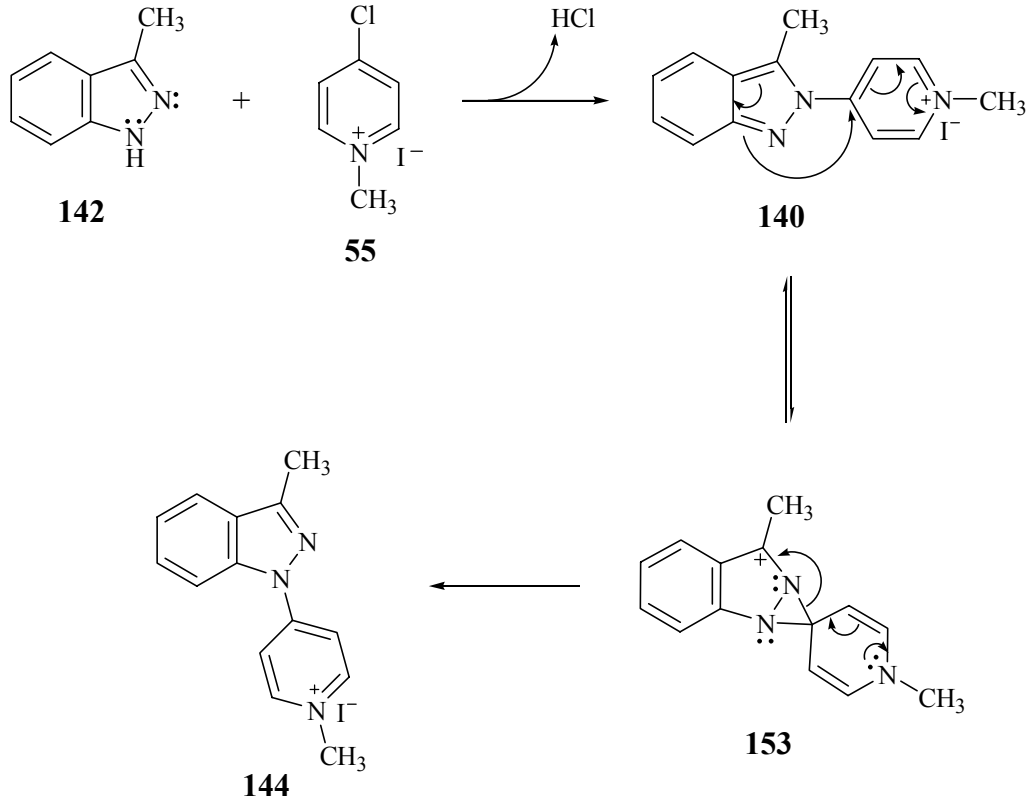

The enthalpies of reaction for the formation of **153** from **140** ($\Delta H_{rxn} = \Delta H_{\mathbf{153}} - \Delta H_{\mathbf{140}}$) and hypothetical intermediate **154** that will be derived from 4-(2*H*-protioindazolyl)-1-methylpyridinium iodide [**112** ($\Delta H_{rxn} = \Delta H_{\mathbf{154}} - \Delta H_{\mathbf{112}}$)] were calculated[196] and the additional stabilization introduced by the methyl group was estimated to be 6 kcal/mol. Although our results had demonstrated unambiguously the requirement of TMP for the rearrangement reaction of the 2*H*-protioindazolylpyridinium **112**, it is possible that the rearrangement of **140** may take place in the absence of base due to this additional stabilization. This additional stabilizing factor is not present in **154** where the attack by TMP is obligatory to mount the energy barrier for the rearrangement reaction to take place.

[196] Bond elongation was observed for intermediates **153** and **154** upon minimization at the semi empirical AM1 level. Therefore single point energies were calculated at AM1 level following molecular mechanics (MM) minimization.

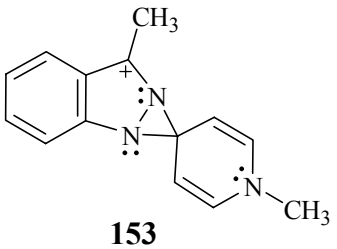

153

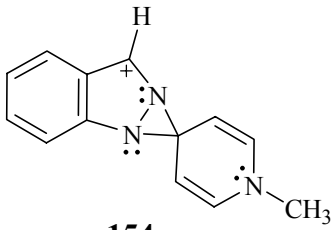

154

In order to evaluate the possibility of such a spontaneous rearrangement reaction, attention was turned to the isolation of the 2*H*-3-methylindazolylpyridinium species **140** which we assumed was the minor product observed in the reaction between 3-methylindazole and **55** in the absence of TMP (Fig. 11). Preparative HPLC (10 injections) provided a solution of what appeared to be a sample of **140** free of the 1*H*-isomer **144** (Fig. 17a). The mobile phase (50% acetonitrile, 50% pH 4.7 aqueous containing 1% triethylamine and 0.6% acetic acid) was evaporated under vacuum at 60 ^{o}C to yield a pink residue. The residue was analyzed by HPLC-DA to confirm the purity of the material. Indeed a single peak was observed in the HPLC-DA tracing (Fig. 17b). Much to our surprise, however, the retention time of this peak corresponded to the retention time of the major product of the reaction (characterized as the 1*H*-isomer **144**) but not to the retention time of the minor product.

Figure 17. HPLC-DA analysis of the collected fractions before (a) and after (b) evaporation of the solvent.

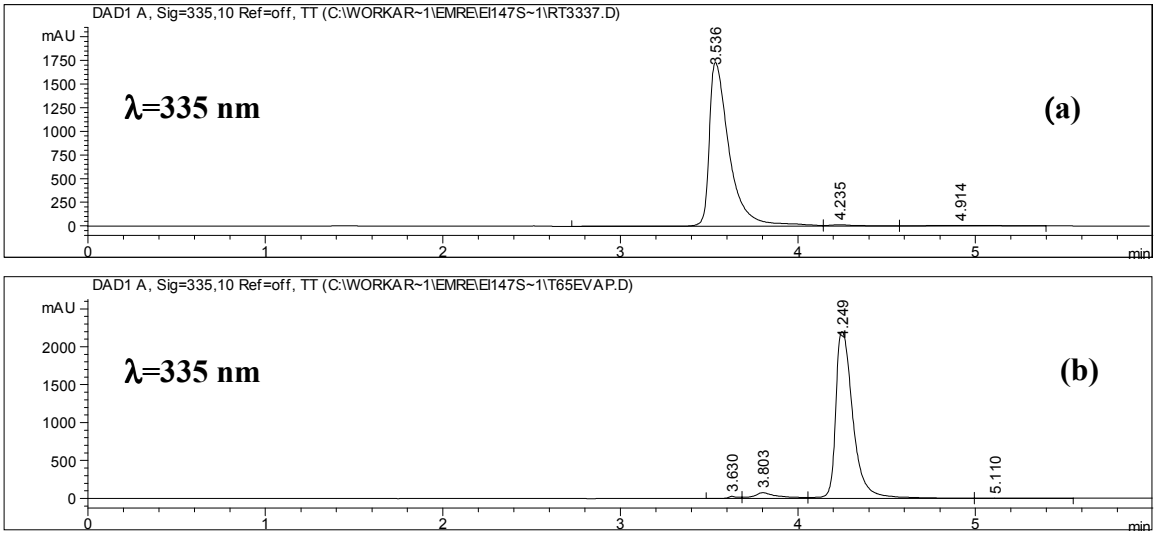

One possible explanation of this behavior was the spontaneous thermal rearrangement of the 2*H*-3-methylindazolylpyridinium species **140** to the 1*H*-isomer **144** during the evaporation of the mobile phase. Another possibility would be the presence of triethylamine in the mobile phase used in the HPLC separation that could catalyze the rearrangement reaction. In any event, the isolation of the minor product was repeated and this time the mobile phase was removed via freeze drying to prevent a thermal rearrangement reaction. HPLC-DA analysis of the residue showed a single peak with a retention time corresponding to the minor product. Following the isolation, ^{1}H NMR analysis of the residue was obtained (Fig. 18). The aromatic region of the spectrum was different from corresponding region in the spectrum obtained for the 1*H*-isomer **144** (Fig. 13) and consistent with the 2*H*-3-methylindazolylpyridinium species **140**.

Figure 18. Aromatic region of the ^{1}H NMR spectrum of the minor product obtained in the reaction between 3-methylindazole and 55 in the absence of TMP.

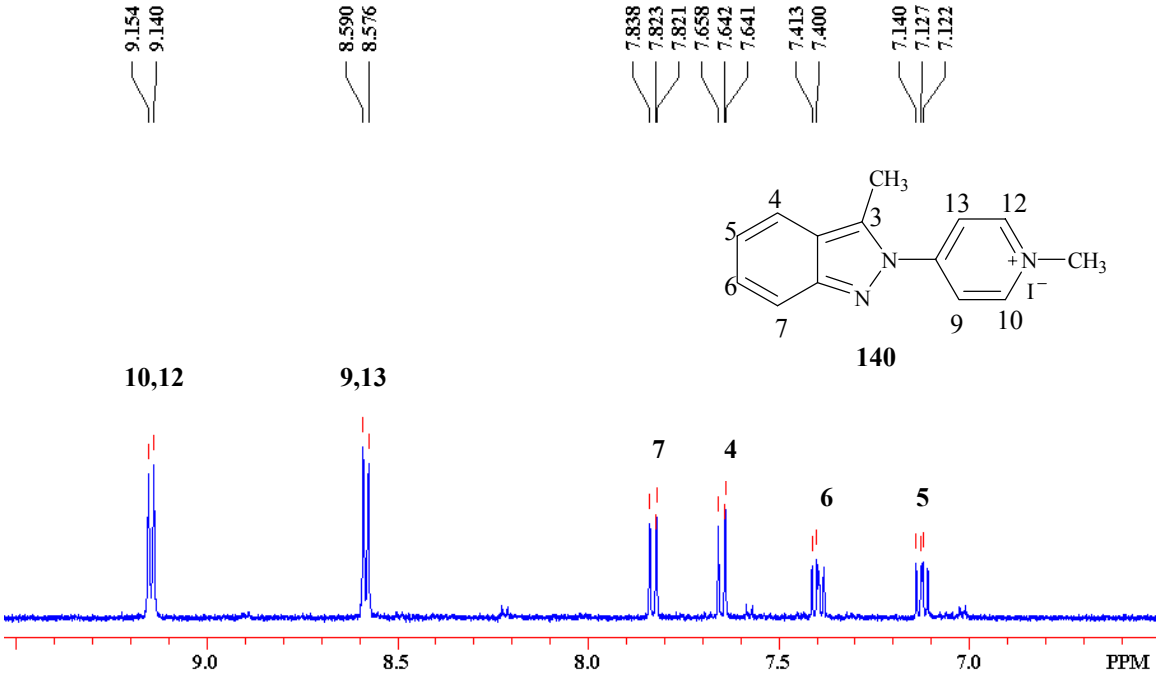

There were three signals appearing as singlets in the upfield region of the ^{1}H NMR spectrum (Fig. 19) at 4.39 ppm, 2.95 ppm and 1.53 ppm. Each signal integrated to 3 protons. In comparison with the 1*H*-isomer **144**, the signal at 4.39 ppm was assigned to

the protons of N-methyl group and the signal at 2.95 ppm was assigned to the protons of 3-methyl group of **140**. The unassigned signal at 1.53 ppm was not present in the ^{1}H NMR spectrum of the 1*H*-isomer **144**.

Figure 19. Upfield region of the ^{1}H NMR spectrum (500 MHz) obtained for the minor product of the reaction between 3-methylindazole and 55 in the absence of TMP.

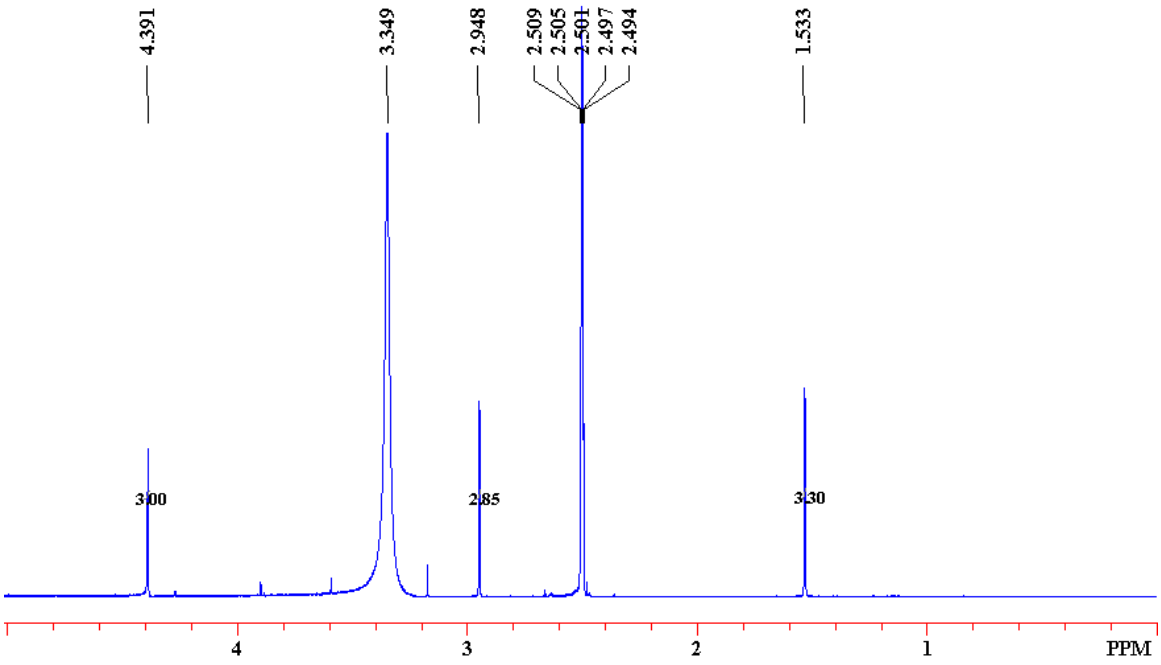

Since the mobile phase had been removed before the NMR analysis, it was unlikely that the signal at 1.53 ppm is a solvent peak. One possibility would involve the exchange of iodide with acetate to give 4-(2*H*-3-methylindazolyl)-1-methylpyridinium acetate with loss of HI during the freeze drying process. The ^{1}H NMR spectrum of potassium acetate (Fig. 20) showed that the signal corresponding to the protons of the methyl group appear at 1.52 ppm, consistent with this proposal.

Figure 20. ^{1}H NMR spectrum (500 MHz) of potassium acetate in DMSO-d_6.

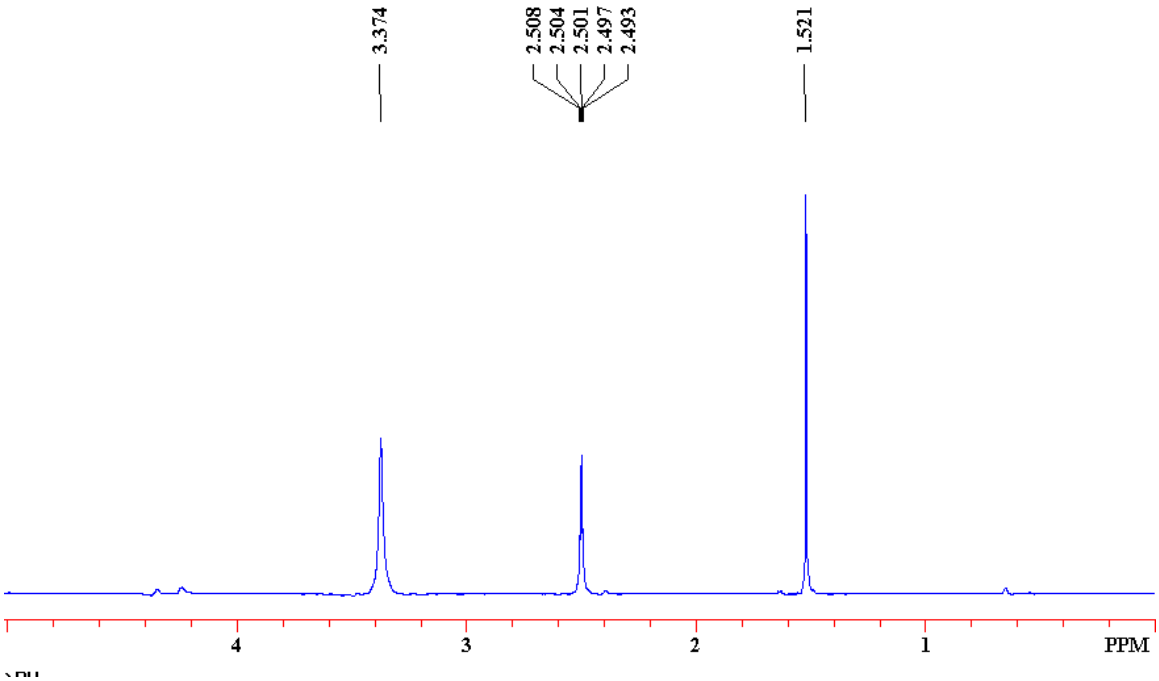

The ^{1}H NMR suggested that the pyridinium acetate salt of the 2*H*-isomer **140** was obtained rather than the pyridinium iodide salt. The stability of this compound in the absence of TMP was investigated by HPLC-DA at room temperature in DMF. HPLC-DA tracings are shown in Figure 21.

Figure 21. HPLC-DA monitoring of the stability of 140 in DMF at room temperature.

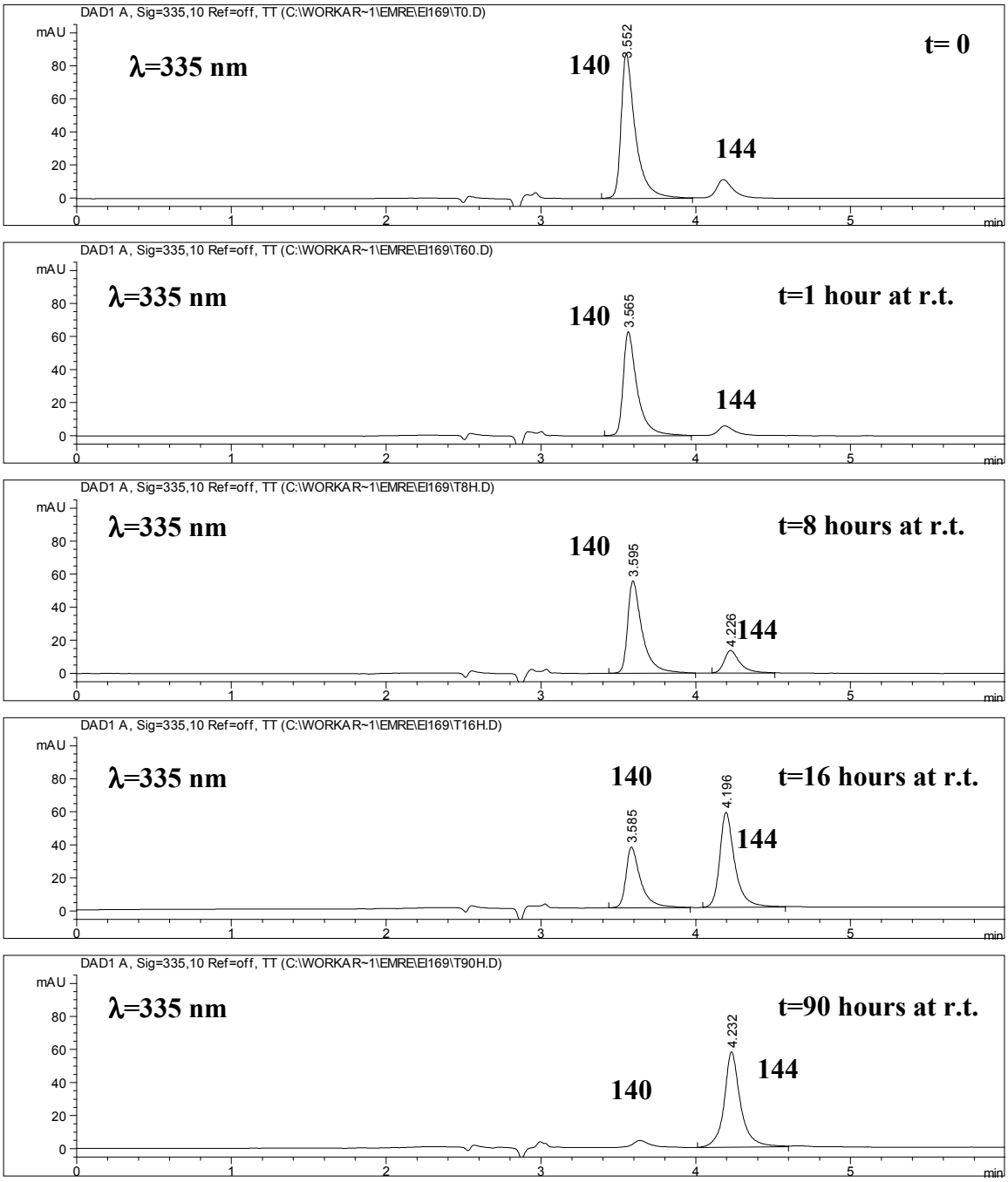

As shown in Figure 22, the intensity of the peak corresponding to **140** decreased over time and a new peak corresponding to the 1*H*-isomer **144** appeared. HPLC-DA

tracing obtained after 4 days showed the replacement of the peak corresponding to **140** completely with the peak corresponding to **144**.

These results brought to our attention the possibility that the rearrangement of **140** to **144** was mediated by acetate present in the sample of **140** as the counter ion. An independent synthesis of acetate free **140** was pursued. A retrosynthetic analysis is given in Scheme 54. The regioselective bromination of the 4-(2*H*-indazolyl)pyridine (**157**) is expected to result in the formation of the corresponding 3-bromo derivative **156**. Compound **156** can be converted to the 2*H*-3-methylindazolylpyridine species **155** via lithium-bromine exchange followed by treatment of the lithiated intermediate with iodomethane. The desired 2*H*-isomer **140** is expected to form following methylation of **155**.

Scheme 54. Retrosynthetic approach to the 4-(2*H*-3-methylindazolyl)-1-methylpyridinium iodide (140).

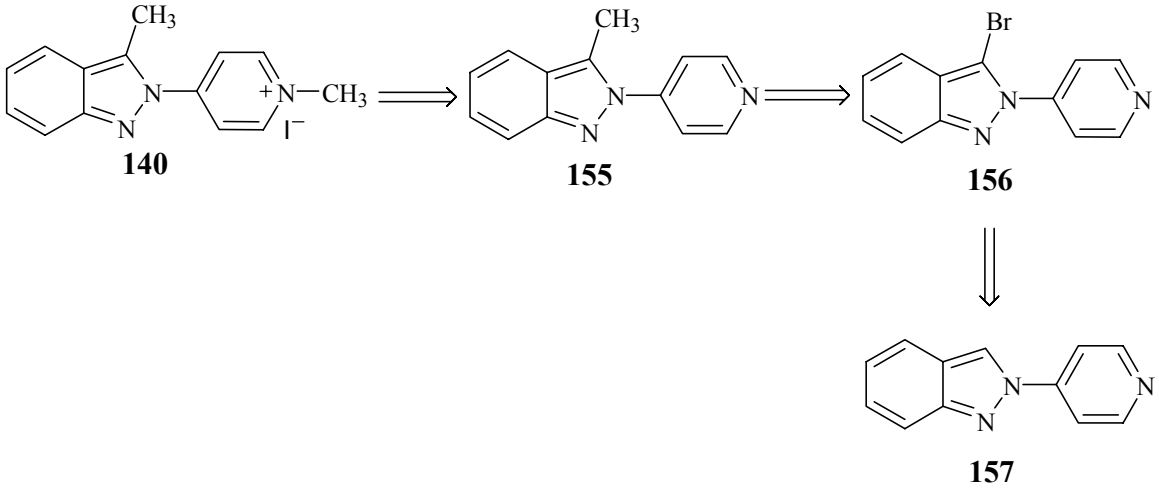

As previously reported,[197] the reaction between indazole and 4-chloropyridine (**158**) resulted in the formation of a mixture of the 1*H*- and 2*H*-indazolylpyridines **111** and **157** as shown in Scheme 55. The solid 2*H*-isomer **157** separated readily from the oily 1*H*-isomer **111** upon cooling the material obtained after the work-up. Hence, the original procedure was improved by eliminating the chromatographic separation step.

[197] Reference 185.

Scheme 55. Synthesis of 2*H*-indazolylpyridine 157.

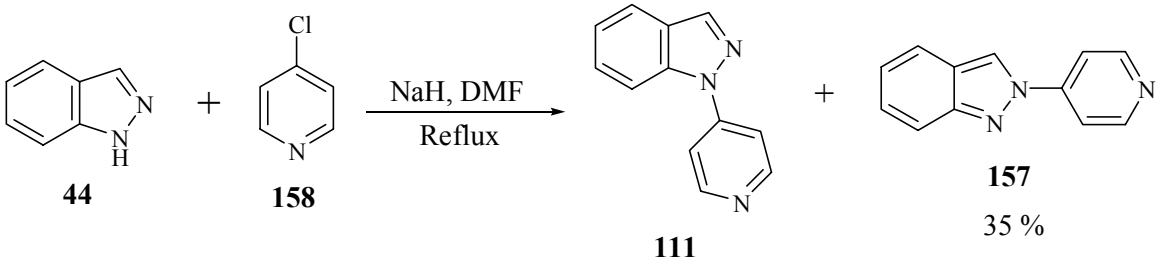

44 **158** **111** **157** 35 %

Bromination of **157** was attempted with the same bromine/dioxane complex used to brominate indazole.[198] This time the yield was lower due to the undesired formation of the hydrobromide salt of unreacted **157** as shown in Scheme 56. The ^{1}H NMR spectrum of the product in $CDCl_3$ (Fig. 22) lacked the signal corresponding to the proton attached to C-3 showing that the bromination had taken place regiospecifically at C-3 as expected. Unreacted 2*H*-indazolylpyridine **157** was recovered quantitatively as the hydrobromide salt.

Scheme 56. Bromination of 157 forming 2*H*-3-bromoindazolylpyridine species 156 together with the hydrobromide salt of 157.

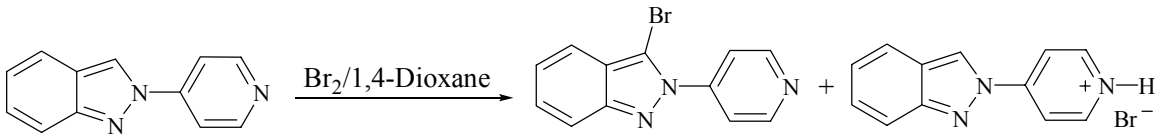

157 **156** 32 % **157.HBr**

[198] Reference 193.

Figure 22. ^{1}H NMR spectrum (500 MHz) of the product obtained from the reaction shown in Scheme 56.

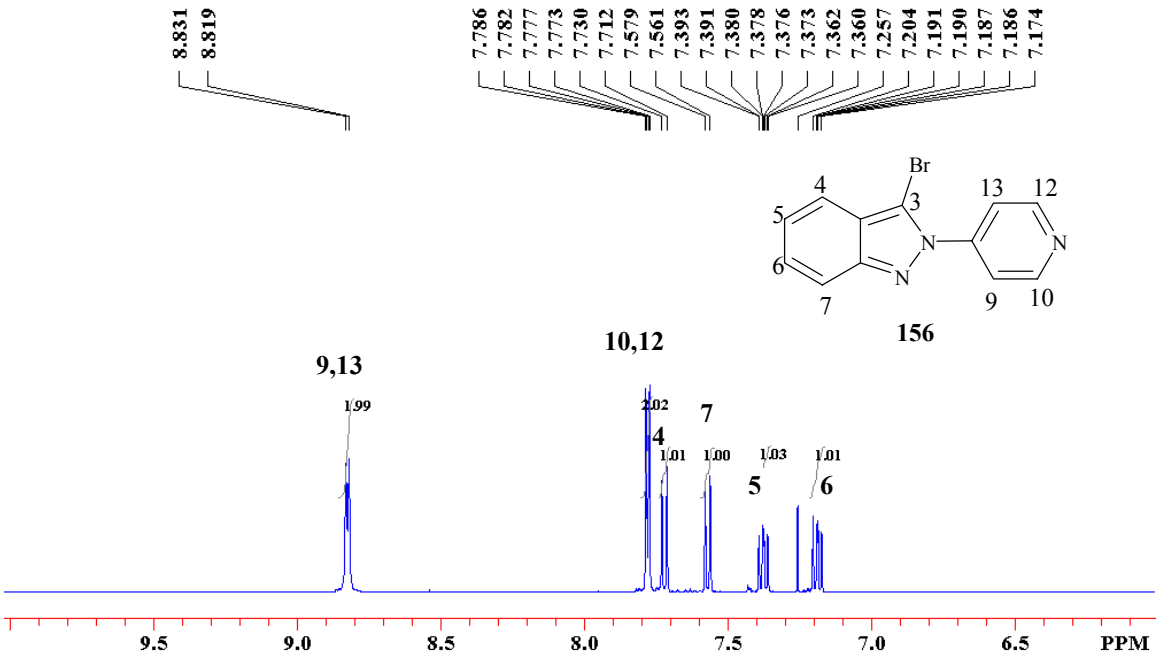

Methylation of **156**, via lithium-bromine exchange followed by treatment with iodomethane, resulted in the desired 2*H*-3-methylindazolylpyridine **155** (Scheme 57). In addition to the desired product, GC-MS analysis showed the presence of 2*H*-protioindazolylpyridine **157** and an isomeric monomethylated product. The isomeric monomethylated product was isolated. The ^{1}H NMR spectrum of this product displayed signals for five aromatic indazolyl protons suggesting that the methylation was taking place on the pyridine ring. Further characterization of the unknown product (**159**) was not attempted except for confirming its molecular formula via exact mass analysis.

Scheme 57. Formation of 2*H*-3-methylindazolylpyridine 155 via bromine-lithium exchange followed by methylation.

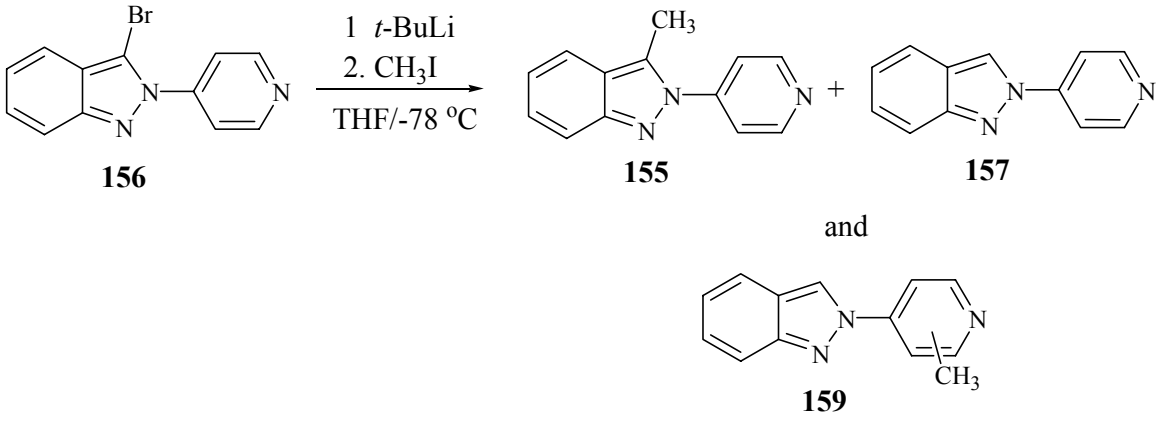

Despite our purification efforts by column chromatography followed by preparative thin layer chromatography, we could not obtain **155** in pure form. Instead a mixture of the 2*H*-protioindazolylpyridine **157** and **155** was obtained. The subsequent methylation reaction was carried out on this mixture (Scheme 58) to yield a mixture of 2*H*-protioindazolylpyridinium **112** and 2*H*-3-methylindazolylpyridinium **140**. The ^{1}H NMR spectrum of the mixture of **112** and **140** is shown in Figure 23a. The signals corresponding to the protons of compound **140** in the mixture were identical to the signals present in the ^{1}H NMR spectrum of the 2*H*-3-methylindazolylpyridinium species (Fig. 23b) obtained via preparative HPLC.

Scheme 58. Methylation of the mixture consisting of 2*H*- indazolylpyridines 157 and 155 to yield the corresponding 2*H*-indazolylpyridinums 112 and 140.

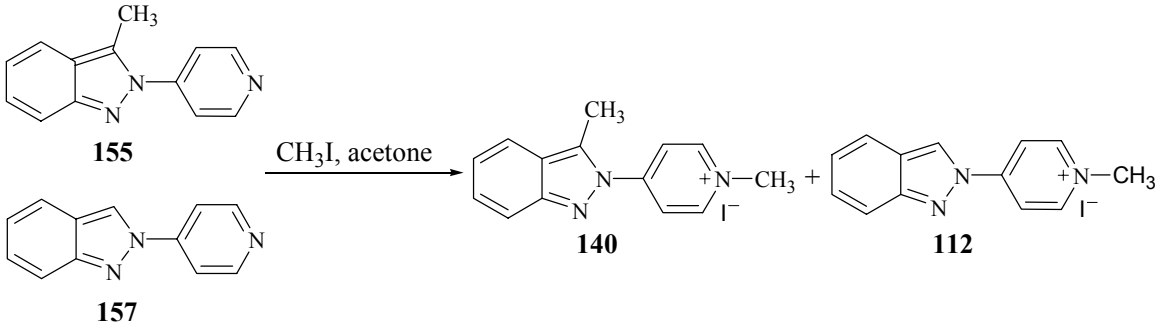

Figure 23. ^{1}H NMR spectrum (500 MHz) of the mixture of 112 and 140 (a) and the ^{1}H NMR spectrum (500 MHz) of 140 obtained via preparative HPLC from the reaction between 55 and 3-methylindazole in the absence of TMP (b).

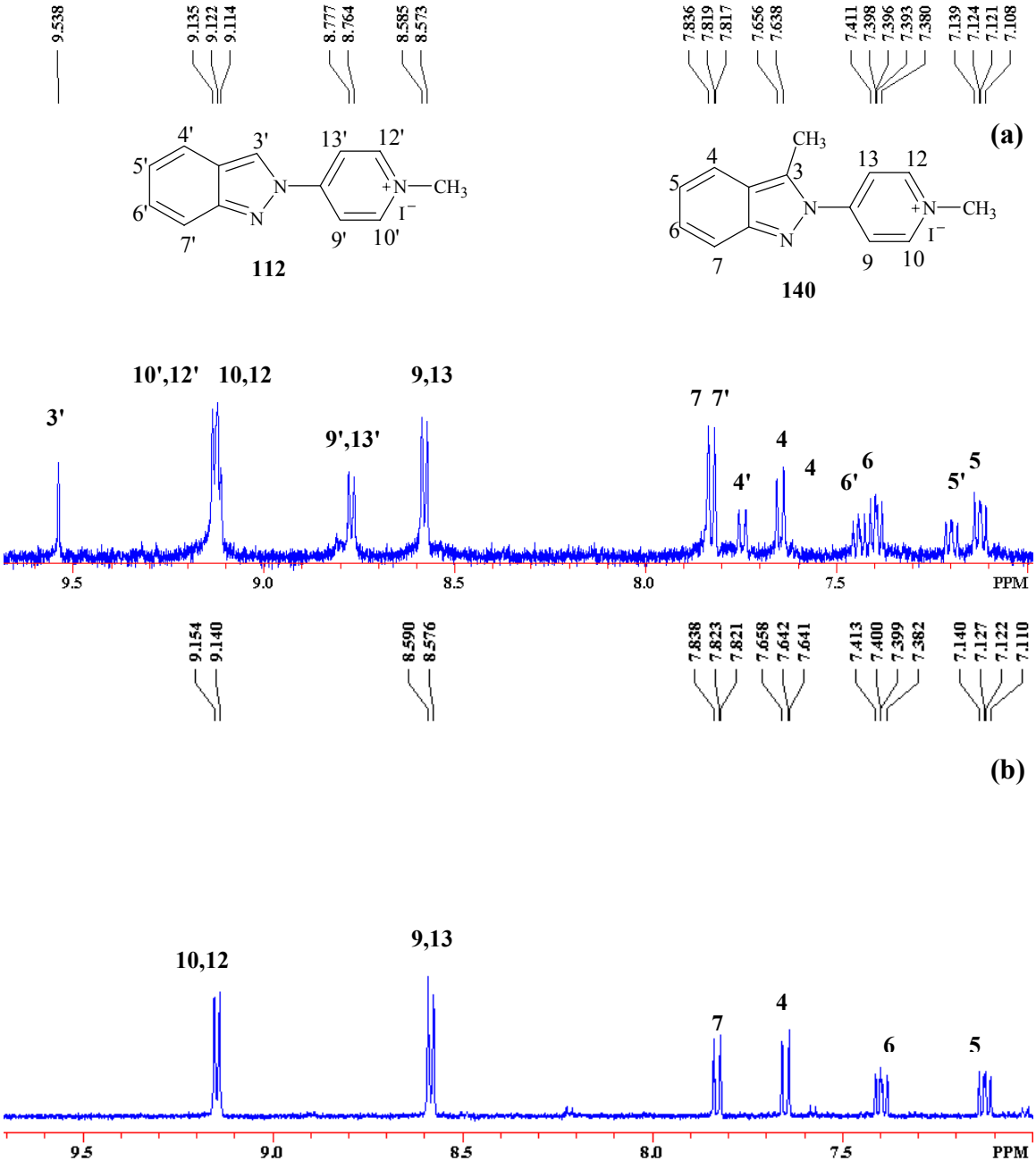

The stability of **140** in the mixture obtained from the reaction shown in Scheme 58 was investigated in the absence of TMP. Since HPLC-DA tracings were expected to be complex, ^{1}H NMR spectroscopy was used to monitor the reaction. The separation of

the two signals corresponding to the protons of N-methyl groups of **112**, **140** and the 1*H*-isomer **144**, made the use of ^{1}H NMR feasible (Fig. 24). The mixture of **112** and **140** in DMSO-d_6 was heated at 90 ^{o}C and ^{1}H NMR spectra shown in Figure 25 were obtained. After heating the mixture at 90 ^{o}C for 12 hours, there was no change in the ^{1}H NMR spectrum and the appearance of the signal corresponding to the N-methyl protons of the 1*H*- isomer **144** was not observed (Fig. 25).

Figure 24. ^{1}H NMR spectrum of the mixture of 112 and 140(a) and ^{1}H NMR spectrum of 1*H*-3-methylindazolylpyridinium 144 (b).

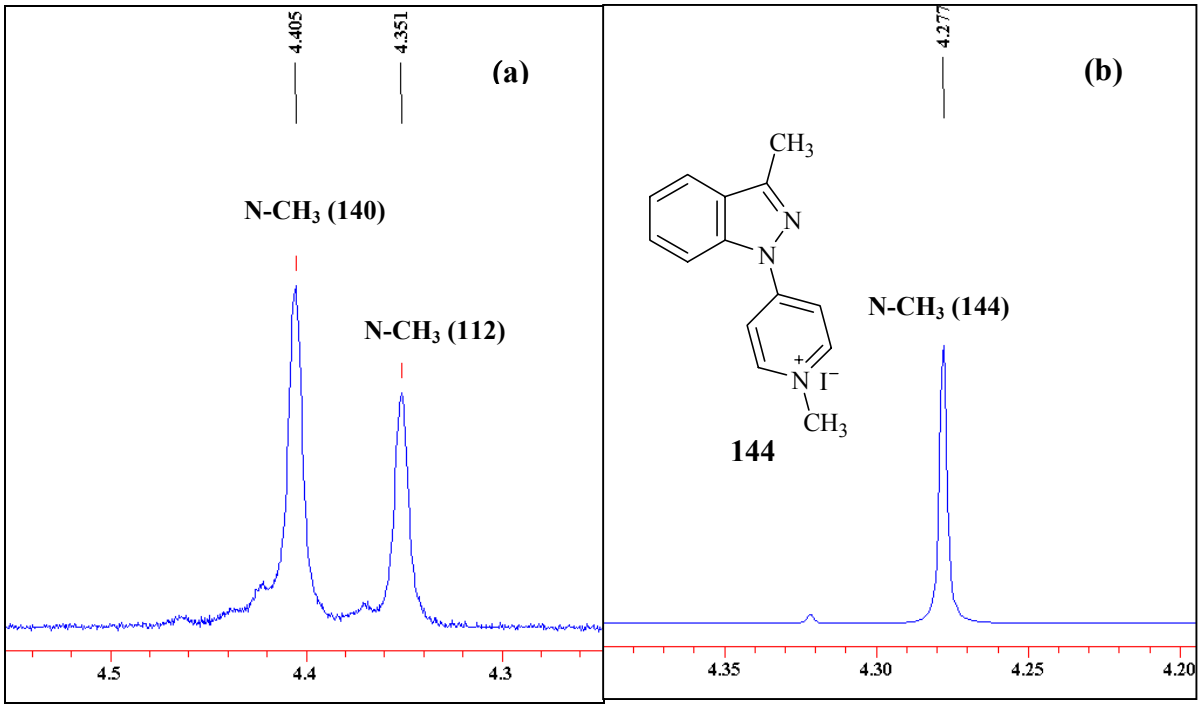

Figure 25. ^{1}H NMR monitoring of the stability of 140 in the absence of TMP.

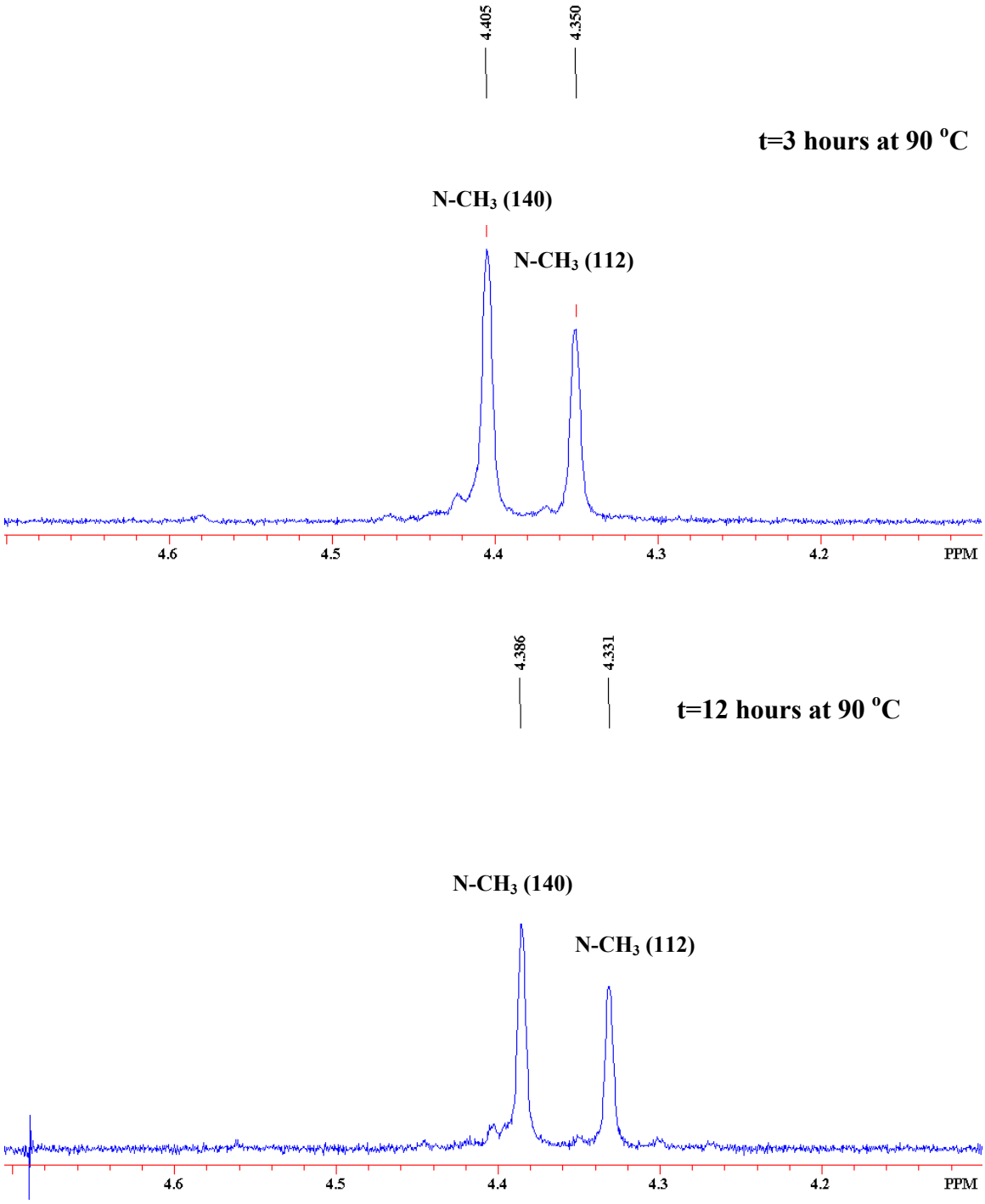

This outcome showed that a spontaneous thermal rearrangement of **140** to the 1*H*-isomer **144** was not taking place. Therefore, we considered it likely that the previously observed rearrangement of **140** was mediated by the acetate counter ion. In order to

investigate this possibility, the stability of the 2*H*-protioindazolylpyridinium species **112** in the presence of potassium acetate was monitored by ^{1}H NMR (Fig. 26).

Figure 26. ^{1}H NMR (400 MHz) monitoring of the stability of 2*H*-protioindazolylpyridinium derivative 112 in the presence of potassium acetate at room temperature.

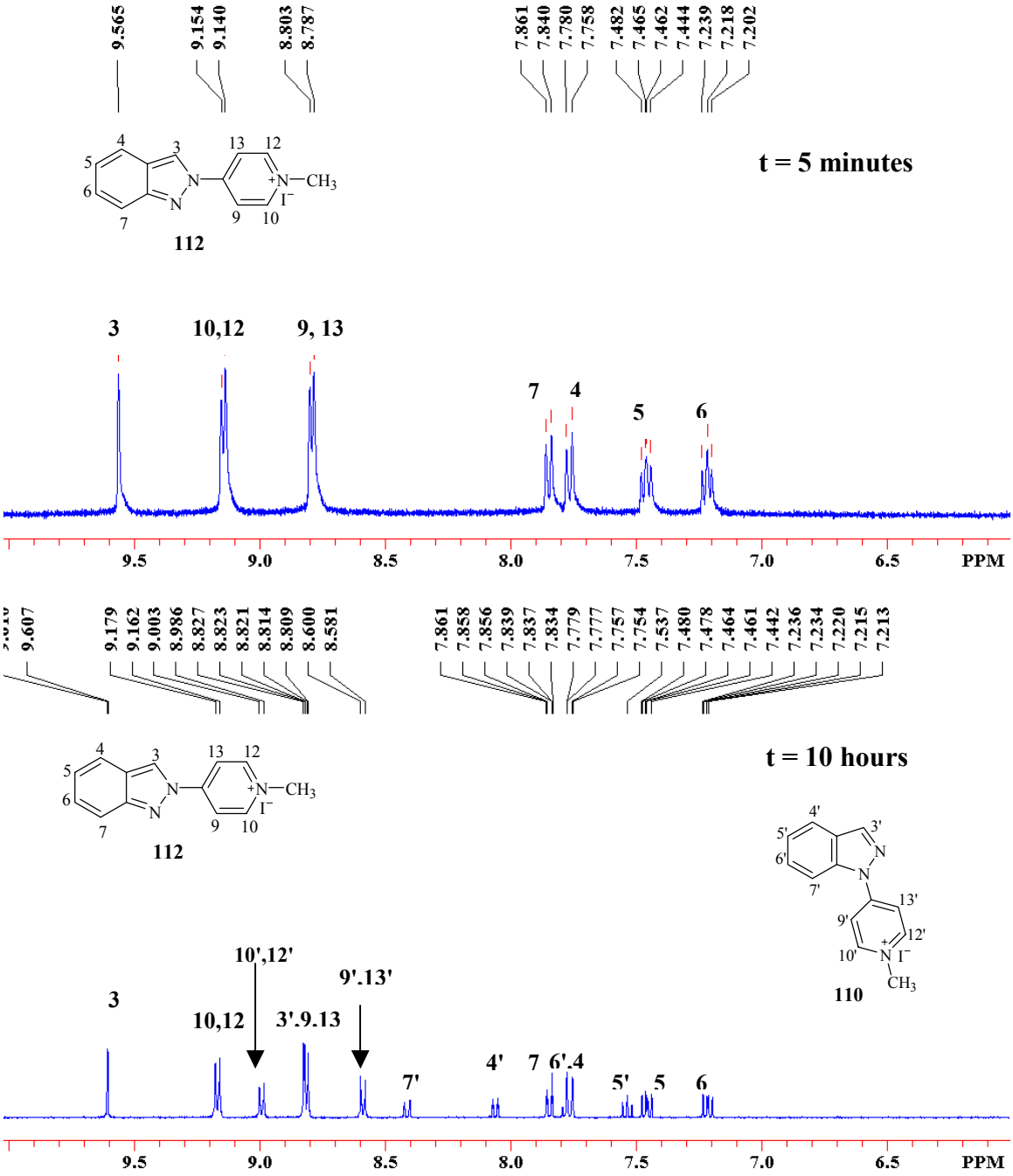

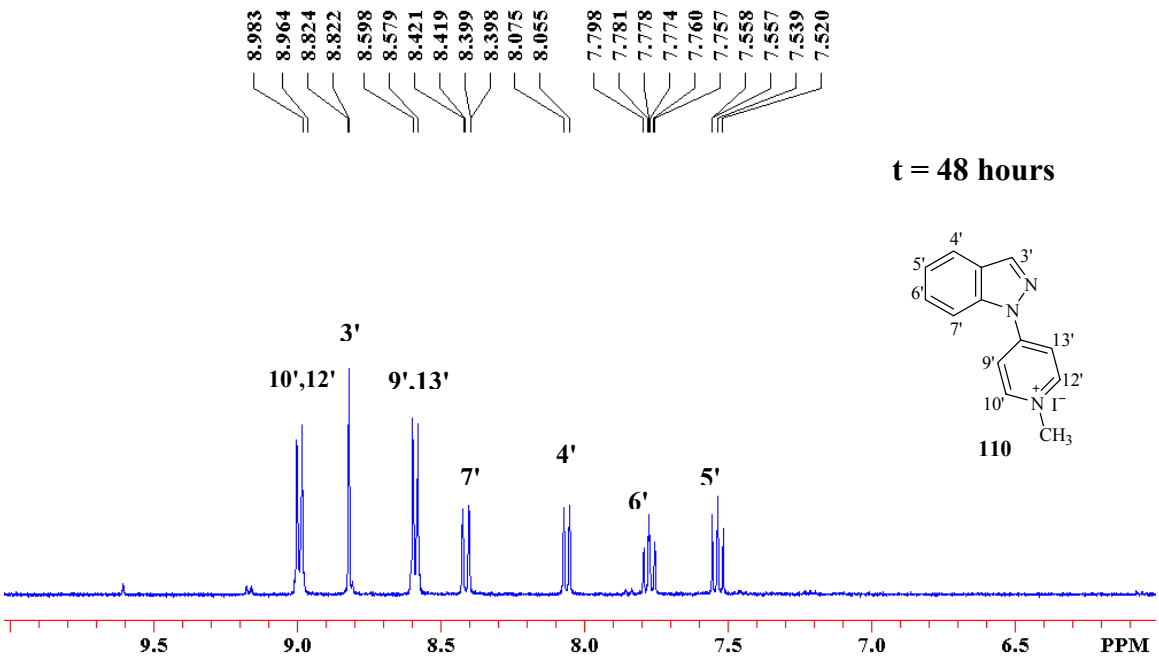

As shown in Figure 26, the 2*H*-isomer **112** rearranged to the 1*H*- isomer in the presence of acetate after 48 hours. This finding demonstrated that the rearrangement of **140** to **144** observed earlier was not a unimolecular reaction (Scheme 53) but mediated by acetate ion.

In the absence of the considered unimolecular thermal rearrangement, it was suggested that the 1*H*-isomer must form independently in the reaction between 3-methylindazole and **55** in the absence of TMP. As discussed above, the formation of the high energy intermediate **152** (Scheme 52) leading to the 1*H*-isomer **144** seemed unlikely. Furthermore, since the lone pair of the N-1 nitrogen of the indazole nucleus is part of the π-system, the nucleophilicity of N-1 is considerably lower compared to N-2. Consistent with this reasoning, the attack by N-1 has been shown to take place only in the presence of a base that generates the indazolyl anion. These considerations have prompted us to speculate that 3-methylindazole itself may serve as a base to form the 3-methylindazolyl anion (**160**) and 3-methylindazolium (**161**) through a disproportionation reaction (Scheme 59). The presence of even a low concentration of **160** could be sufficient to account for the very slow reaction leading to the 1*H*-3-methylindazolylpyridinium **144**.

Scheme 59. Formation of 3-methylindazolyl anion (160) and 3-methylindazolium (161) through disproportionation followed by the reaction of 3-methylindazolyl anion with 55 to give 1*H*-3-methylindazolylpyridinium 144.

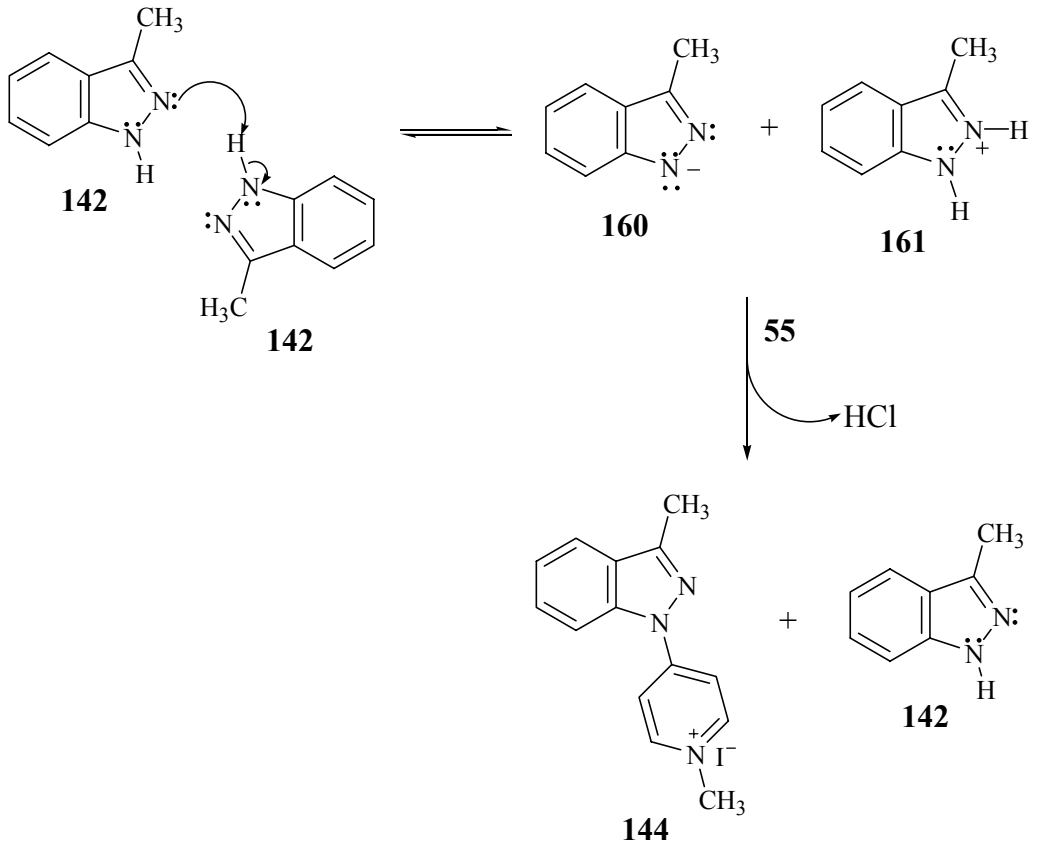

The proposed disproportionation reaction should be facilitated by the increased basicity of 3-methylindazole compared to the unsubstituted indazole. The analogous disproportionation reaction presumably does not take place with indazole which would account for the exclusive formation of the 2*H*-indazolylpyridinium species in the uncatalyzed addition-elimination reaction.

Alternatively, an *in situ* tautomerization reaction of 3-methylindazole may result in the formation of the less stable 2*H*-tautomer of 3-methylindazole (**162**) prior to the reaction with 4-chloro-1-methylpyridinium iodide (**55**). The attack by the N-1 nitrogen atom of the 2*H*-tautomer **162** would be expected to give intermediate **163** which can be stabilized through delocalization favoring the formation of 1*H*-3-methylindazolylpyridinium **144** as shown in Scheme 60.

Scheme 60. The tautomerization of 3-methylindazole to give the 2*H*- tautomer 162.

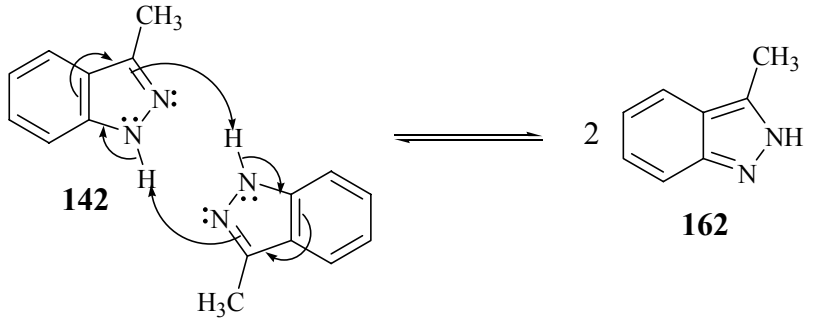

Scheme 61. Formation of stabilized intermediate 163 via the reaction between of 2*H*-tautomer 162 and 55.

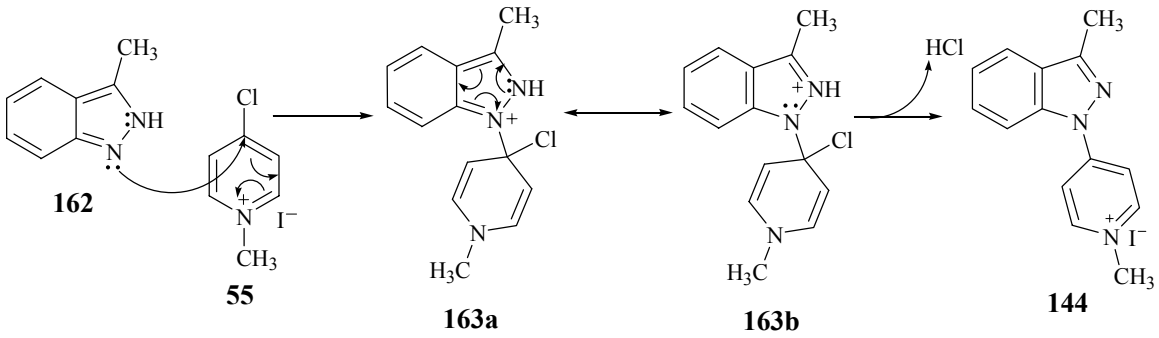

The disproportionation reaction shown in Scheme 59 [as well as the tautomerization reaction (Scheme 60)] can be considered as a pre-equilibrium process with an equilibrium constant K_{eq} (Scheme 62, Equation 1) where the concentration of **160** is expected to be approximately equal to the concentration of **161**. Therefore, the rate of the addition-elimination reaction (Scheme 62, Equation 2) can be expressed as shown in Equation 4 of Scheme 62. The initial concentration of 3-methylindazole (**142**) will be equal to the concentration of the remaining neutral 3-methylindazole plus twice the concentration of the 3-methylindazolyl anion (Scheme 62, Equation 5). The concentration of 3-methylindazolyl anion is expected to be very small compared to neutral 3-methylindazole at any given point during the course of the reaction. Therefore, the concentration of neutral 3-methylindazole can be considered to be constant and equal to the starting concentration (Scheme 62, Equation 7). According to this analysis the

reaction between 3-methylindazole anion (**160**) and **55** leading to the formation of 1*H*-3-methylindazolylpyridinium **144** is expected to be first order in 3-methylindazole (Scheme 62, Equation 8). As shown in Figure 16 (page 84), the reaction of 3-methylindazole and **55** in the absence of TMP is indeed first order in 3-methylindazole, consistent with both proposed pathways. This analysis does not allow us to distinguish between the two pathways.

Scheme 62. Kinetic analysis of the reaction between 3-methylindazolyl anion (160) and 55.

$$2\ \mathbf{142} \rightleftharpoons \mathbf{160} + \mathbf{161} \quad K_{eq} = \frac{[\mathbf{160}][\mathbf{161}]}{[\mathbf{142}]^2} \qquad (1)$$

$$\mathbf{160} + \mathbf{55} \longrightarrow \mathbf{144} \quad \text{Rate} = k[\mathbf{160}][\mathbf{55}] \qquad (2)$$

$$[\mathbf{160}] = [\mathbf{161}] \Longrightarrow [\mathbf{160}] = [\mathbf{142}]\, K_{eq}^{1/2} \qquad (3)$$

$$\Longrightarrow \text{Rate} = k[\mathbf{142}]\, K_{eq}^{1/2}[\mathbf{55}] \qquad (4)$$

$$[\mathbf{142}]_{initial} = [\mathbf{142}] + 2[\mathbf{160}] \qquad (5)$$

$$\Longrightarrow [\mathbf{142}] = [\mathbf{142}]_{initial} - 2[\mathbf{160}] \qquad (6)$$

$$\Longrightarrow [\mathbf{142}] = [\mathbf{142}]_{initial} \qquad (7)$$

$$\Longrightarrow \text{Rate} = k[\mathbf{142}]_{initial}\, K_{eq}^{1/2}[\mathbf{55}] \qquad (8)$$

The TMP catalyzed rearrangement reaction of the 2*H*-isomer **140** to the corresponding 1*H*-isomer **144** at 90 ^{o}C starting with the previously obtained mixture of **112** and **140** was examined next. The signals corresponding to the protons of the N-methyl groups were monitored (Fig. 27). This time, we took advantage of the presence of the 2*H*-protioindazolylpyridinium species **112** as part of the mixture for comparing the rates of rearrangement.

Figure 27. ^{1}H NMR (400 MHz) monitoring of the rearrangement reaction in the presence of TMP at 90 ^{o}C.

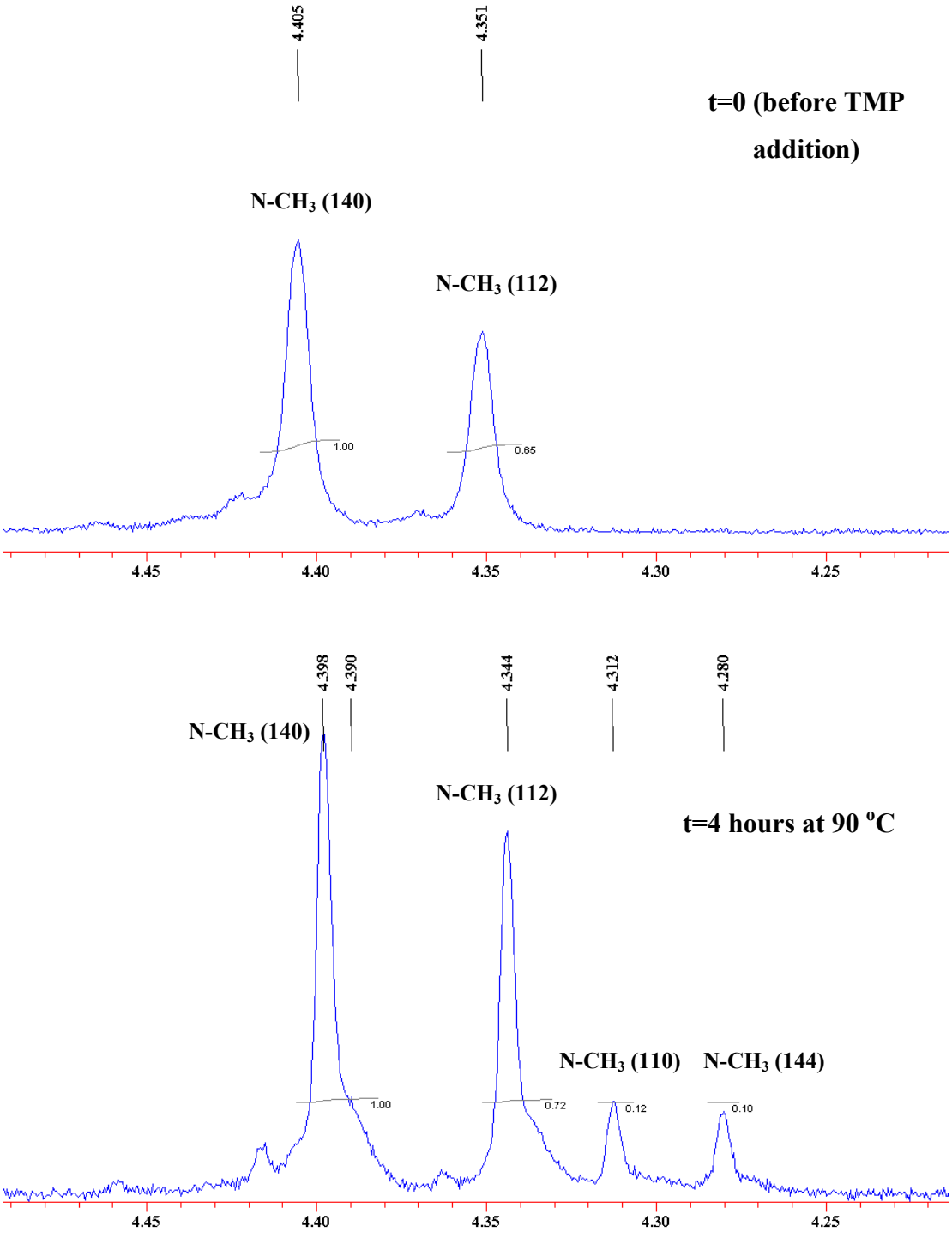

After 4 hours at 90 ^{o}C in the presence of 1 equivalent of TMP, rearrangement of 2*H*-3-methylindazolylpyridinium **140** to the corresponding 1*H*-isomer **144** was observed as expected (Fig. 27). Furthermore, the rate of rearrangement of **140** was comparable to that of **112**. This was rather unexpected considering the calculated energies of the spirodiaziridinyl intermediates **121** and **164** that will form from the 2*H*-protio and 2*H*-3-methylindazolylpyridiniums, respectively. The calculated enthalpy of reaction for the formation of intermediate **121** from **112** [$\Delta H_{rxn} = \Delta H_{\mathbf{121}} - (\Delta H_{\mathbf{112}} + \Delta H_{TMP}) = 31$ kcal/mol] is significantly lower than the calculated enthalpy of reaction for the formation of intermediate **164** from **140** [$\Delta H_{rxn} = \Delta H_{\mathbf{164}} - (\Delta H_{\mathbf{140}} + \Delta H_{TMP}) = 49$ kcal/mol]. This difference in energy should lead to a slower rate of isomerization for 2*H*-3-methylindazolylpyridinium species compared to the 2*H*-protio species **112**. A possible rationale for this behavior would involve attack of TMP at C-6 to give intermediate **165**. In this case, the 3-methyl substituent would not cause steric hindrance. However, the enthalpy of reaction for the formation of intermediate **165** is still high due to the disturbance of aromaticity making the attack at C-6 unlikely. At this point, attack by hydroxide ion, which might form *in situ* via the equilibrium reaction between TMP and water present in DMSO, was considered. In this case the steric hindrance exerted by the methyl group should be less significant leading to a smaller difference between the enthalpies of reaction for the formation of the expected spirodiaziridinyl intermediates **166** and **167**.

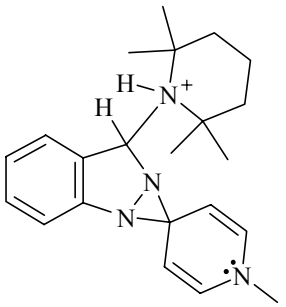

121

ΔH_{rxn} = 29 kcal/mol (AM1)

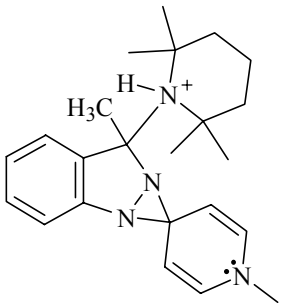

164

ΔH_{rxn} = 49 kcal/mol (AM1)

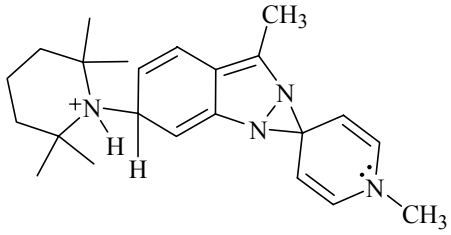

165

ΔH_{rxn} = 49 kcal/mol (AM1)

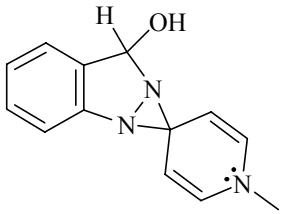

166

ΔH_{rxn} = -164 kcal/mol (AM1)

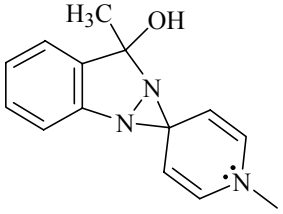

167

ΔH_{rxn} = -158 kcal/mol (AM1)

Although the equilibrium reaction between TMP and water is expected to be shifted towards TMP (pK_a 11) allowing the formation of only very low concentrations of hydroxide ion,[199] this may be sufficient to catalyze the rearrangement reaction. It is important to note that, since the formation of hydroxide ion will be a pre-equilibrium process, the rearrangement reaction will be still first order in TMP, consistent with our earlier kinetic analyses. However, the results of the previous experiments using piperidine for the rearrangement reaction had suggested that nucleophilic molecules, which are not hindered, would attack at C-4 leading to a cleavage reaction (Section 3.4, Scheme 41). TMP was thought to be nucleophilic enough to attack at C-3 to catalyze the rearrangement reaction but too hindered to attack at C-4 to result in cleavage.

[199] The amount of hydroxide ion that would be present was calculated to be 400 μM where the concentration of TMP is 0.01 M. The concentration of water present in DMSO-d_6 was estimated to be 0.14 M by integrating the water peak and comparing with the signal corresponding to the methyl protons of TMP.

Nevertheless the stability of the 2*H*-proteindazolylpyridinium **112** was investigated in the presence of approximately 1 equivalent of KOH (Fig. 28).

Figure 28. ^{1}H NMR (400 MHz) Monitoring of 112 in the presence of KOH at room temperature.

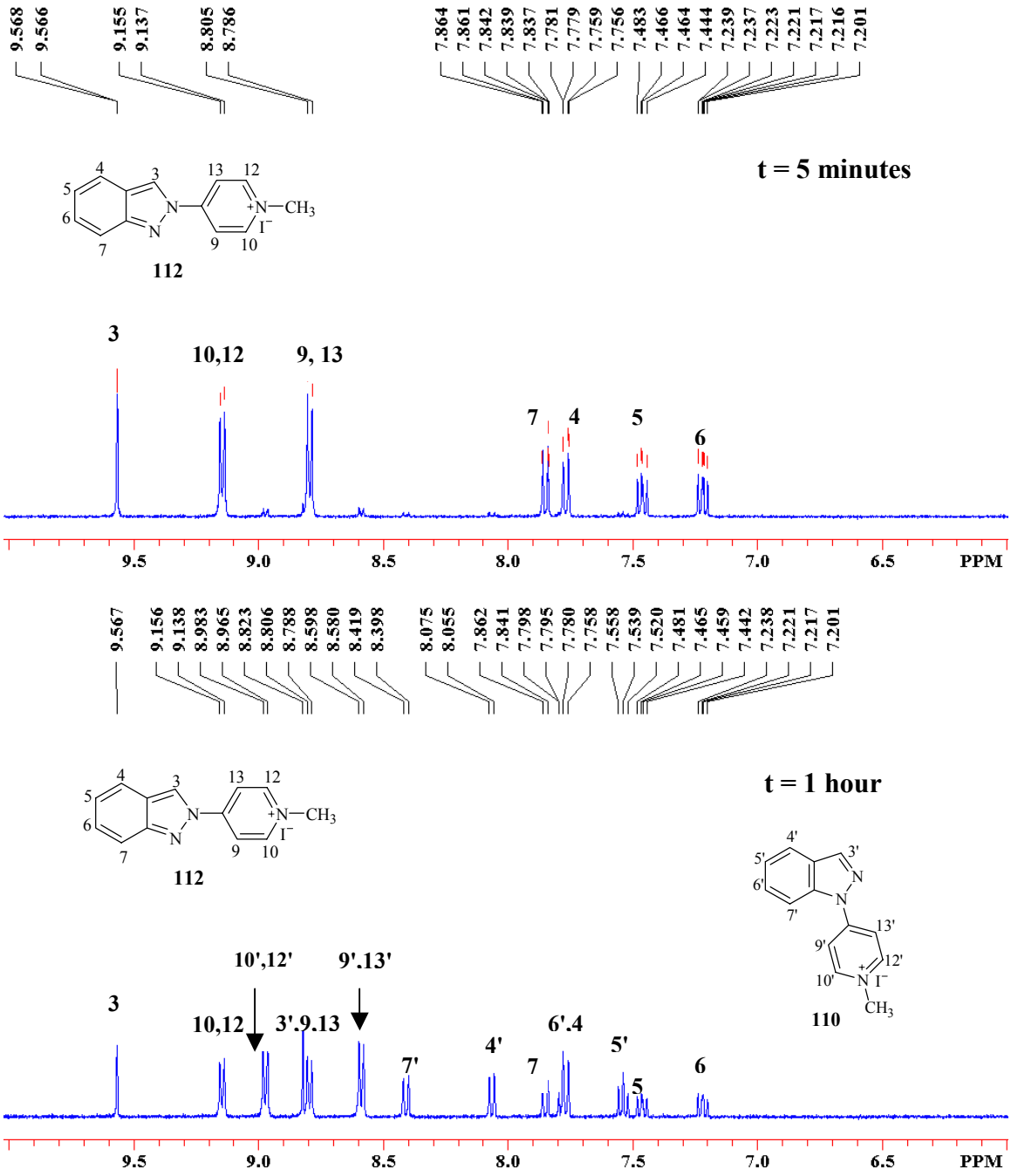

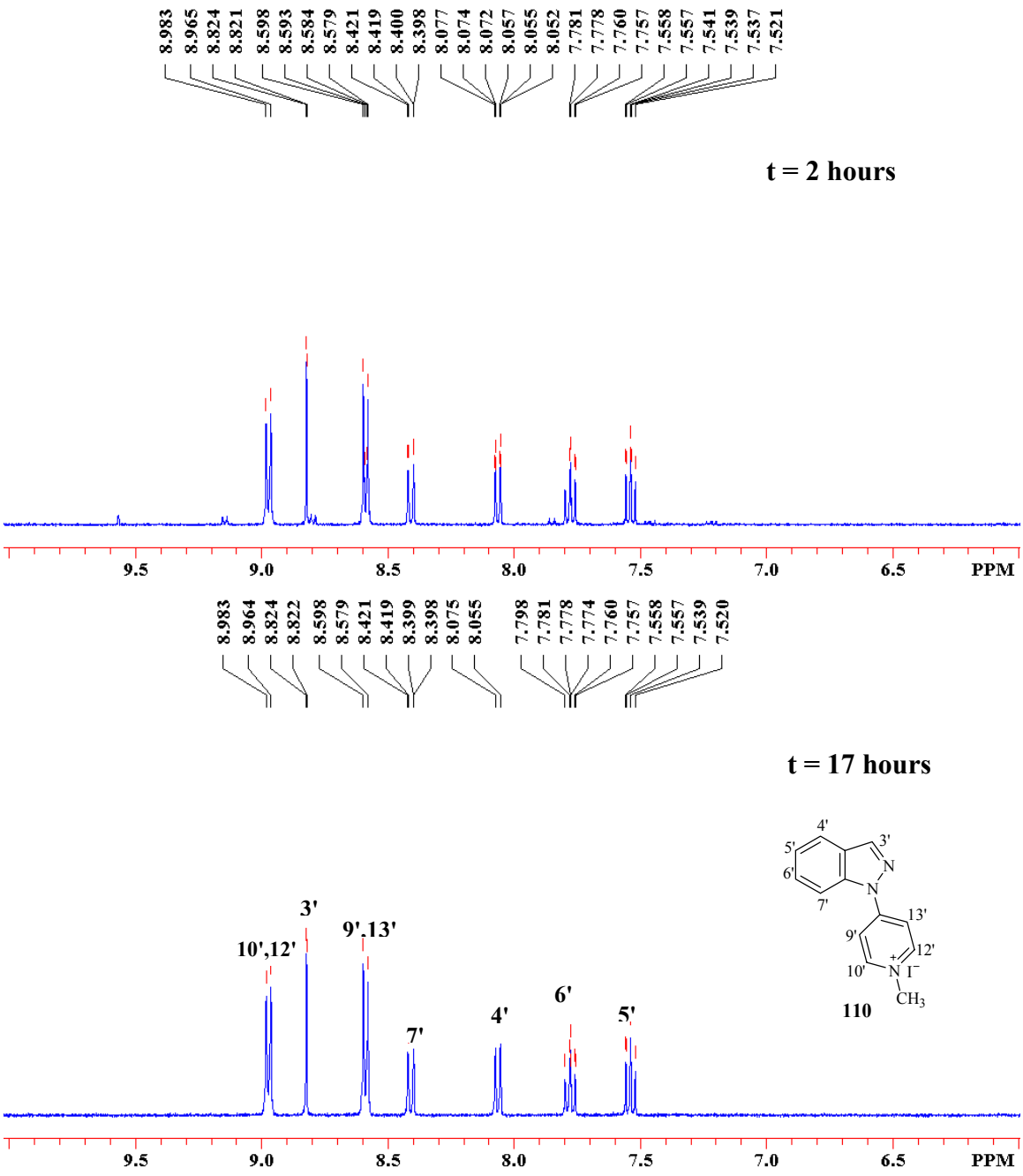

The ^{1}H NMR spectra showed a decrease for the peaks corresponding to the protons of **112** over time and appearance of the peaks corresponding to the protons of 1*H*- isomer **110** at room temperature. The rearrangement reaction was complete after 3 hours (Fig. 28). There was no indication of the cleavage reaction even after 17 hours. This was rather unexpected since the hydroxide ion, being a much smaller and more nucleophilic molecule than piperidine, would be expected to attack at C-4 leading to the

cleavage reaction. One rationale for this outcome is the lower acidity of the OH proton compared to the piperidinium proton. After the reversible formation of the intermediate **131** via attack of piperidine at C-4 of pyridinyl moiety, deprotonation takes place readily resulting in the cleavage reaction (Page 70, Scheme 41). In the case of intermediate **168**, however, the OH proton may not be acidic enough to favor the forward reaction upon deprotonation (Scheme 63) at least under these reaction conditions.

Scheme 63. Proposed hydroxide mediated cleavage reaction leading to indazole (44) and 1-methyl-4-pyridone (169)

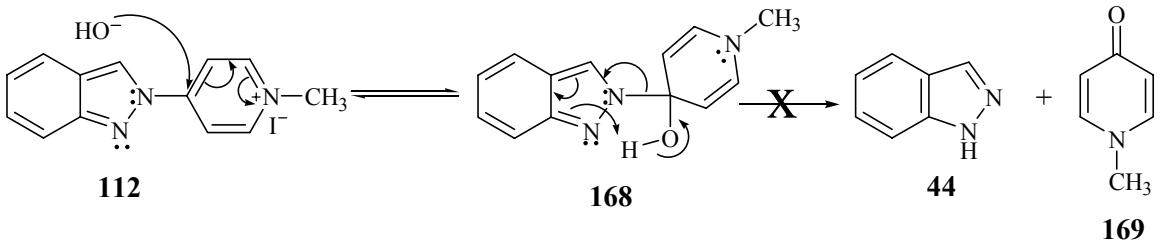

In order to investigate further, the equilibrium reaction between TMP and water leading to the formation of hydroxide ion, the rate of the rearrangement reaction was compared in "dry" vs. "wet" DMSO-d_6. DMSO-d_6 was stirred over CaH_2 overnight, freshly distilled and stored over 3 Å molecular sieves prior to use. The rearrangement reaction of **112** was attempted in the presence of 1 equivalent of TMP at 90 ^oC. The water content of DMSO-d_6 was estimated by integrating the water peak, to be 0.14 M and 0.02 M before and after the drying process, respectively, compared to 0.01 M TMP. After 4 hours ^1H NMR spectra showed that the extent of rearrangement was 28% in "dry" DMSO-d_6 versus 20% in "wet" DMSO-d_6. The rearrangement reaction was expected to proceed more rapidly in "wet" DMSO-d_6 due to the anticipated higher concentration of hydroxide ion formed through the TMP-water equilibrium. However, even under "dry" conditions, trace amounts of water present may be sufficient to form enough hydroxide ion to catalyze the rearrangement reaction. Furthermore, under "dry" conditions, the solvent medium will have a more aprotic character which is likely to increase the nucleophilicity of the hydroxide ion enhancing the rate of the rearrangement reaction. Therefore, this issue remains poorly resolved although it is still possible that the

rearrangement reaction is being catalyzed by the hydroxide ion forming *in situ* through the equilibrium reaction between TMP and water.

After studying the effects of the 3-methyl substituent on the coupling and the rearrangement reactions, we expanded our efforts to 3-bromoindazole and the corresponding 1*H*- and 2*H*-3-bromoindazolylpyridiniums **145** and **141**. The bromo group provides an opportunity to characterize the effect of introducing an electronegative atom at C-3 on the rate of the rearrangement reaction. Also the 2*H*-3-bromoindazolylpyridinium species **141** might offer an opportunity to obtain direct evidence for the site of attack by TMP as shown in Scheme 61. After the formation of the putative intermediate **170**, bromide may leave in the form of HBr via an intramolecular proton transfer reaction leading to the TMP adduct **171**. We were concerned, however, that the 4-membered transition state required for the proposed intramolecular proton transfer may prevent the displacement reaction shown in Scheme 64.

Scheme 64. Proposed formation of TMP adduct 171 via the displacement of bromide through an intramolecular proton transfer.

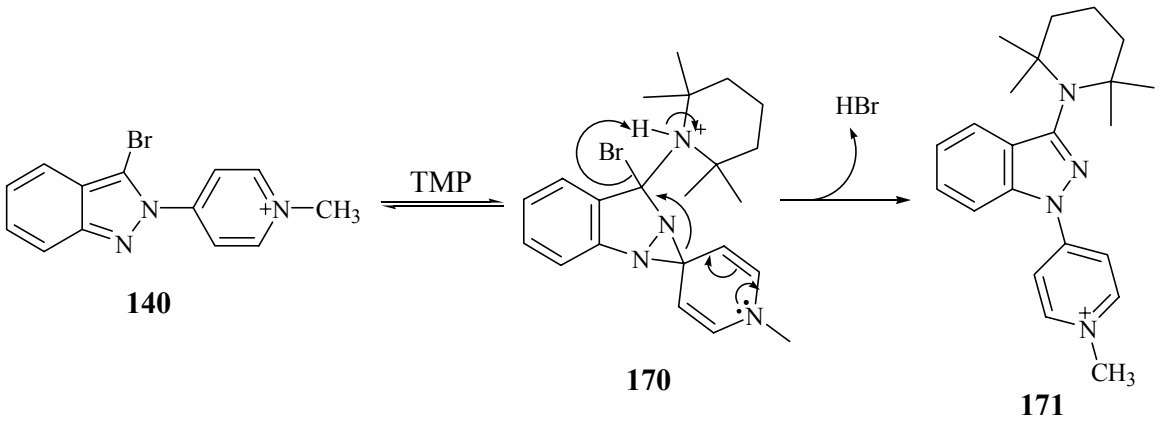

140 **170** **171**

The coupling reaction of 3-bromoindazole (**143**) with 4-chloro-1-methylpyridinium iodide (**55**) was attempted in the absence of TMP and monitored by HPLC-DA. Even at 100 ^{o}C, the reaction proceeded too slowly to be of synthetic utility. This was expected based on the results obtained for the analogous reaction of 3-methylindazole. Due to the failure of the coupling reaction, we prepared the 2*H*-3-

bromoindazolylpyridinium **141** via methylation of the previously synthesized (Scheme 56) 2*H*-3-bromoindazolylpyridine (**156**) as shown in Scheme 65.

Scheme 65. Synthesis of 2*H*-3-bromoindazolylpyridinium 141 via the methylation of 156.

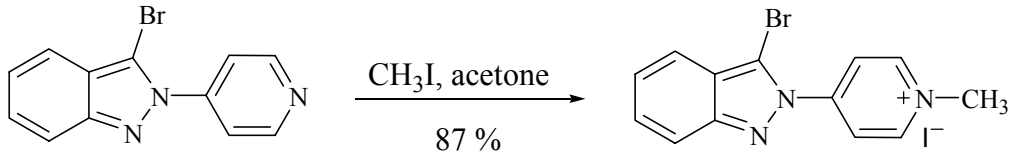

156 **141**

The fate of **141** was monitored in the presence of 1 equivalent of TMP via HPLC-DA (Fig. 29). The HPLC-DA tracings document the disappearance of **141** at room temperature over time and the appearance of a new peak which we expected to be either **145**, produced from the rearrangement reaction, or **171** from a displacement reaction.

Figure 29. HPLC-DA monitoring of the stability of 141 in the presence of TMP at room temperature.

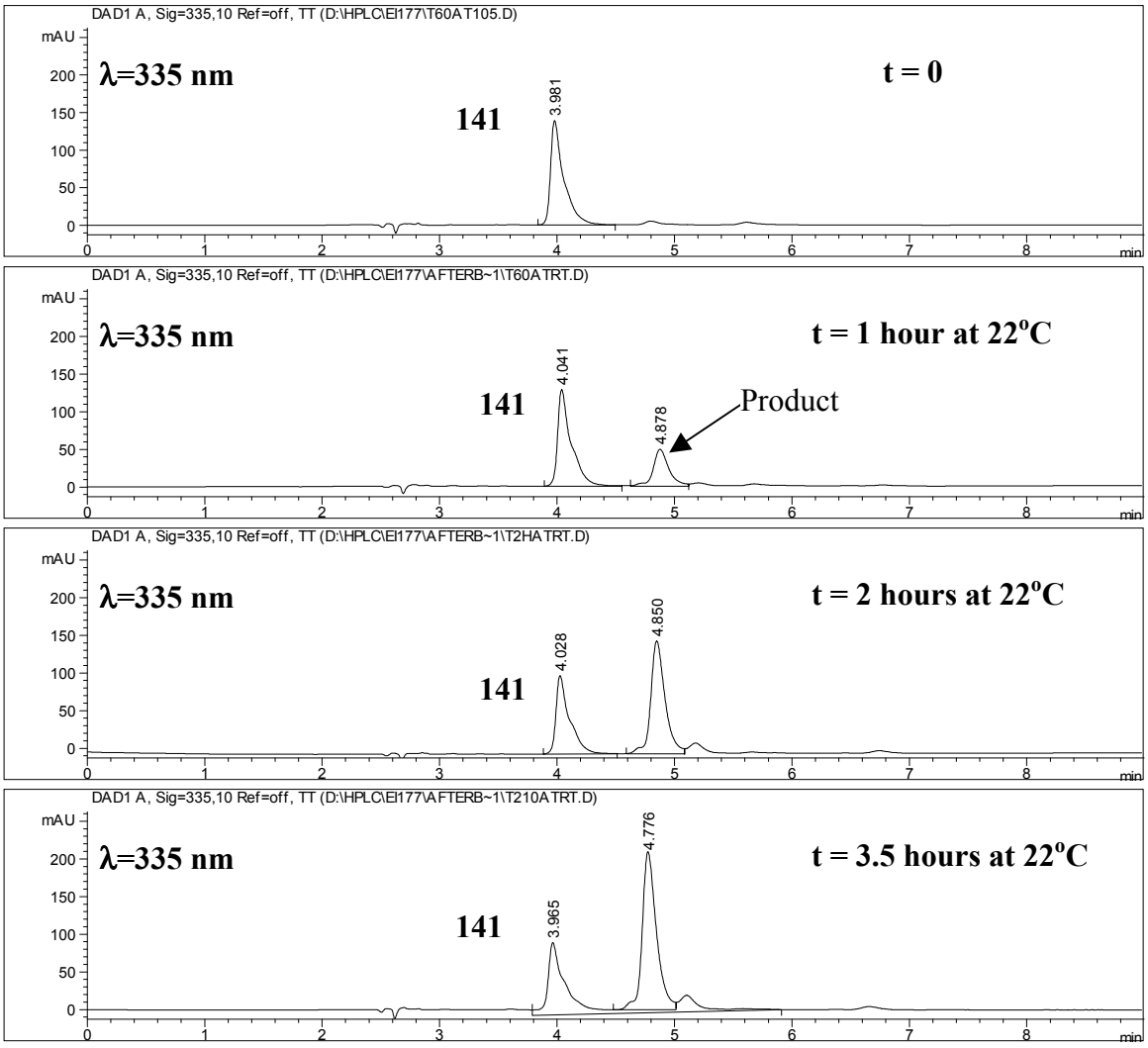

An independent synthesis of **145** was readily achieved by reaction between 3-bromoindazole and **55** in the presence of TMP at room temperature. A single product was obtained and was characterized as the expected 1*H*-3-bromoindazolylpyridinium species **145** (Scheme 66).

Scheme 66. Synthesis of 1*H*-3-bromoindazolylpyridinium 145 via the reaction between 3-bromoindazole (143) and 55 in the presence of TMP at room temperature.

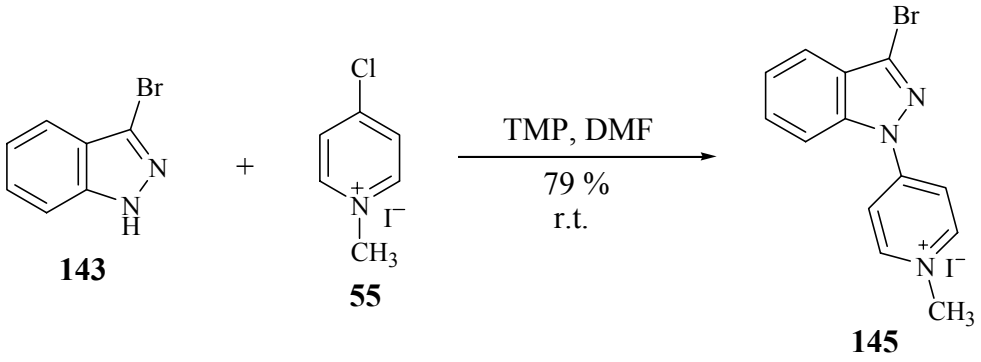

The retention time and the UV spectrum of the product obtained from the reaction of the 2*H*-isomer **141** with TMP corresponded to that of the 1*H*-3-bromoindazolylpyridinium **145** (Fig. 30). Also the ^{1}H NMR spectrum of this compound was identical with that of the independently synthesized 1*H*-isomer **144** (Fig. 31). Thus, treatment of **141** with TMP leads exclusively to the rearranged product **145**. There was no evidence for the formation of TMP adduct **171**.

Figure 30. (a) UV spectrum of the rearranged product (t_R = 4.8 min) and (b) UV spectrum of synthetic 1*H*-3-bromoindazolylpyridinium 145.

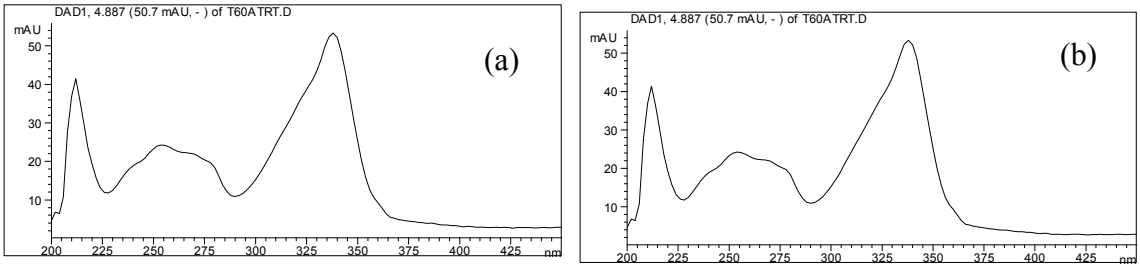

Figure 31. (a) ^{1}H NMR spectrum (500 MHz) of the reaction mixture containing the 2*H*-3-bromoindazolylpyridinium species 141 taken after 3 days in the presence of TMP at room temperature. (b)^{1}H NMR spectrum (500 MHz) of synthetic 1*H*-3-bromoindazolylpyridinium 145.

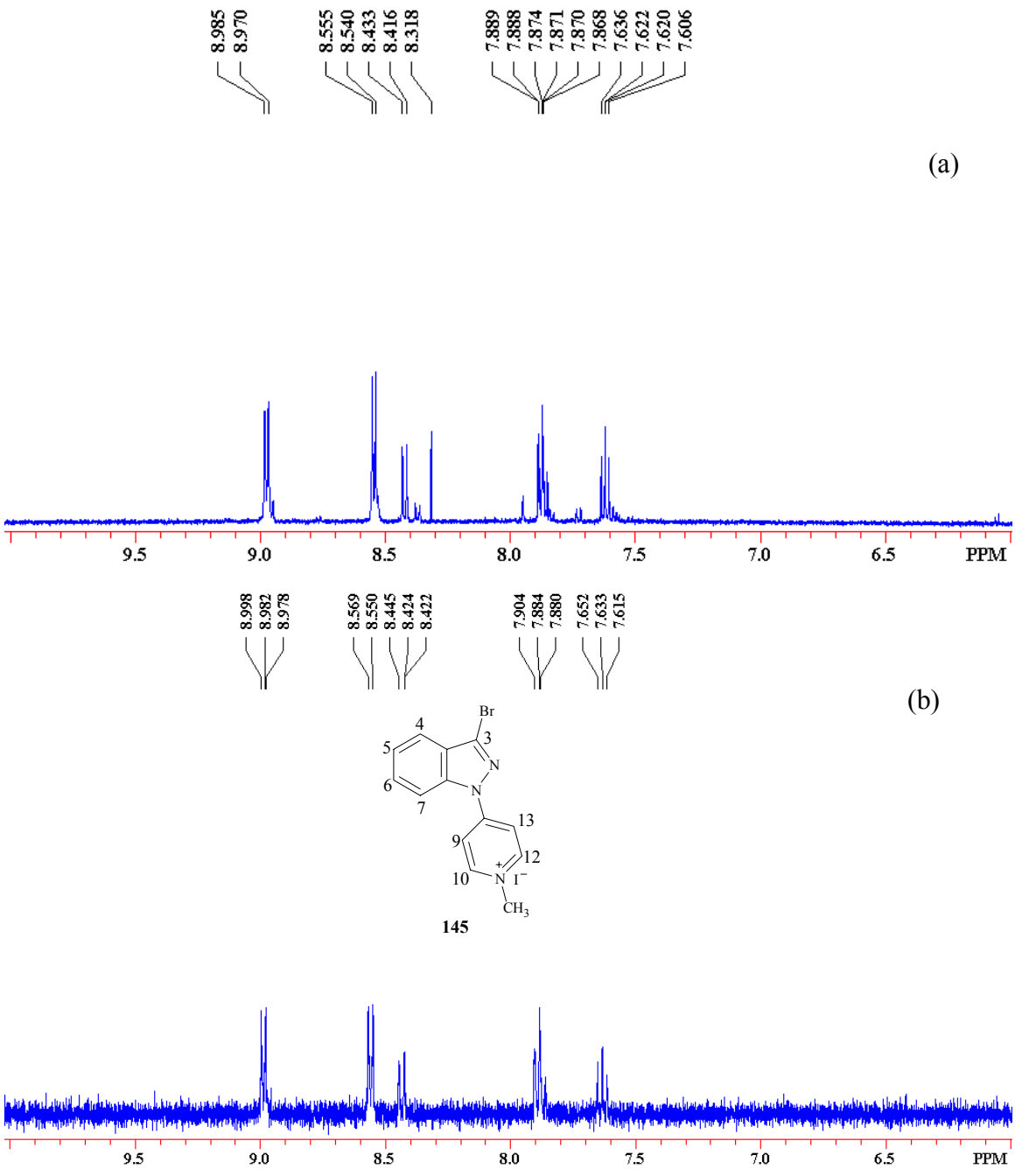

Unlike the elevated temperature required for the TMP catalyzed rearrangement of the previously investigated 2*H*-protio and 2*H*-3-methylindazolylpyridinium species, the

2*H*-3-bromoindazolylpyridinium species rearranged readily in the presence of TMP at room temperature. The enthalphies of reaction for the formation of the spirodiaziridinyl intermediates **164** and **170** derived from 2*H*-3-methyl and 2*H*-3-bromoindazolylpyridinium species, respectively, are similar, suggesting that steric factors are comparable. Steric factors being equivalent, the enhanced rate of rearrangement observed for the 2*H*-3-bromoindazolylpyridinium analog may be explained by the enhanced electropositivity of C-3 due to the electronegativity of the bromine atom at the expected site of attack. The increased electropositivity of C-3 should facilitate the attack by TMP and result in an increase in the rate of the rearrangement reaction. According to this analysis, increase in the rate of the rearrangement reaction observed with 3-bromo substitution is consistent with the attack by TMP at the C-3 position.

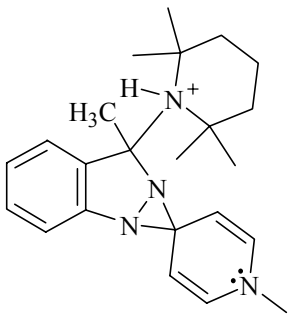

164

ΔH_{rxn} = 49 kcal/mol (AM1)

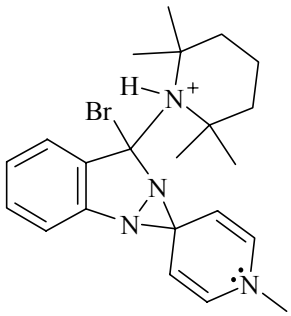

170

ΔH_{rxn} = 50 kcal/mol (AM1)

3.5.2. Studies on 6-Substituted Indazolylpyridinium Analogs

The results obtained so far on the rearrangement of 2*H*-indazolylpyridinium species are consistent with the attack of TMP at C-3 position. Nevertheless, we decided to investigate further the possibility of attack by TMP at C-6 as an alternative pathway for the TMP catalyzed rearrangement. In order to explore the potential electronic effects of substitution at C-6 on the rate of the rearrangement reaction, we undertook the preparation of 2*H*-6-bromo and 2*H*-6-methoxyindazolylpyridinium analogs **174** and **175** and the corresponding 1*H*-isomers **176** and **177**.

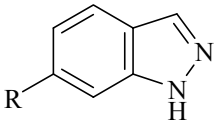

172: R = Br
173: R = OCH_3

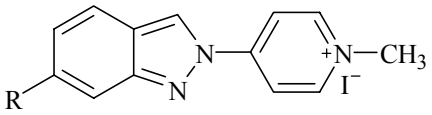

174: R = Br
175: R = OCH_3

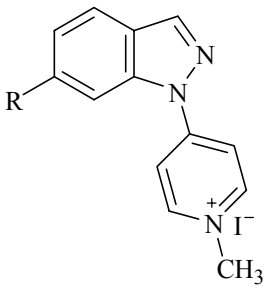

176: R = Br
177: R = OCH_3

3.5.2.1. Synthesis

The synthesis of the starting indazoles **172** and **173** was attempted via the diazotization of the corresponding methylanilines **178** and **179** followed by *in situ* cyclization. This method has been employed previously for the preparation of 7-NI.[200] The synthesis of 6-bromoindazole (**172**) was achieved successfully in 63 % yield as shown in Scheme 67. Compound **172** was fully characterized as described in the experimental section.

Scheme 67. Synthesis of 6-bromoindazole (168) via the diazotization of 174 followed by cyclization.

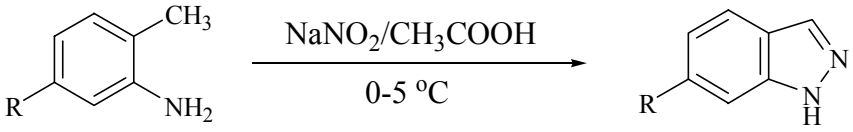

178: R = Br
179: R = OCH_3

172: R = Br
173: R = OCH_3

When the preparation of 6-methoxyindazole was attempted in a similar manner, the GC-MS TIC tracings showed the appearance of two peaks early in the course of the reaction. After 5 minutes (Fig. 32a), the intensity of the peak (t_R = 9.32 minutes) with $M^{\cdot+}$ 148, expected for the anticipated product **173**, was approximately equal to that of a

[200] Barbet, O., Minjat, M., Petovy, A. (1986) Phenyl urees derives de l'indazole; recherché de l'activite anthelminthique, effect des substituants. *Eur J. Med.Chem. –Chim Ther*. **21**, 359-362.

second peak with t_R = 8.32 minutes which had $M^{\cdot+}$ 180. By 2 hours (Fig. 32b) only starting aniline (t_R = 9.44 minutes) and the unexpected peak at t_R = 8.32 minutes were present.

Figure 32. GC-MS monitoring of the attempted synthesis of 6-methoxyindazole via diazotization of 5-methoxy-2-methylaniline (179).

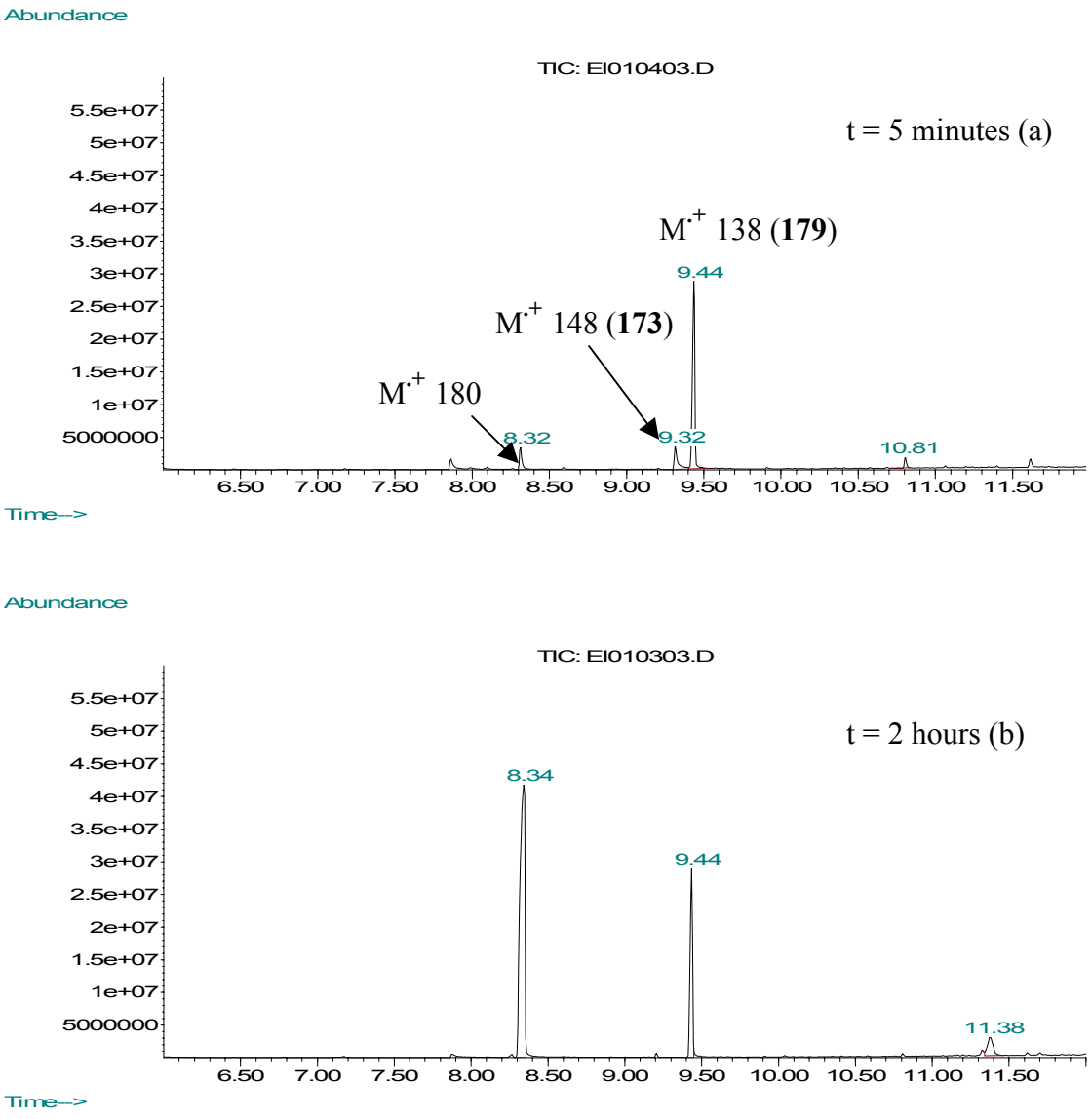

The mass spectrum of the unknown peak is shown in Figure 33. The parent ion of 180 Da corresponds to 2-acetoxy-5-methoxytoluene (**181**, Scheme 66) which is likely to be formed by the reaction of the diazonium intermediate **180** with solvent acetic acid.

Figure 33. Mass spectrum of the unknown peak with the retention time of 8.32.

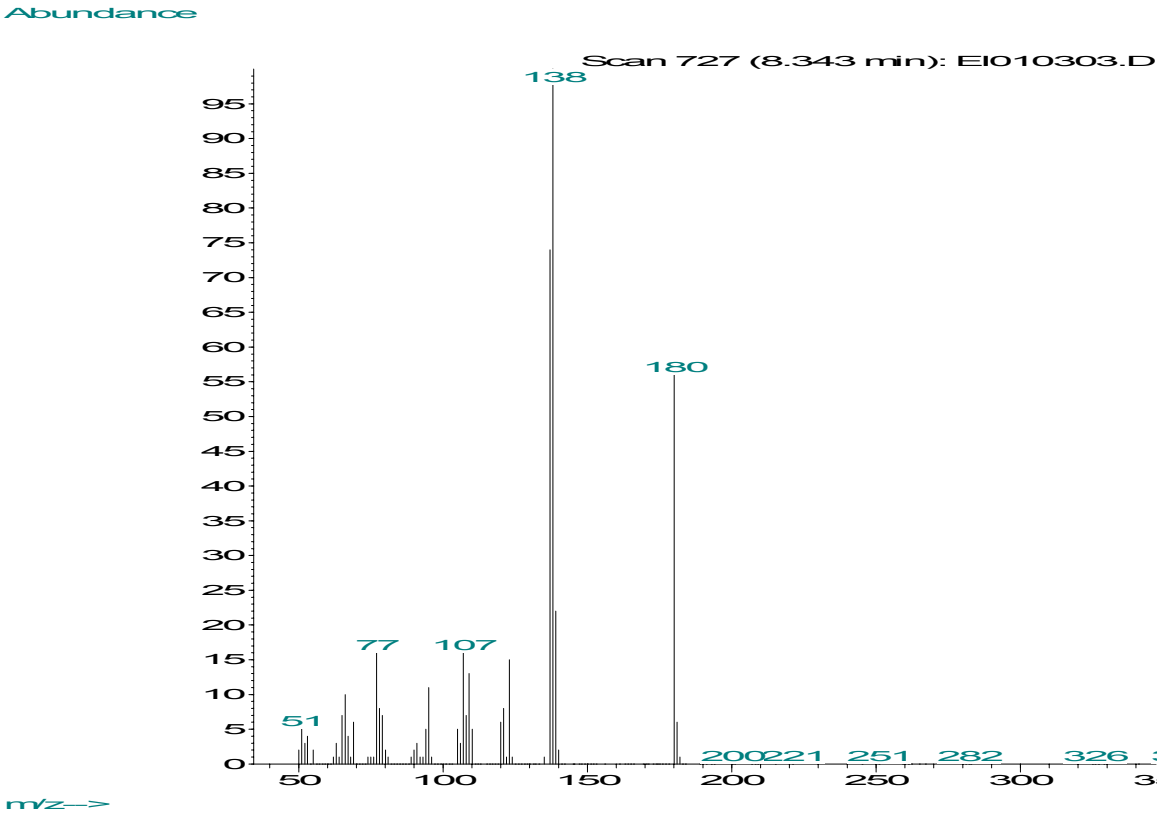

It seems likely, therefore, that the presence of **173** in the reaction mixture resulted from cyclization of **180** in the injection port of the GC (Scheme 68). Although compound **181** was not characterized fully, the loss of ketene from the parent ion proposed in Scheme 69 is consistent with the major fragment m/z 138. A literature search did not reveal an example of this type of a conversion (formation of **181** from **180**).

Scheme 68. Formation of 6-methoxyindazole and 180 from the diazonium species 181.

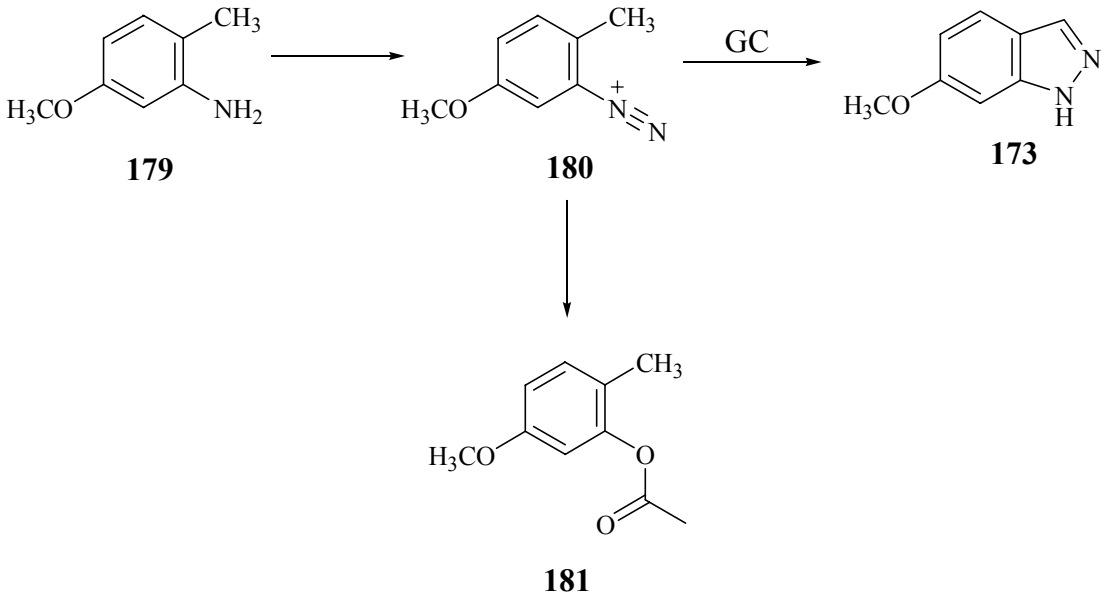

Scheme 69. Proposed fragmentation of 181 to give 182 and ketene.

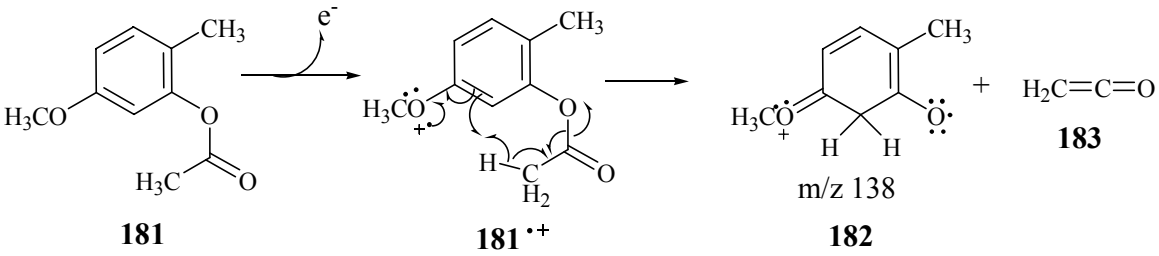

Due to the failure of the above approach, we attempted the synthesis of 6-methoxyindazole by first isolating the diazonium intermediate as the tetrafluoroborate salt (**181**) followed by cyclization using potassium acetate in the presence of 18-crown-6 as shown in Scheme 70.[201]

[201] Reference 195.

Scheme 70. Synthesis of 6-methoxyindazole.

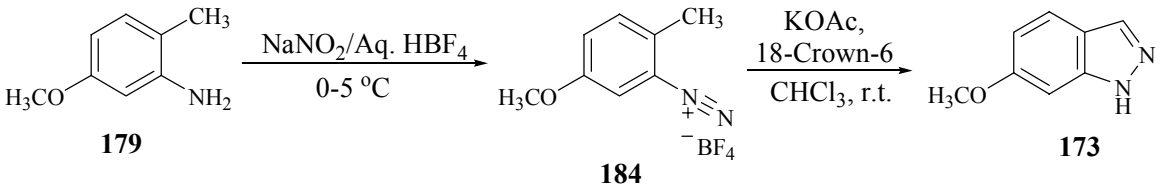

The tetrafluoroborate salt **184** was obtained in 93% yield. However, when kept at room temperature, **184** decomposed with gas evolution to give 2-fluoro-4-methoxytoluene (**185**) as shown in Scheme 71. This is a known pathway to fluorobenzene derivatives.[202] We also observed the formation of a product in the GC-MS TIC tracings corresponding to phenol **186**.

Scheme 71. Decomposition of diazonium tetrafluoroborate 184.

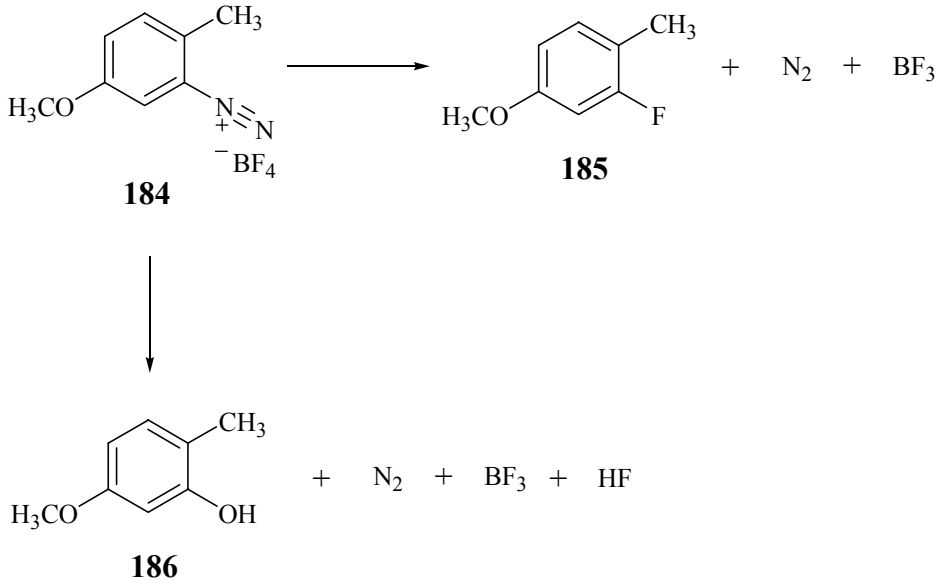

The tetrafluoroborate salt **184** was freshly prepared prior to the cyclization reaction shown in Scheme 70 or kept in the refrigerator after its preparation. The cyclization reaction of **184** resulted in the formation of 6-methoxyindazole (**173**) in 36% yield.

[202] Balz, Schieman (1927) *Ber.* **60**, 1186.

The coupling reaction between 6-bromoindazole and **55** in the absence of TMP at 100 ^{o}C resulted in the exclusive formation of the 2*H*-6-bromoindazolylpyridinium **174** as expected in 72 % yield (Scheme 72). When the coupling reaction was attempted in the presence of TMP at room temperature, HPLC-DA analysis indicated that a mixture of 1*H*- and 2*H*-6-bromoindazolylpyridinium products had been produced. Only the 1*H*-isomer **176** was isolated from the reaction mixture and fully characterized as the major product of the reaction. These results are in agreement with the outcome of the coupling reaction between indazole and **55**.

Scheme 72. Synthesis of 1*H*- and 2*H*-6-bromoindazolylpyridium derivatives 176 and 174.

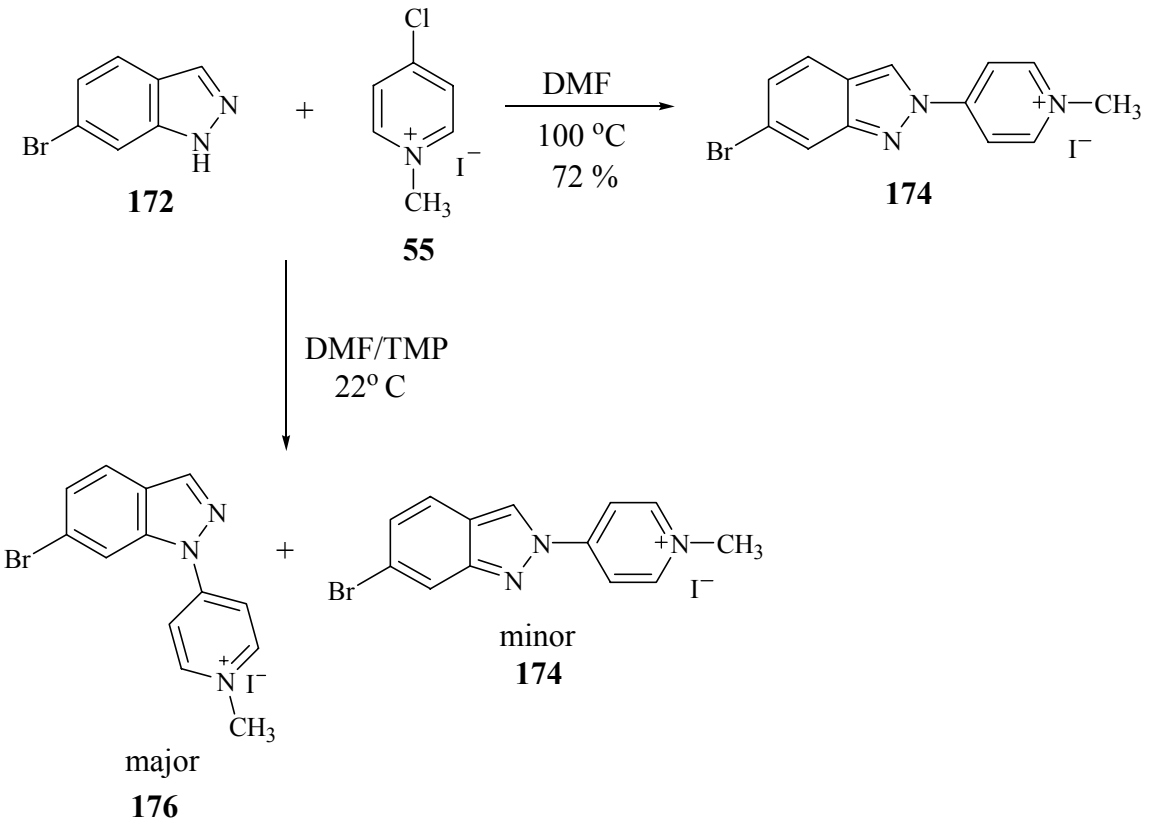

The synthesis of the 6-methoxyindazolypyridinium analogs **175** and **177** was examined next. First, the reaction between 6-methoxyindazole and **55** shown in Scheme 73 was carried out in the absence of TMP and monitored by HPLC-DA. As shown in Figure 34, formation of a single product was observed to take place slowly even at room

temperature (In Fig. 34 panel b, the HPLC tracing at 369 nm is included instead at 269 nm in order to demonstrate the product formation more clearly). In contrast, the reaction between indazole (or 6-bromoindazole) and **55** in the absence of base results in product formation only at elevated temperatures (100 ^{o}C).[203] The product was obtained in 56% yield and characterized as the 2*H*-isomer **177** as expected.

Scheme 73. Addition elimination reaction between 6-methoxyindazole (177) and 55.

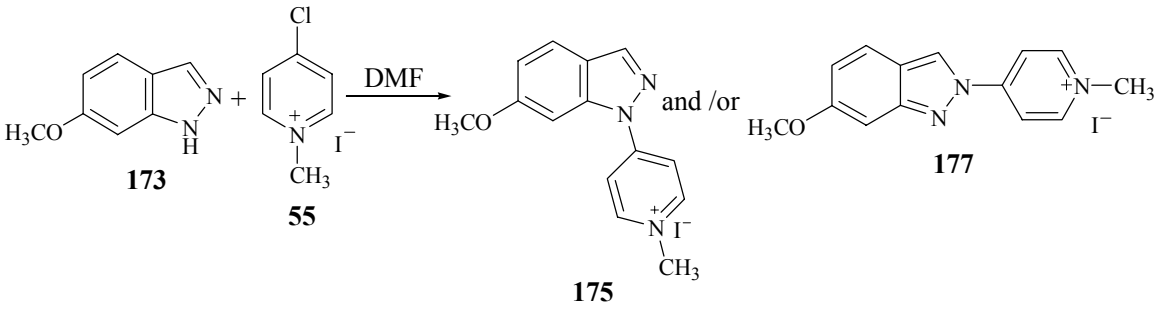

173 **55** **175** **177**

[203] For a detailed explanation for the high temperature requirement see Section 2.2.1.2.

Figure 34. HPLC-DA monitoring of the reaction between 6-methoxyindazole and 55 in the absence of TMP.

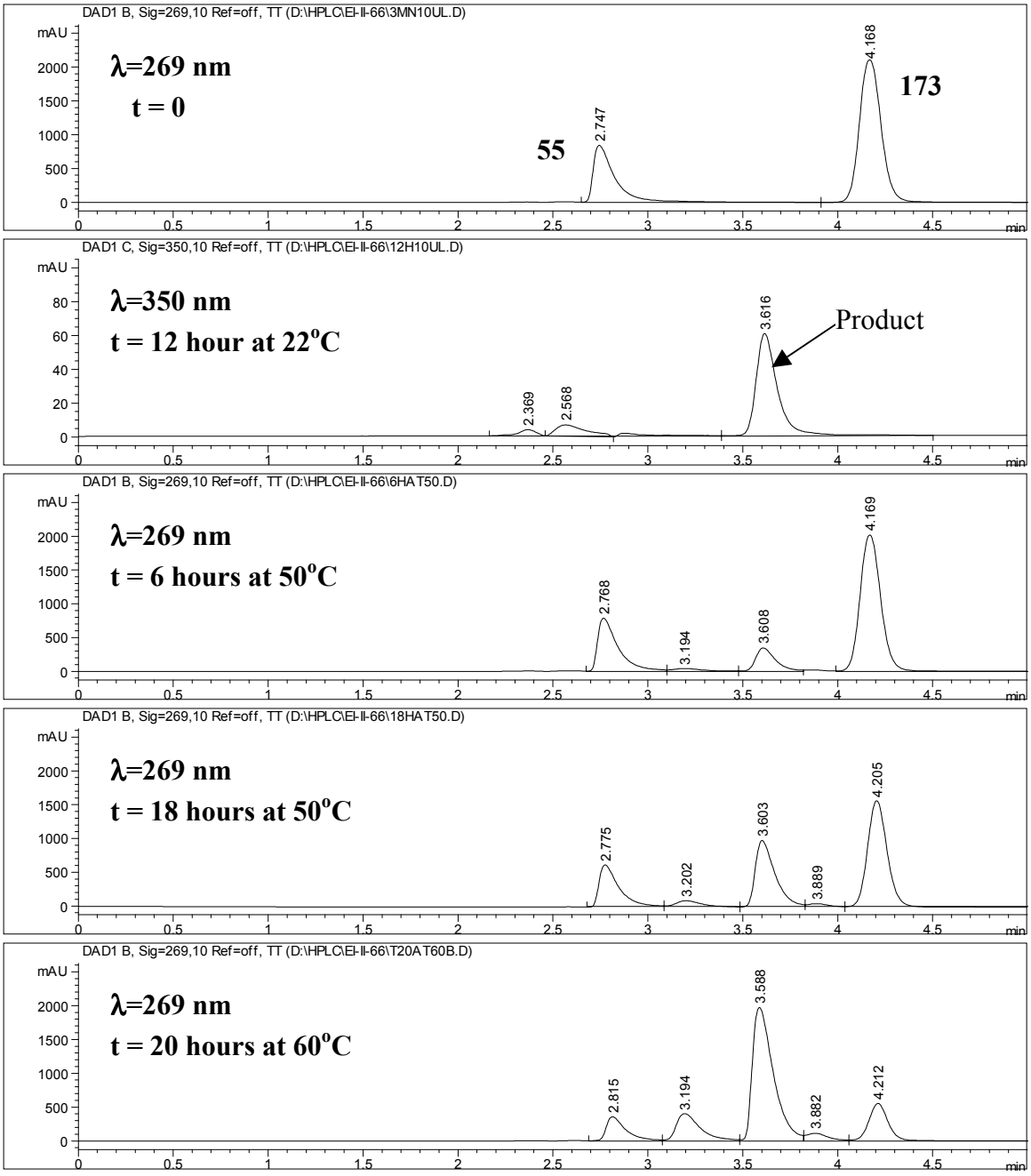

The enhanced reactivity of 6-methoxyindazole compared to the protio and 6-bromoindazole is consistent with the expected increase in nucleophilicity of the N-2 nitrogen of **173** due to the electron donating properties of the methoxy substituent. Also,

the resonance stabilization of the positively charged intermediate **187** facilitates the product formation (Scheme 74).

Scheme 74. Resonance stabilization of intermediate 187 increasing the rate of the reaction leading to 2*H*-6-methoxyindazolylpyridinium 174.

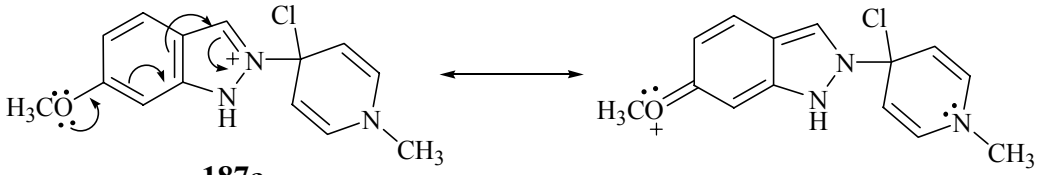

187a **187b**

The corresponding 1*H*-isomer **177** was prepared as a reference compound for the monitoring of the rearrangement reaction. This time, the reaction between 6-methoxyindazole and **55** was carried in the presence of TMP at room temperature. Although, the formation of the 2*H*-isomer was observed by HPLC-DA in this reaction, the major product was the 1*H*-isomer **177** which was obtained in 70 % yield. This outcome was in agreement with the previously investigated reactions between indazole derivatives and **55** in the presence of TMP at room temperature.

3.5.2.2. Investigation of the Rearrangement Reaction

The rearrangement of 4-(2*H*-6-bromoindazolyl)-1-methylpyridinium iodide (**174**) was attempted in the presence of TMP and monitored by HPLC-DA. As in the case of 4-(2*H*-3-bromoindazolyl)-1-methylpyridinium (**141**), the isomerization of **174** to the corresponding 1*H*-isomer **176** proceeded at room temperature in contrast to the protio analog **112** which rearranged at a comparable rate only when heated to 60 ^{o}C. However, the rate of the rearrangement was approximately 4 times slower than that of the 3-bromo analog **141**. Assuming attack of TMP at C-3, a slower rate of rearrangement for **174** would be expected due to the lower electropositivity at C-3 for this analog compared to **141**. The increase in the rate of isomerization of **141** compared to the 2*H*-protio compound **112** is also consistent with the increased electropositivity of the indazole nucleus.

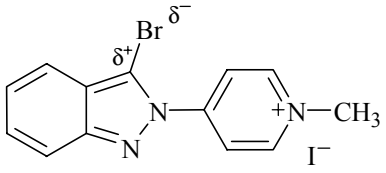

141

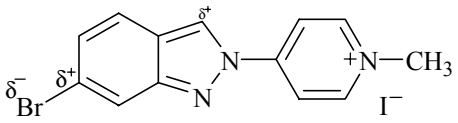

174

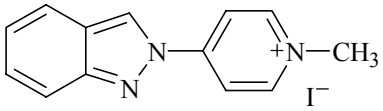

112

An alternative rationale to account for the more rapid rearrangement of **174** compared to **112** is the attack by TMP at C-6 instead of C-3 since the electropositivity of C-6 will be enhanced due to the bromine substitution at this position. On the basis of our calculations, however, this possibility is considered unlikely in view of the much higher energy of the spirodiaziridinyl intermediate **188** generated by the attack of TMP at C-6 compared to the benzenoid spirodiaziridinyl intermediate **189** which will form upon attack at C-3.

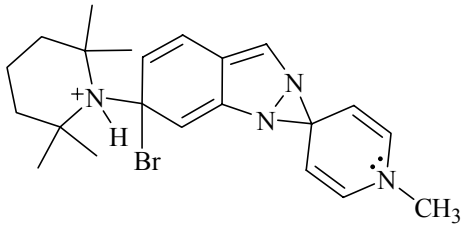

188

ΔH_{rxn} = 70 kcal/mol (AM1)

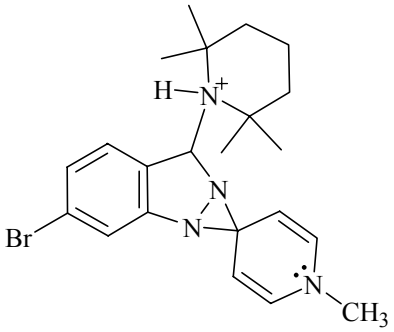

189

ΔH_{rxn} = 29 kcal/mol (AM1)

Therefore, we conclude that the increased rate of rearrangement observed for **174** compared to **112** must be due to the bromine substitution at C-6 increasing the electropositive character at C-3 inductively, where the attack by TMP is expected to take place. The rate of the rearrangement reaction is still slower than the rate observed for 2*H*-3-bromoindazolylpyridinium species **141** since the electropositivity of C-3 will be considerably higher in **141** compared to **174**.

Next, the rearrangement of 2*H*-6-methoxyindazolylpyridinium **175** to the corresponding 1*H*-isomer was investigated. When the stability of **175** was monitored by HPLC-DA in the absence of TMP, no change was observed even at 150 ^{o}C. Consequently, the increase in nucleophilicity of N-1 due to the presence of the 6-methoxy substituent (Scheme 75, resonance structure **175b**) is not sufficient to lead to a unimolecular rearrangement reaction through the hypothetical intermediate **190**.

Scheme 75. Possible unimolecular formation of spirodiaziridinyl intermediate 190 facilitated by the 6-methoxy substituent.

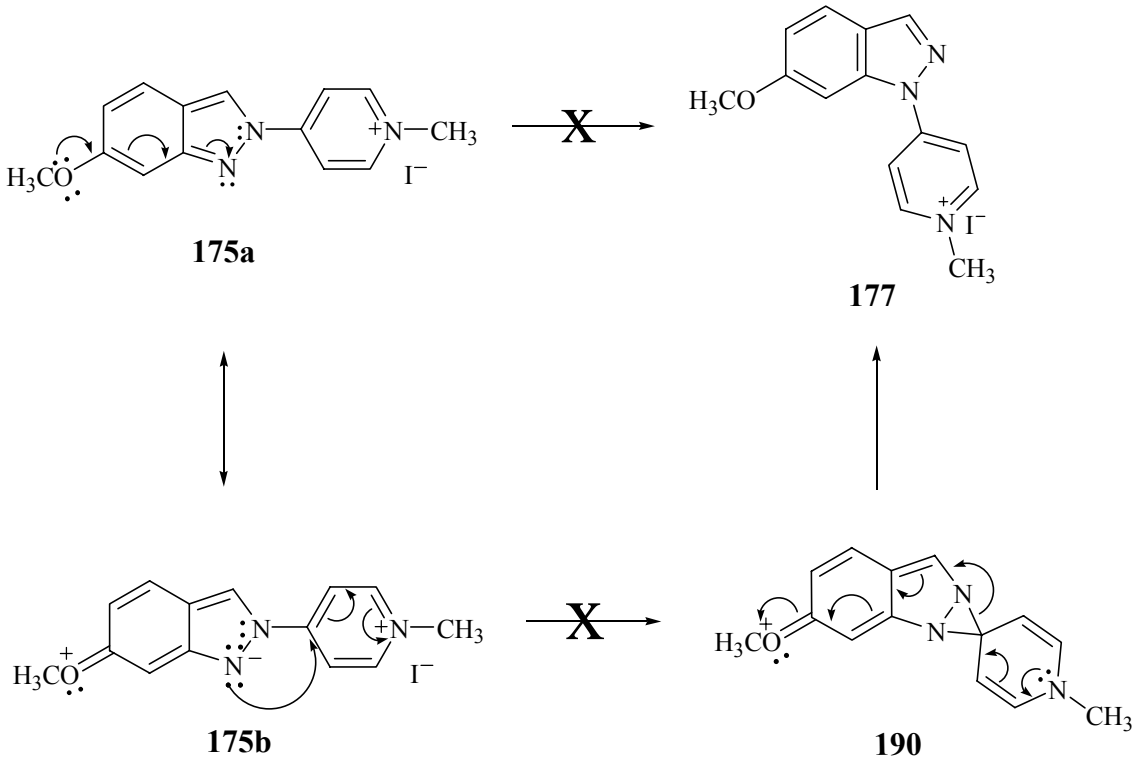

The stability of the 2*H*-isomer **175** was also monitored in the presence of 1 equivalent of TMP at 90 ^{o}C by ^{1}H NMR. It was seen that **175** was rearranging at a rate comparable to that observed with the 2*H*-protioindazolylpytridinium derivative **112**. Since the methoxy substituent at C-6 is expected to increase the electropositivity at this position, the possible attack of TMP at C-6 is likely to increase the rate of the rearrangement compared to **112**. Therefore, observed rate of rearrangement for **175** is consistent with the attack of TMP at C-3.

3.5.3. Studies on the 5-Substituted Indazolylpyridinium Derivatives

As discussed in Section 5.3.2.2, the increased rate of rearrangement observed for 4-(2*H*-6-bromoindazolyl)-1-methylpyridinium iodide (**174**) compared to the 2*H*-protio derivative **112** is likely to be due to the increased electropositivity of the indazole nucleus due to the presence of bromine atom. This outcome led us to study the rearrangement reaction of the 2*H*-5-bromoindazolylpyridinium derivative **193** to the corresponding 1*H*-isomer **195** in order to investigate the effect of changing the position of bromine substitution. The 5-methoxy analog **194** was also included in order to examine the effect of an electron donating substituent at C-5.

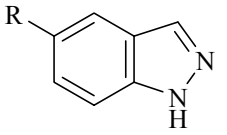

191: R = Br
192: R = OCH_3

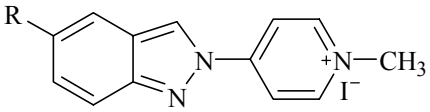

193: R = Br
194: R = OCH_3

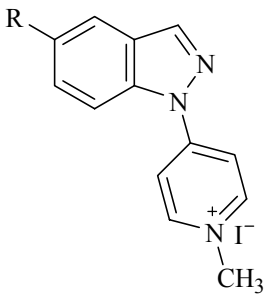

195: R = Br
196: R = OCH_3

The synthesis of 2*H*-5-bromoindazolylpyridinium species **193** was carried out as previously described for the corresponding 6-bromo substituted derivative (Scheme 72). The rearrangement of the 2*H*-isomer **193** to the corresponding 1*H*-isomer **195** in the presence of TMP took place at room temperature at a rate comparable to that observed with 2*H*-6-bromoindazolylpyridinium **174**. This outcome provided further evidence for the inductive effect of bromo substitution at C-5 or C-6 increasing the electropositivity at C-3 which leads to the enhancement of the rate of isomerization observed for **174** and **193** compared to the 2*H*-protioindazolylpyridinium **112**.

Next, the preparation of 4-(2*H*-5-methoxyindazolyl)-1-methylpyridinium iodide (**194**) was attempted via the addition-elimination reaction between 5-methoxyindazole (**192**) and **55** in the absence of base. Product formation was observed even at room temperature at a rate comparable to that observed for the analogous reaction between

6-methoxyindazole (**173**) and **55**. Since 5-methoxy substituent is not expected to increase the nucleophilicity of N-2 directly, it is not possible to explain the enhanced rate of the reaction between 5-methoxyindazole and **55** in the absence of TMP, at this point.

The rearrangement of 4-(2*H*-5-methoxyindazolyl)-1-methylindazolylpyridinium iodide (**190**) was attempted in the presence of TMP at 90 ^{o}C and monitored by ^{1}H NMR. The rate of rearrangement was compared with 4-(2*H*-indazolyl)-1-methylpyridinium iodide (**112**). As in the case of the 6-methoxy analog **175**, the rate of the rearrangement of **190** was comparable to that observed with the 2*H*-isomer **112**. Although the methoxy group is expected to increase the electron density at C-3 via resonance (Scheme 76), disfavoring the attack by TMP, the rearrangement reaction appeared not to be retarded. This outcome suggests that contribution of resonance structure **194b** is not significant.

Scheme 76. Increased electron density on C-3 due to the electron donating effect 5-methoxy substituent.

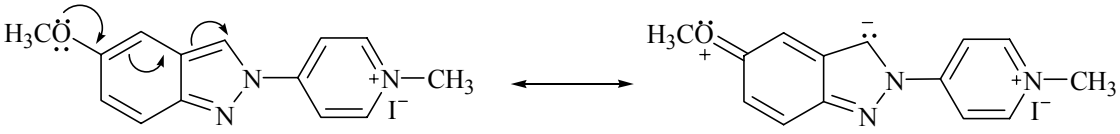

194a **194b**

CHAPTER 4
STUDIES ON THE CYANIDE MEDIATED REARRANGEMENT OF 2*H*-INDAZOLYLPYRIDINIUM DERIVATIVES

4.1. Cyanide Mediated Rearrangement of 2*H*-3-bromoindazolylpyridinium 141.

The results of all the experiments carried out so far on the rearrangement reaction are consistent with a nucleophilic pathway. We suspect that attack takes place at the C-3 carbon of the indazolyl moiety resulting in the formation of a spirodiaziridinyl intermediate which leads to the isomerization of the 2*H*-indazolylpyridiniums to the thermodynamically more stable 1*H*- isomers. However, no direct evidence documenting the site of attack is available. Attempts to displace the 3-bromo group by TMP failed, perhaps because of the unfavored 4-membered transition state of intramolecular proton transfer step. In the light of this observation, the use of a strong nucleophile with poor leaving group properties was considered. Therefore, it was decided to examine cyanide as a potential nucleophile which might displace bromide to give the 1*H*-3-cyano adduct **198** as shown in Scheme 77. Bromide is a better leaving group than cyanide and could leave preferentially after the formation of the spirodiaziridinyl intermediate **197**. Furthermore, formation of a new, strong carbon-carbon bond could favor the cyano adduct **198** over the 1*H*-3-bromoindazolylpyridinium species **145**.

Scheme 77. Proposed displacement of bromide by cyanide leading to the cyano adduct 198 vs. formation of isomerization product the 1*H*-3-bromoindazolylpyridinium 145.

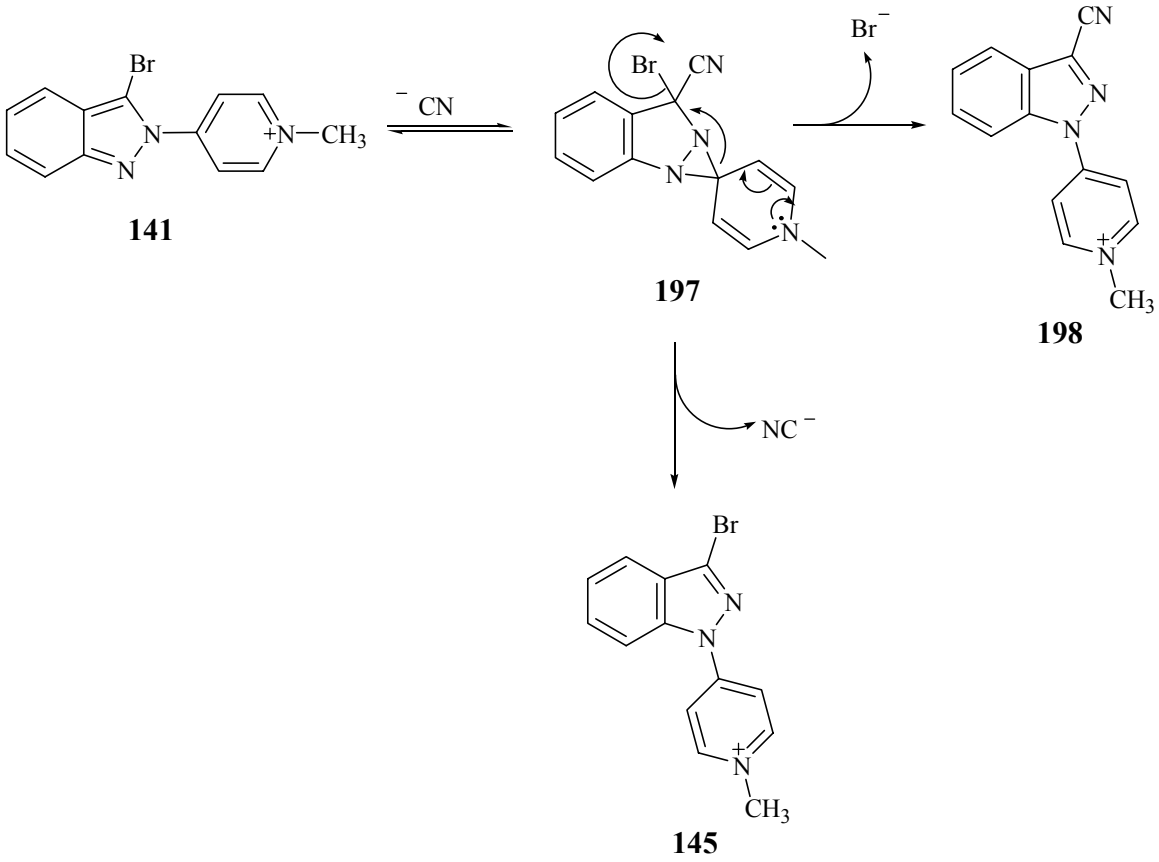

To a solution of the 2*H*-isomer **141** in DMSO-d_6 1 equivalent of cyanide was added as a KCN/DMSO-d_6 solution in an NMR tube. A color change from yellow to green and to dark green-black was observed immediately after the cyanide addition. Eventually the color of the reaction mixture turned orange. The progress of the reaction was monitored by ^{1}H NMR. The results are shown in Figure 35.

Figure 35. ^{1}H NMR (500 MHz) monitoring of the reaction between 141 and cyanide at room temperature.

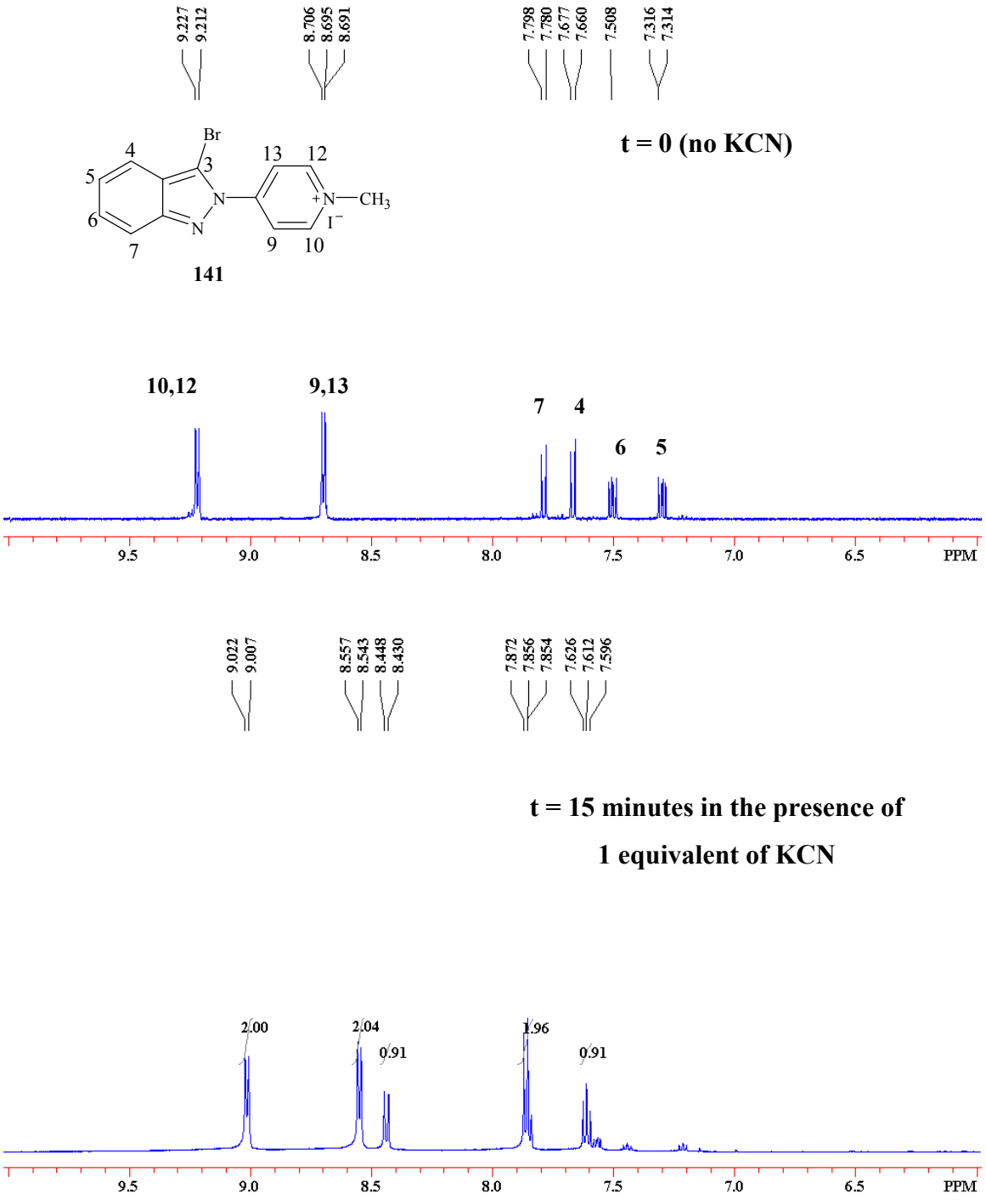

The signals corresponding to the 2*H*-isomer **141** disappeared completely within 15 minutes and a new set of signals, consistent with an indazolylpyridinium structure, appeared (Fig. 35). Some minor peaks also were present in the ^{1}H NMR spectrum. A comparision of this spectrum with the spectrum of synthetic 1*H*-3-bromoindazolylpyridinium iodide [(**145**), Fig. 36], established that the product to be the 1*H*-isomer **145**.

Figure 36. Synthetic 1*H*-3-bromoindazolylpyridinium 145.

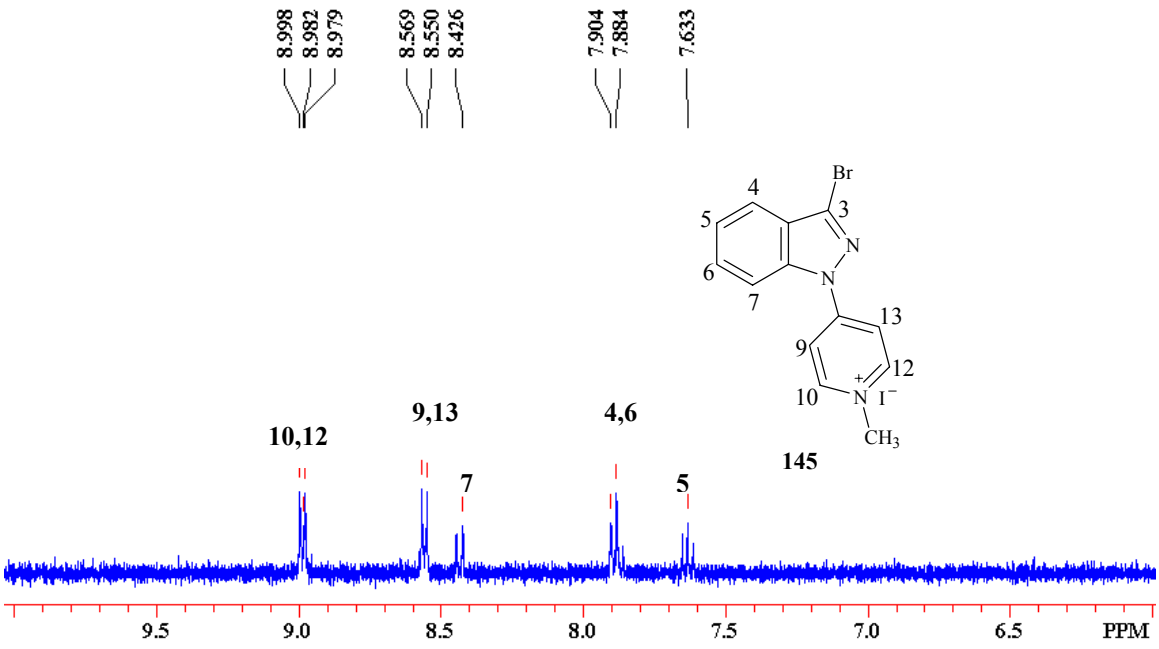

This outcome did not appear to be consistent with the better leaving group properties of bromide vs. cyanide. At this point an alternative mechanism was considered for the rapid cyanide promoted rearrangement reaction that also would account for the retention of bromine in the rearranged product.

4.2. Proposed Cyanide Mediated Rearrangement of 140 via a Radical Pathway

One electron reduction of **141** by cyanide (Scheme 78) may result in the formation of the pyridinyl radical **199** which could lead to the neutral spirodiaziridinyl radical intermediate **200**. Following ring opening to **201**, a single electron transfer from the rearranged product to another molecule of **141** could serve as a propagation step in a chain reaction. The mechanism shown in Scheme 78 is attractive since it would account for the retention of bromine in the rearranged product **145**.

Scheme 78. Proposed cyanide catalyzed radical initiated rearrangement reaction.

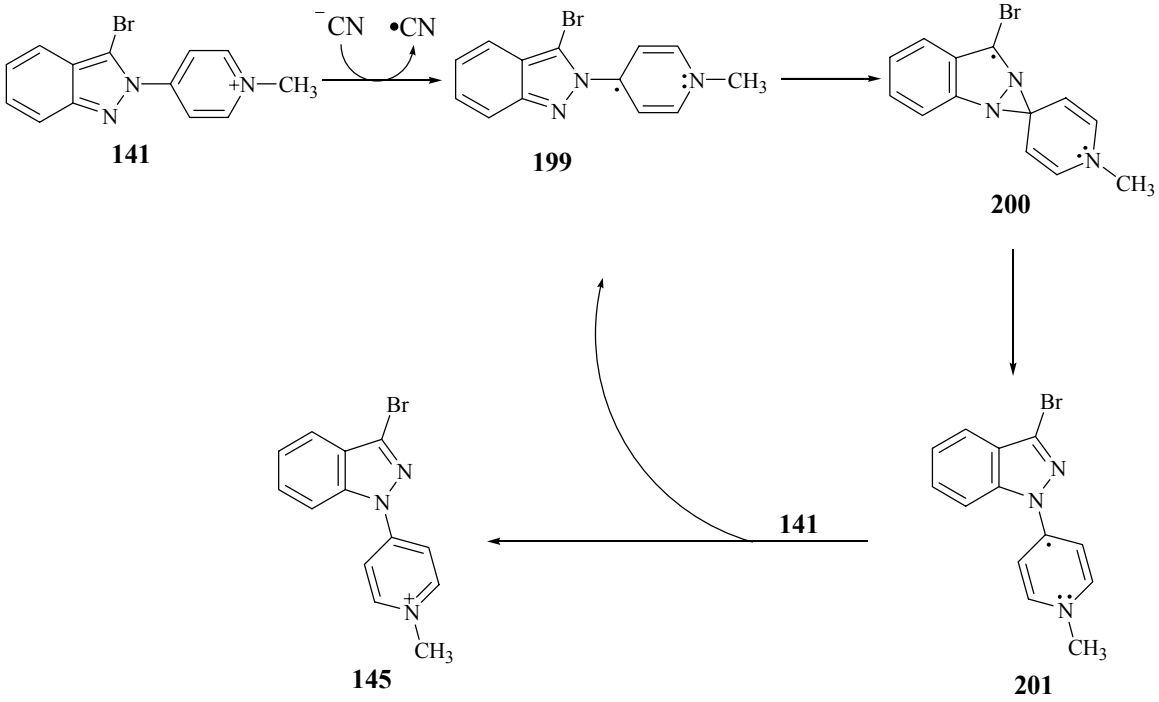

The following is a brief review of the one electron reduction of pyridinium species.

4.2.1. One Electron Reduction of Pyridinium Species.

One electron reduction of pyridinium species to form dihydropyridinyl radicals[204] has been reported in the literature[205] in part because of interest in the biologically important reductive cofactor nicotinamide adenine dinucleotide (NADH).[206] Mairanovskii *et al*. was first to propose the one electron electrochemical reduction of N-alkylpyridinium species to form dihydropyridinyl radicals that undergo dimerization.[207.208] Both chemical and electrochemical reductions of quaternary pyridinium salt, e.g. the 1-methylpyridinium species **202**, to the reactive dihydropyridinyl radical intermediate **203** have been reported to result in the subsequent rapid formation of the dimeric species **204** as shown in Scheme 79. [209] Gaudiello *et al.* provided evidence for the formation of the transient radical intermediate **203** via electron spin resonance (ESR) spectroscopy after spin trapping **203** by α-phenyl-N-*t*-butylnitrone (**205**) to form **206**.[210] Gaudiello's research group has also determined the formal reduction potential of the 1-methylpyridinium species **202** in aqueous 1.0 M KCl to be 1.372 V vs. NHE. The regiochemistry and stereochemistry of the dimerization of substituted dihydropyridinyl radicals have been studied extensively.[211,212,213]

---

[204] In the literature, the term 1,4-dihydropyridyl is also used. See for example Reference 211.
[205] Gaudiello, J.G., Larkin, D., Rawn, D.J., Sosnowski, J.J. (1982) On the mechanism of electrochemical reduction of N-methylpyridinium ion. *J. Electroanal. Chem.* **131**, 203-214.
[206] Lavilla, R. (2002) Recent developments in the chemistry of dihydropyridines. *J. Chem. Soc. Perkin Trans. 1*, 1141-1156.
[207] Mairanovskii, S.G. (1956) Polarographic behavior of quaternary pyridine salts. *Dokl. Akad. Nauk USSR* **110**, 593-596.
[208] Mairanovskii, S.G. (1957) Nature of catalytic hydrogen currents in polarography. *Dokl. Akad. Nauk USSR* **114**, 1272-1275.
[209] Lavilla, R., Spada, A., Carranco, I., Rayo, M., Llorente, N., Diaz, J.L. Bernabeu (2002) Productive trapping of NAD^+ type of radicals. Non-biomimetic reduction of pyridinium salts. *Chem. Commun.* 850-851.
[210] Gaudiello, J.G., Larkin, D., Rawn, D.J. Sosnowski, J.J. (1982) On the mechanism of the electrochemical reduction of N-methylpyridinium ion. *J. Electronanal. Chem.* **131**, 203-214.
[211] Carelli, I., Cardinali, M.E., Casini, A., Arnone, A. (1976) Electrochemical reduction of 3-cyano-1-methylpyridinium iodide, a nicotinamide adenine dinucleotide model compound. *J. Org. Chem.* **41**, 3967-3969.
[212] Carelli, V., Liberatore, F., Casini, A., Tortorella, S., Scipione, L., Di Renzo, B. (1998) On the regio- and stereoselectivity of pyridinyl radical. *New. J. Chem.* **22**, 999-1004.
[213] Gaillard, F., Sung, Y.-E., Bard, A.J. (1999) Hot electron generation in aqueous solution at oxide-covered tantalum electrodes. Reduction of methylpyridinium and electrogenerated chemiluminescence of Ru(bpy)32+. *J. Phys. Chem. B*. **103**, 667-674.

Scheme 79. Dimerization of the dihydropyridinyl radical 203.

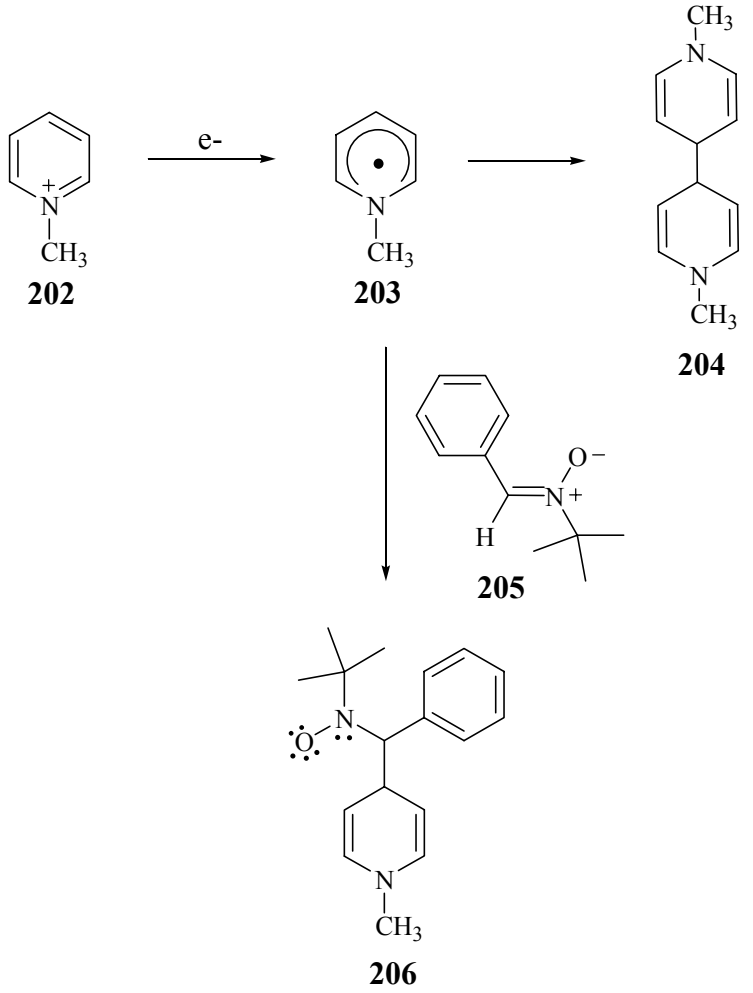

With the aid of microelectrode cyclic voltammetry, Foster has determined the dimerization rate of the 1-methylcarbamidopyridinyl radical **208**, which was derived from the corresponding pyridinium perchlorate salt **207**, to the dihydropyridine dimer **209** to be 9.0×10^6 $M^{-1}s^{-1}$ in DMF (Scheme 80).[214] The rate of dimerization in aqueous medium was larger by two orders of magnitude.

[214] Forster, R.J. (1999) Mechanism and kinetics of homogenous 1-methyl-carbamidopyridinyl radical reactions. *Phys. Chem. Chem. Phys.* **1**, 1543-1548.

Scheme 80. Dimerization of pyridinyl radical 208 formed by the reduction of 1-methyl-carbamidopyridinium perchlorate (207) to give bis-dihydropyridine 209.

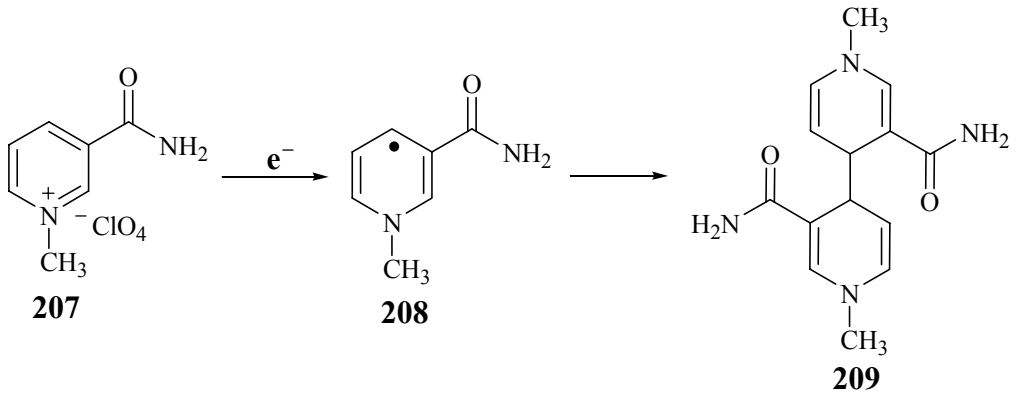

A recent report by Lavilla *et al.* describes the trapping of a variety of dihydropyridinyl radicals, such as **210**, by 1-chloroacrylonitrile (**211**) in the presence of Zn-CuI to form γ-addition products of the structure **212**, as shown in Scheme 81, as well as dimeric products. However, the reaction was reported to fail for unactivated pyridinium derivatives like 1-methylpyridinium iodide. No product formation of the structure **212** was observed when electrochemical reduction or other reducing agents were utilized.

Scheme 81. Trapping of dihydroypridinyl radical 210 by chloroacrylonitrile (211).

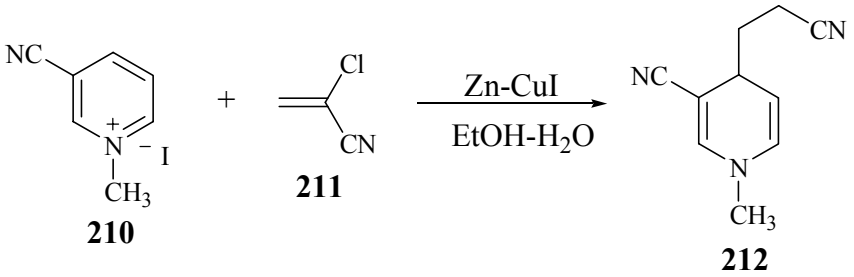

As discussed above, one electron reduction of pyridinium compounds has been an area of interest for some time. The resulting pyridinyl radicals are very reactive species leading to the rapid formation of dimerization products. Although the reduction of 2*H*-3-bromoindazolylpyridinium iodide (**141**) by cyanide (Scheme 78) is possible, there is no literature precedence for such a reaction. Furthermore, the rearrangement of **141** to the

corresponding 1*H*-isomer **145** is a clean reaction; no evidence for the formation of dimers has been observed. Therefore, if the rearrangement reaction is proceeding through the radical pathway described in Scheme 78, the transfer of an electron from the rearranged radical intermediate **201** to **141** must be proceeding at a rate greater than the rate of dimerization.

Despite these considerations, the proposed radical pathway was investigated via a series of experiments. In these experiments 4-(2*H*-5-bromoindazolyl)-1-methylpyridinium iodide (**193**) or 4-(2*H*-6-bromoindazolyl)-1-methylpyridinium iodide (**174**) were used due to their ready availability. These two compounds were shown to behave in the same way in the presence of cyanide as the 2*H*-3-bromoindazolylpyridinium analog **141**.

4.2.2. Investigation of the Proposed Radical Pathway

In the first experiment, 2,2,6,6-tetramethyl-1-piperidinyloxy radical (TEMPO) was included in a solution of **193** in DMSO-d_6 prior to the addition of cyanide solution. Being a radical scavenger, addition of TEMPO might prevent or at least slow down a possible radical mediated isomerization reaction. However, the cyanide catalyzed rearrangement reaction in the presence of TEMPO proceeded at a comparable rate to the analogous reaction carried in the absence of TEMPO.

A second approach utilized sodium bisulfite in place of cyanide as a known one electron reducing agent with poor nucleophilic character in an attempt to catalyze the rearrangement reaction. However, the 2*H*-isomer **174** was stable in the presence of excess bisulfite suggesting that the proposed one electron reduction of **174** leading to the isomerization was not taking place.

Although it was not possible to rule it out at this point, we could not obtain any evidence to favor a radical pathway. Furthermore, all of the experimental results obtained were consistent with a nucleophilic pathway. However, assuming that the rearrangement reaction proceeded through a nucleophilic pathway we could not account for the retention of bromine in the cyanide mediated rearrangement of **141**.

4.3. Stereochemical Examination of the Rearrangement Reaction

According to the proposed pathway, the conversion of intermediate **197** to the rearranged product **145** proceeds via an E2 type of elimination reaction (Scheme 82). The leaving group, whether cyanide or bromide, should be anti-coplanar with the bond connecting N-2 of indazole and C-4 of the pyridinyl moiety. Therefore the resulting product of the rearrangement reaction will depend on which diastereomer (**a** or **b**) of intermediate **197** forms.

Scheme 82. Conversion of intermediate 197 to the 1*H*-isomers 198 or 145 via an E2 type of elimination reaction.

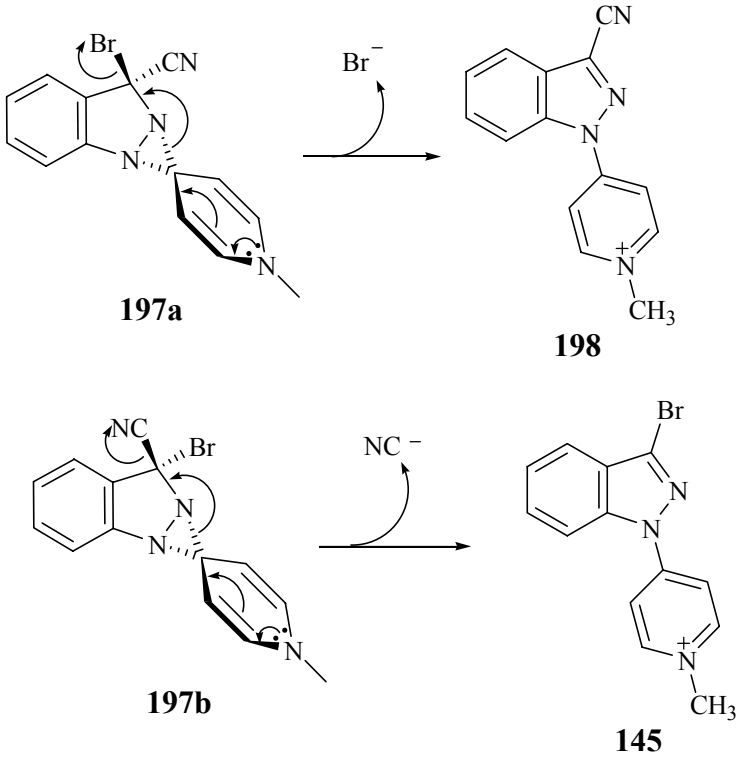

The retention of bromine in the final product suggests the exclusive formation of diastereomer **197b** following the attack by cyanide at C-3. It is possible that this outcome is dictated by the difference in the enthalpies of reaction for the formation of diastereomeric intermediates **197a** and **197b**. Calculated enthalpies of reaction (AM1) showed that the diastreomer **197a** was favored over the diastereomer **197b** by 2 kcal/mol.

In any case, it was concluded that the difference in energies was too small to result in the exclusive formation of one diastereomer over the other.

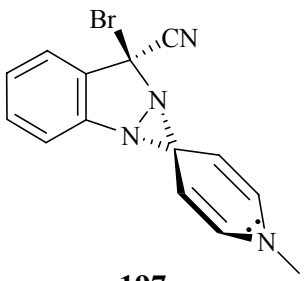

197a

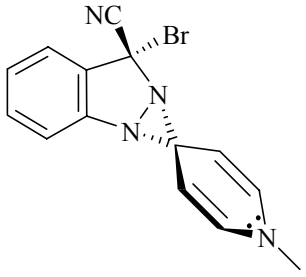

197b

In the light of these observations, the stereospecific formation of intermediate **197b** via a concerted Michael type 1,4-addition reaction is proposed. Attack by cyanide at C-3 of the planar indazole moiety from the top directs the pyridinyl ring below the plane resulting in the exclusive formation of intermediate **197b** which will be converted to the 1*H*-3-bromoindazolylpyridinium **145** (Scheme 83 and Fig. 37).

Scheme 83. Stereospecific formation of diastereomer 195b via a concerted stereospecific Michael addition.

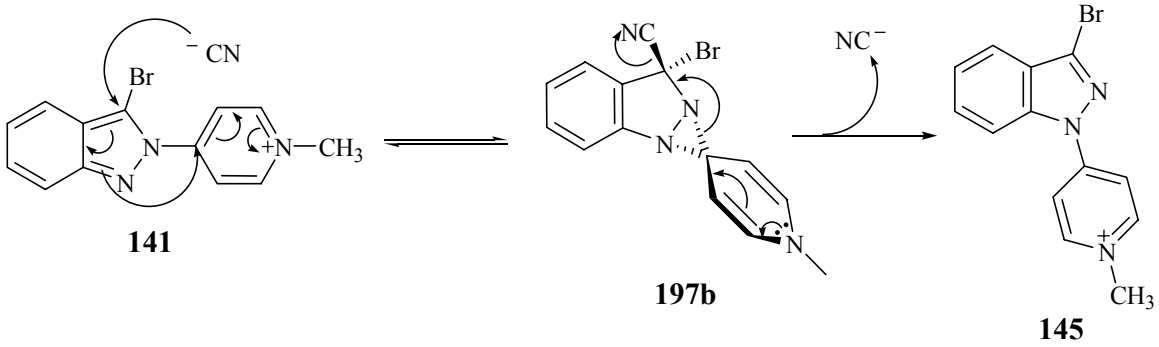

141 **197b** **145**

Figure 37. Three dimensional representation of the reaction shown in Scheme 83 with minimized structures.

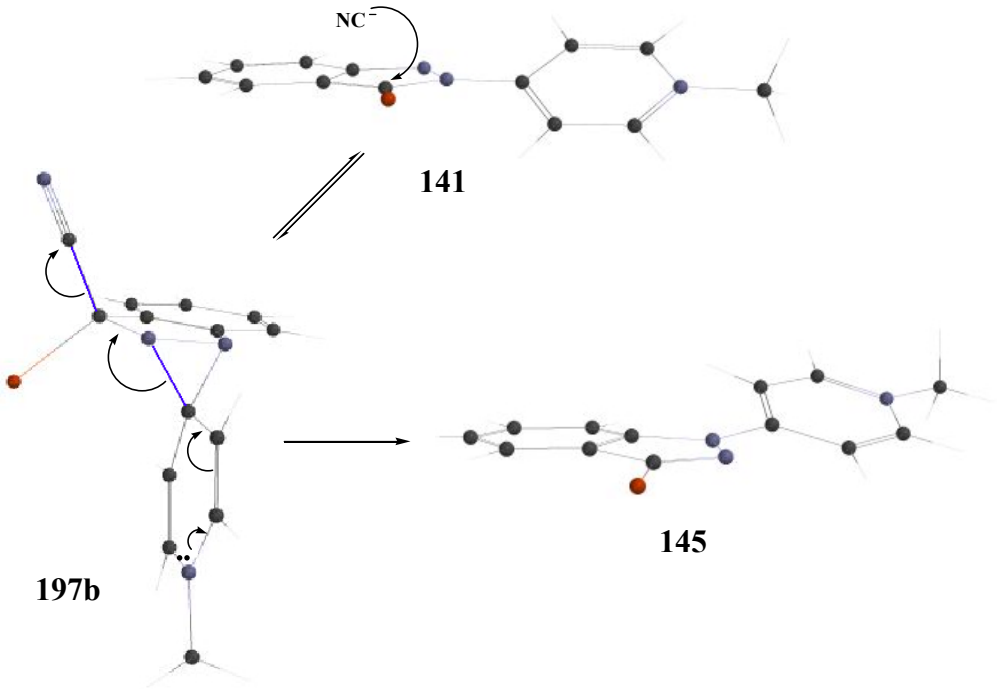

Interestingly, the addition of TMP to acetylene **122** gives exclusively the *E* isomer of the α,β-unsaturated ester **123** described in Section 3.2. Scheme 38 is a good literature example of a stereocontrolled Michael addition (Scheme 83 and Fig. 37).

4.4. Investigation of the Stoichiometry of the Cyanide Mediated Rearrangement Reaction.

The results obtained on the cyanide mediated rearrangement reaction of 2*H*-3-bromoindazolylpyridinium **141** support a nucleophilic pathway. Further supporting evidence that the cyanide mediated rearrangement reaction operates through the same mechanism as that of the TMP mediated reaction was sought by demonstrating a catalytic role of cyanide. Due to its availability and the good HPLC baseline separation of the 1*H*- and the 2*H*-isomers, the 2*H*-6-bromoindazolylpyridinium analog **174** was utilized in this series of experiments. Compound **174** was treated with 0.1 equivalent of KCN in DMSO-d_6 and the progress of the rearrangement reaction was monitored by ^{1}H NMR as shown in Figure 38.

Figure 38. ^{1}H NMR (400 MHz) monitoring of the progress of the rearrangement reaction in the presence of 0.1 equivalent of KCN.

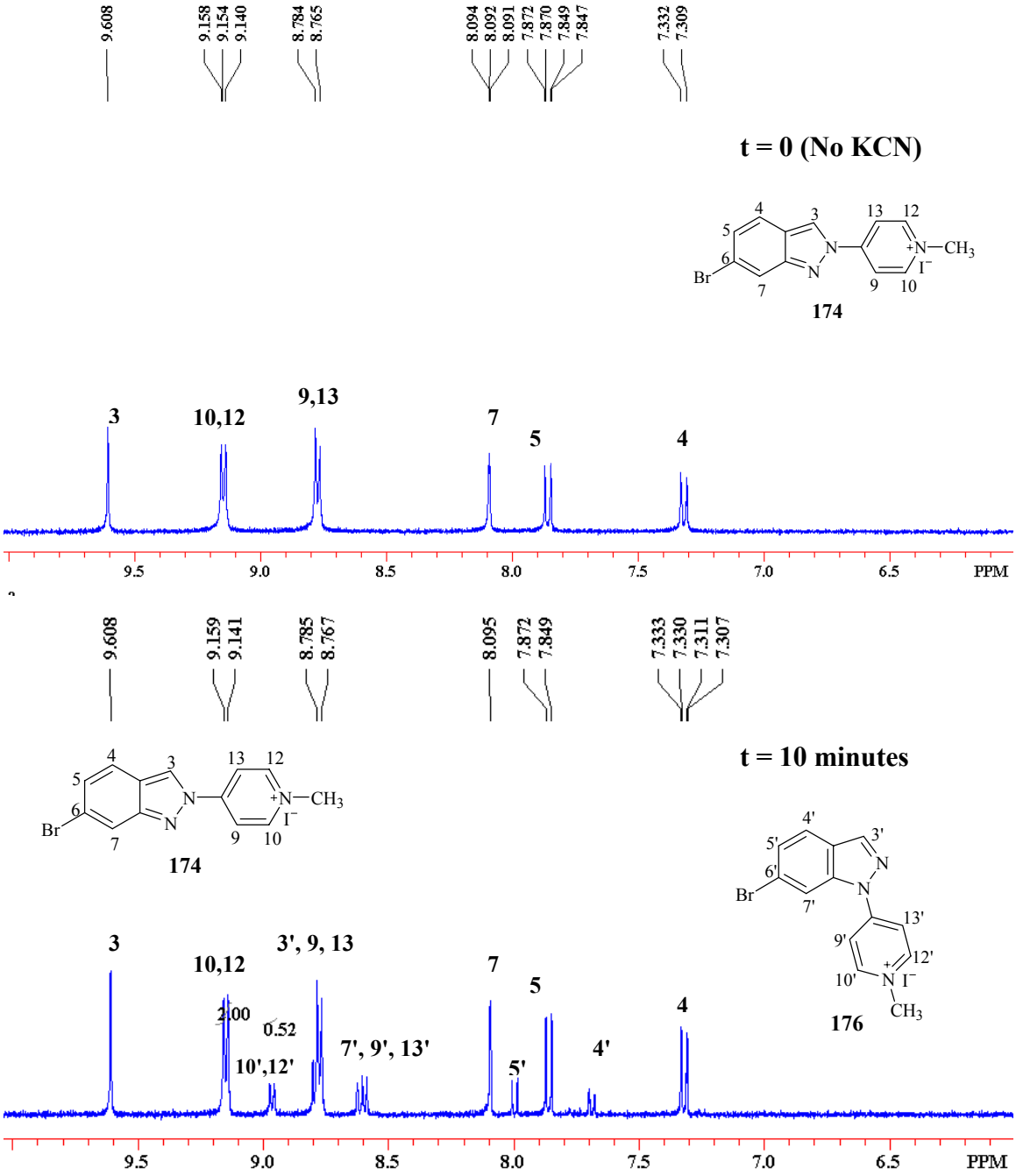

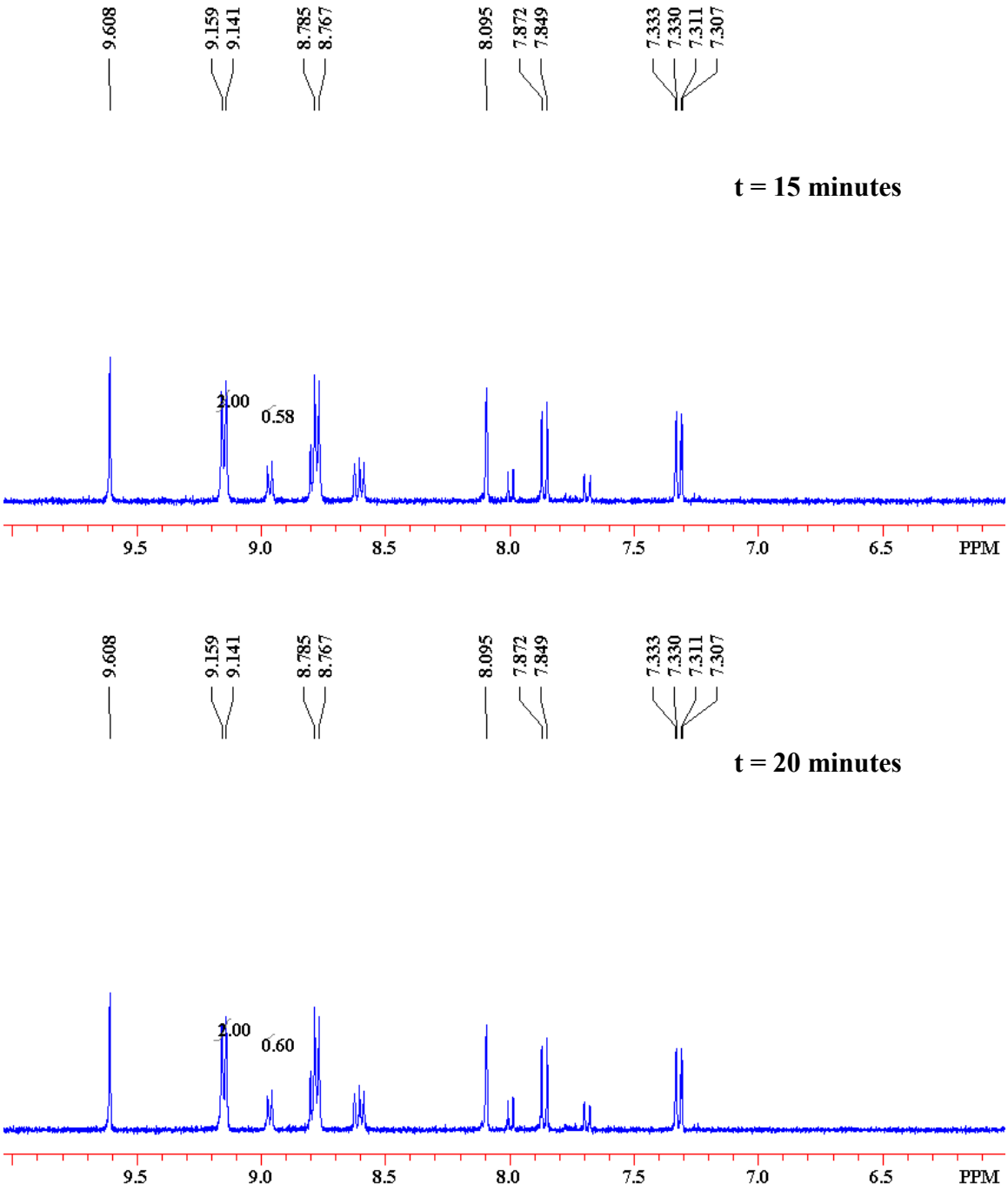

After 10 minutes approximately 20 % of the starting 2*H*-isomer had been converted to the corresponding 1*H*-isomer. Although the isomerization reaction seemed to proceed rapidly at the beginning, as seen in Figure 38c and d, the composition of reaction mixture was stable after 10 minutes. Consequently, it appeared suggesting that the cyanide had been consumed during the first 10 minutes of the reaction after which

that rearrangement reaction had stopped. In an attempt to determine the amount of cyanide required for the quantitative conversion of the 2*H*-isomer **174** to the 1*H*-isomer **176**, stability of **174** was monitored in the presence of increasing amounts of KCN by HPLC-DA. DMSO-d_6 was used due to its compatibility with the subsequent NMR analyses. The results are summarized in Figure 39.

Figure 39. HPLC-DA determination of the amount of cyanide required for the quantitative conversion of the 2*H*-6-bromoindazolylpyridinium 174 to the corresponding 1*H*-isomer 176.

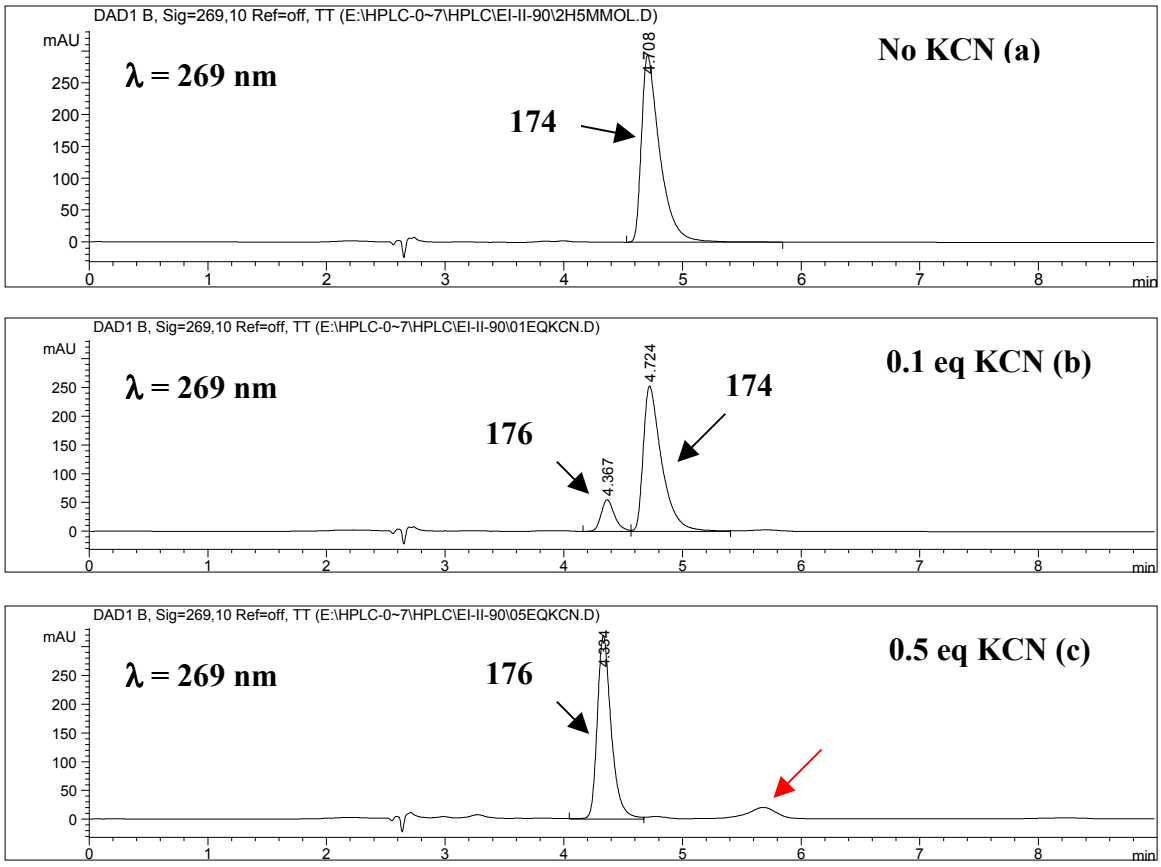

The HPLC tracings (Fig. 39) demonstrate that the conversion of **174** to **176** was complete when 0.5 equivalents of cyanide was used. The appearance of a very minor peak at t_R = 5 minutes was also noted (Fig. 39c). This outcome demonstrated that the rearrangement reaction was not catalytic in cyanide. On the other hand, a stoichiometric amount of cyanide was not required to achieve complete conversion of **174** to **172**. This

finding suggested the possibility that the cyanide was being consumed via an alternative pathway unrelated to the rearrangement reaction. Therefore, we focused our attention on the minor peak (t_R = 5.7 minutes, Fig. 39c) which we expected would be the product or one of the products of the reaction resulting in the consumption of cyanide. In order to facilitate the formation of the product corresponding to the new peak, we carried out the rearrangement reaction in the presence of 1 and 2 equivalents of KCN. The HPLC tracings are shown in Figure 40.

Figure 40. HPLC tracings obtained for the reaction of 174 with 1 and 2 equivalents of KCN.

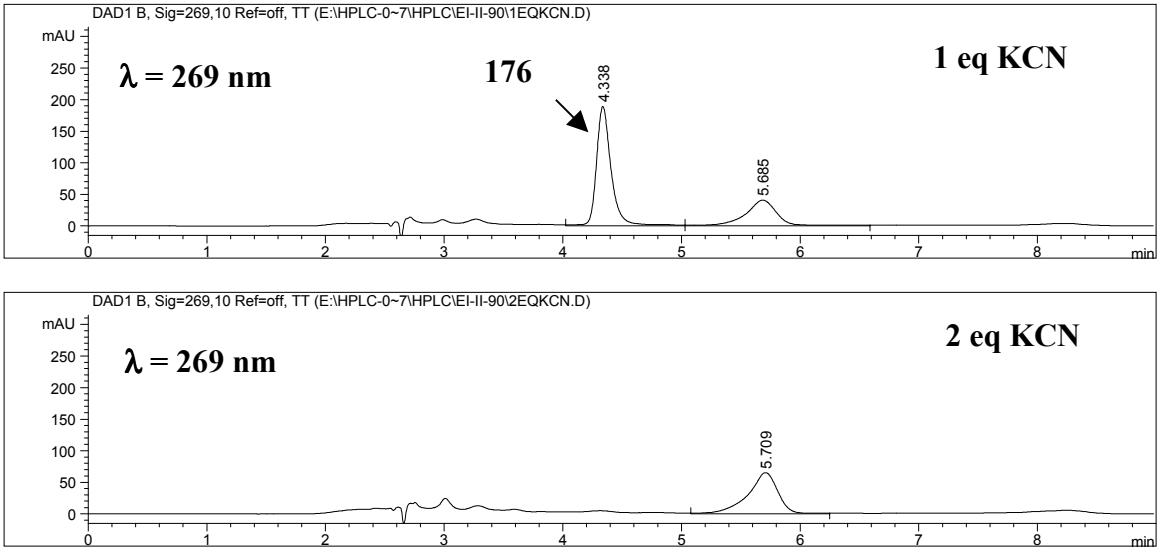

When 2 equivalents of KCN were used, the only peak present in the HPLC tracing was the peak with the retention time of 5.7 minutes. The retention time and the UV spectrum of this new peak it corresponded to 6-bromoindazole (**172**). Comparison of the ^{1}H NMR spectrum of the reaction mixture with the ^{1}H NMR spectrum of synthetic 6-bromoindazole revealed that the major product of the reaction between **174** and 2 equivalents of cyanide was indeed 6-bromoindazole (Fig. 41).

Figure 41. ^{1}H NMR spectrum (400 MHz) of the reaction mixture (a) and ^{1}H NMR spectrum (500 MHz) of synthetic 6-bromoindazole [172 (b)].

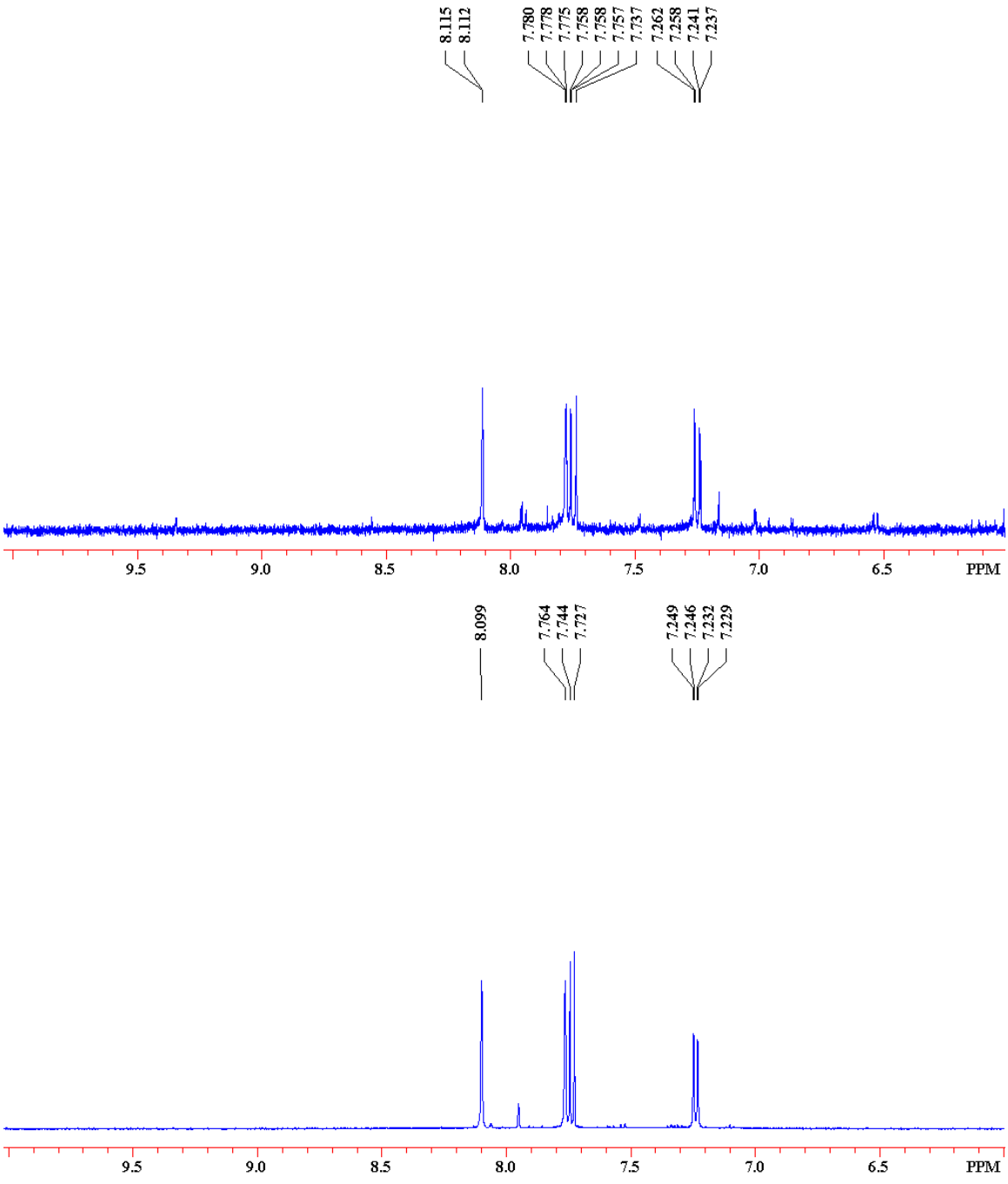

A possible pathway to account for the formation of **168** would involve the attack of cyanide at the C-4 carbon of the pyridinium ring of the 2*H*-isomer **174**. The resulting intermediate, **213**, could collapse to form 6-bromoindazole via protonation and 4-cyano-

1-methylpyridinium (**214**) as shown in Scheme 84. The proton source of such a reaction accounted for by the presence of water in DMSO-d_6.

Scheme 84. Proposed formation of 6-bromoindazole (172) and 4-cyano-1-methylpyridinium (214) via the reaction between KCN and 174.

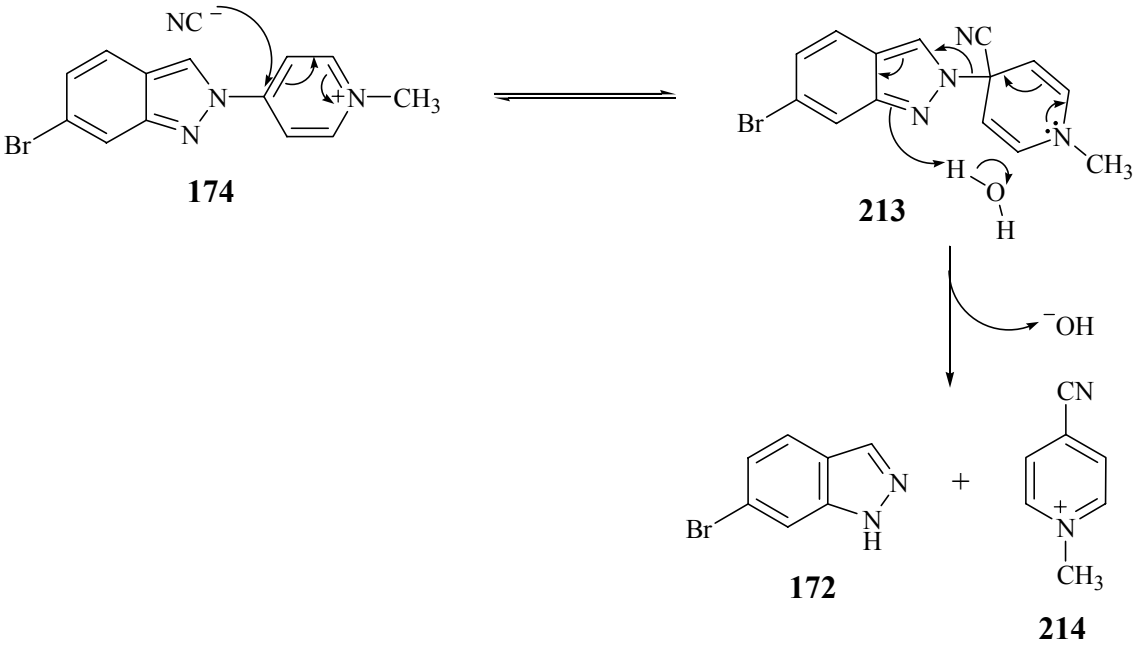

Although, the above pathway is consistent with the formation of 6-bromoindazole and the consumption of cyanide, the ^{1}H NMR spectra did not display any signals corresponding to the 4-cyano-1-methylpyridinium species **214** nor its hydrolysis product, 1-methyl-4-pyridone [(**169**), Scheme 85]. This aspect of the reaction will be discussed in detail in Section 4.6.

Scheme 85. Hydrolysis of 214 to form 1-methyl-4-pyridone (169).

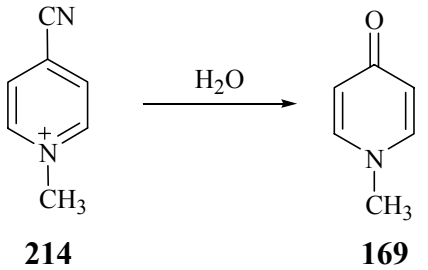

Another noteworthy observation is related to the amount of cyanide consumed. According to the above pathway, the amount of cyanide consumed must be stoichiometric with respect to the amount of 6-bromoindazole formed. However, the ^{1}H NMR spectrum obtained for the 0.5 equivalent KCN experiment demonstrates that approximately 25 % of **174** is converted to 6-bromoindazole instead of the expected 50 %. The remaining 75 % of **174** is present as the rearranged product **176**. One possible explanation is the attack of cyanide at C-4 of the pyridinyl moiety taking place only after the formation of the spirodiaziridinyl intermediate as shown in Scheme 86. In other words, the cyanide consumption would be expected to stop once the rearrangement of the 2*H*-isomer **174** to the 1*H*-isomer **176** was complete. In this case, the cyanide mediated decomposition reaction will be second order in cyanide and as the concentration of KCN is increased, the decomposition reaction will be favored over the rearrangement reaction. When 2 equivalents of KCN is used, it is possible that the decomposition reaction becomes the only reaction to take place leading to the exclusive formation of 6-bromoindazole.

Scheme 86. An alternative pathway for the decomposition of the 2*H*-isomer 174 in the presence of cyanide.

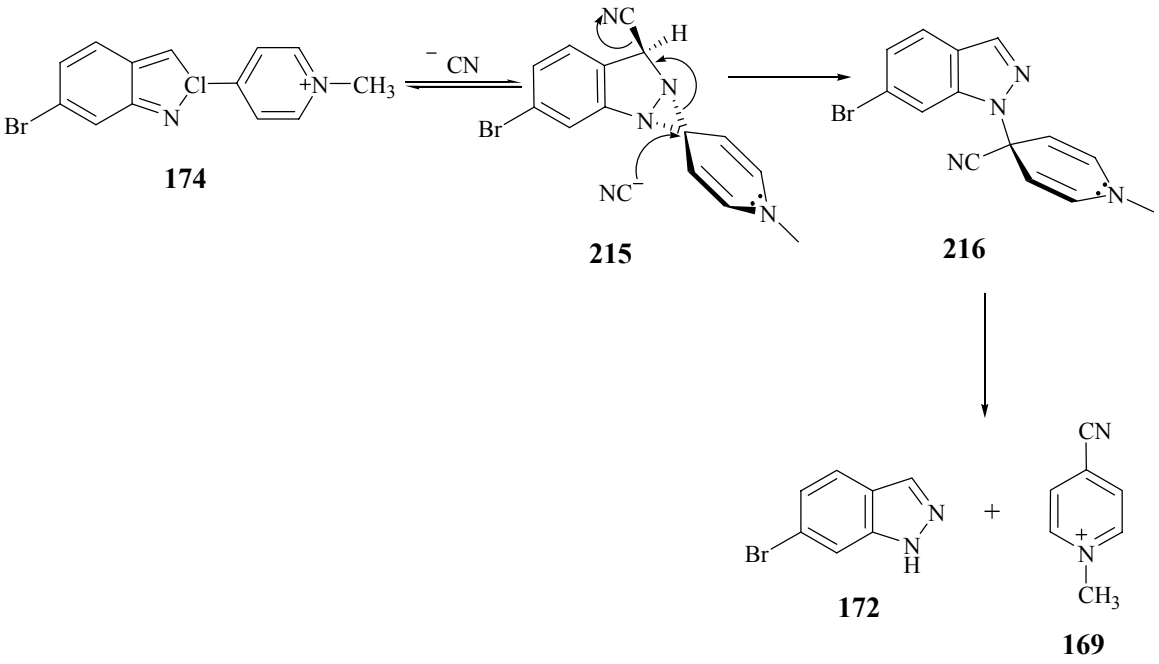

In order to obtain a better understanding of the decomposition mechanism, the progress of the rearrangement/decomposition reaction of **174** in the presence of 2 equivalents of KCN was monitored by HPLC-DA as shown in Figure 42.

Figure 42. HPLC monitoring of the stability of 174 in the presence of 2 equivalents of KCN.

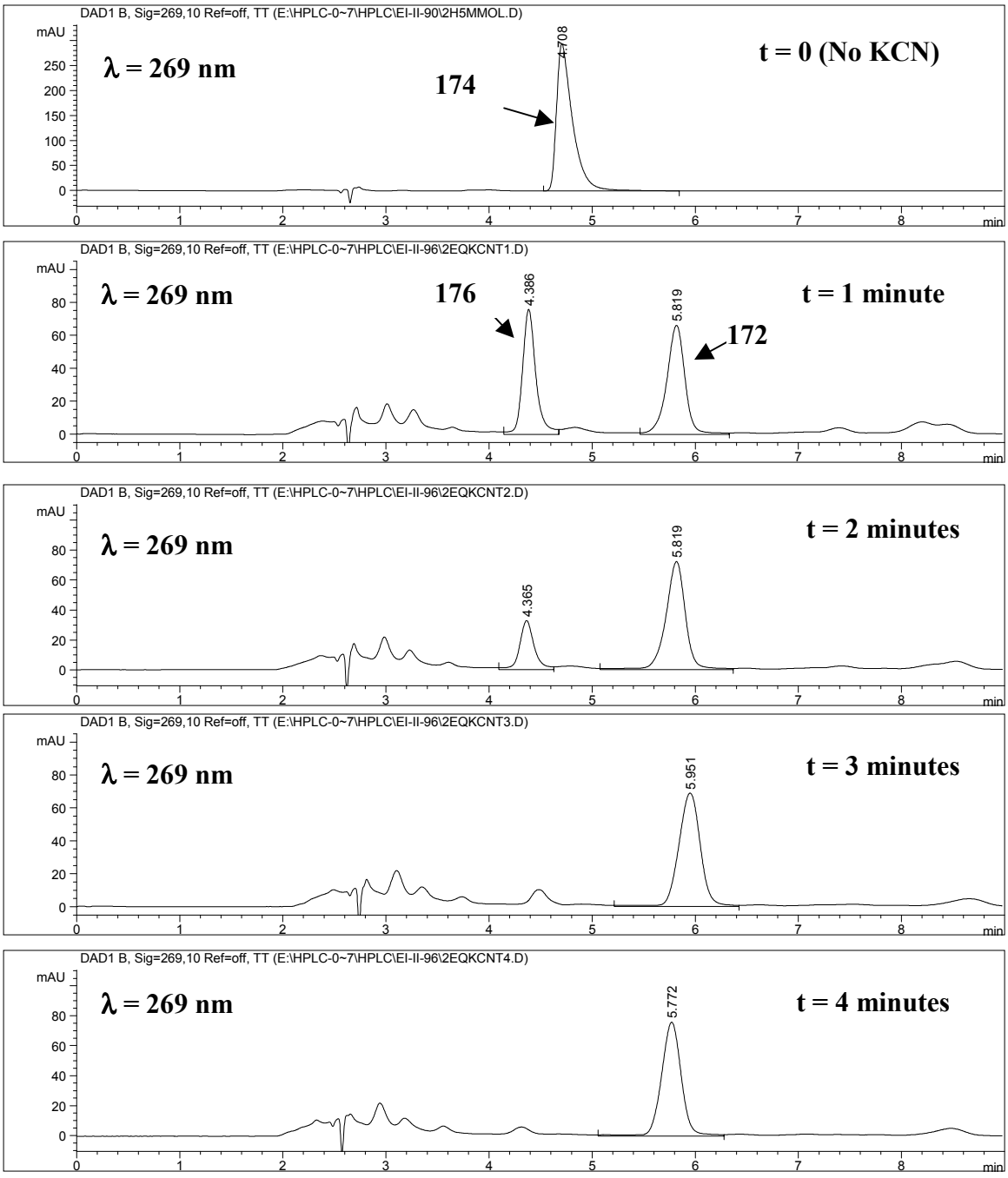

After 1 minute the peak corresponding to the 2*H*-isomer had disappeared. In addition to the rearrangement product **176**, 6-bromoindazole (**172**) was observed. After 2 minutes, the intensity of the peak corresponding to the 1*H*-isomer decreased and after 4 minutes, it was completely replaced by the peak corresponding to 6-bromoindazole. This

outcome demonstrates that the decomposition reaction proceeds even after the rearrangement of the 2*H*-isomer **174** to the 1*H*-isomer **176** is complete. This finding led us to study the stability of **176** in the presence of cyanide. Indeed, decomposition of **176** to 6-bromoindazole was observed in the presence of cyanide (Fig. 43).

Figure 43. Stability of 1*H*-6-bromoindazolylpyridinium 176 in the presence of 2 equivalents of KCN.

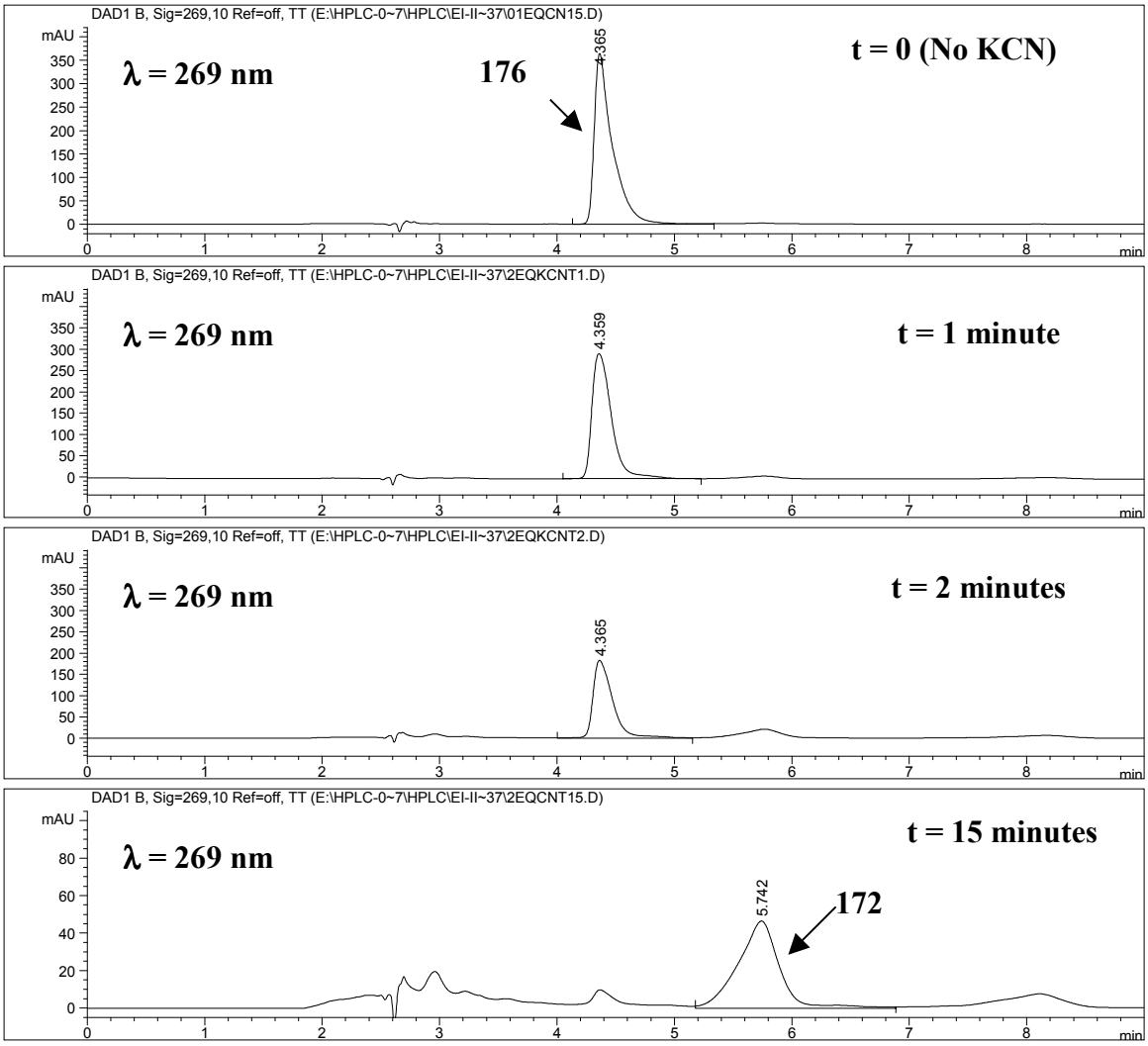

The comparison of the HPLC tracings obtained 1 minute after the KCN addition to the 2*H*-isomer **174** versus the 1*H*-isomer **176** shows that the amount of 6-bromoindazole present (i.e. the extent of decomposition) is significantly more in the case of the 2*H*-isomer. Therefore, it was concluded that, although 6-bromoindazole must be

forming from both isomeric 6-bromoindazolylpyridinium species, the decomposition of **174** takes place more readily than does the decomposition of **176**. This is in agreement with the enhanced stability of **174** due to its benzenoid structure. At this point it is not possible to rule out the pathway proposed in Scheme 86 where the cyanide attack takes place after the formation of the spirodaziridinyl intermediate from **174**. However, this is unlikely with the 1*H*-isomer **176** since the formation of the spirodiaziridinyl intermediate from this compound is not expected to be a favored reaction.

4.5. The Role of Water in the Cyanide Mediated Decomposition Reaction

Regardless of the source of 6-bromoindazole, a trace amount of water should be present in the DMSO-d_6 to account for the protonation of the 6-bromoindazolyl anion and 6-bromoindazole formation. In order to evaluate this proposal, the extent of decomposition of the 1*H*-6-bromoindazolylpyridinium **176** was investigated after drying DMSO-d_6 over 3Å molecular sieves over night. Although the ^{1}H NMR spectrum of the "dried" DMSO-d_6 still showed the presence of a trace amount of water, the water content was reduced significantly. The stability of the 1*H*-isomer **176** in the presence of 2 equivalents of KCN (dried in the vacuum oven) in "dry" and "wet" DMSO-d_6 was compared (Fig. 44).

Figure 44. ^{1}H NMR spectrum (400 MHz) of the 1*H*-isomer 176 in the presence of "dry" (a) and "wet" (b) DMSO-d_6.

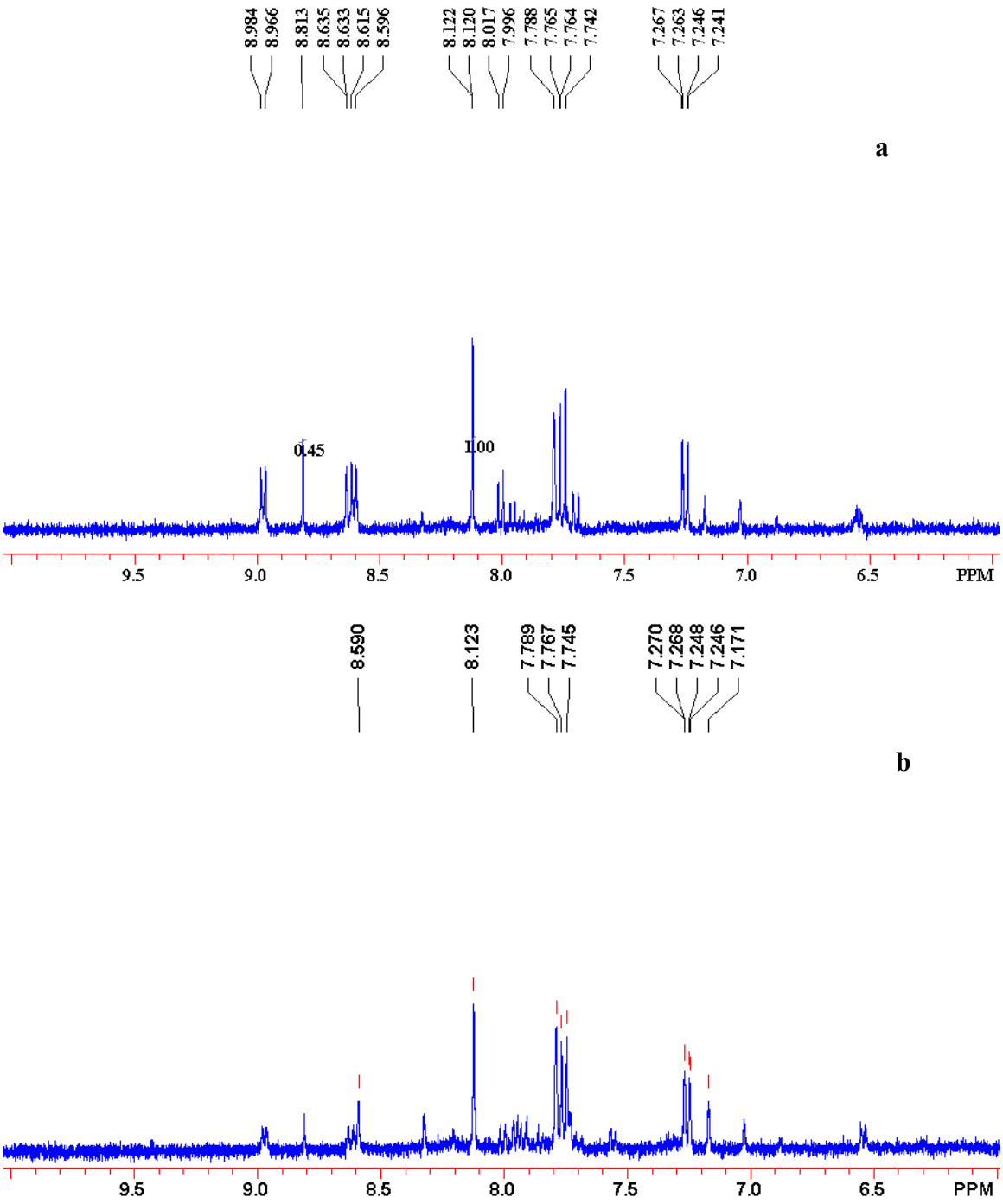

The ratio of signals corresponding to the protons attached to C-3 of 6-bromoindazole and **176** was 1 to 0.45 after 30 minutes in "dry" DMSO-d_6. When "wet" DMSO-d_6 was used, this ratio was almost 1 to 0.1. Therefore, the water in DMSO-d_6 must be promoting the decomposition reaction, most likely due to the protonation step shown in Scheme 84.

4.6. Investigation of the Fate of the 4-Cyano-1-methylpyridinium Species

The mechanism proposed in Scheme 84 accounts for the decomposition of the 6-bromoindazolylpyridinium species and formation of 6-bromoindazole. However, as mentioned earlier, the fate of the putative co-product, the 4-cyano-1-methylpyridinium species following its formation, was not clear. The fact that it could not be detected in the ^{1}H NMR spectra suggested that, if formed, it was undergoing further reaction or reactions. Furthermore, the amount of cyanide consumed could not be explained only by the pathway of Scheme 84 since more cyanide was being consumed than the amount of 6-bromoindazole formed These seemingly controversial results led us to investigate the fate of KCN via a labeling experiment. In this experiment, 0.1 equivalent of 2*H*-5-bromoindazolyl pyridinium **193** was added to a solution of 1 equivalent K^{13}CN in DMF-d_7 and the reaction was monitored by ^{13}C NMR. Due to the low concentration of **193**, possible interference by its ^{13}C signals was expected to be eliminated. Almost immediately after the addition of **193**, the signal corresponding to the carbon of K^{13}CN disappeared completely and a new set of reaction product signals appeared (Fig. 45). The multiple ^{13}C signals shows that $^{13}CN^-$ is involved in several reactions.

Figure 45. ^{13}C NMR monitoring of consumption of $K^{13}CN$ in the presence of 193.

t = 0 (No 193)

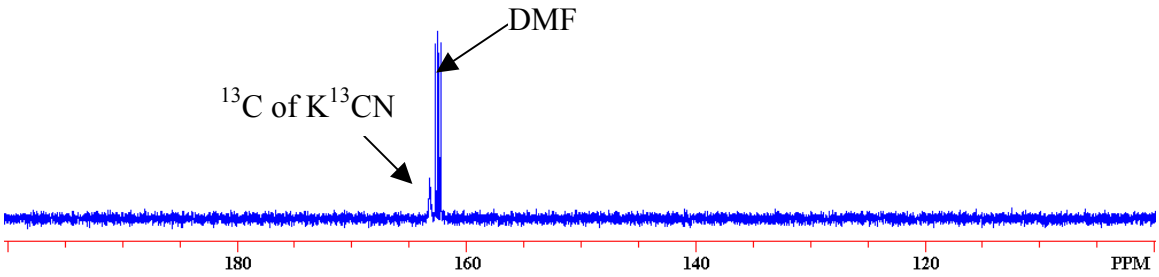

t = 10 minutes in the presence of 0.1 equivalent of 193

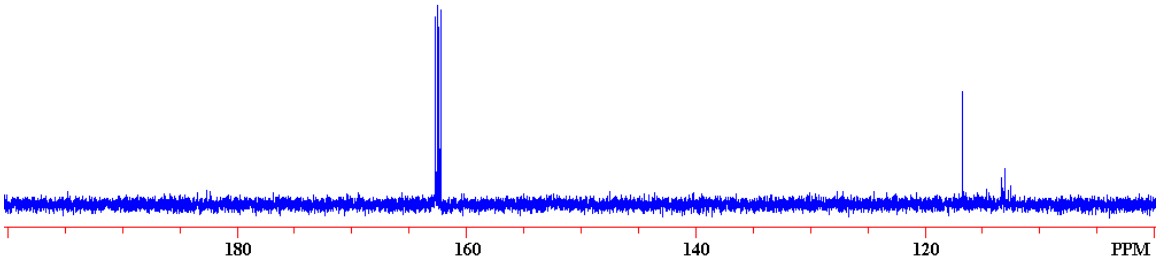

Next, in an attempt to characterize the cyano adducts formed from the reaction between 2*H*-6-bromoindazolylpyridinium species **174** and KCN, ^{1}H NMR spectrum of the reaction mixture containing **174** and 2 equivalents of KCN was obtained (HPLC-DA tracing of this reaction mixture is shown in Figure 42) The ^{1}H NMR spectrum was complex. There were many signals present both in the aromatic and aliphatic regions in addition to the signals corresponding to the protons of the major product, 6-bromoindazole (Fig. 46).

Figure 46. ^{1}H NMR (400 MHz) spectrum of 174 in DMSO-d_6 after the addition of 2 equivalents of KCN.

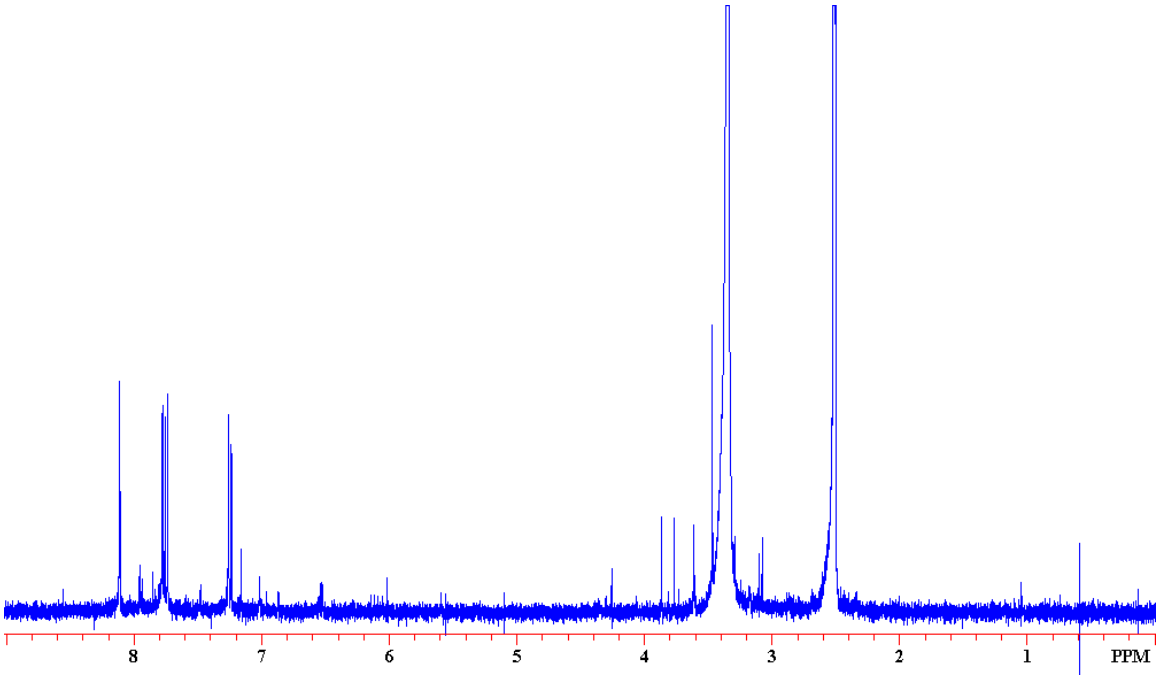

Since the information obtained from NMR and HPLC-DA analysis was limited, it was decided to use LC-MS in an attempt to identify the cyano adducts. Atmospheric pressure chemical ionization (APCI) was used as the ionization source leading to the detection of positively charged species (MH^+). The reaction mixture containing the 2*H*-6-bromoindazolylpyridinium derivative **174** and 1 equivalent of KCN (unlabelled) was analyzed by LC-MS. First, the presence of the 4-cyano-1-methylpyridinium species and 1-methyl-4-pyridone was investigated by extracting ions with MH^+ 119 and 110, respectively. However, there was no evidence for the presence of these compounds. When the total ion chromatogram for the region of 3-5 minutes[215] [the region of 2-3.5 minutes in HPLC-DA tracings with a cluster of peaks (Fig. 40)] was examined, no distinct peak was observed (Fig. 47a). However, mass spectra showed that a compound (or compounds) with MH^+ 135 (Fig. 47c) was eluting first (3-4 minutes), followed by co-elution with another compound with MH^+ 160 [(Fig. 47b), 4-5 minutes]. The MH^+

[215] The difference in retention times between HPLC-DA and HPLC-MS analyses is due to the change in the mobile phase. See Experimental for details.

observed for the peak with t_R = 17.7 minutes (8.5 minutes in HPLC-DA analysis) was 329/331 (Fig. 48d), consistent with a bromine containing product. The mass spectrum obtained for the peak with t_R = 6.1 minutes (Fig. 48b) corresponded to the remaining 1*H*-isomer **176** and the mass spectrum obtained for the peak with t_R = 13.4 minutes (Fig. 48c) corresponds to the decomposition product, 6-bromoindazole (**172**). Results of the LC-MS analyses are shown in Figures 47 and 48.

Figure 47. LC-MS tracings (3-10 minutes) obtained for the reaction of 2*H*-6-bromoindazolylpyridinium 174 with 1 equivalent of KCN.

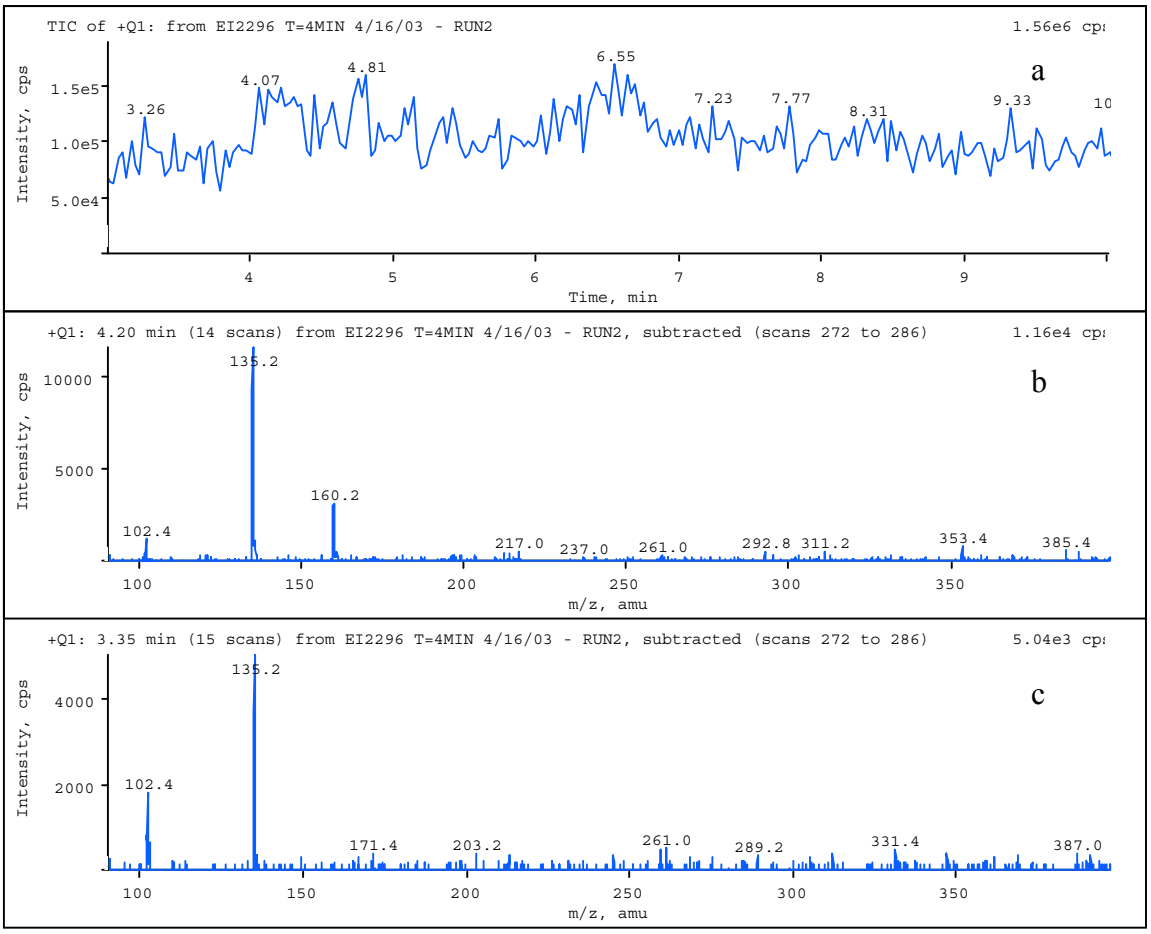

Figure 48. LC-MS tracings (4.5 minutes-20 minutes) obtained for the reaction of 2*H*-6-bromoindazolylpyridinium 174 with 1 equivalent of KCN.

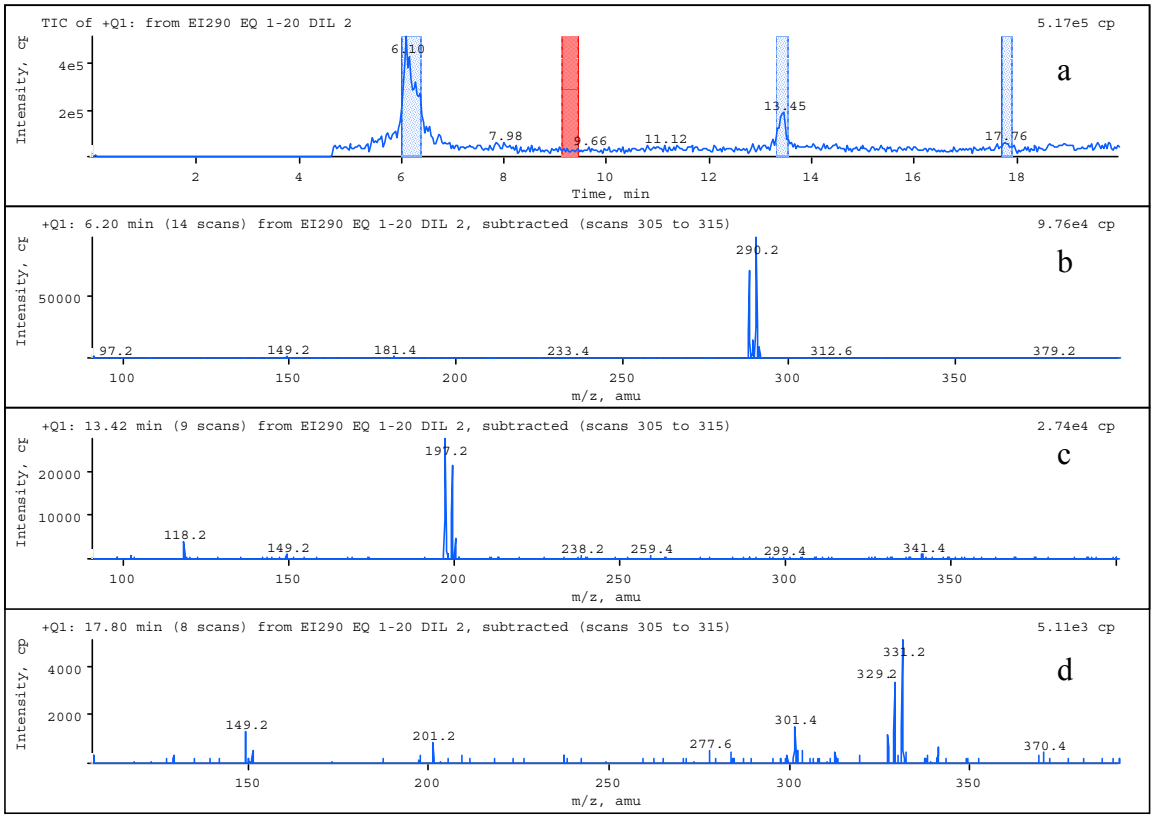

The mass spectra of the polar compounds (t_R = 2-3.5 minutes; MH^+ 135 and 160) show that they do not possess a bromine atom. Therefore, it was concluded that they must be derived from the pyridinyl moiety of the starting material, possibly following the formation of the 4-cyano-1-methylpyridinium species upon decomposition of the 6-bromoindazolylpyridinium species as shown in Scheme 84. The non-polar decomposition product (t_R = 8.5 minutes) with the MH^+ of 329/331 is likely to be formed upon the reaction between cyanide and the 6-bromoindazolylpyridinium species with MH^+ 288/290, since the bromine atom is conserved (Scheme 87). Also the higher molecular weight suggests the presence of the pyridinyl moiety together with the indazolyl nucleus.

Scheme 87. Summary of cyanide mediated reactions of 1*H*- and 2*H*-6-bromoindazolylpyridinium derivatives.

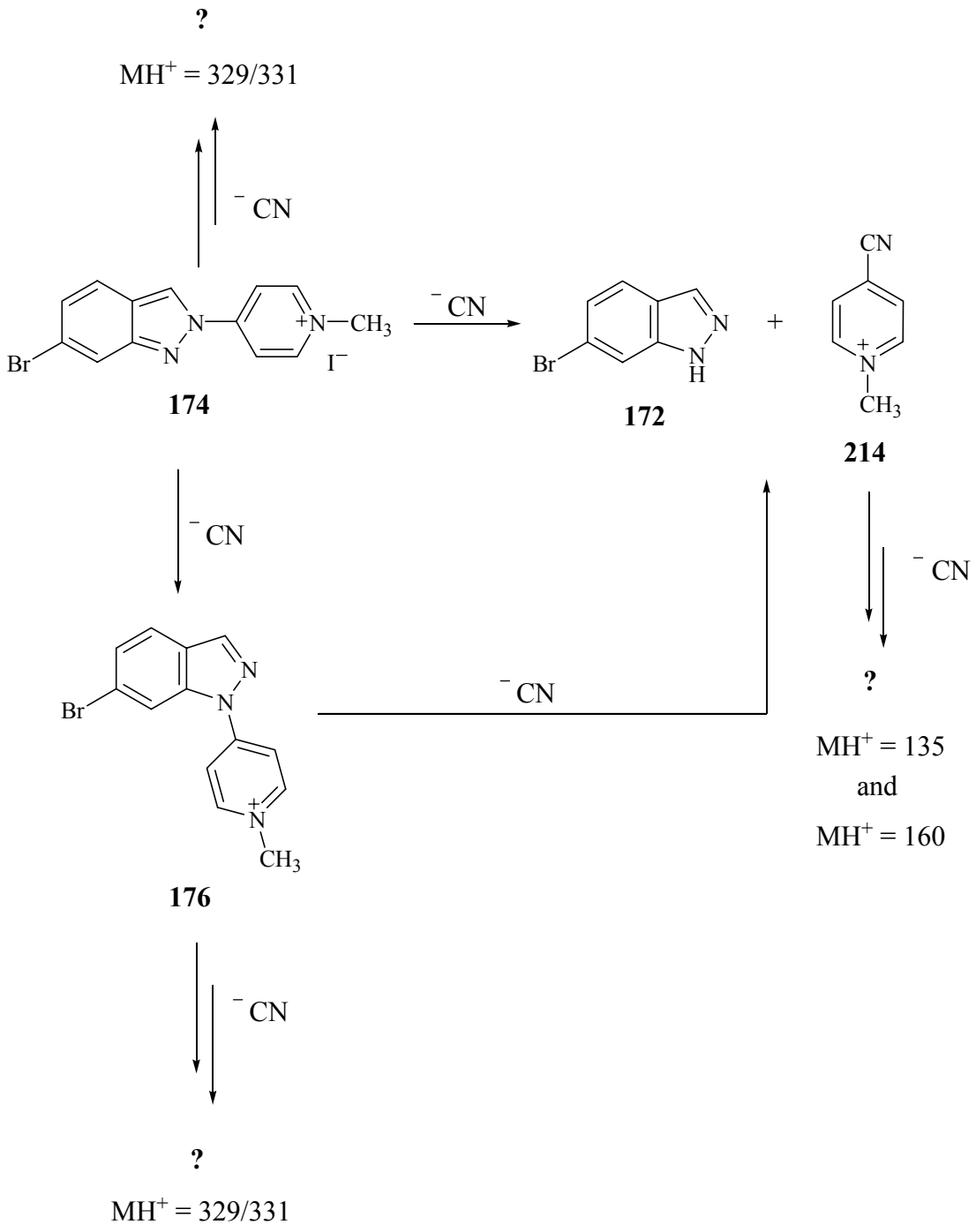

Consideration of the limited number of possible structures consistent with MH^+ 135 led to **218** as a candidate for this product. This compound could be obtained from the

reaction of **214** with cyanide as shown in Scheme 88. The attack of cyanide at C-2 of 4-cyano-1-methylpyridinium species **214** will result in the formation of intermediate **217**. Oxidation (air oxidation or disproportionation) of **217** leads to the aromatic dicyano adduct **218**. Hydrolysis of **218** will give pyridones **219** and/or **220** with the APCI generated protonated forms (**221** and **222**) having MH^+ of 135.

Scheme 88. Formation of protonated cyano adducts 221 and/or 222 with MH^+ 135.

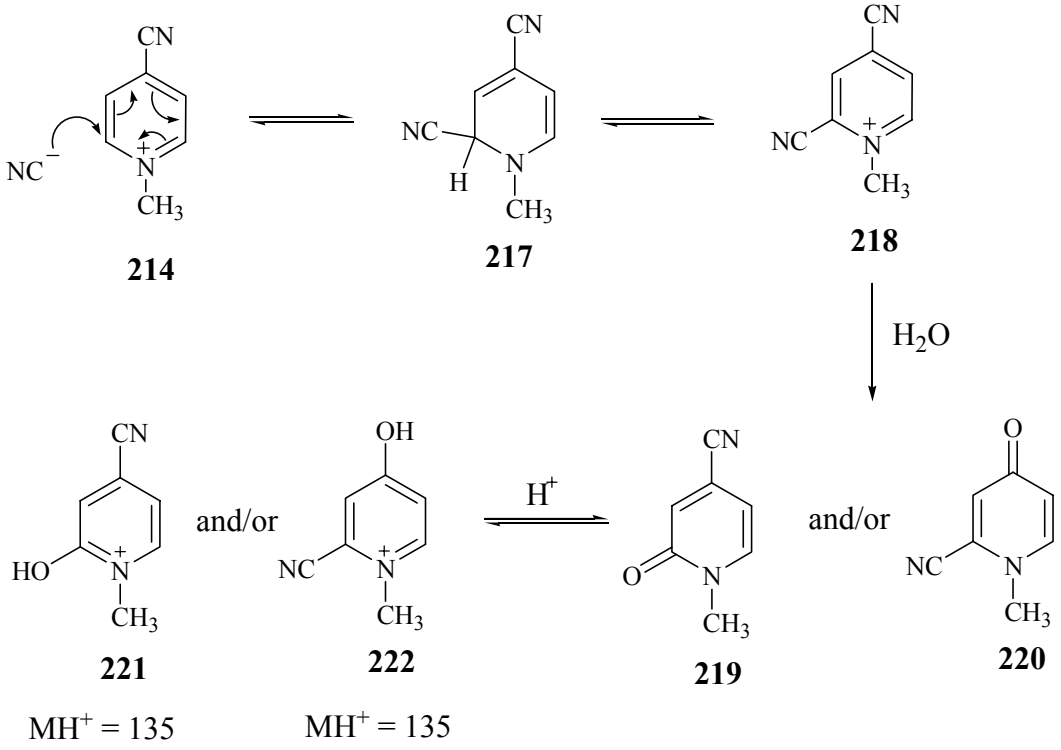

MH^+ = 135 MH^+ = 135

In addition to hydrolysis, the dicyanopyridinium species **218** may undergo a second cyanation step forming intermediate **223**, oxidation of which will give the tricyanopyridinium intermediate **224** as shown in Scheme 89. As in the case of **218**, hydrolysis of **224** may yield pyridones **225** and/or **226** with MH^+ species **227** and **228** observed in the APCI mass spectrum with MH^+ 160.

Scheme 89. Formation of protonated cyano adducts 227 and/or 228 with MH^+ 160.

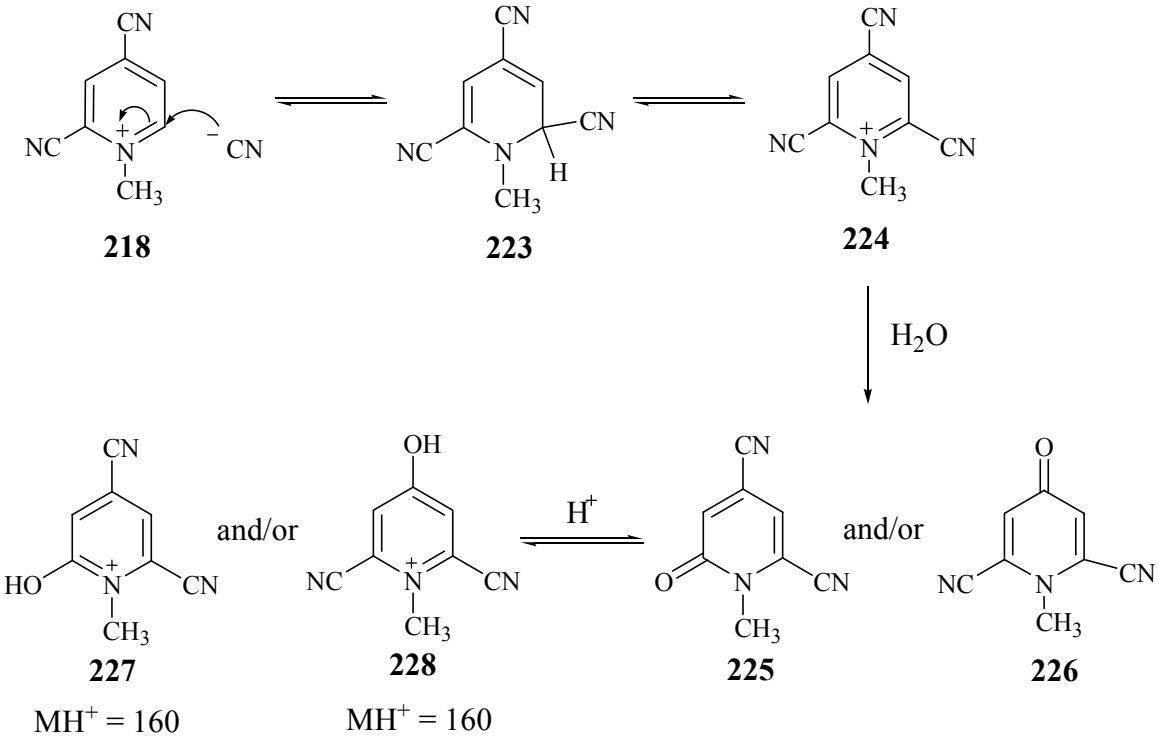

The reactions shown in Schemes 88 and 89 were investigated further, this time by treating 4-cyano-1-methylpyridinium iodide (**214**) with ^{13}C labeled KCN in DMF. In Scheme 90 some of the possible products of this reaction are shown based on the information obtained by LC-MS analysis of the cyanide mediated decomposition of 6-bromoindazolylpyridinium derivative **174**. The product analysis of this reaction was carried out by GC-MS with electron impact (EI) ionization instead of LC-APCIMS. Unlike APCI, the molecular ions will be detected as $M^{\cdot+}$ instead of MH^+ which is expected to provide supporting evidence for the characterization of the cyano adducts.

Scheme 90. Proposed products of the reaction between 214 and ^{13}C labeled KCN.

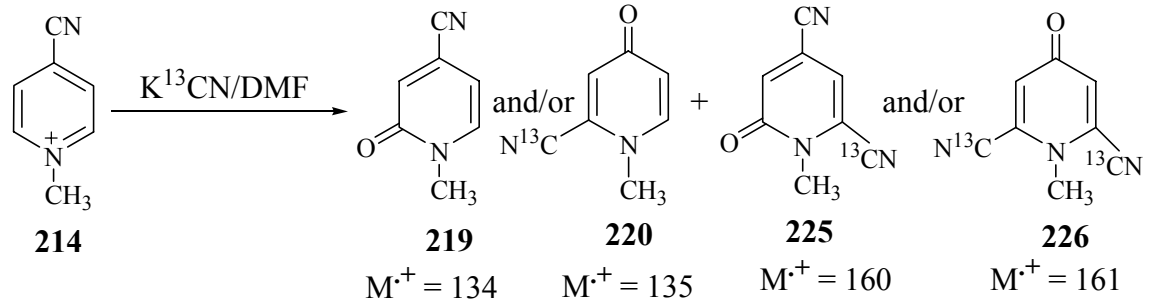

Immediately after the addition of $K^{13}CN$, the reaction mixture turned black. After 30 minutes, the reaction mixture was partitioned between dichloromethane and water. The organic layer was dried, dichloromethane was evaporated and the residue was analyzed by GC-MS. The GC-MS TIC tracing obtained was complex. Therefore, the molecular ions corresponding to the proposed products were extracted. The molecular ions with $M^{\cdot+}$ 135 and 161 were not present. However, when the molecular ions $M^{\cdot+}$ 134 and 160 were extracted two peaks were obtained as shown in Figure 49a and b with the mass spectra shown in Figure 50.

Figure 49. Extracted ion chromatogram for molecular ions $M^{\cdot+}$ 134 (a) and $M^{\cdot+}$ 160 (b).

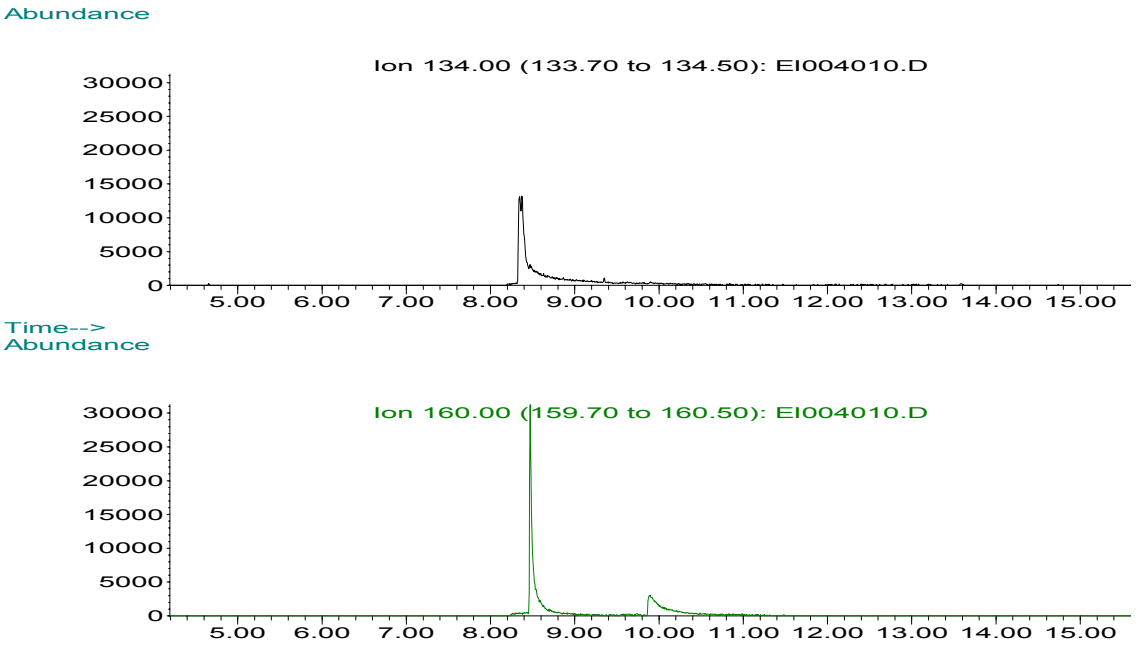

Figure 50. Mass spectra for the peaks with the molecular ions $M^{\cdot+}$ 134 (a) and $M^{\cdot+}$ 160 (b).

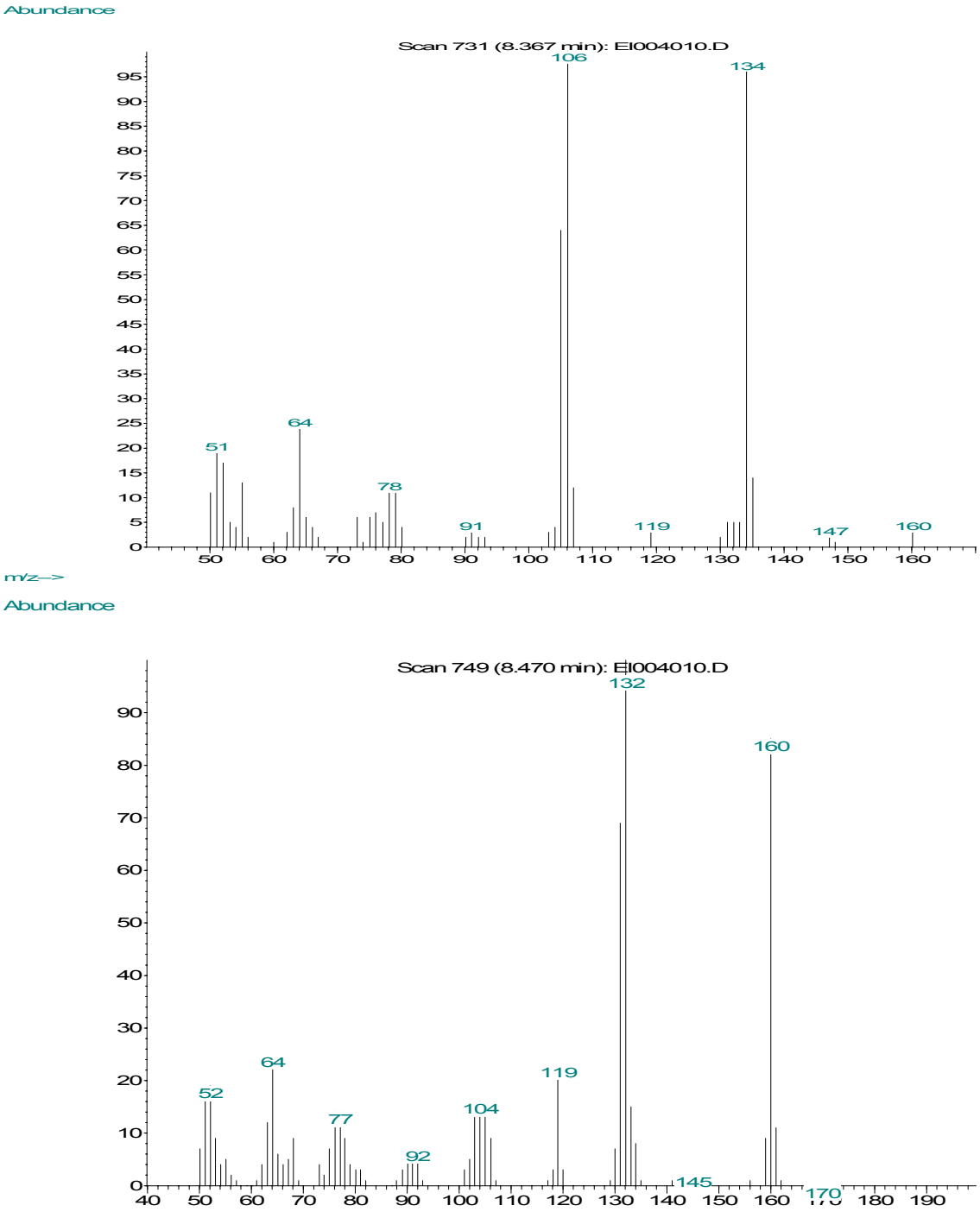

This outcome was consistent with and strongly supported the formation of cyano pyridones **219** and **225** via the pathways proposed in Schemes 88 and 89. Also, the use of ^{13}C labeled KCN provided an opportunity to distinguish between the isomeric pyridones **219**, **220** and **225**, **226**. The attempts to isolate the pyridone derivatives failed due to the complex mixture of products. The complexity of mixture of products is consistent with the formation of dicyanodihydropyridine **217** (Scheme 88) which is expected to be highly reactive based on the literature report on the reactivity of 4-cyano-1-methyl-1,2-dihdyropyridine (**229**). It was shown that captodative diene **229** dimerizes to compound **230** even at –45 ^{o}C which in turn isomerizes to **231** at –20 ^{o}C as shown in Scheme 91.

Scheme 91. Dimerization of captodative diene 229.

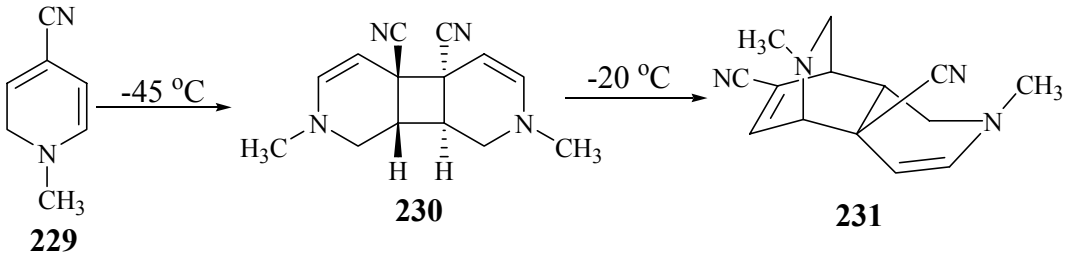

229 **230** **231**

4.7. Investigation of Cyano Adducts Derived from the 6-Bromoindazolylpyridinium Species

After the identification of the cyanopyridone adducts **219** and **225** we turned our attention to the peak with t_R = 8.5 minutes observed in LC-MS tracings with MH^+ 329/331. As discussed above, the presence of bromine established the retention of the 6-bromoindazolyl group in the molecule. Therefore, in the light of the results obtained for the 4-cyano-1-methylpyridinium species, we considered attack of cyanide at the pyridinium moiety of the 1*H* and/or 2*H*-6-bromoindazolylpyridinium derivative via a pathway analogous to the one shown for compound **214** in Scheme 88. As shown in Scheme 92, attack of cyanide at C-2 of the pyridinyl ring of the 1*H*-6-bromoindazolylpyridinium **176** (or the corresponding 2*H*-isomer) results in the formation of cyanodihydropyridine **232**. Oxidation of **232** to cyanopyridinium **233** followed by a second cyanide attack gives dicyanodihydropyridine **234**. Hydrolysis of dicyanopyridinium **235**, the oxidation product of **234**, leads to the formation of pyridone

236. The protonated forms of the expected products **236** and **237** are consistent with the observed MH^+ of 329/331 (Scheme 93).

Scheme 92. Formation of cyanopyridone 236 from 4-(1*H*-6-bromoindazolyl)-1-methylindazolylpyridinium iodide (176).

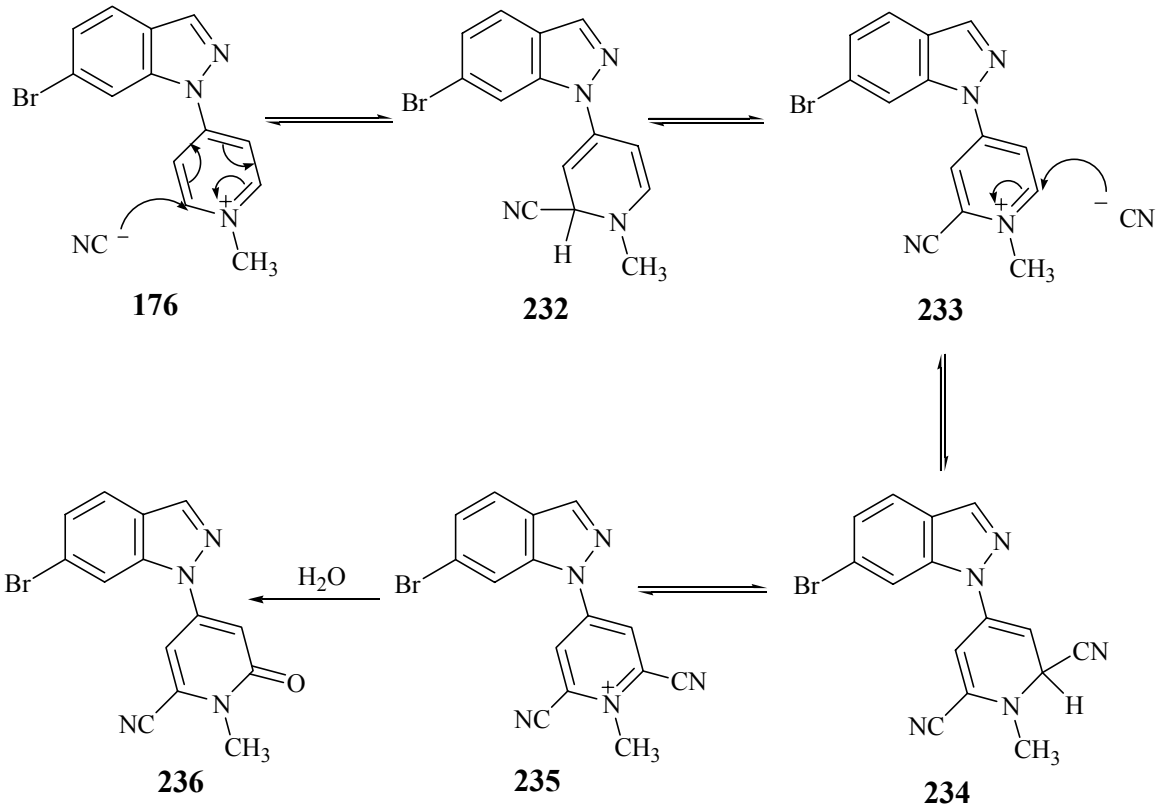

Scheme 93. Formation of cyanopyridones 237 and/or 236 from the corresponding 6-bromoindazolylpyridinium derivatives 174 and 176.

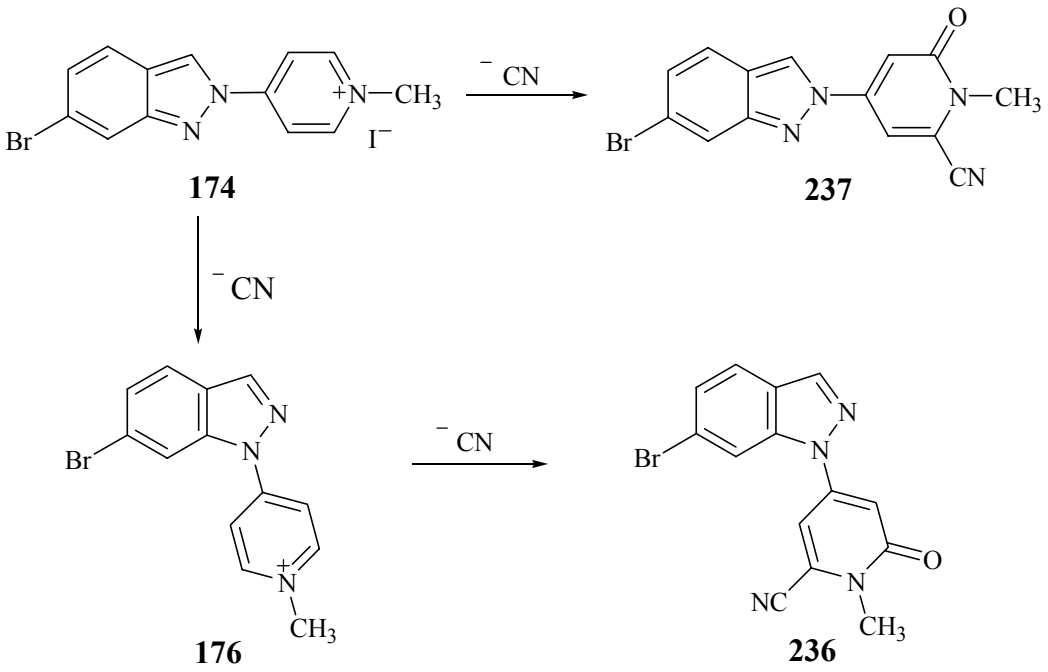

The reaction mixture containing the decomposition products of 2*H*-6-bromoindazolylpyridinium (LC-MS analysis for this reaction mixture is shown in Figures 47 and 48) was partitioned between ethyl acetate and water. The organic layer was analyzed by GC-MS. The major peak in the TIC tracings corresponded to 6-bromoindazole as expected. When the molecular ion $M^{\cdot+}$ 328 was extracted, two peaks were observed as shown in Figure 51 with the mass spectra shown in Figure 52.

Figure 51. Extracted ion chromatogram for molecular ions $M^{\cdot+}$ 328.

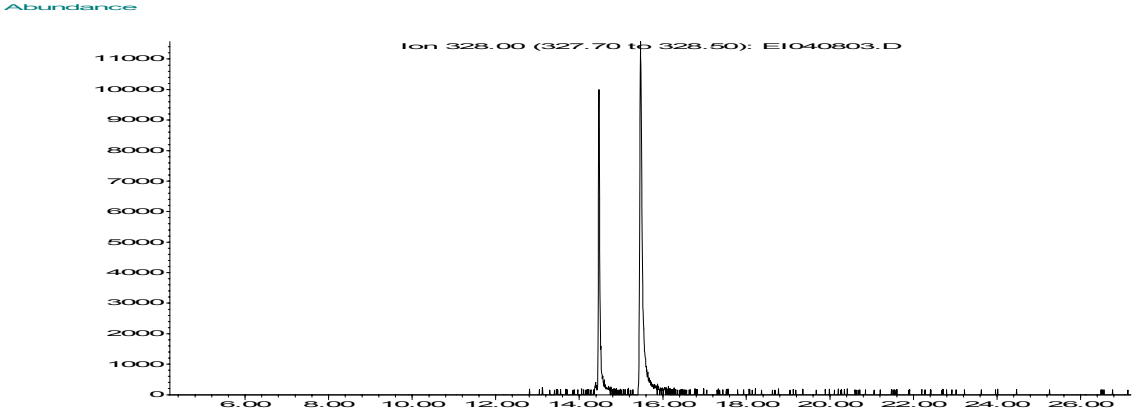

Figure 52. Mass spectra for the peaks with the molecular ion $M^{\cdot+}$ 328/330.

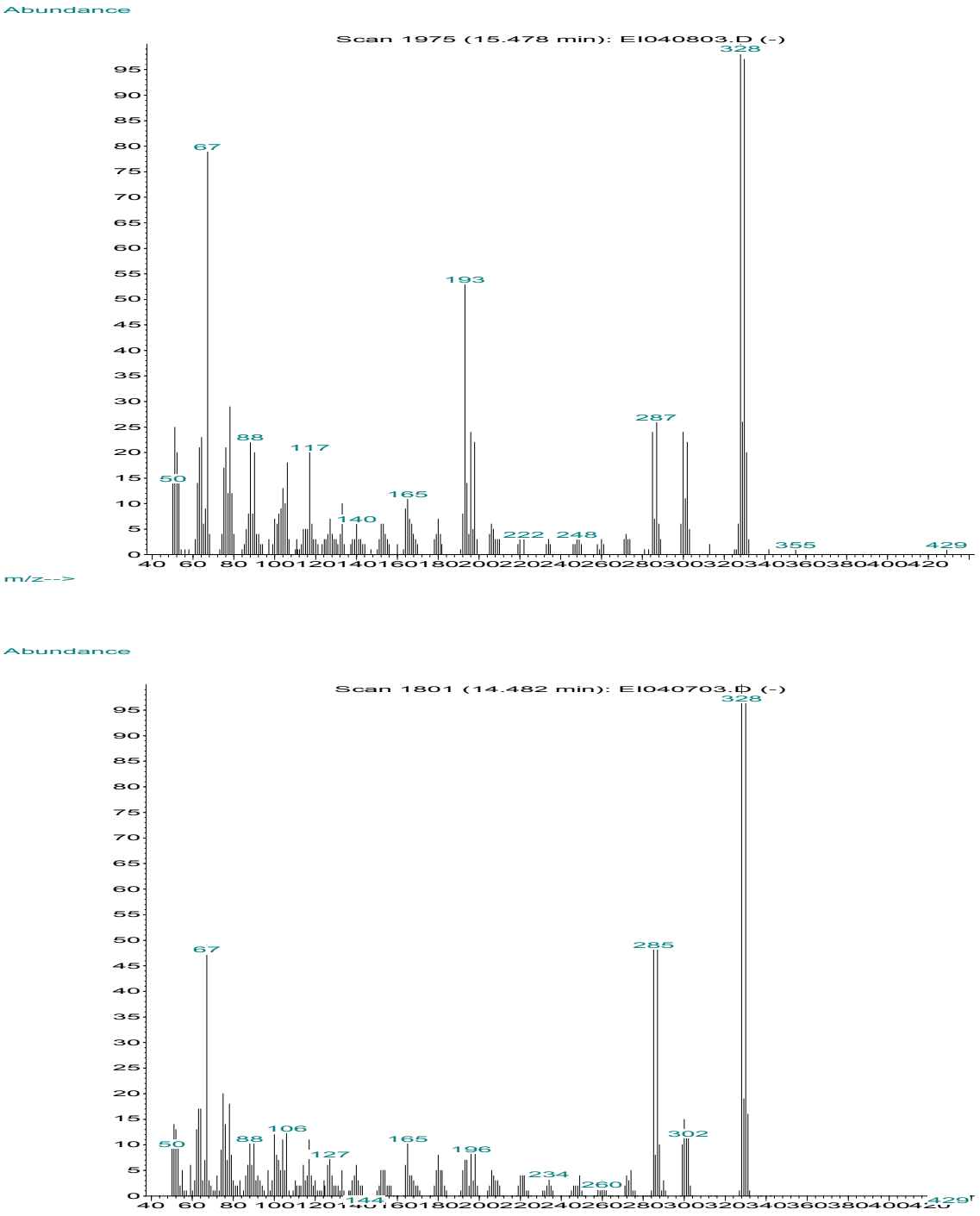

GC-MS analysis shows that cyanide attack is taking place before as well as after the rearrangement of the 2*H*-isomer **174** to the 1*H*-isomer **176** resulting in the formation of the regioisomeric cyano adducts **237** and **236**, respectively. A similar analysis was

conducted on the reaction mixture containing the decomposition products formed by the treatment of the 4-(1*H*-6-bromoindazolyl)-1-methylpyridinium iodide (**176**) with 2 equivalents of cyanide. As shown in Figure 53, only a single peak with $M^{\cdot+}$ 328 was present. This was expected since the 1*H*-isomer **176** does not rearrange to the 2*H*-isomer **174**.

Figure 53. Extracted ion chromatogram for molecular ion $M^{\cdot+}$ 328

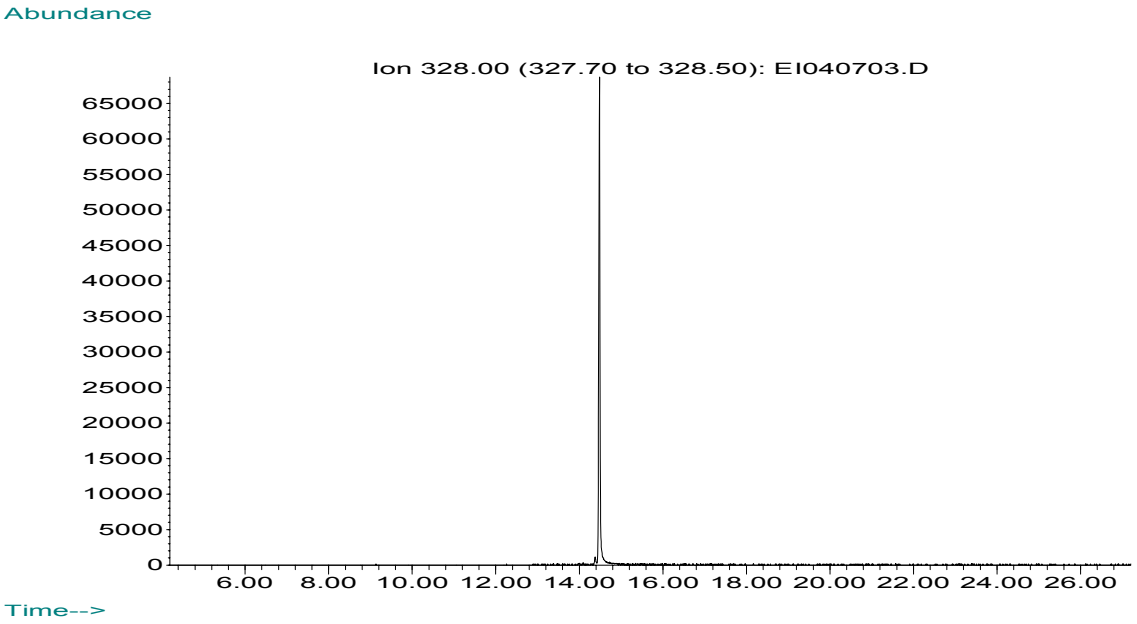

4.8. Investigation of the role of oxygen in the decomposition reaction.

As shown in Scheme 88, oxidation of cyanodihydropyridine **217** gives pyridinium **218**, hydrolysis of which leads to the formation of pyridone **219**. This oxidation step as well as the subsequent oxidation leading to pyridone **225** may be mediated by dioxygen. Another possibility is the disproportionation of 4-cyano-1-methylpyridinium (**214**) leading to the formation pyridinium **218** and 4-cyano-1-methyl-1,2-dihydropyridine (**238**) as shown in Scheme 94. A similar disproportionation reaction has been reported previously in the literature for MPTP derivatives.[216]

---

[216] Peterson, L.A., Caldera, P.S., Trevor, A., Chiba, K., Castagnoli, N., Jr. (1985) Studies on the 1-methyl-4-phenyl-2,3-dihydropyridinium species 2,3-$MPDP^{+}$, the monoamine oxidase catalyzed oxidation product of the nigrostriatal toxin 1-methyl-4-phenyl-1,2,3,6-tetrahydropyridine (MPTP). *J. Med. Chem.* **28**, 1432-1436.

Scheme 94. Proposed mechanism for disproportionation of 214.

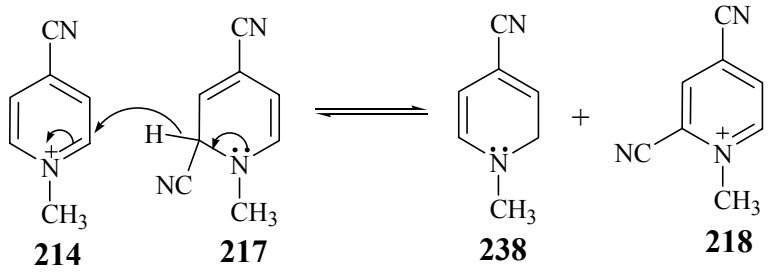

In an attempt to examine the role of dioxygen in the oxidation reaction, the addition of cyanide to 4-(2*H*-6-bromoindazolyl)-1-methylpyridinium iodide (**174**) under anaerobic conditions was examined. A solution of **174** in DMSO-d_6 was degassed in an NMR tube under vacuum via three subsequent freeze thaw cycles. After freezing the solution of **174**, a solution of 2 equivalents of KCN in DMSO-d_6 was added to the solution containing **174** under a blanket of nitrogen. The contents of the NMR tube were degassed once again and kept under nitrogen until a homogenous solution formed. The ^{1}H NMR spectrum of the mixture was obtained (Fig. 54a) and compared with the ^{1}H NMR spectrum of the reaction carried out under aerobic conditions (Fig. 54b). The ^{1}H NMR spectrum obtained for the anaerobic reaction was still complicated. However, some of the peaks present for the aerobic reaction were missing in the spectrum obtained for the anaerobic reaction. Although, the outcome was not conclusive, the results suggest that both dioxygen dependent and the disproportionation reaction proposed in Scheme 94 may be playing roles in the cyanide mediated decomposition reactions.

Figure 54. ^{1}H NMR (400 MHz) spectrum of 4-(2*H*-6-bromoindazolyl)-1-methylpyridinium iodide (174) in the presence of 2 equivalents of KCN under anaerobic conditions (a) and aeorobic conditions (b).

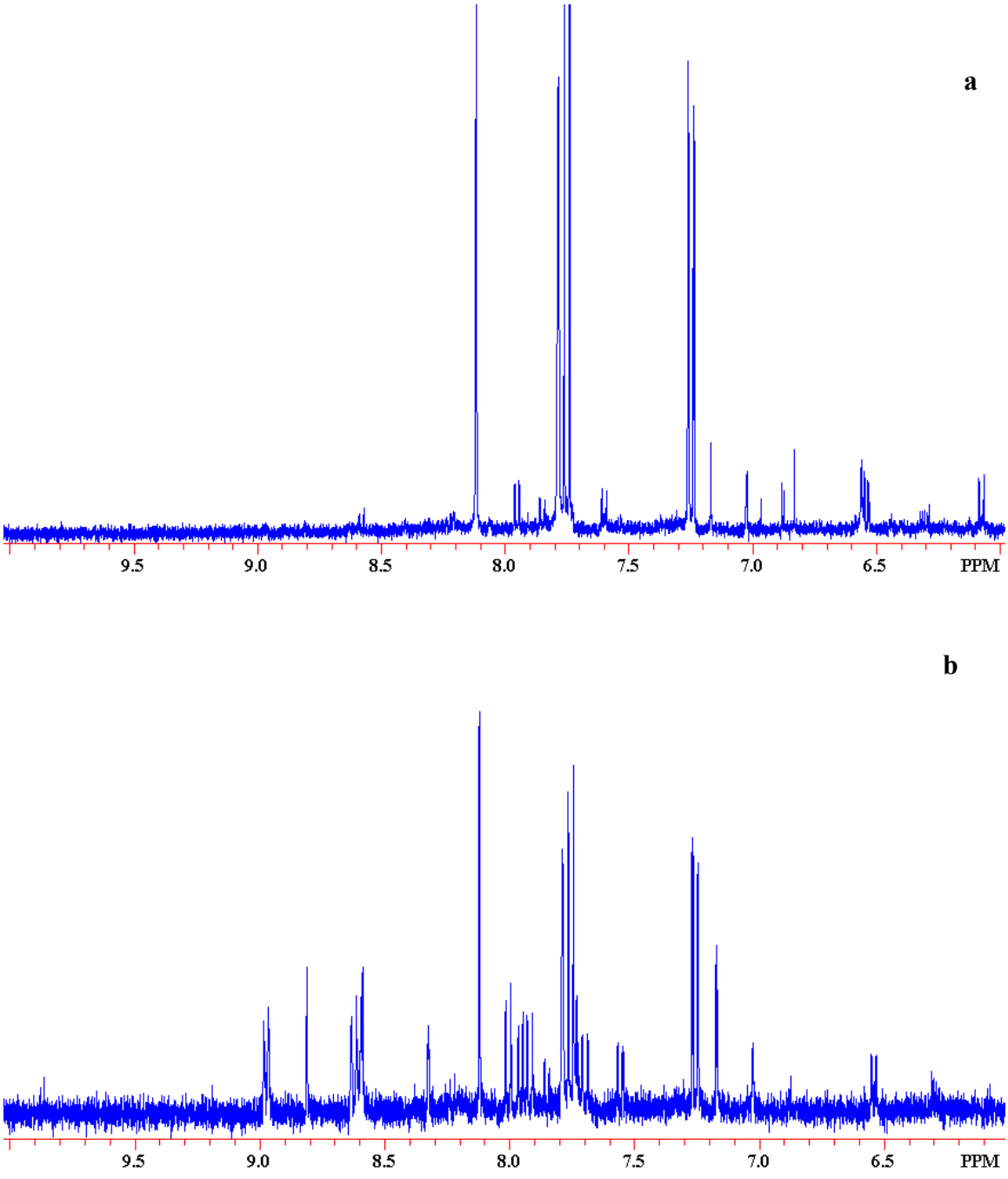

4.9. Comparison of the Stability of 2*H*-6-bromoindazolylpyridinium Derivative 174 in the Presence of Cyanide in DMSO-d_6, DMF-d_7 and D_2O

The effect of solvent on the cyanide mediated rearrangement of **174** was investigated using various deuterated solvents. The rearrangement reaction took place in a few minutes at room temperature in the presence of 0.5 equivalent of KCN when carried out in DMSO-d_6 or DMF-d_7. The rate of the rearrangement reaction was comparable in both solvents. The rearrangement reaction was also attempted in D_2O. The stability of **174** in water in the presence of 0.5 equivalent of KCN at room temperature was monitored by HPLC-DA. No significant change was observed even after 52 hours (Fig. 55).

Figure 55. Monitoring the stability of 174 in the presence of 0.5 equivalent of KCN in D_2O.

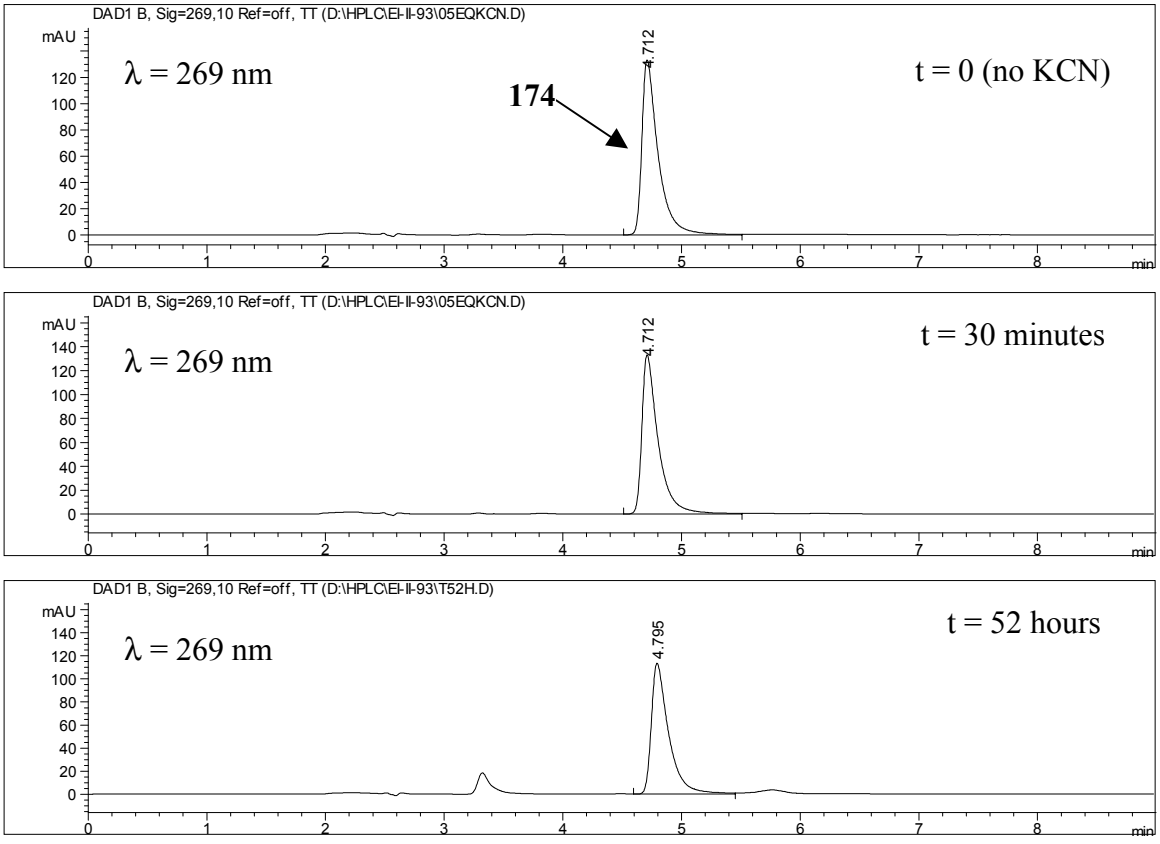

The effect of solvent on the rate of the rearrangement reaction is consistent with a nucleophilic pathway. In a polar, aprotic solvent the nucleophilicity of cyanide will be enhanced resulting in the rapid rearrangement of 2*H*-indazolylpyridinium derivatives. However, in a polar protic solvent like water, the nucleophilicity of cyanide is masked due to solvation which may account for the stability of **174** in aqueous solution in the presence of cyanide.

4.10. Investigation of Other Negatively Charged Nucleophiles.

The rapidity of the cyanide mediated rearrangement reaction is consistent with the nucleophilic character of cyanide. The rearrangement reaction was complete in few minutes in the presence of cyanide. We also examined the rate of the rearrangement reaction in the presence of other negatively charged species with different nucleophilicities. The stability of 4-(2*H*-5-bromoindazolyl)-1-methylpyridinium iodide (**193**) in DMSO-d_6 was monitored by ^{1}H NMR spectroscopy in the presence of sodium azide. The rearrangement of **193** required 7 hours to reach completion at room temperature. When the analogous experiment was carried out in the presence of sodium perchlorate, or sodium iodide, no evidence for the rearrangement reaction was observed even after 2 days. These results are consistent with the increasing nucleophilic character in going from perchlorate and iodide to azide to cyanide. The studies on the rearrangement of the 2*H*-proteindazolylpyridinium **112** showed that the rearrangement was complete in 3 hours at room temperature in the presence potassium hydroxide and in 48 hours at room temperature in the presence of potassium acetate (Section 3.5.1). These results are also in agreement with the relative nucleophilicity of hydroxide versus acetate.

4.11. Summary of Results for the Cyanide Mediated Rearrangement Reaction of 2*H*-Indazolylpyridinium Derivatives.

Although the results obtained for the TMP catalyzed rearrangement reaction supported a nucleophilic pathway, the site of attack by TMP was not obvious. Calculated energies of the intermediates showed that attack at C-3 should be favored due to the benzenoid nature of the corresponding spirodiaziridinyl intermediate. This finding led us to explore the possibility of providing direct evidence for the site of attack via the

concomitant displacement of a 3-bromo substituent from 4-(2*H*-3-bromoindazolyl)-1-methylpyridinium iodide (**141**). The proposed displacement reaction was shown not to occur using TMP, an outcome that might reflect the involvement of an unfavored intramolecular proton transfer. The use of cyanide instead of TMP was examined as an alternative approach where bromide might leave preferentially following the formation of the spirodiaziridinyl intermediate. However, in the presence of cyanide the bromine atom was retained in the rearrangement product of **141**. At this point, a radical pathway was considered which might account for the retention of bromine atom. Although it was not possible to rule it out completely, no evidence was obtained to support a radical pathway. A more plausible explanation for the retention of bromine was the concerted formation of a single diastereomeric spirodiaziridinyl intermediate via a stereospecific Michael type addition of cyanide. The collapse of the spirodiaziridinyl intermediate via an E2 type pathway requires the cyanide group to leave preferentially.

Another interesting finding of these studies relates to the stoichiometry of the cyanide mediated rearrangement reaction. According to the proposed nucleophilic pathway, cyanide was expected to have a catalytic role in mediating the rearrangement reaction as in the case of TMP. However, it was shown that a catalytic amount of cyanide was not sufficient for the completion of the rearrangement reaction. On the other hand, a stoichiometric amount of cyanide also was not necessary. This outcome suggested that cyanide was being consumed via a reaction or reactions unrelated to the isomerization process. The decomposition of both 1*H*- and 2*H*-indazolylpyridinium derivatives in the presence of cyanide was demonstrated to take place resulting in the formation of the corresponding indazole and possibly the 4-cyano-1-methylpyridinium species **214**. The formation of indazole upon decomposition was confirmed by mass spectrometry and NMR spectroscopy. However, no evidence was obtained for the formation of 4-cyano-1-methylpyridinium species suggesting that this compound was undergoing rapid decomposition following its formation. The decomposition of **214** was shown to result in the formation of a complex mixture of products which was expected on the basis the documented reactivity of cyanodihydropyridinyl derivatives. Two pyridone derivatives were identified as decomposition products derived from **214** by mass spectrometry via ^{13}C labeling studies. It was also shown that the attack of cyanide at C-2 of pyridinyl

moiety of 1*H*- and 2*H*-indazolylpyridinium derivatives was leading to additional pyridone derivatives with analogous structures.

Additional experiments were carried out to assess the effect of solvent on the rate of the cyanide mediated rearrangement reaction. The results were consistent with the proposed nucleophilic pathway. When cyanide is replaced with other negatively charged nucleophiles including azide and perchlorate, it was shown that the rates of the rearrangement reaction followed the nucleophilicities of these compounds.

Although the initial aim of unambiguous determination of the site of attack via the displacement of bromine failed, additional evidence supporting the nucleophilic pathway and insight into the stereochemistry of the rearrangement reaction were obtained.